UNIVERSIDADE ESTADUAL DE CAMPINAS
FACULDADE DE ENGENHARIA MECÂNICA
E INSTITUTO DE GEOCIÊNCIAS

MARCELO ANUNCIAÇÃO JACULLI

DYNAMIC BUCKLING WITH FRICTION INSIDE DIRECTIONAL WELLS

FLAMBAGEM DINÂMICA COM ATRITO DENTRO DE POÇOS DIRECIONAIS

CAMPINAS
[2017]

MARCELO ANUNCIAÇÃO JACULLI

DYNAMIC BUCKLING WITH FRICTION INSIDE DIRECTIONAL WELLS

FLAMBAGEM DINÂMICA COM ATRITO DENTRO DE POÇOS DIRECIONAIS

Dissertation presented to the Mechanical Engineering Faculty and Geosciences Institute of the University of Campinas in partial fulfillment of the requirements for the degree of Master in Petroleum Sciences and Engineering in the area of Exploitation.

Dissertação apresentada à Faculdade de Engenharia Mecânica e Instituto de Geociências da Universidade Estadual de Campinas como parte dos requisitos exigidos para a obtenção do título de Mestre em Ciências e Engenharia de Petróleo na área de Explotação.

Orientador: Prof. Dr. José Ricardo Pelaquim Mendes

Este exemplar corresponde à versão final da Dissertação defendida pelo aluno Marcelo Anunciação Jaculli e orientada pelo Prof. Dr. José Ricardo Pelaquim Mendes.

Assinatura do Orientador

CAMPINAS

[2017]

Agência(s) de fomento e nº(s) de processo(s): CAPES, 33003017

Ficha catalográfica
Universidade Estadual de Campinas
Biblioteca da Área de Engenharia e Arquitetura
Luciana Pietrosanto Milla - CRB 8/8129

J169d
Jaculli, Marcelo Anunciação, 1992-
Dynamic buckling with friction inside directional wells / Marcelo Anunciação Jaculli. – Campinas, SP : [s.n.], 2017.

Orientador: José Ricardo Pelaquim Mendes.
Dissertação (mestrado) – Universidade Estadual de Campinas, Faculdade de Engenharia Mecânica.

1. Flambagem (Mecânica). 2. Dinâmica. 3. Colunas. 4. Poços de petróleo. I. Mendes, José Ricardo Pelaquim,1971-. II. Universidade Estadual de Campinas. Faculdade de Engenharia Mecânica. III. Título.

Informações para Biblioteca Digital

Título em outro idioma: Flambagem dinâmica com atrito dentro de poços direcionais
Palavras-chave em inglês:
Buckling (Mechanic)
Dynamics
Columns
Oil well completion
Área de concentração: Explotação
Titulação: Mestre em Ciências e Engenharia de Petróleo
Banca examinadora:
José Ricardo Pelaquim Mendes [Orientador]
Paulo Roberto Ribeiro
Isamu Ikeda Junior
Data de defesa: 14-02-2017
Programa de Pós-Graduação: Ciências e Engenharia de Petróleo

UNIVERSIDADE ESTADUAL DE CAMPINAS
FACULDADE DE ENGENHARIA MECÂNICA
E INSTITUTO DE GEOCIÊNCIAS

DISSERTAÇÃO DE MESTRADO ACADÊMICO

DYNAMIC BUCKLING WITH FRICTION INSIDE DIRECTIONAL WELLS

Autor: Marcelo Anunciação Jaculli
Orientador: Prof. Dr. José Ricardo Pelaquim Mendes

A Banca Examinadora composta pelos membros abaixo aprovou esta Dissertação:

Prof. Dr. José Ricardo Pelaquim Mendes, Presidente
Departamento de Energia / Faculdade de Engenharia Mecânica / UNICAMP

Prof. Dr. Paulo Roberto Ribeiro
Departamento de Energia / Faculdade de Engenharia Mecânica / UNICAMP

Dr. Isamu Ikeda Junior
PETROBRAS

A Ata da defesa com as respectivas assinaturas dos membros encontra-se no processo de vida acadêmica do aluno.

Campinas, 14 de fevereiro de 2017.

DEDICATÓRIA

Dedico esse trabalho a Angela, Marcos e Gisele, os três pilares que me sustentam e me dão forças para prosseguir. Não seria possível ter chegado até aqui sem o seu amor e apoio incondicionais. Amo muito vocês.

AGRADECIMENTOS

Agradeço primeiramente a Deus pelo dom da vida.

Agradeço aos meus pais, Angela e Marcos, e à minha irmã, Gisele, seja pelo apoio incondicional, pelas palavras de incentivo ou pela compreensão nas dificuldades.

Agradeço ao meu orientador, Prof. Dr. José Ricardo P. Mendes, pela oportunidade e pelo apoio contínuo desde a graduação até o mestrado. Nos últimos 5 anos sob sua orientação, tive a oportunidade de aprender muito tanto sobre a minha área de pesquisa como também sobre a profissão de docente. Agradeço também ao Dr. Kazuo Miura por enriquecer o debate com comentários e ideias sempre muito pertinentes em relação ao tema desse trabalho. Agradeço ao Prof. Dr. Paulo Roberto Ribeiro, ao Prof. Dr. Marco Lucio Bittencourt, ao Dr. Isamu Ikeda Junior e ao Dr. Cristiano Agostini por aceitarem participar da avaliação e correção deste trabalho. Agradeço também à CAPES por financiar este trabalho.

I would also like to thank D. Sc. Stefan Miska and Ph. D. Guohua Gao for answering some questions regarding the subject and especially regarding their paper, which was the basis for this work.

Agradeço aos funcionários da FEM que me ajudaram nos últimos 7 anos, em especial aos das secretarias de graduação e pós-graduação e aos do DEP.

Agradeço a todos meus amigos, sejam eles da escola, da graduação ou da pós-graduação, pelas discussões e ideias, pelas risadas e pelas muitas histórias para contar ao longo dos últimos anos.

ABSTRACT

The exploration of offshore fields and the construction of deep and directional wells brought the necessity to understand the behavior of columns on such conditions – being them either risers, drill strings or tubings. Complete understanding of their behavior means to be able to design and operate them while avoiding any problems. In the present work, the differences observed on the measurements of friction during operations of tripping in and tripping out a tubing were studied, one of the problems associated to columns inside directional wells. It is worth noting that this problem can occur in various operations, such as lowering a sand screen curled on a pipe inside an open hole segment, lowering a tubing string inside a cased hole, or lowering a coiled tubing inside a tubing string. Generally, projects – and even commercial software – consider only the associated static problem, which proved as not being able to justify the measurement differences obtained on the field. Therefore, the present work introduces a dynamic model in opposition to the static model to explain the mentioned phenomenon. The main hypothesis is that column buckling inside the well would cause it to vibrate differently during tripping in and tripping out. During tripping in, the column is being compressed and thus can suffer buckling, displacing itself angularly inside the well to form either a sinusoid or a helix; meanwhile, during tripping out, the column is under tension and thus there is no buckling, meaning that the column will remain in contact with the lowest portion of the well the whole time. Using the models developed to characterize the column during tripping in and out, it was observed that, in fact, friction is different on both cases, thus reinforcing the hypothesis that buckling is responsible for the observed differences on friction during operations of tripping in and out a column.

Keywords: buckling (mechanics), dynamics, columns, oil well completion

RESUMO

A exploração de campos *offshore* e a construção de poços profundos e direcionais trouxe a necessidade de entender o comportamento de colunas nestas condições – sejam elas *risers*, colunas de perfuração ou colunas de produção. Entender completamente seu comportamento significa ser capaz de projetá-las e operá-las sem que ocorram quaisquer problemas. Neste trabalho, estuda-se um dos problemas associados a colunas dentro de poços direcionais: as diferenças observadas nas medições de atrito durante operações de descida ou de subida de uma coluna de produção. Nota-se que esse problema pode ser observado em vários tipos diferentes de operações, como, por exemplo, na descida de uma tela atrelada a um tubo base por dentro de um trecho de poço aberto; na descida de uma coluna de produção por dentro de um revestimento; ou na descida de um flexitubo por dentro de uma coluna de produção. Tradicionalmente, os projetos – e até mesmo *software* comerciais – consideram somente o problema estático associado, o que se provou não ser suficiente para justificar as diferenças medidas em campo. Sendo assim, este trabalho introduz um modelo dinâmico, em oposição ao modelo estático, para explicar o fenômeno mencionado. A principal hipótese é de que a flambagem da coluna dentro do poço faria com que ela vibrasse de forma diferente durante a sua descida e a sua subida. Durante a descida, a coluna está comprimida e, portanto, pode sofrer flambagem, deslocando-se angularmente dentro do poço para formar uma senóide ou um helicoide; já durante a subida, a coluna está tracionada e, portanto, não ocorre flambagem, de forma que ela permanece em contato com a parte mais baixa do poço o tempo todo. Utilizando-se os modelos desenvolvidos para se caracterizar a coluna durante a sua descida e a sua subida, observou-se que, de fato, o atrito é diferente nos dois casos, reforçando-se assim a hipótese de que a flambagem é a responsável pelas diferenças observadas no atrito durante operações de descida e subida de coluna.

Palavras-chave: flambagem (mecânica), dinâmica, colunas, poços de petróleo

LIST OF ILLUSTRATIONS

LIST OF TABLES

LIST OF ABBREVIATIONS AND ACRONYMS

ANP	Agência Nacional do Petróleo, Gás Natural e Biocombustíveis (Brazilian National Petroleum, Natural Gas and Biofuels Agency)
BHA	Bottom Hole Assembly
DPS	Dynamic Positioning System
KOP	Kickoff Point
RAO	Response Amplitude Operator
SVD	Singular Value Decomposition
USA	United States of America
WOB	Weight-on-bit

LIST OF SYMBOLS

A	Cross sectional area, m²
$\vec{a}$	Acceleration vector, m/s²
a	Center of Taylor's series expansion
$\vec{b}$	Binormal unitary vector
C	Courant number
C_f	Friction coefficient
c	Propagation speed of waves on a solid medium, m/s
dx	Infinitesimal element of length, m
E	Young's modulus, N/m²
$\vec{F}$	Internal force vector, N
$\vec{F}_f$	Total friction force, N
$\vec{F}_{f1}$	Friction force component on the axial direction, N
$\vec{F}_{f2}$	Friction force component on the tangential direction, N
F_x	Internal force component on the $\hat{\imath}$ direction, N
F_r	Internal force component on the $\hat{p}$ direction, N
F_y	Internal force component on the $\hat{\jmath}$ direction, N
F_z	Internal force component on the $\hat{k}$ direction, N
F_ϑ	Internal force component on the $\hat{q}$ direction, N
$\vec{f}$	External forces per unit of length vector, N/m
f	Total dynamic friction coefficient
f_1	Dynamic friction coefficient on the axial direction
f_2	Dynamic friction coefficient on the tangential direction
$f(x)$	Function of a single variable
g	Gravitational acceleration, m/s²
$\vec{H}_0$	Angular momentum vector, kg*m²/s
h	Interval for discretization
I	Area moment of inertia, m^4
I_p	Mass moment of inertia per unit of length, kg*m
$\hat{\imath}$	Axial direction vector (direction vector on *x* axis)

i	Space index for discretization
$\hat{\jmath}$	Direction vector on y axis
j	Time index for discretization
$\hat{k}$	Direction vector on z axis
k	Vector norm of $\partial\vec{\tau}/\partial x$
k_r	Component of $\vec{\tau}$ on the $\hat{p}$ direction
k_ϑ	Component of $\vec{\tau}$ on the $\hat{q}$ direction
L	Column length, m
$\vec{M}$	Internal moment vector, N*m
M_r	Internal moment component on the $\hat{p}$ direction, N*m
M_ϑ	Internal moment component on the $\hat{q}$ direction, N*m
m_p	Mass per unit of length, kg/m
$\vec{N}$	Normal force vector, N
N	Normal contact force per unit of length, N/m
$\vec{n}$	Normal unitary vector
$\vec{P}$	Linear momentum vector, kg*m/s
$\hat{p}$	Normal direction vector
$\vec{q}_p$	Weight force vector, N
$\hat{q}$	Tangential direction vector
$\vec{r}$	Position vector, m
r	Clearance between the column and the well, m
r_c	Well radius, m
T	Total time interval, s
t	Time variable
U_h	Heave amplitude, m
$u(x,t)$	Axial displacement function
u_a	Axial displacement due to axial tension/compression, m
u_b	Axial displacement due to bending, m
u_x	Total axial displacement, m
$\vec{v}$	Velocity vector, m/s
v_1	Velocity on the axial direction, m/s
v_2	Velocity on the tangential direction, m/s
x	Space coordinate on the axial direction

α	Well inclination angle, rad
Δt	Time interval for discretization, s
Δx	Space interval for discretization, m
θ	Angular displacement, rad
ρ	Material specific mass, kg/m³
$\vec{\tau}$	Position unitary vector
$\vec{\Omega}$	Angular velocity vector, rad/s
ω	Column rotational angular frequency, rad/s
ω_h	Heave angular frequency, rad/s
ω_r	Component of $\vec{\Omega}$, rad/s
ω_ϑ	Component of $\vec{\Omega}$, rad/s

CONTENTS

1. INTRODUCTION

Since the technology of directional drilling was improved on the USA in the 70s, directional wells became the reality of the oil industry. In Brazil, the first directional wells were drilled in the 80s, while the first horizontal wells were drilled on the 90s, as can be seen on Figures 1.1 and 1.2, respectively.

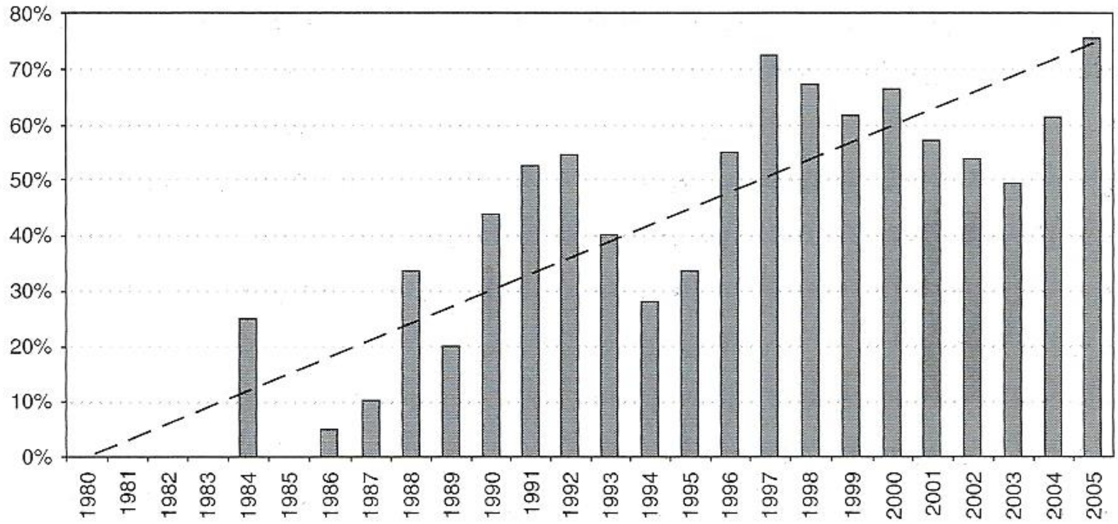

Figure 1.1: Percentage of directional and horizontal offshore wells drilled in respect to the total number of offshore wells drilled in each year (Rocha et al., 2006).

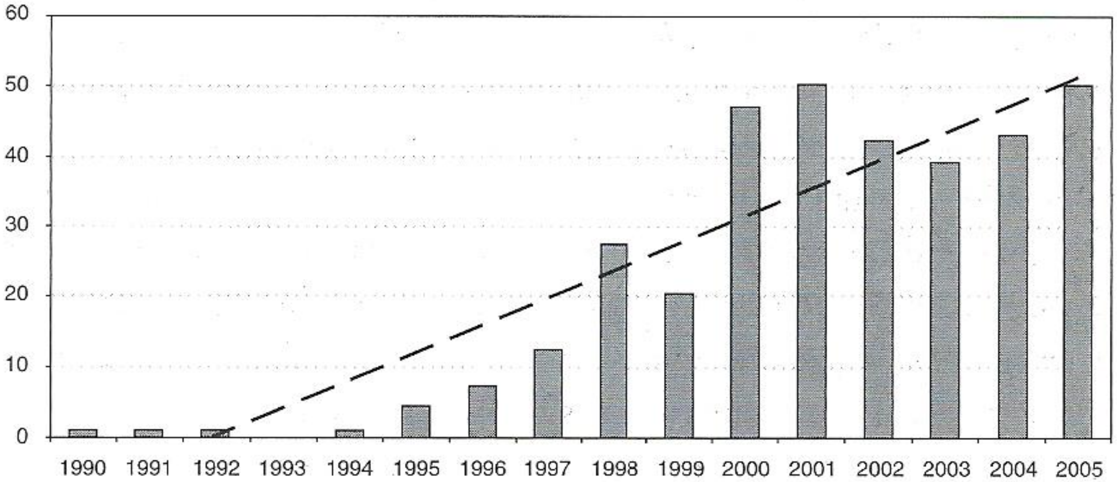

Figure 1.2: Number of horizontal offshore wells drilled in each year (Rocha et al., 2006).

Through the years, the percentage of directional and horizontal wells relative to the total wells kept increasing, reaching around 75% of the wells drilled in 2005. Directional and horizontal wells have innumerous advantages over vertical ones, such as increasing the well productivity by increasing the area in contact with the reservoir. Directional drilling became pretty much the standard way of constructing a well for offshore environments, a fact that can be observed on the ANP (2012) report, shown on Table 1.1. The red column is the total number of wells in each basin; the blue columns are the number of directional, horizontal and directional plus horizontal wells in each basin; and the green columns are the percentages of directional, horizontal and directional plus horizontal wells in respect to the total number of wells in each basin; finally the last row contains the total numbers of each respective column. It is important to note that the basins with onshore and offshore portions were separated as being two different basins. As can be seen, the basins with the highest percentages of directional wells are the ones located offshore – either entirely, such as the Ceará basin, or considering just the offshore portion, such as the Campos basin. The total percentage – 21% – may still be small, but is important to note that there are still old vertical production wells functioning and exploratory wells may be drilled as vertical due to smaller costs.

Table 1.1: Distribution of directional and horizontal wells in each Brazilian basin, sorted by the highest percentage of total directional and horizontal wells in respect to the total number of wells in the basin (adapted from ANP, 2012).

BASIN	# WELLS	# NON-VERTICAL WELLS			% NON-VERTICAL WELLS		
		DIR	HOR	TOTAL	DIR	HOR	TOTAL
CAMPOS ONSHORE	**3**	0	2	**2**	0,0%	66,7%	**66,7%**
CAMPOS OFFSHORE	**3141**	1210	692	**1902**	38,5%	22,0%	**60,6%**
POTIGUAR OFFSHORE	**419**	185	4	**189**	44,2%	1,0%	**45,1%**
CEARA	**227**	94	6	**100**	41,4%	2,6%	**44,1%**
SERGIPE OFFSHORE	**476**	204	3	**207**	42,9%	0,6%	**43,5%**
RECONCAVO OFFSHORE	**7**	0	3	**3**	0,0%	42,9%	**42,9%**
ESPIRITO SANTO OFFSHORE	**265**	36	41	**77**	13,6%	15,5%	**29,1%**
ALAGOAS ONSHORE	**835**	232	0	**232**	27,8%	0,0%	**27,8%**
PARNAIBA	**87**	20	0	**20**	23,0%	0,0%	**23,0%**
ESPIRITO SANTO ONSHORE	**1595**	193	155	**348**	12,1%	9,7%	**21,8%**
JEQUITINHONHA OFFSHORE	**34**	6	0	**6**	17,6%	0,0%	**17,6%**
SANTOS	**473**	56	23	**79**	11,8%	4,9%	**16,7%**

ALMADA ONSHORE	**6**	1	0	**1**	16,7%	0,0%	**16,7%**
SERGIPE ONSHORE	**4047**	623	16	**639**	15,4%	0,4%	**15,8%**
RECONCAVO ONSHORE	**6494**	953	33	**986**	14,7%	0,5%	**15,2%**
CAMAMU OFFSHORE	**59**	6	0	**6**	10,2%	0,0%	**10,2%**
POTIGUAR ONSHORE	**7703**	743	29	**772**	9,6%	0,4%	**10,0%**
MUCURI ONSHORE	**42**	3	0	**3**	7,1%	0,0%	**7,1%**
MUCURI OFFSHORE	**16**	1	0	**1**	6,3%	0,0%	**6,3%**
ALMADA OFFSHORE	**18**	1	0	**1**	5,6%	0,0%	**5,6%**
PARA-MARANHAO	**34**	1	0	**1**	2,9%	0,0%	**2,9%**
PARANA	**125**	2	0	**2**	1,6%	0,0%	**1,6%**
TUCANO SUL	**132**	2	0	**2**	1,5%	0,0%	**1,5%**
AMAZONAS	**213**	3	0	**3**	1,4%	0,0%	**1,4%**
TOTAL	**26451**	4575	1007	**5582**	17,3%	3,8%	**21,1%**

Aside from increasing the productivity, directional wells have a number of different applications (Rocha et al., 2006; Bourgoyne et al., 1986). These include drilling multiple development wells from a single platform, thus lowering costs; using directional drilling to reach hard objectives, such as for formations below urban and environmental protected areas; sidetracking, an operation in which the well is deviated from its original trajectory, in order to avoid anything restricting the path such as "fishes"; exploring fractured reservoirs; drilling relief wells for controlling blowouts; and multilateral wells, which are wells with several "legs" producing from different zones. Therefore, directional wells are extremely important for the oil industry and understanding the behavior of all the equipment during operations of directional drilling becomes vital to ensure safety. The present work focuses on the dynamic behavior of columns used on completion operations inside a directional well. During completion – and, by extension, on interventions as well – several operations involve the use of a column inside another column, such as lowering a tubing string inside a cased hole; a coiled tubing string inside a tubing string; or a sand screen using a work string inside an open hole. Thus, these columns vibrate freely during such operations while being constrained by the well or another column; these vibrations are the object of study of the present work.

1.1. Motivation

During completion operations, it was observed that the friction on the column – measured indirectly through the hook load – was different during operations of tripping in and out of the well. This problem originally appeared when measurements of hook load during tripping in and out – which were taken since tubing auxiliary lines were failing – indicated that the friction force would be different in both cases. This was unexpected because none of the current models and software can explain this effect or even consider that the column can have different friction forces. Since this problem did not happen with drill strings – which are stiffer than tubings and coiled tubings – the cause would probably be associated with buckling. During tripping in, the tubing is being lowered inside the well using its own weight, and compressive forces can act on it due to contact with the wellbore; meanwhile, during tripping out, the tubing is being pulled from the well, thus it is subjected to a tension force instead. Therefore, since forces occur in different directions during tripping in and tripping out, the hypothesis here is that the tubing is suffering buckling during its tripping in due to compression, while the tubing is not buckled during tripping out due to tension. The fact that the column buckles in only one scenario could explain the difference on the friction forces.

Another thing to consider is that the problem may be related directly to the dynamic response of the system instead of its static response. The problem could not be explained by the most common commercial software available in the market – considering that they are based on analyzing the static behavior of the column – thus leading this author to believe that the cause is dynamical.

1.2. Objectives

The objective of the present work is to describe the dynamic buckling behavior of columns inside directional wells through a mathematical model. Such model can work together with current models in the literature, since the former is dynamic and the latter are static. Also, by using this dynamic model, differences observed in practice regarding friction during tripping in from tripping out operations can be explained.

The results obtained showed that, in fact, the friction force is different during tripping in from tripping out. Then, a more complex model to consider the well trajectory as well as the heave motion of a column fixed on a floating vessel was developed, and the friction force remained different in the two cases. Also, it was possible to see the effects of the well inclination and the heave motion on the dynamic behavior of columns.

1.3. Structure of the present work

To better understand the proposed model and its implications, the present work is divided in six chapters with two appendices.

- On this chapter, the problem is discussed on its context, stating the motivations and objectives together with the main hypothesis;
- On chapter 2, a literature review regarding the problem of columns vibrating is done, by presenting the static and dynamic approaches for buckling, as well as references for directional drilling and numerical methods, which will be needed in order to solve the model;
- On chapter 3, the model itself is presented, divided in four steps; each step represents a gradual progress starting from a base model, thus explaining the role of each hypothesis on the final model;
- On chapter 4, the methodology and applications are shown, by providing a simple study case for a directional well scenario given by Rocha et al. (2006);
- On chapter 5, the results for the presented scenario are shown and a discussion of the results is made;
- Finally, on chapter 6, the final conclusions are presented, further commenting the results for the proposed problem and giving advice for future works regarding the subject;
- On Appendix A, the mathematical deduction of Models I through III is presented in more detail;
- On Appendix B, a more in-depth discussion of the finite differences method is made, including an analysis regarding the stability of the algorithm, in order to further enrich the proposed model.

2. LITERATURE REVIEW

On this chapter, a literature review regarding the subject is made. First, a historical background about the problem of vibrations in columns is presented, and then a brief review regarding directional drilling is also made. The buckling problem itself is presented next, by showing firstly the literature regarding the static approach and then recent works for the dynamic approach. Lastly, a brief review about numerical methods is made – focusing on the finite differences method – since solving the resulting motion equations can present several numerical challenges.

2.1. Historical background

The exploration of offshore fields and the construction of deep and directional wells brought the necessity to understand the behavior of columns under such conditions – whether they are risers, drilling strings or tubing strings. Several works regarding the subject were published starting from the 60s, remaining the focus of intense studies up until now. Bailey & Finnie (1960) and Finnie & Bailey (1960) are perhaps the pioneers on the subject of the behavior of columns. Since then, there were many other works about columns vibrations, characterizing its three vibration modes – axial, torsional and lateral – as well as the coupling between these three modes. On axial vibrations, the ones that stand out are Chung & Whitney (1981), Sparks et al. (1982) and Niedzwecki & Thampi (1988), whereas on lateral vibration there are Park et al. (2002) and Sparks (2002). It is evident that there are several other works exploring the topic; however, only a few hypothesis and/or boundary conditions are changed, always keeping the essence of the original problem – for axial and torsional vibrations, the wave equation firstly proposed by Jean d'Alembert in 1746; for lateral vibrations, the beam models deducted by Leonhard Euler and Daniel Bernoulli around 1750 and by Stephen Timoshenko in 1921. Han & Benaroya (2002) studied the behavior of columns using the Euler-Bernoulli and Timoshenko beam models, whereas, more recently, Chin (2014) studied the effect caused by the coupling of the three vibration modes; both works also presented numerical solutions for the motion equations of their respective problems. Chakrabarti (1987) presents the necessary modeling to study the dynamic behavior of offshore structures, such as vessels and floating platforms; such analysis is needed for the study of offshore wells, since the motion of such structures is transmitted to the column, thus making the offshore problem essentially different from an onshore one – where there is not such kind of motion. An example of problem associated with column vibrations can be seen on Figure 2.1. The figure exemplifies a common operation during drilling wells: the drilling rig – represented by the floating vessel – lowers a BOP – represented by the lumped mass at the bottom – using a riser – represented by the column. As the floating vessel vibrates with amplitude u_0, caused by the ocean waves, the motion is transmitted through the column to the lumped mass below, which vibrates with a different amplitude u_B.

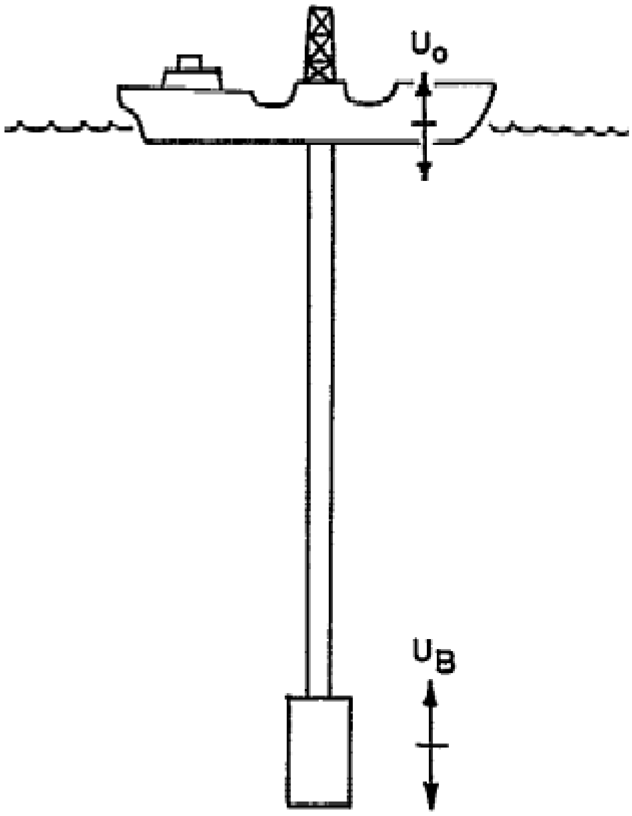

Figure 2.1: Example of a column vibrating on an offshore environment (adapted from Chung & Whitney, 1981).

Despite the progress on studying vibrations of such systems – a problem which is intrinsically dynamic – there were still phenomena associated with the static problem, such as column buckling. Lubinski et al. (1962) published one of the first works on the subject. The initial concern was only for vertical wells; in such cases, there was the possibility that the tubing string would buckle due to loadings caused by temperature and fluid pressure. Since the column was virtually fixed on its lower end due to the packer, such loadings could cause compression and, consequently, buckling. In the case that buckling would occur, the column would suffer changes on its length, which would be reduced; therefore, the authors focused on how to estimate such changes, calculating the so-called effective length. Figure 2.2 exemplifies this effect, showing the length reduction caused by buckling.

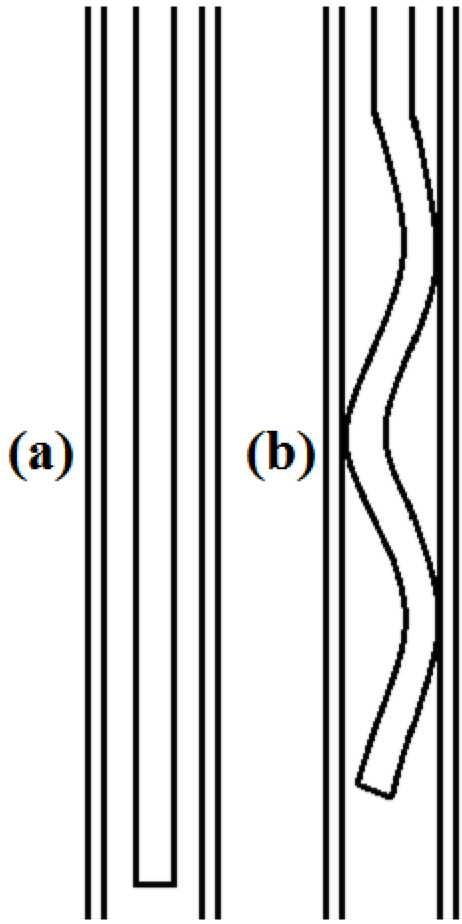

Figure 2.2: Example of (a) non-buckled and (b) buckled tubing string inside a well (adapted from Lubinski et al., 1962).

As the construction of wells became more complex, with the beginning of the practice of building directional wells, the solutions for vertical wells were no longer enough to describe the column behavior. Paslay & Bogy (1964) and, later, Dawson & Paslay (1984), noted that a model which considered the effects of the well inclination on buckling was needed. For such, the authors deducted a formula to calculate the critical buckling force – the maximum compressive force that the column could resist without suffering buckling – considering the well inclination. This criterion for the critical force is still widely accepted for solving problems associated to buckling, being used on commercial software. Works after Dawson & Paslay (1984) tried to improve the criterion by including, for example, the influence of friction.

Lastly, more recently, Gao & Miska (2010a) published a work analyzing the dynamic behavior of a column in an already buckled configuration. Through the dynamic analysis, it is possible to compare the column behavior under a buckled condition with its non-buckled condition. These differences can explain phenomena observed in practice and/or experimentally, such as the differences on the friction force during the column tripping in and its tripping out.

Evidently, the interest in both the vibration of continuous systems and the buckling of columns is not exclusive to the oil exploration activities. Timoshenko (1937) had already presented the equations for the axial vibration of bars, torsional vibration of shafts and lateral vibrations of beams way before any other work mentioned here; in 1757, Euler had already deducted the Euler's critical load, the maximum load that a column could support without buckling. Rao (2007) gathers the motion equations for the most commons continuous systems in engineering applications, as well as the analytical methods of Newton and Lagrange, used to deduct the equations.

2.2. Directional drilling

Since the present work is based on directional wells, a short review regarding directional drilling is in place. A classical book regarding drilling is the one from Bourgoyne et al. (1986), while Rocha et al. (2006) focused specifically on directional drilling.

On Bourgoyne et al. (1986), several aspects of drilling are discussed, such as required equipment, drilling fluids, cementing and drilling hydraulics. The interesting part of their book for this work is chapter 8, in which directional drilling is discussed. The authors provide insight on the technology, such as applications, special equipment and trajectory planning and control. Meanwhile, on Rocha et al. (2006) a much more in-depth discussion is made, especially regarding the practices adopted in Brazil. The book provides examples of directional wells trajectories, which will be used on this present work. Figure 2.3 illustrates an onshore directional well.

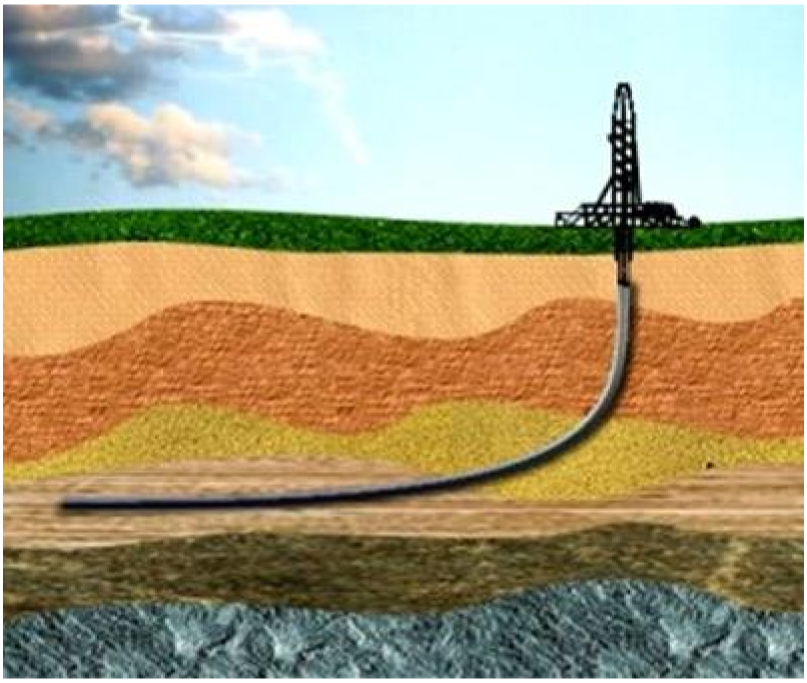

Figure 2.3: Example of an onshore directional well. The well starts vertical, but then it gains curvature until becoming horizontal.

2.3. Column buckling – static approach

As previously mentioned, the concern of authors regarding the buckling phenomenon was always in respect to the static problem, not the dynamic one. Therefore, until today the majority of published works – as well as the commercial software developed specially for this kind of problem – worried only about the static approach, with more or less the same goal: to estimate which compressive force will cause buckling – i.e. the critical buckling load – and to find the new column length after buckling – i.e. the effective length. What distinguishes the innumerous works in the literature are the possible nuances in the model: different boundary conditions, different column configurations, the effect of dry friction, the effect of well inclination. Among these innumerous works, the ones that stand out are the pioneers and still widely referenced today: Lubinski et al. (1962), Paslay & Bogy (1964) and Dawson & Paslay (1984). It is interesting to note as well the work done by Mitchell (2008), who did a summary of the state of the art about column buckling, by narrating the historic of publications on the subject and enunciating the challenges which remain to be analyzed to understand it even fuller.

Lubinski et al. (1962) make an analysis on the effect of internal and external pressures and temperature on the static behavior of a tubing string. According to them, the column might suffer helical buckling both when the packer used to settle it can seal its motion completely as well when the motion is permitted. In case buckling occurs, the original length of the column will reduce. Therefore, the authors propose models to calculate the column length reduction and explored practical cases for each one of the possible scenarios: packer without any column motion restrictions, packer with partial column motion restriction, packer with complete column motion restriction and permanent corkscrewing – phenomenon in which the column suffers plastic strain and retains the helical configuration even under tension. These calculations aim to mitigate the buckling effects during the tubing string installation and/or operation, thus predicting, for example, which maximum compressive force can be applied to avoid buckling. The authors also remark that buckling can cause operational problems even when it does not cause tubing failure; if the tubing is buckled, the passage of tools using wireline may become impossible.

Paslay & Bogy (1964), using energy methods, do an extensive analysis regarding the stability of a bar subjected to tension loads and confined inside an inclined cylinder. Considering the hypothesis that the bar always remains in contact with the internal surface of the cylinder, the authors conclude that the bar will always be stable, as long as there are no restrictions for its rotational motion. They also concluded that for a bar of small diameter – compared to the diameter of the external cylinder – the confinement effect becomes negligible and thus the critical buckling load in this case reduces itself to the traditional Euler’s critical load. These results were fundamental for subsequent works to elaborate more robust criteria regarding the critical buckling load.

Dawson & Paslay (1984) suggest corrections for the work of Paslay & Bogy (1964), aiming to consider the effect of floatability of the drill string. As observed by the authors, the critical load for a column calculated by Paslay & Bogy (1964) for slant wells results in a higher value than for the same column inside a vertical well; therefore, the drill string is more resistant to buckling in directional wells than on vertical ones. Since the column is more resistant in that scenario, there is the possibility of tripping in under compression on the slant segment without the risk of buckling. Also, with a lesser risk of buckling, the BHA weight can be reduced, which in turn will reduce the torque and drag during operations as well. Even so, there is still the possibility that the column buckles under an excessive compressive load; therefore, the authors develop a criterion to avoid buckling, taking into account the weight-on-bit (WOB) and the column wet weight. Controlling these two variables, it is possible to avoid that the compressive load surpasses the critical buckling load. Lastly, the authors remark that, as the time passes, the mechanical properties of the joints degrade, becoming less rigid, lighter and, consequently, more susceptible to buckling, thus influencing on the results obtained through usage of the buckling models. Also, the analyses are valid only for slant segments of well – which have constant inclination – because drastic changes on the inclination can compromise the column resistance to buckling by reducing the critical buckling load.

Based on these classical works, there is a vast list of other works which give contributions starting from these initial models. Following up, only a few of these works are presented; the ones which the author of this present dissertation considers relevant in building the knowledge on the subject. They are organized in chronological order, but also grouped based on the kind of contribution given.

Mitchell (1986) makes a simplified analysis aiming to consider the effect of the dry friction force on the critical buckling load. The author concludes that the friction force reduces the compressive force acting on the tubing string, thus attenuating the effects of buckling. If the buckling effect is attenuated, the column original length will not reduce as much as predicted on previous works, which in turn gives more freedom when designing packers – a problem which had been already identified by Lubinski et al. (1962). However, the author also concludes that his model still needs improvements. Such improvements were made by himself in Mitchell (1996b), in which the model also considers the load history on the column – for the case in which the column is loaded once, the load is removed and then a new load is applied – thus being able to pinpoint the direction of the friction force during the second loading. Later, Mitchell (2007), knowing that the column could either slip on the wellbore or roll without slipping, modifies Dawson & Paslay's (1984) criterion to consider such effects; the difference between each criterion is the presence of a term respective to the torsional rigidity. Following Mitchell's (2007) footsteps, Gao & Miska (2009) recognize that the friction force possesses components in more than one direction; there is lateral friction due to the angular motion of the column inside the well, as well as axial friction due to the axial strain of the column.

Chen et al. (1990) are perhaps the first ones to recognize and distinguish the existence of two different buckling modes: sinusoidal – also commonly called lateral –

and helical. Figure 2.4 shows the two modes of buckling. The authors then establish criteria that would separate the two kinds of buckling and could recognize which one would happen first. They conclude that firstly sinusoidal buckling would happen – when the critical buckling load is reached – and only then helical buckling could happen – which requires an even larger load than the critical load. The authors also find out the existence of another critical value even higher, in which a phenomenon called lock-up would occur: the column would lock inside the well in its helical configuration and would not be able to move on the axial direction any longer, even under tension.

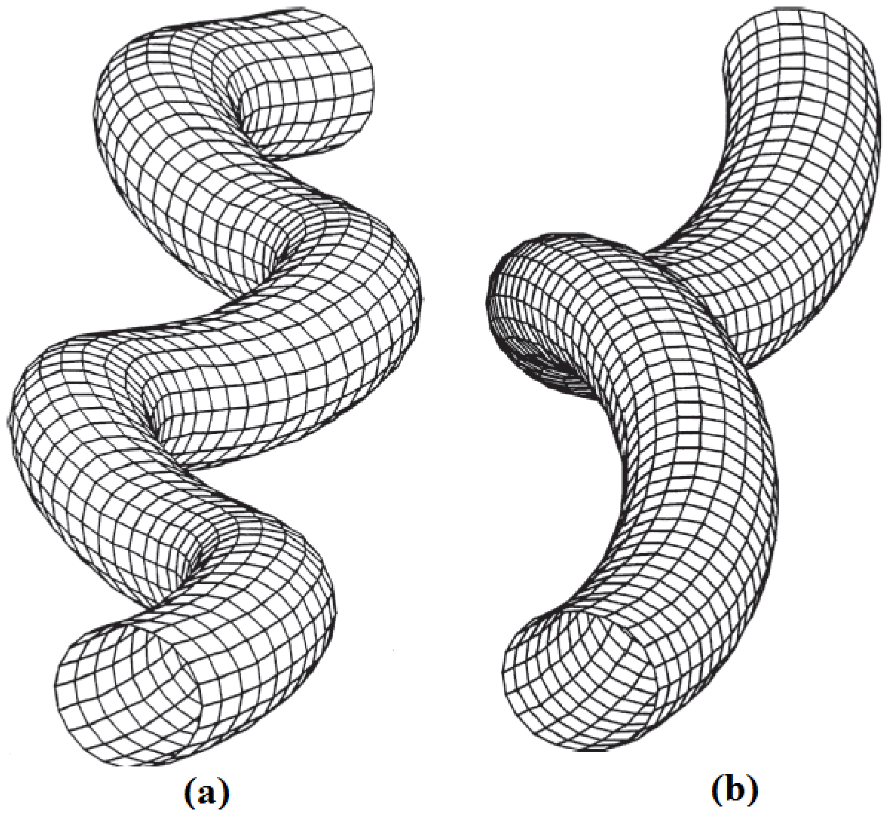

Figure 2.4: Example of (a) sinusoidal and (b) helical buckling (Mitchell, 2008).

Saliés (1994) makes an experimental study to measure the critical buckling load. A schematic of the experiment can be seen on Figure 2.5. The author varies several parameters to observe the effect of each one of them on the final result: different pipe diameters and thickness, different materials for different dry friction coefficients, different well inclinations ranging from vertical until horizontal. The author then compared the obtained results with the existing models in the literature, such as Lubinski et al. (1962), Dawson & Paslay (1984) and Chen et al. (1990). The experimental results are satisfactory, with good congruence when compared to the values calculated from the models. The author also concludes that the friction, aside from increasing the critical buckling load as already observed previously by Mitchell (1986), also creates a hysteresis effect during loading and unloading of the pipe. Lastly, he also concludes that the tendency is for the column to suffer helical buckling, with sinusoidal buckling happening only on its first mode before it moves to helical.

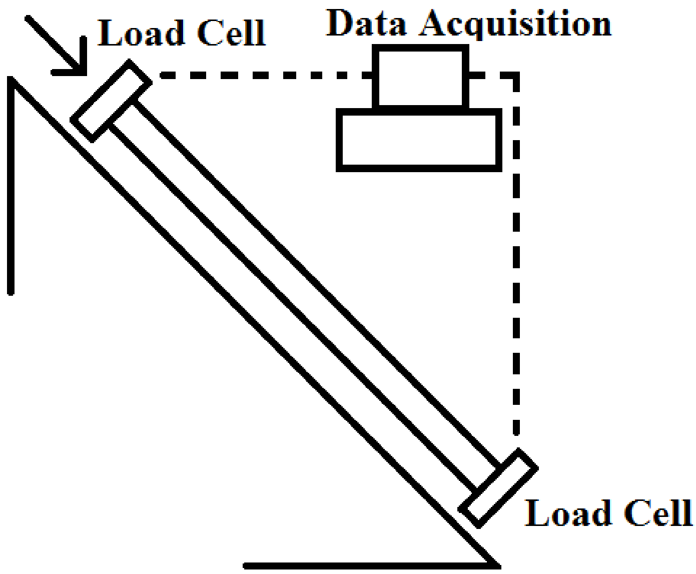

Figure 2.5: Schematic of an experiment for measuring the critical buckling load (adapted from Saliés, 1994).

He & Kyllingstad (1995) improve the model from Dawson & Paslay (1984) to consider the well curvature. Up until then, Dawson & Paslay's (1984) model only considered that the column was on an inclined well segment with constant curvature; the consequence of such model was that the critical buckling load calculated from it was still too conservative when compared with measured data. For this very reason, the authors consider the effect of the well curvature, which increases the critical buckling load and thus is less conservative. Later, Mitchell (1999) reformulated the criteria for the critical buckling load initially proposed by Dawson & Paslay (1984), by taking into account the work from He & Kyllingstad (1995).

Using the Euler-Bernoulli slender beam model, Mitchell (1988) proposes an equilibrium equation to calculate the static displacements of a column already under buckling inside a vertical well. After that, in Mitchell (1996a) and Mitchell (1997), the author improves the model to also consider directional wells. Lastly, Mitchell (2002) seeks analytical solutions for the presented equilibrium equations, especially for the cases of vertical and horizontal wells. Starting from Mitchell's (1988) model, Gao & Miska (2009) study the effects of the boundary conditions and friction force on the static configuration of the column after buckling occurred. They concluded that for slender pipes, the effect of the boundary conditions can be neglected without affecting the result, whereas the effect of the friction force becomes even more relevant, since the critical buckling load is increased – something that was already mentioned by Mitchell (1986). Similar to Paslay & Bogy (1964), they also conclude that for non-slender pipes the effect of the wellbore could be neglected. These results are expanded in Gao & Miska (2010b).

Miska & Cunha (1995) performed an extensive analysis regarding the critical buckling load, considering six different combinations: whether the column had weight or not, combined with either pure axial loading, pure torsional loading or both loads. The authors note that the torque reduces the critical buckling load, besides also reducing the helix pitch during helical buckling. Such effects are more noticeable in wells with smaller inclinations or in more flexible columns. These results are later expanded in Qiu et al. (1998) and in Qiu et al. (1999), where the authors improve the model from Miska & Cunha (1995) for the 3D case, besides analyzing the influence of the column initial configuration on the buckling phenomenon. Wicks et al. (2007) propose a critical buckling load criterion for long cylinders by taking into account the effects of compression and torsion, while also concluding that more studies are required to include the gravity and friction effects properly as well.

Mitchell (2008) makes a summary of the state of the art of the column buckling problem. The author presents the criteria for the critical buckling load developed by Dawson & Paslay (1984), Chen et al. (1990) and He & Kyllingstad (1995), in respect to the two possible buckling configurations: sinusoidal and helical. It also shows the corrections to consider the friction effect, obtained by Mitchell (2007). Lastly, the author presents the equilibrium equations for the column after buckling, initially obtained by Lubinski et al. (1962) and expanded by Miska & Cunha (1995) and Mitchell (2002). As for the challenges remaining to be overcome, the author mentions the modeling of columns with segments with different properties – known as tapered strings, shown on Figure 2.6, which bring uncertainties to the problem due to the change of diameter, the effect of the boundary conditions on directional wells, besides fully understanding the role of the friction force on the problem. Despite the fact that papers like Mitchell (1986) approached the effect of the friction force, the author judges that this effect is not completely described and understood.

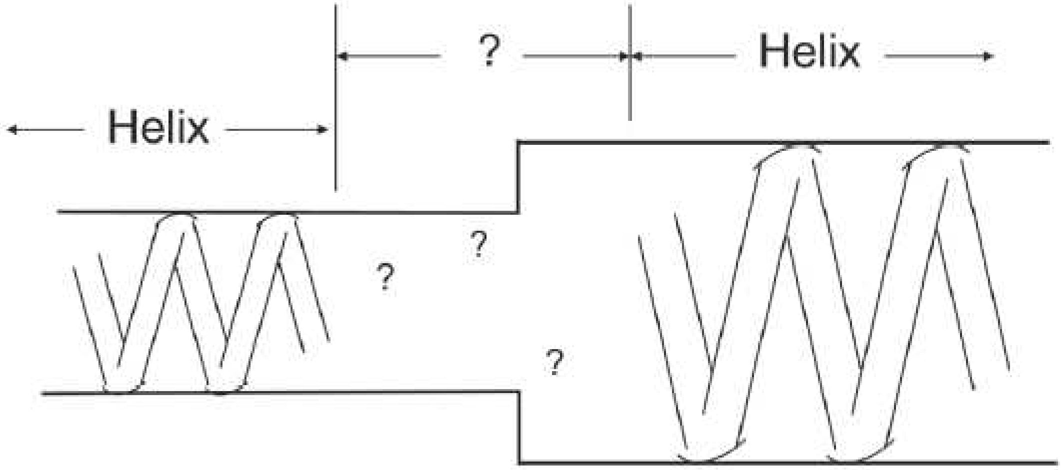

Figure 2.6: Example of a tapered-string problem (Mitchell, 2008).

Recent works have focused in comparing results obtained from literature models with experimentally measured data, such as in Arslan et al. (2014); or improving even further the models for the static configuration after buckling, as in Huang et al. (2015a) and Huang et al. (2015b).

2.4. Column buckling – dynamic approach

Differently from the static problem, the dynamic problem associated to column buckling has received little attention from authors. However, there are two plausible explanations for this fact. Firstly, the dynamic analysis has little contribution in creating criteria to evaluate if the column will buckle or not. This happens because the dynamic analyses already consider that the column will buckle regardless, similar to what was done by Gao & Miska (2009) for the column configuration after buckling on the static case. Secondly, the motion equations describing the column become complex due to the coupling which appears between axial and angular displacements, resulting on a system of non-linear partial differential equations. Analytical solutions become impossible – unless several simplifications are made – thus numerical methods being the only possible path to follow.

Gao & Miska (2010a) is the most relevant work regarding the dynamic approach. There, the authors deduct a dynamic model to describe the vibration of a column under an already buckled condition. Such model results in a system of partial differential equations relating axial displacement, angular displacements, axial internal force and normal contact force between the column and the well. After several simplifications, the authors are able to find an analytical solution and analyze the phenomena that occur during the vibration of the buckled column. They observe that depending on the amplitude of vibration, the column might have two different behaviors, called the first and second modes of snaking motion. On the first mode, the column vibrates only in contact with half of the well; in other words, starting from the equilibrium position at the lowest point of the well, it can vibrate and reach the highest point of the well only in contact with one of the two sides. Meanwhile, on the second mode, the column is free to vibrate in contact with any point of the well. The authors conclude that the model still needs improvements, since it neglects the dry friction force, which is most likely relevant on the phenomenon. In Sun et al. (2014), the authors expand Gao & Miska's (2010a) work, finding approximated analytical solutions and comparing with numerical solutions, reaching good results. Figure 2.7 shows a schematic of the problem proposed by Gao & Miska (2010a).

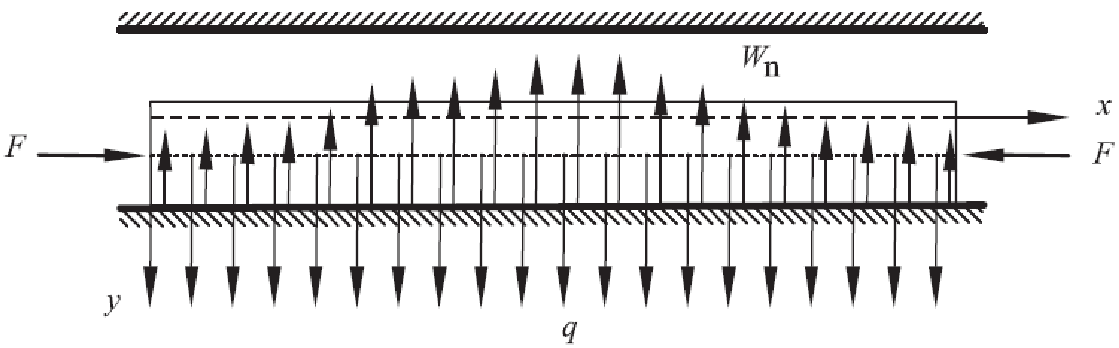

Figure 2.7: Example of a column inside a horizontal segment of well. W_n is the distributed normal force, q is the column distributed weight and F is a compressive force (adapted from Sun et al., 2014).

Despite a robust model already existing to explain the dynamic problem associated to column buckling, there is still a lot to be done. As explained by Gao & Miska (2010a), the two biggest simplifications of their model are the friction force being neglected and the analysis being valid only for a horizontal well. The goal of this present work is exactly to push forward on these two hypotheses while also exploring the implications of what was already deducted by them.

2.5. Numerical methods

Due to the natural complexity of the motion equations associated with the vibration of continuous media, which is the case of columns, an analytical solution becomes unfeasible. For this reason, it is necessary to select and apply an appropriate numerical method. The most commonly used methods are the finite differences and the finite elements; on this work, the finite differences method is used. Despite having a higher computational cost than the finite elements, it is much easier to do the discretization for finite differences.

The finite differences method finds innumerous applications on the most diverse engineering, physics and math problems; therefore, the literature on this topic is extremely vast. Here, in respect to the finite differences method, it is worth mentioning the books by Leveque (2005) and Strang (2007), besides the work from Fornberg (1988). A discussion regarding the stability of the method is made on Courant et al. (1928), in which the authors provide a criterion for choosing the appropriate space and time discretization steps, while in Arfken (1985) a discussion regarding badly-scaled matrices is made, which is a common problem that arises when applying the finite differences method.

In Leveque (2005) and Strang (2007), several methods for finite differences discretizing are presented, such as the Euler approximations and the Runge-Kutta methods. The discretization is then applied to classical differential equations in the literature, such as the wave equation, the heat equation and the Poisson’s equation. A discussion regarding the stability of these equations is also made, especially regarding the errors associated with discretization and how to choose properly the space and time steps to enable numerical convergence.

Fornberg (1988) presents the necessary equations to deduct the finite differences discretization for derivatives of first, second, third and fourth orders for centered, forward and backward differences, while also doing the discretization for the grid points themselves or for half-way points between two adjacent grid points. The author presents results with a higher order of precision than what is commonly found on literature, such as, for example, a discretization of eighth order for the first and second derivatives, which requires the information from nine points of the grid to obtain the derivative of a single point. The usage of a discretization of higher order enhances the precision of the results, but does not solve any problems related to the algorithm stability.

Courant et al. (1928) make an analysis of different kinds of partial differential equations – namely elliptic, hyperbolic and parabolic equations – in respect of their stability. It was on this work that the authors deduct the Courant number and propose the Courant-Friedrichs-Lewy stability condition, a necessary condition for the finite differences discretization to be numerically stable, especially for the case of hyperbolic partial differential equations, category in which the wave equation belongs.

In Arfken (1985), the author presents several necessary tools for solving mathematical problems, such as vectors, matrices, determinants, functions, series and transformations. Regarding matrices, he discusses the matrix conditioning number and the requirements to determine if a matrix is well or badly conditioned; if a matrix is badly conditioned, it means it is close to being singular, thus making it harder to solve. This analysis is fundamental for the finite differences method, because sometimes the resulting matrix associated with the discretization can be badly-scaled.

3. THEORETICAL FOUNDATION

In order to fulfill the proposed objectives, mathematical models will be described on this section. The procedure used to create the model was incremental: four models were developed, with each model pushing the previous one a step further.

The solution starts with Model I, which is exactly the same as proposed by Gao & Miska (2010a). This is considered the base model, since it the most simplified one. On this model, there is no friction, the well segment is always horizontal and the boundary at $x = 0$ is fixed. Improving this model there is Model II, which considers the friction force – but the segment is still horizontal and the boundary at $x = 0$ is still fixed. It is worth noting that Model II is the minimum requirement to verify the hypothesis that the friction force is different during tripping in and tripping out. Moving further, Model III considers the well inclination as well; therefore, any well trajectory can be studied, as long as the angle at each depth is provided. Finally, Model IV considers a periodic excitation at the boundary $x = 0$. This is a necessary improvement to consider a sea environment, since the column is subjected to a heave motion caused by the vessel heave motion; Models I to III can be applied only to onshore wells, where the column does not suffer any kind of periodic motion. Finally, while all models are subdivided into a tripping in case and a tripping out case, the column is not actually moving forward or backward; all models consider a fixed length of column vibrating around its equilibrium position for that very specific length, but under different hypotheses depending if the column is on a tripping in case or on a tripping out case. Table 3.1 sums up the hypotheses of all models.

Table 3.1: Summary of hypothesis for all four models.

	Friction force	Slant segments	Periodic motion on boundary
Model I			
Model II	X		
Model III	X	X	
Model IV	X	X	X

3.1. Model I – Column without friction

In order to understand the column behavior during its tripping in and tripping out, a dynamic model which relates its displacements inside the well becomes necessary. On a directional well, the column is free to vibrate on all three directions, aside from rotating around its own axis. On the following model, only a horizontal segment of well is considered and the column remains in contact with the well throughout its whole length and during the whole time, thus reducing the number of variables from three – initially the displacements on the x, y and z axis – to two – axial displacement along the well axis and angular displacement as defined by Figure 3.1. To help with modeling, two unitary vectors $\hat{p}$ and $\hat{q}$ are defined – normal and tangential, respectively, to the contact point between the column and the wellbore. Both the well radius and the column radius are considered constant for the whole horizontal segment and the clearance between the two radii is considered small.

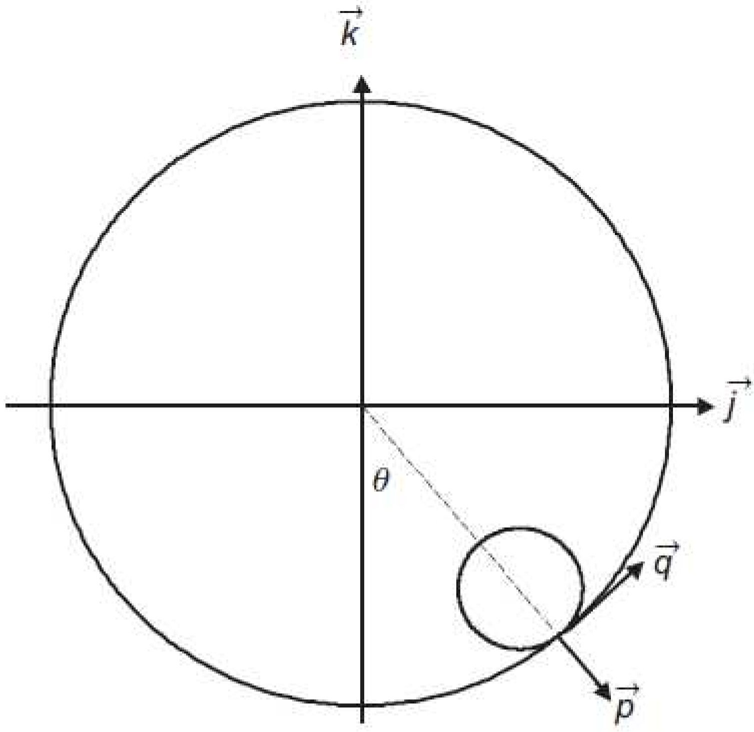

Figure 3.1: Column inside a well scheme. The column is represented by the smaller circle, while the well is represented by the larger circle. The angle θ is defined between the z axis of the well and the normal vector $\hat{p}$ (Gao & Miska, 2010a).

There are some simplifications regarding the loads on the column. The effect of viscous damping was neglected and there is no imposed torque on the two ends, while the column rotary speed is constant. Lastly, as mentioned before for this model, the effect of friction is neglected.

Figure 3.2 shows the column buckled configuration inside the well, from planes *xz* and *yz*, with plane *yz* containing the cross section and the *x* axis providing the position along the horizontal segment. Initially, the column is not subjected to any kind of load on the axial direction; consequently, it is not buckled and rests on the lowest portion of the well, such as in (a). When a compressive force high enough to cause buckling is acting on the column, it suffers simultaneously axial and angular displacements. It is important to observe that the column final position is a consequence of both the axial contraction u_a and the contraction caused by bending u_b, as seen in (b). The axial displacement is defined as positive on the positive direction of the *x* axis, while the angular displacement is defined positive on the counterclockwise direction, starting from the *z* axis. Thus, to describe the column dynamic behavior, it is necessary to understand how the axial and angular displacements occur as a function of time.

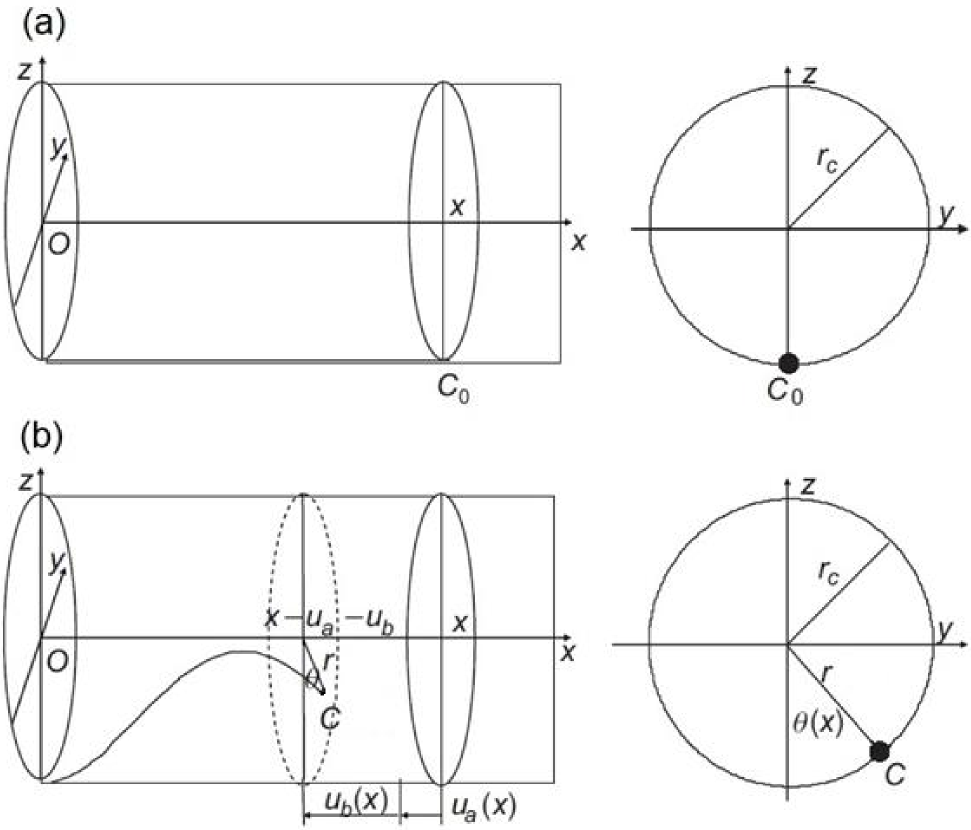

Figure 3.2: (a) Column resting position when it is not subjected to compressive loads. (b) Column buckled position caused by compressive loads (adapted from Gao & Miska, 2009).

The model presented on this section, as said before, is the same from Gao & Miska (2010a). The idea behind using this model, despite it neglecting the friction force, is to do an initial observation regarding the effects of buckling on the column dynamic behavior, especially the contact force between the column and the well.

Finally, it is worth pointing that despite the text referring to the internal cylindrical element as "column" and the external cylindrical element as "well", the model is not restricted to only this scenario. As mentioned before, several operations involve the use of columns inside another column, such as lowering a tubing string inside a cased hole; a coiled tubing string inside a tubing string; or a sand screen using a work string inside an open hole. Therefore, usage of terms "column" and "well" is only to improve understanding. Lastly, the model by Gao & Miska (2010a) was developed for drill strings, which rotate while moving forward. This does not happen in completion scenarios; however, the effect of rotation is kept, thus the model can still be of use for analyzing drill strings.

3.1.1. Model for tripping in

During tripping in, the column will be subjected to compressive loads which will cause buckling. Therefore, the point C_0 from Figure 3.2(a) which is initially on the lower portion of the well with coordinates *(x, 0, -r)* will displace to the position of point *C* from Figure 3.2(b) with coordinates $(x + ux, r*sin\theta, -r*cos\theta)$ on a certain time t. To keep the sign convention consistent, the displacement u_x is added up, despite being negative since it is a contraction. This displacement includes the effects of axial contraction u_a and bending contraction u_b, as explained beforehand. The coordinate x is the initial position along the horizontal segment of well, the coordinate θ is the angle defined between the z axis and the normal vector $\hat{p}$ and the distance r is the difference between the well radius and the column radius – also known as clearance.

The step-by-step deduction can be seen on Appendix A. Here, only the final motion equations will be shown:

$$EA\frac{\partial^2 u_x}{\partial x^2} - m_p\frac{\partial^2 u_x}{\partial t^2} + EAr^2\frac{\partial \theta}{\partial x}\frac{\partial^2 \theta}{\partial x^2} = 0 \tag{1}$$

$$
\begin{aligned}
EIr\left[\frac{\partial^4\theta}{\partial x^4} - 6\left(\frac{\partial\theta}{\partial x}\right)^2\frac{\partial^2\theta}{\partial x^2}\right] \\
- EAr\left[\frac{\partial u_x}{\partial x}\frac{\partial^2\theta}{\partial x^2} + \frac{\partial^2 u_x}{\partial x^2}\frac{\partial\theta}{\partial x} + \frac{3}{2}r^2\frac{\partial^2\theta}{\partial x^2}\left(\frac{\partial\theta}{\partial x}\right)^2\right] \\
- I_p r\omega\left[2\frac{\partial^2\theta}{\partial x\partial t}\frac{\partial\theta}{\partial x} + \frac{\partial\theta}{\partial t}\frac{\partial^2\theta}{\partial x^2}\right] + m_p g\sin\theta \\
+ m_p r\frac{\partial^2\theta}{\partial t^2} = 0
\end{aligned} \tag{2}
$$

$$
F_x(x,t) = -EA\frac{\partial u_x}{\partial x} - \frac{1}{2}EAr^2\left(\frac{\partial\theta}{\partial x}\right)^2 \tag{3}
$$

$$
\begin{aligned}
N(x,t) = -EIr\left[\left(\frac{\partial\theta}{\partial x}\right)^4 - 3\left(\frac{\partial^2\theta}{\partial x^2}\right)^2 - 4\frac{\partial^3\theta}{\partial x^3}\frac{\partial\theta}{\partial x}\right] \\
- EAr\left[\frac{\partial u_x}{\partial x}\left(\frac{\partial\theta}{\partial x}\right)^2 + \frac{1}{2}r^2\left(\frac{\partial\theta}{\partial x}\right)^4\right] \\
+ I_p r\omega\left[\frac{\partial^3\theta}{\partial x^2\partial t} - \frac{\partial\theta}{\partial t}\left(\frac{\partial\theta}{\partial x}\right)^2\right] + m_p g\cos\theta \\
+ m_p r\left(\frac{\partial\theta}{\partial t}\right)^2
\end{aligned} \tag{4}
$$

The final problem consists of four equations to determine four unknowns: u_x, θ, F_x and N.

3.1.2. Model for tripping out

For the problem of tripping out, the equations previously presented are severely simplified. This happens because the column does not suffer buckling and thus remains in contact with the lowest portion of the well for its whole length and for the whole time. During tripping out, the point C_0 from Figure 3.2(a) displaces itself from $(x, 0, -r)$ to $(x + u_x, 0, -r)$. Once again, the full deduction is shown on Appendix A. Here are the final motion equations:

$$
EA\frac{\partial^2 u_x}{\partial x^2} - m_p\frac{\partial^2 u_x}{\partial t^2} = 0 \tag{5}
$$

$$
F_x(x,t) = -EA\frac{\partial u_x}{\partial x} \tag{6}
$$

$$N(x,t) = -m_p r \frac{\partial^3 u_x}{\partial x \partial t^2} + m_p g \tag{7}$$

The final problem is now only three equations for three unknowns: u_x, F_x and N.

3.1.3. Solution for tripping in

Due to the complexity of the problem of tripping in, an analytical solution is not possible. Therefore, a numerical solution using the finite differences method will be used. The steps for discretizing the problem are shown on Appendix A, resulting in the following equations:

$$\begin{aligned} U_{i,j+1} = 2U_{i,j} - U_{i,j-1} + \frac{EA\Delta t^2}{m_p \Delta x^2}\left(U_{i+1,j} - 2U_{i,j} + U_{i-1,j}\right) \\ + \frac{EAr^2\Delta t^2}{2m_p\Delta x^3}\left(\theta_{i+1,j} - \theta_{i-1,j}\right)\left(\theta_{i+1,j} - 2\theta_{i,j} + \theta_{i-1,j}\right) \end{aligned} \tag{8}$$

$$\begin{aligned} &\frac{I_p r\omega\left(\theta_{i+1,j} - \theta_{i-1,j}\right)}{4\Delta x^2 \Delta t}\theta_{i+1,j+1} \\ &+ \left[\frac{I_p r\omega\left(\theta_{i+1,j} - 2\theta_{i,j} + \theta_{i-1,j}\right)}{2\Delta x^2\Delta t} - \frac{m_p r}{\Delta t^2}\right]\theta_{i,j+1} \\ &- \frac{I_p r\omega\left(\theta_{i+1,j} - \theta_{i-1,j}\right)}{4\Delta x^2\Delta t}\theta_{i-1,j+1} \\ &= \frac{I_p r\omega\left(\theta_{i+1,j} - 2\theta_{i,j} + \theta_{i-1,j}\right)}{2\Delta x^2\Delta t}\theta_{i,j-1} \\ &- \frac{I_p r\omega\left(\theta_{i+1,j} - \theta_{i-1,j}\right)}{4\Delta x^2\Delta t}\left(-\theta_{i+1,j-1} + \theta_{i-1,j-1}\right) \\ &+ \frac{m_p r}{\Delta t^2}\left(-2\theta_{i,j} + \theta_{i,j-1}\right) \\ &+ \frac{EIr}{\Delta x^4}\Big[\left(\theta_{i+2,j} - 4\theta_{i+1,j} + 6\theta_{i,j} - 4\theta_{i-1,j} + \theta_{i-2,j}\right) \\ &- \frac{3}{2}\left(\theta_{i+1,j} - \theta_{i-1,j}\right)^2\left(\theta_{i+1,j} - 2\theta_{i,j} + \theta_{i-1,j}\right)\Big] \\ &- \frac{EAr}{2\Delta x^3}\Big[\left(U_{i+1,j} - U_{i-1,j}\right)\left(\theta_{i+1,j} - 2\theta_{i,j} + \theta_{i-1,j}\right) \\ &+ \left(U_{i+1,j} - 2U_{i,j} + U_{i-1,j}\right)\left(\theta_{i+1,j} - \theta_{i-1,j}\right) \\ &+ \frac{3r^2}{4\Delta x}\left(\theta_{i+1,j} - 2\theta_{i,j} + \theta_{i-1,j}\right)\left(\theta_{i+1,j} - \theta_{i-1,j}\right)^2\Big] \\ &+ m_p g \sin\theta_{i,j} \end{aligned} \tag{9}$$

$$F_{i,j} = -\frac{EA}{2\Delta x}\left[\left(U_{i+1,j} - U_{i-1,j}\right) + \frac{r^2}{4\Delta x}\left(\theta_{i+1,j} - \theta_{i-1,j}\right)^2\right] \tag{10}$$

$$\begin{aligned} N_{i,j} = -\frac{EIr}{\Delta x^4}\Bigg[&\frac{1}{16}\left(\theta_{i+1,j} - \theta_{i-1,j}\right)^4 - 3\left(\theta_{i+1,j} - 2\theta_{i,j} + \theta_{i-1,j}\right)^2 \\ &- \left(\theta_{i+2,j} - 2\theta_{i+1,j} + 2\theta_{i-1,j} - \theta_{i-2,j}\right)\left(\theta_{i+1,j} \right. \\ &\left. - \theta_{i-1,j}\right)\Bigg] \\ &- \frac{EAr}{8\Delta x^3}\left[\left(U_{i+1,j} - U_{i-1,j}\right)\left(\theta_{i+1,j} - \theta_{i-1,j}\right)^2 \right. \\ &\left. + \frac{r^2}{4\Delta x}\left(\theta_{i+1,j} - \theta_{i-1,j}\right)^4\right] \\ &+ \frac{I_p r\omega}{2\Delta x^2 \Delta t}\left[\left(\theta_{i+1,j} - 2\theta_{i,j} + \theta_{i-1,j} - \theta_{i+1,j-2} \right.\right. \\ &\left. + 2\theta_{i,j-2} - \theta_{i-1,j-2}\right) \\ &\left. - \frac{1}{4}\left(\theta_{i,j} - \theta_{i,j-2}\right)\left(\theta_{i+1,j} - \theta_{i-1,j}\right)^2\right] + m_p g \cos\theta_{i,j} \\ &+ \frac{m_p r}{4\Delta t^2}\left(\theta_{i,j} - \theta_{i,j-2}\right)^2 \end{aligned} \tag{11}$$

Where subscript *i* denotes the space and subscript *j* represents time. On Eqs. (8) and (9), the terms with subscript *j + 1* were isolated, which represent the unknowns of the problem, as long as the values for intervals *j* and *j – 1* are known. Meanwhile, on Eqs. (10) and (11), the time derivatives were discretized using the backward difference to facilitate their solutions. For the axial displacement u_x, it is easy to note that the value for each point *i* can be found independently of adjacent points *i + 1* and *i – 1*, thus eliminating the need of solving a system. However, for the angular displacement θ, the value at each point *i* is dependent of the adjacent points *i + 1* e *i – 1*, thus leading to a linear system of equations. It is worth pointing that despite the problem being uncoupled, the two displacements must march together in time. This happens because in order to calculate the axial displacement at interval *j + 1* the angular displacement at interval *j* is needed and vice-versa. Figure 3.3 shows the point mesh needed for solving Eqs. (8) and (9). The level *j + 1*, marked in white, are unknowns that must be calculated, while the levels *j* and *j – 1*, marked in black, represent variables already known.

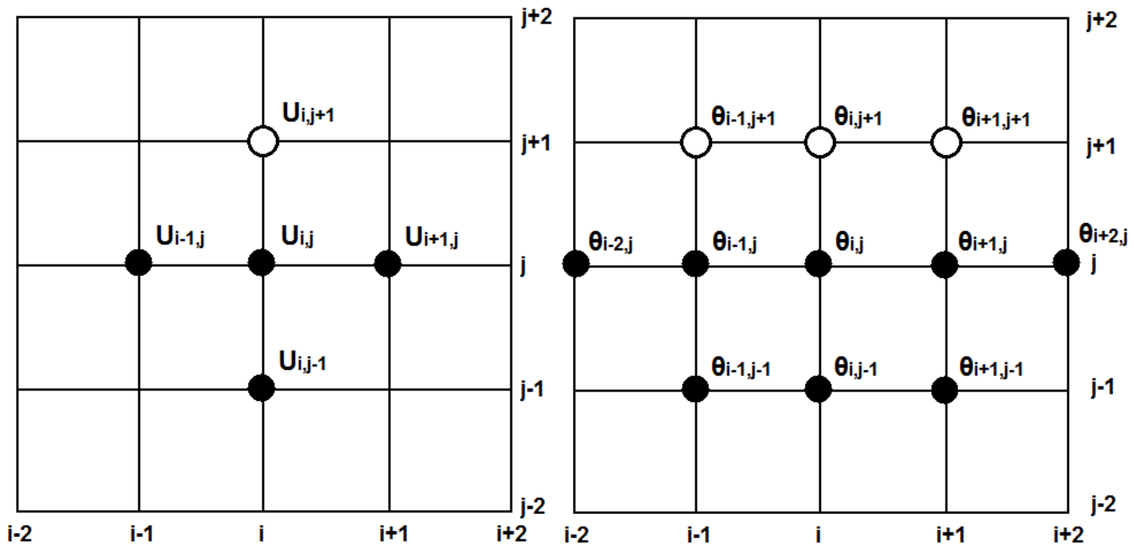

Figure 3.3: Point mesh for variables U and θ.

The spatial discretization divides the column into $N + 1$ points, with points 0 and N being the extremities. Meanwhile, the time discretization starts in $j = 1$, with $j = 1$ being the initial condition for the displacement and $j = 2$ being the initial condition for the velocity. Therefore, the equations shown previously are valid for $j = 3$. The mesh for the spatial discretization can be seen on Figure 3.4. It is important to note that besides dividing the column into $N + 1$ points, from $i = 0$ up to $i = N$, artificial points $i = -1$ and $i = N + 1$ must be created to discretize the boundary conditions.

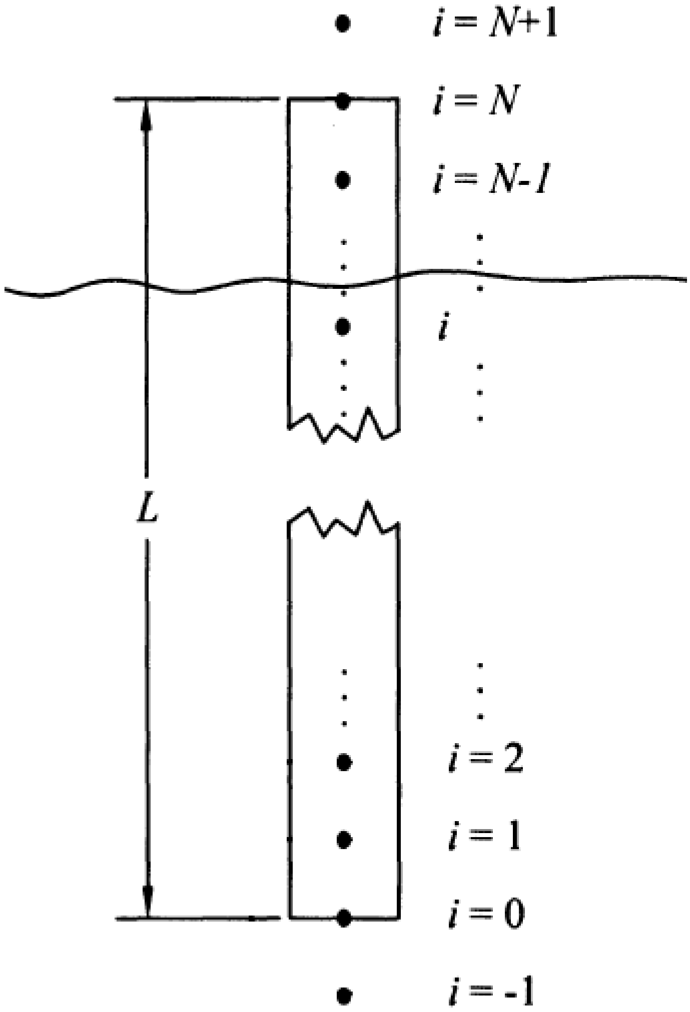

Figure 3.4: Discretization of a column of total length L into $N + 1$ points (adapted from Han & Benaroya, 2002).

More details regarding the method can be seen on Appendix B, including a discussion regarding the algorithm stability. Remains to be defined the initial conditions and the boundary conditions of the problem, so then the equations for points $i = 0$ and $i = N$ and for points $j = 1$ and $j = 2$ can be found. Considering that the column is fixed at $x = 0$ but free to move in $x = L$, the boundary conditions will be given by:

$$u(0) = 0 \tag{12}$$

$$\left.\frac{\partial u}{\partial x}\right|_{x=L} + \frac{r^2}{2}\left(\left.\frac{\partial \theta}{\partial x}\right|_{x=L}\right)^2 = 0 \tag{13}$$

$$\theta(0) = 0 \tag{14}$$

$$\left.\frac{\partial^2\theta}{\partial x^2}\right|_{x=0} = 0 \tag{15}$$

$$\left.\frac{\partial^2\theta}{\partial x^2}\right|_{x=L} = 0 \tag{16}$$

$$\left.\frac{\partial^3\theta}{\partial x^3}\right|_{x=L} = 0 \tag{17}$$

The discretizations of the boundary conditions can be seen on Appendix A. Now for the initial conditions, an initial displacement is imposed for u_x and θ and the initial velocities are considered zero. A small value is given to θ for convergence purposes. The discretizations can be seen on Appendix A as well.

$$u(x,0) = U_0\, sin\left(\frac{\pi x}{L}\right) \tag{18}$$

$$\frac{\partial u(x,0)}{\partial t} = 0 \tag{19}$$

$$\theta(x,0) = 0.1 \tag{20}$$

$$\frac{\partial \theta(x,0)}{\partial t} = 0 \tag{21}$$

3.1.4. Solution for tripping out

Differently from the tripping in case, the equations for tripping out the column are simpler and possess an analytical solution. However, only the numerical solution – which will be the one used – is shown here. The full details on both solutions can be seen on Appendix A. The discretized equations will be:

$$U_{i,j+1} = 2U_{i,j} - U_{i,j-1} + \frac{EA\Delta t^2}{m_p\Delta x^2}\left(U_{i+1,j} - 2U_{i,j} + U_{i-1,j}\right) \tag{22}$$

$$F_{i,j} = -\frac{EA}{2\Delta x}\left(U_{i+1,j} - U_{i-1,j}\right) \tag{23}$$

$$N_{i,j} = -\frac{m_p r}{2\Delta x \Delta t^2}\big(U_{i+1,j} - U_{i-1,j} - 2U_{i+1,j-1} + 2U_{i-1,j-1} + U_{i+1,j-2} - U_{i-1,j-2}\big) + m_p g \quad (24)$$

As in the tripping in case, first Eq. (23) is solved to find and the axial displacements and only then Eqs. (24) and (25) are solved to find the axial and normal forces. Remains to be defined the boundary and initial conditions. As said before, the column is fixed in $x = 0$ and free on $x = L$. The boundary conditions will then be given by:

$$u(0) = 0 \quad (25)$$

$$\left.\frac{\partial u}{\partial x}\right|_{x=L} = 0 \quad (26)$$

And lastly the initial conditions, which will be the same from the tripping in case:

$$u(x,0) = U_0\, sin\left(\frac{\pi x}{L}\right) \quad (27)$$

$$\frac{\partial u(x,0)}{\partial t} = 0 \quad (28)$$

The discretizations can be seen on Appendix A.

3.2. Model II – Column with friction

The effect of the friction force on the column buckling problem had already been studied previously on the literature (Mitchell, 1986; Mitchell, 1996b; Mitchell, 2007; and Gao & Miska, 2009). However, in none of said works the friction force was considered as being part of a dynamic problem, but only for static cases. The objective here is to unify the ideas from Gao & Miska (2009) – whose model is static and has friction – with the ideas from Gao & Miska (2010a) – whose model is dynamic but without friction.

The friction force, differently from other external forces such as the weight and normal contact, does not have a fixed direction as time passes. Its direction is always opposite to the direction of the velocity; since the velocity can change its direction as time passes, the direction of the friction force will change as well. Besides, since the column is free to displace angularly inside the well during its tripping in, two possible scenarios can occur: the column can roll without slipping or roll while slipping. On the first case, the friction force is static – since there is no relative motion between the column and the wellbore – and its modulus can be any value from zero up to the maximum static friction – in which case the column starts slipping. Meanwhile, on the second case, the friction force is dynamic, because there is relative motion between the column and the wellbore; therefore, the friction force has a fixed modulus and can be obtained if the dynamic friction coefficient between the two surfaces and the normal contact force is known. On the present work, it will be assumed that the column rolls while slipping. This hypothesis allows writing the friction force as a function of the normal contact force, thus reducing the number of variables – if the column could roll without slipping, the friction force would be an extra variable, since it would not be written as a function of the normal contact force.

Finally, remains to be defined the direction of the friction force. Both during tripping in and tripping out, the friction force will possess a component on $\hat{\imath}$, whose sign will depend on the direction of the axial velocity $\partial u_x/\partial t$. However, during tripping in, the column also suffers an angular displacement, which will result into a lateral friction on the $\hat{q}$ direction, as shown on Figure 3.5, whose sign will depend on the angular velocity $\partial\theta/\partial t$; this component is not present during tripping out.

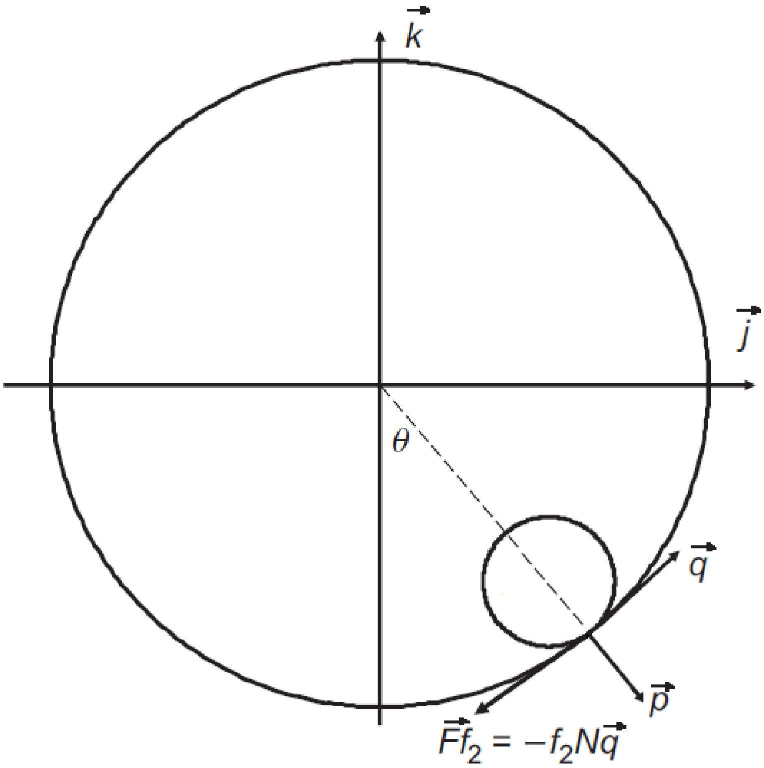

Figure 3.5: Lateral friction caused by the column angular motion inside the well during its tripping in (adapted from Gao & Miska, 2009).

Based on these hypotheses, it is possible to characterize the friction force and then repeat the procedure from the previous section to obtain new equations of motion for the problem. This will be done for both tripping in and tripping out.

3.2.1. Model for tripping in

Once again, the full deduction is left on Appendix A. The friction force will be given by:

$$\vec{F}_f(x,t) = -\frac{fNdx}{\sqrt{\left(\frac{\partial u_x}{\partial t}\right)^2 + r^2\left(\frac{\partial \theta}{\partial t}\right)^2}}\left[sgn\left(\frac{\partial u_x}{\partial t}\right)\left|\frac{\partial u_x}{\partial t}\right|\hat{\imath} + sgn\left(\frac{\partial \theta}{\partial t}\right) r\left|\frac{\partial \theta}{\partial t}\right|\hat{q}\right] \tag{29}$$

The friction force will affect only the equations for the displacements, which will now be given by:

$$EA\frac{\partial^2 u_x}{\partial x^2} - m_p\frac{\partial^2 u_x}{\partial t^2} + EAr^2\frac{\partial\theta}{\partial x}\frac{\partial^2\theta}{\partial x^2} - \frac{sgn\left(\frac{\partial u_x}{\partial t}\right) f \left|\frac{\partial u_x}{\partial t}\right|}{\sqrt{\left(\frac{\partial u_x}{\partial t}\right)^2 + r^2\left(\frac{\partial\theta}{\partial t}\right)^2}}\left\{-EIr\left[\left(\frac{\partial\theta}{\partial x}\right)^4 - 3\left(\frac{\partial^2\theta}{\partial x^2}\right)^2 - 4\frac{\partial^3\theta}{\partial x^3}\frac{\partial\theta}{\partial x}\right] - EAr\left[\frac{\partial u_x}{\partial x}\left(\frac{\partial\theta}{\partial x}\right)^2 + \frac{1}{2}r^2\left(\frac{\partial\theta}{\partial x}\right)^4\right] + I_p r\omega\left[\frac{\partial^3\theta}{\partial x^2\partial t} - \frac{\partial\theta}{\partial t}\left(\frac{\partial\theta}{\partial x}\right)^2\right] + m_p g\cos\theta + m_p r\left(\frac{\partial\theta}{\partial t}\right)^2\right\} = 0 \tag{30}$$

$$EIr\left[\frac{\partial^4\theta}{\partial x^4} - 6\left(\frac{\partial\theta}{\partial x}\right)^2\frac{\partial^2\theta}{\partial x^2}\right] - EAr\left[\frac{\partial u_x}{\partial x}\frac{\partial^2\theta}{\partial x^2} + \frac{\partial^2 u_x}{\partial x^2}\frac{\partial\theta}{\partial x} + \frac{3}{2}r^2\frac{\partial^2\theta}{\partial x^2}\left(\frac{\partial\theta}{\partial x}\right)^2\right] - I_p r\omega\left[2\frac{\partial^2\theta}{\partial x\partial t}\frac{\partial\theta}{\partial x} + \frac{\partial\theta}{\partial t}\frac{\partial^2\theta}{\partial x^2}\right] + m_p g\sin\theta + m_p r\frac{\partial^2\theta}{\partial t^2} + \frac{sgn\left(\frac{\partial\theta}{\partial t}\right) fr \left|\frac{\partial\theta}{\partial t}\right|}{\sqrt{\left(\frac{\partial u_x}{\partial t}\right)^2 + r^2\left(\frac{\partial\theta}{\partial t}\right)^2}}\left\{-EIr\left[\left(\frac{\partial\theta}{\partial x}\right)^4 - 3\left(\frac{\partial^2\theta}{\partial x^2}\right)^2 - 4\frac{\partial^3\theta}{\partial x^3}\frac{\partial\theta}{\partial x}\right] - EAr\left[\frac{\partial u_x}{\partial x}\left(\frac{\partial\theta}{\partial x}\right)^2 + \frac{1}{2}r^2\left(\frac{\partial\theta}{\partial x}\right)^4\right] + I_p r\omega\left[\frac{\partial^3\theta}{\partial x^2\partial t} - \frac{\partial\theta}{\partial t}\left(\frac{\partial\theta}{\partial x}\right)^2\right] + m_p g\cos\theta + m_p r\left(\frac{\partial\theta}{\partial t}\right)^2\right\} = 0 \tag{31}$$

Eqs. (30) and (31) allow calculating the axial displacement u_x and angular displacement θ. Knowing the displacements, the forces F_x and N can then be calculated as well.

3.2.2. Model for tripping out

As in the model without friction, the motion equations become simplified for the tripping out problem. The friction force, in this case, is given by:

$$\vec{F}_f(x,t) = -sgn\left(\frac{\partial u_x}{\partial t}\right) fNdx\hat{\imath} \tag{32}$$

It is interesting to point that the $\hat{\imath}$ component for the friction force during tripping out, given by Eq. (32) is different from the $\hat{\imath}$ component for the friction force during tripping in, given by Eq. (29). This suggests that the friction force in the axial direction is, indeed, different during tripping in and tripping out the column. The final motion equation will be:

$$EA\frac{\partial^2 u_x}{\partial x^2} - m_p\frac{\partial^2 u_x}{\partial t^2} - sgn\left(\frac{\partial u_x}{\partial t}\right) f\left[-m_p r\frac{\partial^3 u_x}{\partial x \partial t^2} + m_p g\right] = 0 \tag{33}$$

Eq. (33) allows calculating the axial displacement u_x. After that, the forces F_x and N can be calculated.

3.2.3. Solution for tripping in

As in the previous case, the solution here must be numeric. The final discretizations will be:

$$
\begin{aligned}
&U_{i,j+1} \\
&= 2U_{i,j} - U_{i,j-1} + \frac{EA\Delta t^2}{m_p \Delta x^2}\left(U_{i+1,j} - 2U_{i,j} + U_{i-1,j}\right) \\
&+ \frac{EAr^2\Delta t^2}{2m_p\Delta x^3}\left(\theta_{i+1,j} - \theta_{i-1,j}\right)\left(\theta_{i+1,j} - 2\theta_{i,j} + \theta_{i-1,j}\right) \\
&- \frac{sgn\left(U_{i,j} - U_{i,j-1}\right) f\Delta t\left|U_{i,j} - U_{i,j-2}\right|}{2m_p\sqrt{\left(\frac{U_{i,j}-U_{i,j-2}}{2\Delta t}\right)^2 + r^2\left(\frac{\theta_{i,j}-\theta_{i,j-2}}{2\Delta t}\right)^2}}\left\{-\frac{EIr}{\Delta x^4}\left[\frac{1}{16}\left(\theta_{i+1,j} - \theta_{i-1,j}\right)^4\right.\right. \\
&- 3\left(\theta_{i+1,j} - 2\theta_{i,j} + \theta_{i-1,j}\right)^2 \\
&\left. - \left(\theta_{i+2,j} - 2\theta_{i+1,j} + 2\theta_{i-1,j} - \theta_{i-2,j}\right)\left(\theta_{i+1,j} - \theta_{i-1,j}\right)\right] \\
&- \frac{EAr}{8\Delta x^3}\left[\left(U_{i+1,j} - U_{i-1,j}\right)\left(\theta_{i+1,j} - \theta_{i-1,j}\right)^2\right. \\
&\left. + \frac{r^2}{4\Delta x}\left(\theta_{i+1,j} - \theta_{i-1,j}\right)^4\right] \\
&+ \frac{I_p r\omega}{2\Delta x^2\Delta t}\left[\left(\theta_{i+1,j} - 2\theta_{i,j} + \theta_{i-1,j} - \theta_{i+1,j-2} + 2\theta_{i,j-2} - \theta_{i-1,j-2}\right)\right. \\
&\left. - \frac{1}{4}\left(\theta_{i,j} - \theta_{i,j-2}\right)\left(\theta_{i+1,j} - \theta_{i-1,j}\right)^2\right] + m_p g \cos\theta_{i,j} \\
&\left. + \frac{m_p r}{4\Delta t^2}\left(\theta_{i,j} - \theta_{i,j-2}\right)^2\right\}
\end{aligned}
\tag{34}
$$

$$
\begin{aligned}
&\frac{I_p r\omega\left(\theta_{i+1,j}-\theta_{i-1,j}\right)}{4\Delta x^2\Delta t}\theta_{i+1,j+1} \\
&+\left[\frac{I_p r\omega\left(\theta_{i+1,j}-2\theta_{i,j}+\theta_{i-1,j}\right)}{2\Delta x^2\Delta t}-\frac{m_p r}{\Delta t^2}\right]\theta_{i,j+1} \\
&-\frac{I_p r\omega\left(\theta_{i+1,j}-\theta_{i-1,j}\right)}{4\Delta x^2\Delta t}\theta_{i-1,j+1} \\
&=\frac{I_p r\omega\left(\theta_{i+1,j}-2\theta_{i,j}+\theta_{i-1,j}\right)}{2\Delta x^2\Delta t}\theta_{i,j-1} \\
&-\frac{I_p r\omega\left(\theta_{i+1,j}-\theta_{i-1,j}\right)}{4\Delta x^2\Delta t}\left(-\theta_{i+1,j-1}+\theta_{i-1,j-1}\right) \\
&+\frac{m_p r}{\Delta t^2}\left(-2\theta_{i,j}+\theta_{i,j-1}\right) \\
&+\frac{EIr}{\Delta x^4}\left[\left(\theta_{i+2,j}-4\theta_{i+1,j}+6\theta_{i,j}-4\theta_{i-1,j}+\theta_{i-2,j}\right)\right. \\
&\left.-\frac{3}{2}\left(\theta_{i+1,j}-\theta_{i-1,j}\right)^2\left(\theta_{i+1,j}-2\theta_{i,j}+\theta_{i-1,j}\right)\right] \\
&-\frac{EAr}{2\Delta x^3}\left[\left(U_{i+1,j}-U_{i-1,j}\right)\left(\theta_{i+1,j}-2\theta_{i,j}+\theta_{i-1,j}\right)\right. \\
&+\left(U_{i+1,j}-2U_{i,j}+U_{i-1,j}\right)\left(\theta_{i+1,j}-\theta_{i-1,j}\right) \\
&\left.+\frac{3r^2}{4\Delta x}\left(\theta_{i+1,j}-2\theta_{i,j}+\theta_{i-1,j}\right)\left(\theta_{i+1,j}-\theta_{i-1,j}\right)^2\right]+m_p g\sin\theta_{i,j} \\
&+\frac{sgn\left(\theta_{i,j}-\theta_{i,j-1}\right)fr\left|\theta_{i,j}-\theta_{i,j-2}\right|}{2\Delta t\sqrt{\left(\frac{U_{i,j}-U_{i,j-2}}{2\Delta t}\right)^2+r^2\left(\frac{\theta_{i,j}-\theta_{i,j-2}}{2\Delta t}\right)^2}}\left\{-\frac{EIr}{\Delta x^4}\left[\frac{1}{16}\left(\theta_{i+1,j}-\theta_{i-1,j}\right)^4\right.\right. \\
&-3\left(\theta_{i+1,j}-2\theta_{i,j}+\theta_{i-1,j}\right)^2 \\
&\left.-\left(\theta_{i+2,j}-2\theta_{i+1,j}+2\theta_{i-1,j}-\theta_{i-2,j}\right)\left(\theta_{i+1,j}-\theta_{i-1,j}\right)\right] \\
&-\frac{EAr}{8\Delta x^3}\left[\left(U_{i+1,j}-U_{i-1,j}\right)\left(\theta_{i+1,j}-\theta_{i-1,j}\right)^2\right. \\
&\left.+\frac{r^2}{4\Delta x}\left(\theta_{i+1,j}-\theta_{i-1,j}\right)^4\right] \\
&+\frac{I_p r\omega}{2\Delta x^2\Delta t}\left[\left(\theta_{i+1,j}-2\theta_{i,j}+\theta_{i-1,j}-\theta_{i+1,j-2}+2\theta_{i,j-2}-\theta_{i-1,j-2}\right)\right. \\
&\left.-\frac{1}{4}\left(\theta_{i,j}-\theta_{i,j-2}\right)\left(\theta_{i+1,j}-\theta_{i-1,j}\right)^2\right]+m_p g\cos\theta_{i,j} \\
&\left.+\frac{m_p r}{4\Delta t^2}\left(\theta_{i,j}-\theta_{i,j-2}\right)^2\right\}
\end{aligned} \tag{35}
$$

$$
F_{i,j}=-\frac{EA}{2\Delta x}\left[\left(U_{i+1,j}-U_{i-1,j}\right)+\frac{r^2}{4\Delta x}\left(\theta_{i+1,j}-\theta_{i-1,j}\right)^2\right] \tag{36}
$$

$$
\begin{aligned}
N_{i,j} = -\frac{EIr}{\Delta x^4}\Bigg[&\frac{1}{16}\left(\theta_{i+1,j}-\theta_{i-1,j}\right)^4 - 3\left(\theta_{i+1,j}-2\theta_{i,j}+\theta_{i-1,j}\right)^2 \\
&- \left(\theta_{i+2,j}-2\theta_{i+1,j}+2\theta_{i-1,j}-\theta_{i-2,j}\right)\left(\theta_{i+1,j} - \theta_{i-1,j}\right)\Bigg] \\
&- \frac{EAr}{8\Delta x^3}\left[\left(U_{i+1,j}-U_{i-1,j}\right)\left(\theta_{i+1,j}-\theta_{i-1,j}\right)^2 + \frac{r^2}{4\Delta x}\left(\theta_{i+1,j}-\theta_{i-1,j}\right)^4\right] \\
&+ \frac{I_p r\omega}{2\Delta x^2 \Delta t}\Bigg[\left(\theta_{i+1,j}-2\theta_{i,j}+\theta_{i-1,j}-\theta_{i+1,j-2} + 2\theta_{i,j-2}-\theta_{i-1,j-2}\right) \\
&- \frac{1}{4}\left(\theta_{i,j}-\theta_{i,j-2}\right)\left(\theta_{i+1,j}-\theta_{i-1,j}\right)^2\Bigg] + m_p g \cos\theta_{i,j} \\
&+ \frac{m_p r}{4\Delta t^2}\left(\theta_{i,j}-\theta_{i,j-2}\right)^2
\end{aligned}
\tag{37}
$$

The boundary conditions and initial conditions are the same given for the previous model and their discretizations can be seen on Appendix A.

3.2.4. Solution for tripping out

Differently from the model without friction, this time there is no analytical solution if friction is included. The final discretizations will be:

$$
\begin{aligned}
U_{i,j+1} = 2U_{i,j} - U_{i,j-1} &+ \frac{EA\Delta t^2}{m_p \Delta x^2}\left(U_{i+1,j}-2U_{i,j}+U_{i-1,j}\right) \\
&- sgn\left(U_{i,j}-U_{i,j-1}\right) f \Bigg[-\frac{r}{2\Delta x}\left(U_{i+1,j}-U_{i-1,j} - 2U_{i+1,j-1}+2U_{i-1,j-1}+U_{i+1,j-2}-U_{i-1,j-2}\right) \\
&+ g\Delta t^2\Bigg]
\end{aligned}
\tag{38}
$$

$$
F_{i,j} = -\frac{EA}{2\Delta x}\left(U_{i+1,j}-U_{i-1,j}\right) \tag{39}
$$

$$
\begin{aligned}
N_{i,j} = -\frac{m_p r}{2\Delta x \Delta t^2}&\left(U_{i+1,j}-U_{i-1,j}-2U_{i+1,j-1}+2U_{i-1,j-1}+U_{i+1,j-2}\right. \\
&\left.- U_{i-1,j-2}\right) + m_p g
\end{aligned}
\tag{40}
$$

The boundary conditions and initial conditions are the same given for the previous model and their discretizations can be seen on Appendix A.

3.3. Model III – Slant wells

The next step for modeling the column is to consider slant segments of well; up to this point, the model could only be applied to horizontal segments. In practice, even horizontal wells start its trajectory as vertical and have to gain angle before reaching the horizontal position. Also, there are types of wells that do not even have horizontal segments, such as slant and S wells.

Figure 3.6 shows a scheme of a slant segment of well. In (a), the segment is horizontal as in the previous section, while in (b) the segment has an inclination with angle α in respect to the vertical direction. Therefore, the model proposed on this section is a generalization of the previous one. The best way to characterize this problem is to keep using the coordinate system *xyz*, but now rotated to follow the well inclination. Observing Figure 3.6(b), it can be noted that the weight is different in this case; it now possesses a component on the x axis besides the plane *yz*; meanwhile, the normal contact force and the friction force still have the same components.

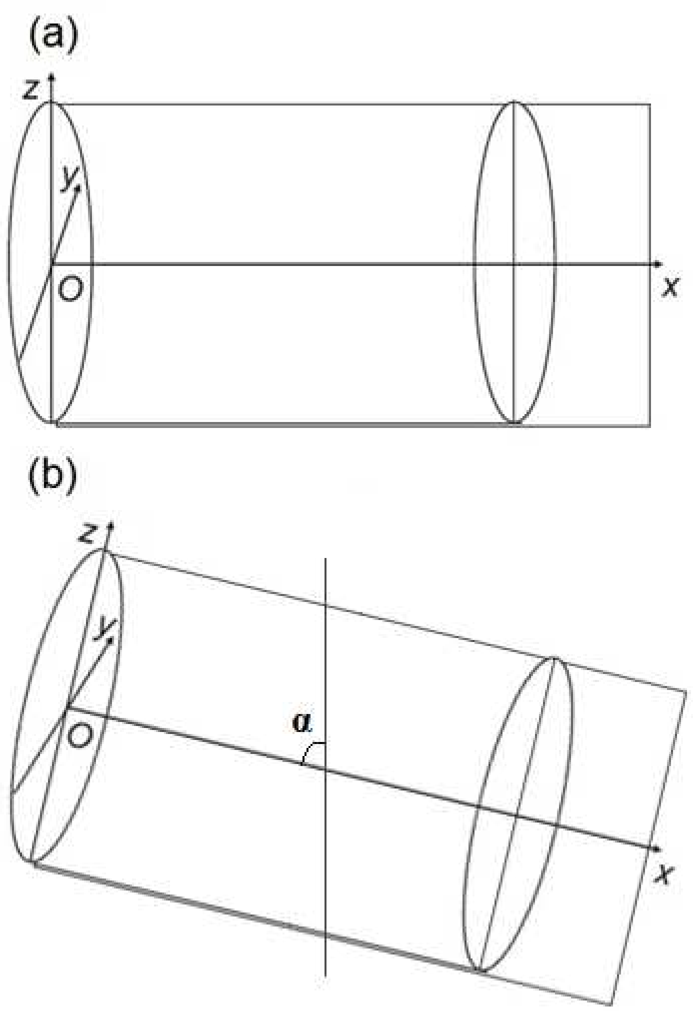

Figure 3.6: (a) Horizontal and (b) slant segment of well. The angle α defines the inclination in respect to the vertical direction (adapted from Gao & Miska, 2009).

It is important to note that the previous hypotheses are still valid, which means that the column still remains always in contact with the wellbore, even if the well segment is not horizontal anymore. The implications of this hypothesis will be tested further on.

3.3.1. Model for tripping in

The full deduction can be seen on Appendix A. The final motion equations will be:

$$
\begin{aligned}
EA\frac{\partial^2 u_x}{\partial x^2} - m_p\frac{\partial^2 u_x}{\partial t^2} + EAr^2\frac{\partial\theta}{\partial x}\frac{\partial^2\theta}{\partial x^2} \\
- \frac{sgn\left(\frac{\partial u_x}{\partial t}\right) f\left|\frac{\partial u_x}{\partial t}\right|}{\sqrt{\left(\frac{\partial u_x}{\partial t}\right)^2 + r^2\left(\frac{\partial\theta}{\partial t}\right)^2}} \Bigg\{ -EIr\left[\left(\frac{\partial\theta}{\partial x}\right)^4 - 3\left(\frac{\partial^2\theta}{\partial x^2}\right)^2\right. \\
\left. - 4\frac{\partial^3\theta}{\partial x^3}\frac{\partial\theta}{\partial x}\right] - EAr\left[\frac{\partial u_x}{\partial x}\left(\frac{\partial\theta}{\partial x}\right)^2 + \frac{1}{2}r^2\left(\frac{\partial\theta}{\partial x}\right)^4\right] \\
+ I_p r\omega\left[\frac{\partial^3\theta}{\partial x^2\partial t} - \frac{\partial\theta}{\partial t}\left(\frac{\partial\theta}{\partial x}\right)^2\right] + m_p g\sin\alpha\cos\theta \\
+ m_p r\left(\frac{\partial\theta}{\partial t}\right)^2\Bigg\} + m_p g\cos\alpha = 0
\end{aligned}
\tag{41}
$$

$$
\begin{aligned}
EIr\left[\frac{\partial^4\theta}{\partial x^4} - 6\left(\frac{\partial\theta}{\partial x}\right)^2\frac{\partial^2\theta}{\partial x^2}\right] \\
- EAr\left[\frac{\partial u_x}{\partial x}\frac{\partial^2\theta}{\partial x^2} + \frac{\partial^2 u_x}{\partial x^2}\frac{\partial\theta}{\partial x} + \frac{3}{2}r^2\frac{\partial^2\theta}{\partial x^2}\left(\frac{\partial\theta}{\partial x}\right)^2\right] \\
- I_p r\omega\left[2\frac{\partial^2\theta}{\partial x\partial t}\frac{\partial\theta}{\partial x} + \frac{\partial\theta}{\partial t}\frac{\partial^2\theta}{\partial x^2}\right] + m_p g\sin\alpha\sin\theta \\
+ m_p r\frac{\partial^2\theta}{\partial t^2} \\
+ \frac{sgn\left(\frac{\partial\theta}{\partial t}\right) fr\left|\frac{\partial\theta}{\partial t}\right|}{\sqrt{\left(\frac{\partial u_x}{\partial t}\right)^2 + r^2\left(\frac{\partial\theta}{\partial t}\right)^2}} \Bigg\{ -EIr\left[\left(\frac{\partial\theta}{\partial x}\right)^4 - 3\left(\frac{\partial^2\theta}{\partial x^2}\right)^2\right. \\
\left. - 4\frac{\partial^3\theta}{\partial x^3}\frac{\partial\theta}{\partial x}\right] - EAr\left[\frac{\partial u_x}{\partial x}\left(\frac{\partial\theta}{\partial x}\right)^2 + \frac{1}{2}r^2\left(\frac{\partial\theta}{\partial x}\right)^4\right] \\
+ I_p r\omega\left[\frac{\partial^3\theta}{\partial x^2\partial t} - \frac{\partial\theta}{\partial t}\left(\frac{\partial\theta}{\partial x}\right)^2\right] + m_p g\sin\alpha\cos\theta \\
+ m_p r\left(\frac{\partial\theta}{\partial t}\right)^2\Bigg\} = 0
\end{aligned}
\tag{42}
$$

$$
\begin{aligned}
N = -EIr\left[\left(\frac{\partial\theta}{\partial x}\right)^4 - 3\left(\frac{\partial^2\theta}{\partial x^2}\right)^2 - 4\frac{\partial^3\theta}{\partial x^3}\frac{\partial\theta}{\partial x}\right] \\
- EAr\left[\frac{\partial u_x}{\partial x}\left(\frac{\partial\theta}{\partial x}\right)^2 + \frac{1}{2}r^2\left(\frac{\partial\theta}{\partial x}\right)^4\right] \\
+ I_p r\omega\left[\frac{\partial^3\theta}{\partial x^2\partial t} - \frac{\partial\theta}{\partial t}\left(\frac{\partial\theta}{\partial x}\right)^2\right] + m_p g\sin\alpha\cos\theta \\
+ m_p r\left(\frac{\partial\theta}{\partial t}\right)^2
\end{aligned}
\tag{43}
$$

The problem consists in solving Eqs. (41), (42) and (43) in order to find the axial and angular displacements and the normal contact force, besides Eq. (3) for the axial force.

3.3.2. Model for tripping out

The full deduction can be seen on Appendix A. The final motion equations will be:

$$EA\frac{\partial^2 u_x}{\partial x^2} - m_p\frac{\partial^2 u_x}{\partial t^2} + m_p g\cos\alpha - sgn\left(\frac{\partial u_x}{\partial t}\right) f\left[-m_p r\frac{\partial^3 u_x}{\partial x\partial t^2} + m_p g\sin\alpha\right] = 0 \quad (44)$$

$$N = -m_p r\frac{\partial^3 u_x}{\partial x\partial t^2} + m_p g\sin\alpha \quad (45)$$

The problem consists of solving Eqs. (44) and (45) to find the axial displacement and normal contact force, besides Eq. (6) for the axial force.

3.3.3. Solution for tripping in

The discretizations for the axial and angular displacements will be given by:

$$
\begin{aligned}
&U_{i,j+1} \\
&= 2U_{i,j} - U_{i,j-1} + \frac{EA\Delta t^2}{m_p \Delta x^2}\left(U_{i+1,j} - 2U_{i,j} + U_{i-1,j}\right) \\
&+ \frac{EAr^2\Delta t^2}{2m_p\Delta x^3}\left(\theta_{i+1,j} - \theta_{i-1,j}\right)\left(\theta_{i+1,j} - 2\theta_{i,j} + \theta_{i-1,j}\right) \\
&- \frac{sgn\left(U_{i,j} - U_{i,j-1}\right) f\Delta t\left|U_{i,j} - U_{i,j-2}\right|}{2m_p\sqrt{\left(\frac{U_{i,j}-U_{i,j-2}}{2\Delta t}\right)^2 + r^2\left(\frac{\theta_{i,j}-\theta_{i,j-2}}{2\Delta t}\right)^2}}\Bigg\{-\frac{EIr}{\Delta x^4}\bigg[\frac{1}{16}\left(\theta_{i+1,j} - \theta_{i-1,j}\right)^4 \\
&- 3\left(\theta_{i+1,j} - 2\theta_{i,j} + \theta_{i-1,j}\right)^2 \\
&- \left(\theta_{i+2,j} - 2\theta_{i+1,j} + 2\theta_{i-1,j} - \theta_{i-2,j}\right)\left(\theta_{i+1,j} - \theta_{i-1,j}\right)\bigg] \\
&- \frac{EAr}{8\Delta x^3}\bigg[\left(U_{i+1,j} - U_{i-1,j}\right)\left(\theta_{i+1,j} - \theta_{i-1,j}\right)^2 \\
&+ \frac{r^2}{4\Delta x}\left(\theta_{i+1,j} - \theta_{i-1,j}\right)^4\bigg] \\
&+ \frac{I_p r\omega}{2\Delta x^2\Delta t}\bigg[\left(\theta_{i+1,j} - 2\theta_{i,j} + \theta_{i-1,j} - \theta_{i+1,j-2} + 2\theta_{i,j-2} - \theta_{i-1,j-2}\right) \\
&- \frac{1}{4}\left(\theta_{i,j} - \theta_{i,j-2}\right)\left(\theta_{i+1,j} - \theta_{i-1,j}\right)^2\bigg] + m_p g \sin\alpha \cos\theta_{i,j} \\
&+ \frac{m_p r}{4\Delta t^2}\left(\theta_{i,j} - \theta_{i,j-2}\right)^2\Bigg\} + \Delta t^2 g \cos\alpha
\end{aligned}
\tag{46}
$$

$$\begin{aligned}
&\frac{I_p r\omega\left(\theta_{i+1,j}-\theta_{i-1,j}\right)}{4\Delta x^2\Delta t}\theta_{i+1,j+1} \\
&+\left[\frac{I_p r\omega\left(\theta_{i+1,j}-2\theta_{i,j}+\theta_{i-1,j}\right)}{2\Delta x^2\Delta t}-\frac{m_p r}{\Delta t^2}\right]\theta_{i,j+1} \\
&-\frac{I_p r\omega\left(\theta_{i+1,j}-\theta_{i-1,j}\right)}{4\Delta x^2\Delta t}\theta_{i-1,j+1} \\
&=\frac{I_p r\omega\left(\theta_{i+1,j}-2\theta_{i,j}+\theta_{i-1,j}\right)}{2\Delta x^2\Delta t}\theta_{i,j-1} \\
&-\frac{I_p r\omega\left(\theta_{i+1,j}-\theta_{i-1,j}\right)}{4\Delta x^2\Delta t}\left(-\theta_{i+1,j-1}+\theta_{i-1,j-1}\right) \\
&+\frac{m_p r}{\Delta t^2}\left(-2\theta_{i,j}+\theta_{i,j-1}\right) \\
&+\frac{EIr}{\Delta x^4}\left[\left(\theta_{i+2,j}-4\theta_{i+1,j}+6\theta_{i,j}-4\theta_{i-1,j}+\theta_{i-2,j}\right)\right. \\
&\left.-\frac{3}{2}\left(\theta_{i+1,j}-\theta_{i-1,j}\right)^2\left(\theta_{i+1,j}-2\theta_{i,j}+\theta_{i-1,j}\right)\right] \\
&-\frac{EAr}{2\Delta x^3}\left[\left(U_{i+1,j}-U_{i-1,j}\right)\left(\theta_{i+1,j}-2\theta_{i,j}+\theta_{i-1,j}\right)\right. \\
&+\left(U_{i+1,j}-2U_{i,j}+U_{i-1,j}\right)\left(\theta_{i+1,j}-\theta_{i-1,j}\right) \\
&\left.+\frac{3r^2}{4\Delta x}\left(\theta_{i+1,j}-2\theta_{i,j}+\theta_{i-1,j}\right)\left(\theta_{i+1,j}-\theta_{i-1,j}\right)^2\right] \\
&+m_p g\sin\alpha\sin\theta_{i,j} \\
&+\frac{sgn\left(\theta_{i,j}-\theta_{i,j-1}\right)fr\left|\theta_{i,j}-\theta_{i,j-2}\right|}{2\Delta t\sqrt{\left(\frac{U_{i,j}-U_{i,j-2}}{2\Delta t}\right)^2+r^2\left(\frac{\theta_{i,j}-\theta_{i,j-2}}{2\Delta t}\right)^2}}\left\{-\frac{EIr}{\Delta x^4}\left[\frac{1}{16}\left(\theta_{i+1,j}-\theta_{i-1,j}\right)^4\right.\right. \\
&-3\left(\theta_{i+1,j}-2\theta_{i,j}+\theta_{i-1,j}\right)^2 \\
&\left.-\left(\theta_{i+2,j}-2\theta_{i+1,j}+2\theta_{i-1,j}-\theta_{i-2,j}\right)\left(\theta_{i+1,j}-\theta_{i-1,j}\right)\right] \\
&-\frac{EAr}{8\Delta x^3}\left[\left(U_{i+1,j}-U_{i-1,j}\right)\left(\theta_{i+1,j}-\theta_{i-1,j}\right)^2\right. \\
&\left.+\frac{r^2}{4\Delta x}\left(\theta_{i+1,j}-\theta_{i-1,j}\right)^4\right] \\
&+\frac{I_p r\omega}{2\Delta x^2\Delta t}\left[\left(\theta_{i+1,j}-2\theta_{i,j}+\theta_{i-1,j}-\theta_{i+1,j-2}+2\theta_{i,j-2}-\theta_{i-1,j-2}\right)\right. \\
&\left.-\frac{1}{4}\left(\theta_{i,j}-\theta_{i,j-2}\right)\left(\theta_{i+1,j}-\theta_{i-1,j}\right)^2\right]+m_p g\sin\alpha\cos\theta_{i,j} \\
&\left.+\frac{m_p r}{4\Delta t^2}\left(\theta_{i,j}-\theta_{i,j-2}\right)^2\right\}
\end{aligned} \tag{47}$$

The boundary conditions and initial conditions discretizations can be seen on Appendix A.

3.3.4. Solution for tripping out

The discretization for the axial displacement will be given by:

$$\begin{aligned}U_{i,j+1} = 2U_{i,j} - U_{i,j-1} + &\frac{EA\Delta t^2}{m_p\Delta x^2}\left(U_{i+1,j} - 2U_{i,j} + U_{i-1,j}\right) \\ &+ g\Delta t^2 \cos\alpha \\ &- sgn\left(U_{i,j} - U_{i,j-1}\right) f\left[-\frac{r}{2\Delta x}\left(U_{i+1,j} - U_{i-1,j}\right.\right. \\ &\left. - 2U_{i+1,j-1} + 2U_{i-1,j-1} + U_{i+1,j-2} - U_{i-1,j-2}\right) \\ &\left. + g\Delta t^2 \sin\alpha\right]\end{aligned} \tag{48}$$

The boundary conditions and initial conditions discretizations can be seen on Appendix A.

3.4. Model IV – Offshore wells

Up until now, all models considered the same boundary conditions: fixed at $x = 0$ and free at $x = L$. However, such boundary conditions are not enough to describe the behavior of columns inside offshore wells. On offshore environments, the environment causes displacements on the platform or vessel, in which the columns are attached; consequently, the column will displace as well due to this motion. These displacements are the consequence of environmental loads, which can be waves, currents and/or wind. The models developed so far can still be used for columns inside onshore wells or attached to fixed platforms, since on these cases the environment cannot cause any meaningful loads and thus the column can be considered fixed. Figure 3.7 shows the types of displacements – also known as degrees of freedom – that can occur on a floating vessel.

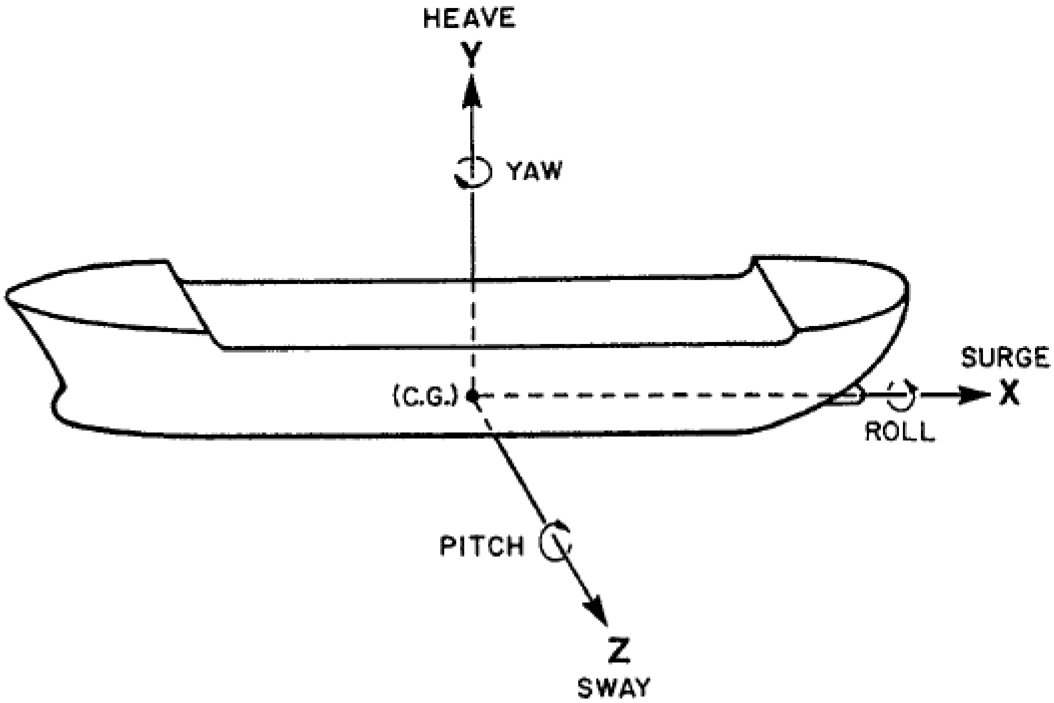

Figure 3.7: Degrees of freedom of an offshore structure (Chakrabarti, 1987).

Observing Figure 3.7, it can be concluded that the vessel will be subjected to three linear displacements on the x, y and z axis – surge, heave and sway, respectively – and three angular displacements around the x, y and z axis – roll, yaw and pitch, respectively. These six motions will be transmitted to any column that is coupled to the vessel. Due to the hypotheses adopted on this work, only the linear displacements can be considered. Regarding them, the most relevant effect is the heave motion; the amplitudes of surge and sway are too small in comparison, since the vessel can absorb these motions due to its dynamic positioning system (DPS). Therefore, only the vessel heave is considered and it is transmitted to the column as a boundary condition for the axial displacement u_x. This methodology was already used by Chung & Whitney (1981). Lastly, it is important to note that the vessel displacement amplitudes are not transmitted entirely to the coupled column. The transmitted amount depends on the motion frequency; this information is given by the response amplitude operators (RAOs) of the vessel. These operators exist for each one of the six degrees of freedom and are characteristic of each vessel. To simplify the analysis, it is considered that the displacement used as a boundary condition is already the column displacement, thus eliminating the need and usage of a RAO.

The boundary condition to be defined here is only for the axial displacement at $x = 0$; this means that from the six boundary conditions defined previously – three for each end, with one being for u_x, one for θ and one for $\partial^2\theta/\partial x^2$ – only one will be changed: u_x at $x = 0$. For u_x at $x = 0$:

$$u(0,t) = U_h \, sin \, \omega_h t \tag{49}$$

Where U_h is the heave amplitude and ω_h is the heave angular frequency. Discretizing Eq. (49):

$$U_{0,j} = U_h \, sin[(j-2)\omega_h \Delta t] \tag{50}$$

The remaining equations for this model are the same developed previously, but remembering that the values for $U_{0,j}$ are no longer zero, thus they do not disappear from the $i = 1$ and $i = 2$ equations. The solutions are valid only starting at $j = 3$, since for $j = 1$ and $j = 2$ the initial conditions are applied instead; that is why on Eq. (50) there is $j - 2$ instead of only j.

4. METHODOLOGY AND APPLICATIONS

A methodology to solve the equations from the previous chapter and to analyze the results obtained is presented here. A summary of the equations and variables involved is made and a study case – based on real data – is also presented.

4.1. Summary of equations and variables

As shown on chapter 3, four models were developed to study the column dynamic buckling problem. Figure 4.1 summarizes the variables of the problem, while Table 4.1 summarizes the equations needed for each model, considering that there is a set of equations for tripping in and for tripping out inside each model.

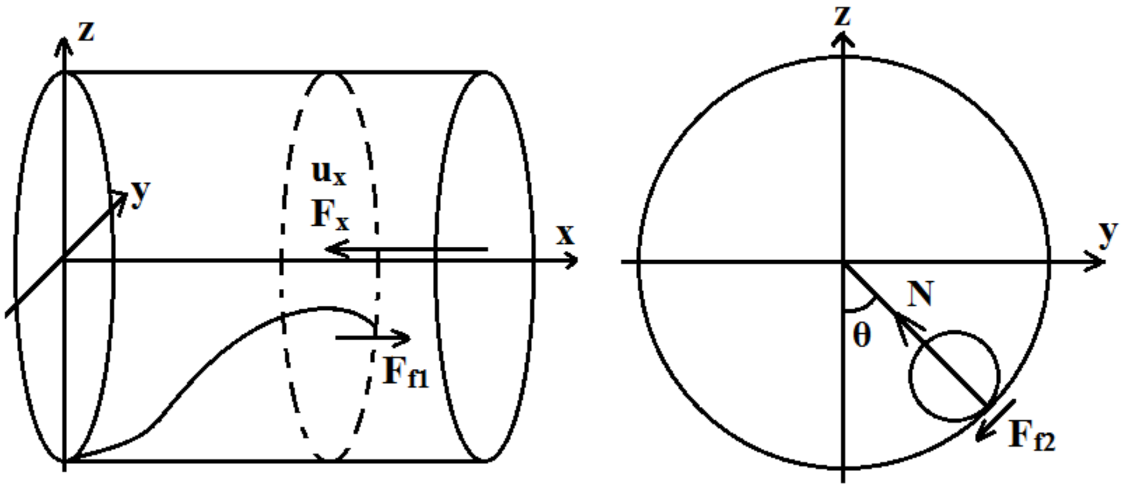

Figure 4.1: Well schematic with all the variables from the problem.

Table 4.1: Summary of all equations needed to solve each model.

Model I	Tripping in	Eqs. (1), (2), (3) and (4)
	Tripping out	Eqs. (5), (6) and (7)
Model II	Tripping in	Eqs. (3), (4), (29), (30) and (31)
	Tripping out	Eqs. (6), (7), (32) and (33)
Model III	Tripping in	Eqs. (3), (29), (41), (42) and (43)
	Tripping out	Eqs. (6), (32), (44) and (45)
Model IV	Tripping in	Eqs. (3), (29), (41), (42) and (43)
	Tripping out	Eqs. (6), (32), (44) and (45)

After doing the discretization using an implicit method, the axial displacement can be calculated independently for each point, whereas the angular displacement results into a system of algebraic equations. After both displacements are calculated, the axial, normal contact and friction forces can then be obtained. Therefore, the problems range from three up to five unknowns. Table 4.2 summarizes all the variables present in each model. For tripping out cases, the angular displacement θ does not exist, while for Model I the friction force components $\vec{F}_{f1}$ and $\vec{F}_{f2}$ do not exist. As seen on Table 4.2, there are a total of 34 variables to be analyzed.

Table 4.2: Summary of all variables of the problem. The X marks if a certain variable appears on the corresponding model.

		u_x	θ	F_x	N	F_f
Model I	Tripping in	X	X	X	X	
	Tripping out	X		X	X	
Model II	Tripping in	X	X	X	X	X
	Tripping out	X		X	X	X
Model III	Tripping in	X	X	X	X	X
	Tripping out	X		X	X	X
Model IV	Tripping in	X	X	X	X	X
	Tripping out	X		X	X	X

4.2. Data used for simulation

In order to simulate each model, a data set is also needed. While some properties remain the same across multiple scenarios – such as the material properties – other inputs may change depending on the operation – such as the diameters. On the present work, a single scenario was considered: a tubing string inside a cased hole. Table 4.3 presents all the data used. It is important to point that the casing is considered to reach from the bottom throughout the whole well until the top; this implicates that a liner is not used. Also, as mentioned before, all the models were developed for a drill string, which rotates; however, the scenario here is for a completion operation, in which the column does not rotate. Also, some data is exclusive to certain models: the dynamic friction force appears only from Model II onwards, since Model I does not have the friction force; the heave is modeled with constant amplitude, constant angular frequency and in phase with the rest of the system, appearing only on Model IV.

Table 4.3: Data used to simulate the tubing-casing scenario.

Property	Value
Tubing string inner diameter	*5.791* in (*0.1471* m)
Tubing string outer diameter	*6.625* in (*0.1683* m)
Inner diameter of a *10 ¾”* casing	*9.56* in (*0.2428* m)
Young’s Modulus	*210* GPa
Specific mass	*7850* kg/m³
Gravitational acceleration	*9.81* m/s²
Rotation angular frequency	*0* rad/s (not rotating)
Dynamic dry friction coefficient (for Models II, III and IV)	*0.1*
Heave amplitude (for Model IV only)	*0.5* m
Heave angular frequency (for Model IV only)	*1* rad/s
Space discretization interval	*10* m
Time discretization interval	*0.0002* s
Space domain	1000 *m* (Models I and II) Figure 4.2 (Models III and IV)
Time domain	10 *s* (20 *s* for Model IV)

Lastly, for Models III and IV, which consider the well inclination, it is possible to define a well trajectory. Although both models only apply for a segment with constant inclination, the key idea here is that a small curved segment of wellbore can be approximated as a segment with constant inclination and thus all equations can be applied. By joining together several of these small segments – with each one of them having their own angle of inclination α according to their position on the well – any given well trajectory can be discretized. Since the solution will be obtained using the finite differences method, a different inclination angle can be assigned to each measured depth and the simulation can calculate the displacements and forces for the whole column inside the well. On this work, a single well trajectory was considered: a horizontal well with two build-ups, as seen on Figure 4.2. All lengths are given in meters.

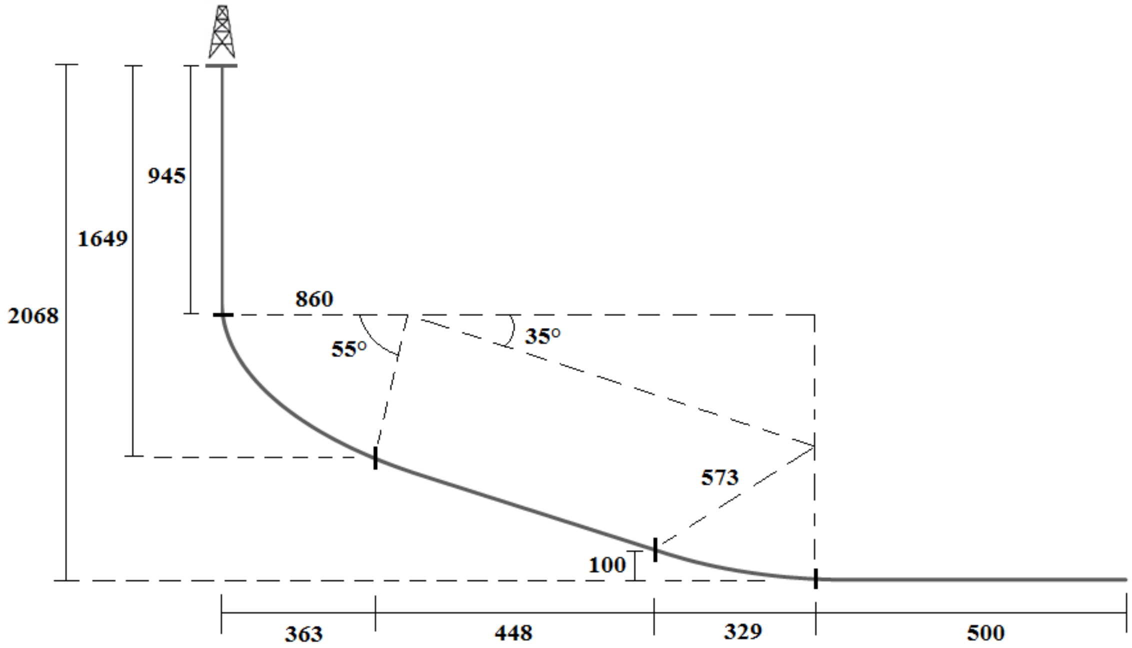

Figure 4.2: Well trajectory for a horizontal well with two build-ups. All lengths are in meters.

The well starts vertical and must reach the objective, which is at a true vertical depth of *2068* m and has a horizontal departure of *1640* m. The kickoff point must be located at a true vertical depth of *945* m. The well starts building its angle with a rate of *2°/30* m until it reaches *55°*. After the slant segment reaches a true vertical depth of *1968* m, the well starts building its angle once more, now with a rate of *3°/30* m until it reaches *90°*. After the horizontal position is reached, the well continues with a purely horizontal segment of *500* m. The remaining values, which are calculated, are also shown on Figure 4.2. The first curved segment has a radius of *860* m, while the second one has a radius of *573* m. The horizontal departure just before the horizontal segment starts is *1140* m. The total measured depth of the well is *3170* m.

Since for Models I and II the well inclination is irrelevant – because the model is only valid for horizontal segments – a length of $L = 1000$ m will be used instead to obtain preliminary results. The trajectories will then be applied to Models III and IV. For comparison purposes between models, the same column length will be used for Models III and IV, when in reality Model IV should have an extra vertical segment at the beginning, representing the column length connecting the vessel with the wellhead along the water depth; the model could still be applied in this case since the column is still constrained – now by a marine riser – through the whole water depth.

5. RESULTS AND DISCUSSION

By using the variables shown on Table 4.2, several comparisons can be drawn: besides comparing tripping in and tripping out for each model and testing several inclinations for Models III and IV, the models can be compared between themselves – for example, Models I and II to see the effect of friction or Models III and IV to see the effect of the heave. Finally, each graph can be made as a function of either time or position; the former would give the behavior of a variable on a fixed point of the column while the latter would give the behavior of a variable for all points on a fixed time instant.

Figure 5.1 shows the column buckled configuration for tripping in using Model I. The column has been reduced to a single line, in which each point is the center of the cross section. The position of each cross section center is given by Eq (A.1). Data was taken for $t = 5$ s. For this graph only, the initial condition for θ was set at 0.7 rad to allow a better visualization.

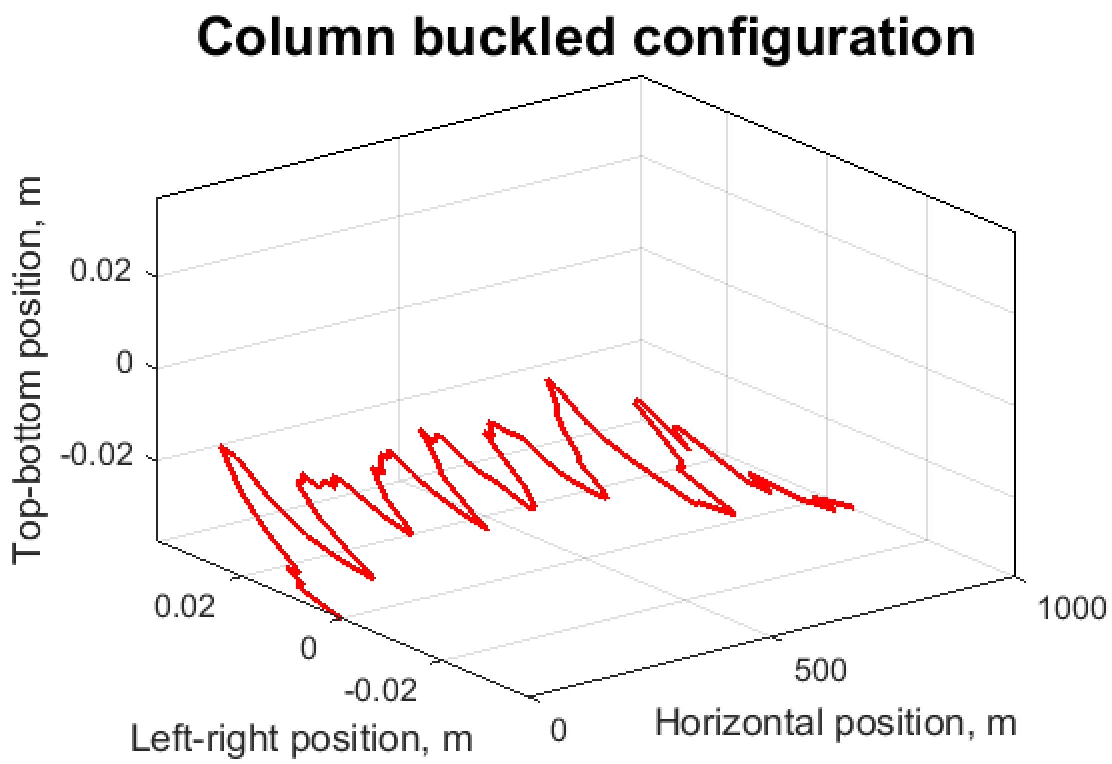

Figure 5.1: Column buckled configuration, given by the positions, in meters, in the three axes. The displacements used are for the time instant $t = 5$ s.

It can be seen on Figure 5.1 that the column remains on the lowest portion of the well – represented by the negative values on the top-bottom position axis – but can reach values around the halfway mark of this portion, which would be $r_c/2$.

Figure 5.2 shows a 3D graph for the horizontal displacement as a function of both horizontal position and time for Model II. By looking at the time axis, it can be seen that the displacement dissipates over time due to friction; meanwhile, by looking at the position axis, the displacement distribution along the length can be seen for a fixed time instant.

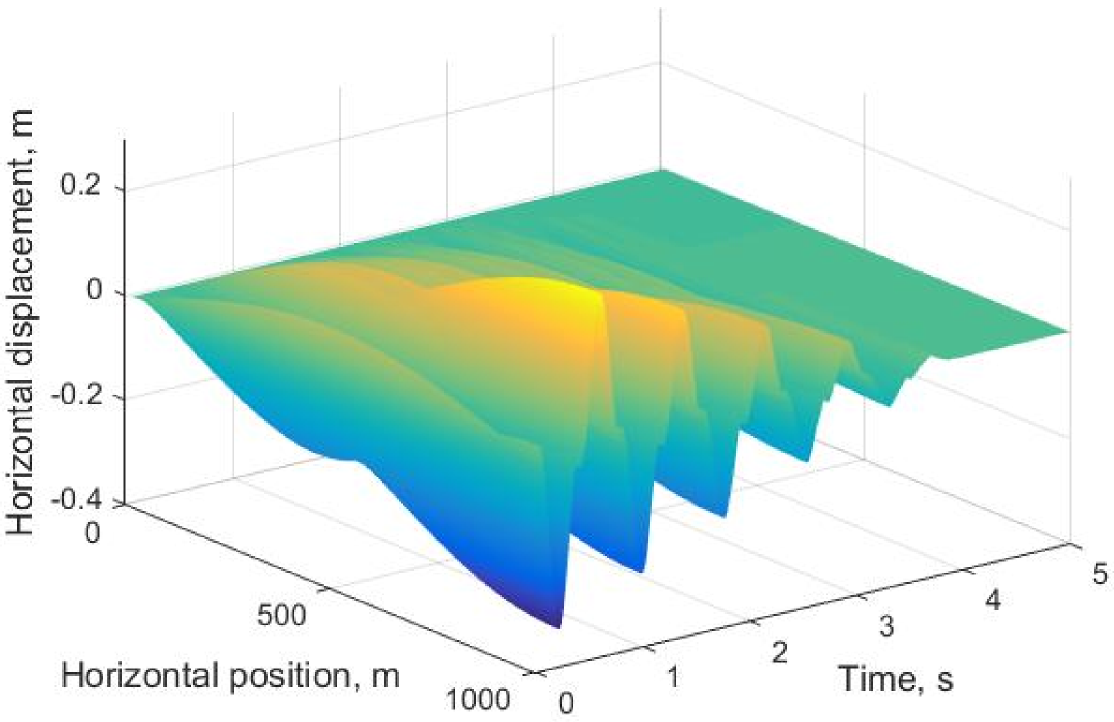

Figure 5.2: Horizontal displacement, in meters, as a function of both horizontal position, in meters, and time, in seconds.

Figure 5.3 shows a comparison of the horizontal displacement between tripping in and tripping out for Model I – which has no friction – while Figure 5.4 does the same for Model II – which has friction. All displacements were taken from a midway point, located at $x = 500$ m.

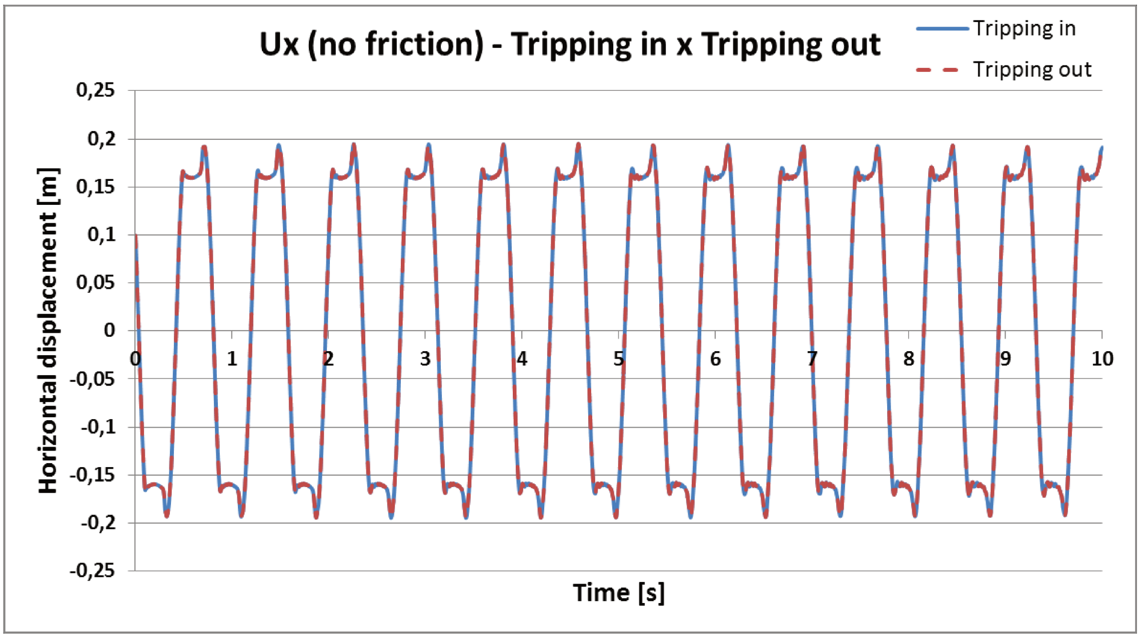

Figure 5.3: Comparison of the horizontal displacement for tripping in and tripping out, in meters, as a function of time, in seconds, for Model I. The displacements used are for the point at $x = 500$ m.

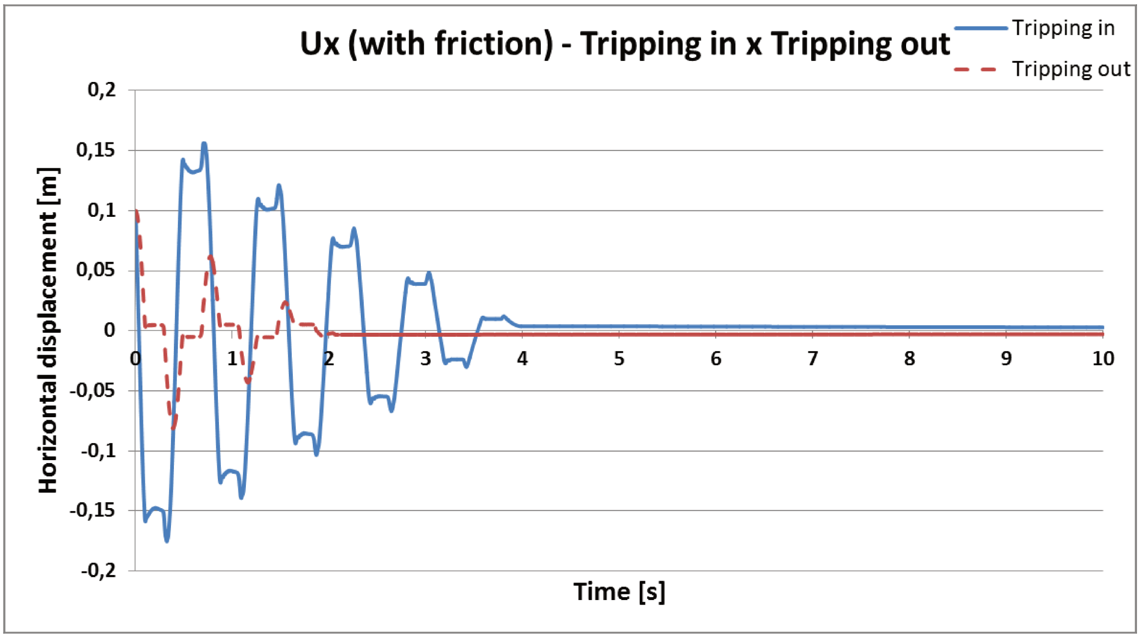

Figure 5.4: Comparison of the horizontal displacement for tripping in and tripping out, in meters, as a function of time, in seconds, for Model II. The displacements used are for the point at $x = 500$ m.

As can be seen on Figure 5.3, there is no difference between tripping in and tripping out when the model does not have friction. However, as seen on Figure 5.4, when friction is added to the model the horizontal displacements become different. The horizontal displacement is greater during tripping in than tripping out. Since the column can buckle during tripping in, there will be a greater contraction and expansion on the horizontal direction due to the formation and dissipation of helices, thus causing greater amplitudes of displacement than on the tripping out case. Also, the displacements become more dependent of each other after the friction is added to the model; this explains why the horizontal displacement is almost unaffected by the angular displacement on Figure 5.3, in which there is no friction, but later is influenced by it on Figure 5.4, in which there is friction. Finally, comparing Figures 5.3 and 5.4, it can be seen that the motion is dissipated through time on Model II; this is coherent considering that on Model I there are no dissipative forces while on Model II the friction force – which is dissipative – is acting.

Figure 5.5 shows a comparison of the angular displacement between Models I and II. Since the column can only suffer angular displacements during tripping in, there is no comparison to be done with the tripping out case. The data is taken again from a point located at $x = 500$ m.

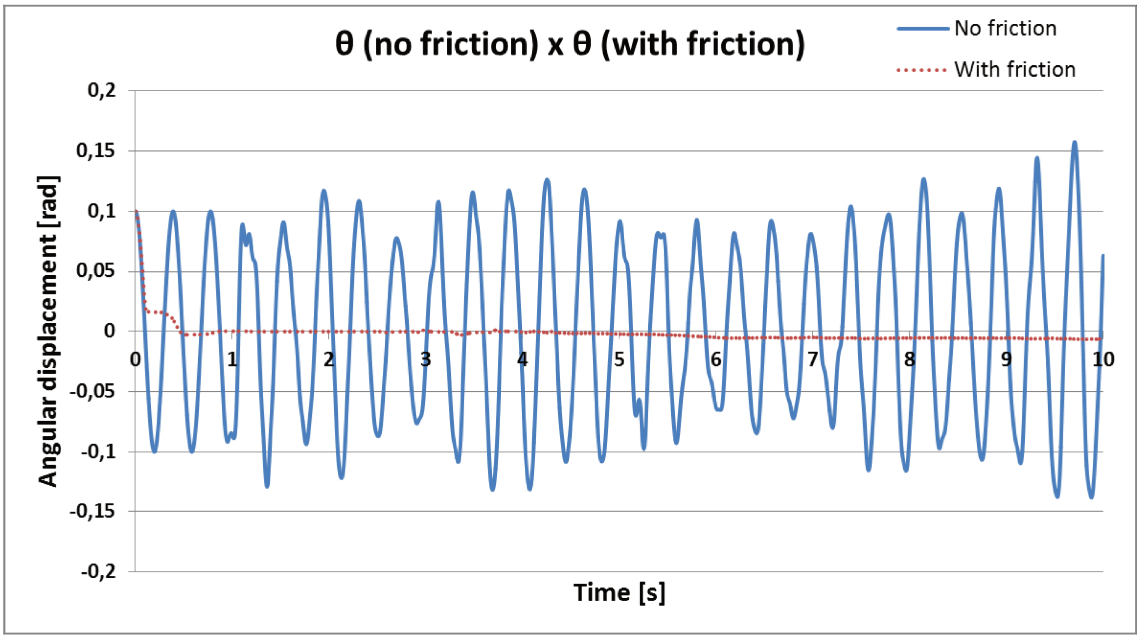

Figure 5.5: Comparison of the angular displacement for Models I and II, in radians, as a function of time, in seconds. The displacements used are for the point at $x = 500$ m.

As seen on Figure 5.5, the angular displacement will not cease for Model I since there is no dissipative force while for Model II the displacement will approach zero quickly due to friction. The angular displacements can be seen on Figure 5.6 through another perspective, as a function of the position instead of time. The values were taken for $t = 1$ s.

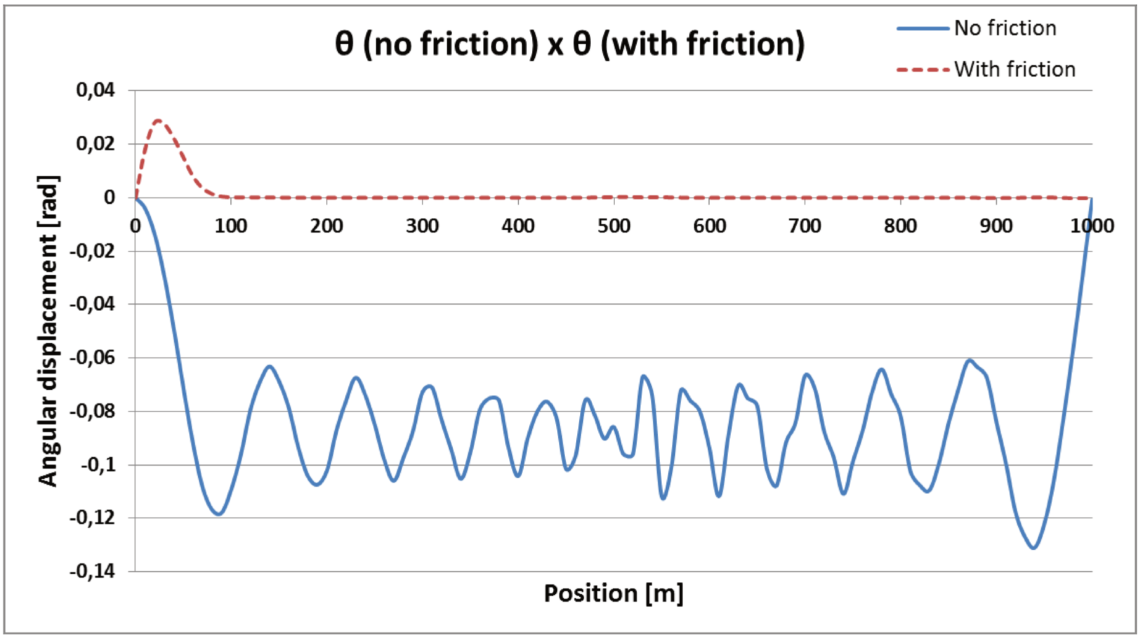

Figure 5.6: Comparison of the angular displacement for Models I and II, in radians, as a function of position, in meters. The displacements used are for the time instant $t = 1$ s.

As seen once more on Figure 5.6, the angular displacement is greatly dissipated due to friction. Even though the angular displacement becomes small, it is sufficient to cause a difference on the horizontal displacement, as observed on Figure 5.4.

Figures 5.7 and 5.8 draw the same comparison as Figures 5.3 and 5.4, but now for the normal contact force per unit of length. Once more, all the results were taken from a point located at $x = 500$ m.

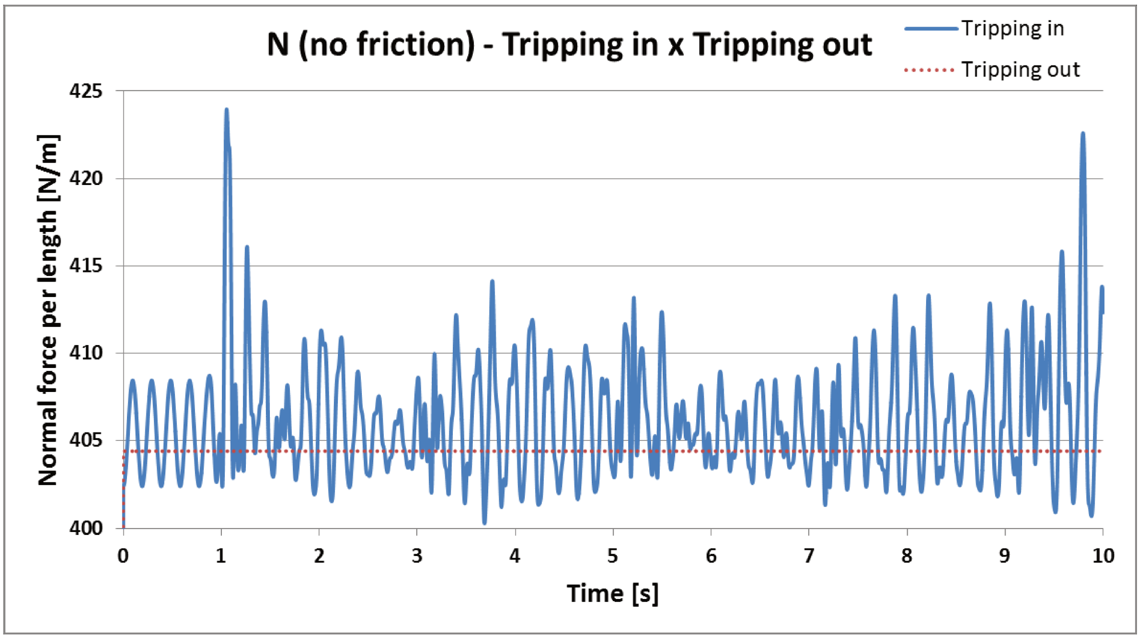

Figure 5.7: Comparison of the normal contact force per unit of length for tripping in and tripping out, in Newton per meter, as a function of time, in seconds, for Model I. The forces used are for the point at $x = 500$ m.

As seen on Figure 5.7, the normal force fluctuates on tripping in, due to the angular displacement behavior seen on Figures 5.5 and 5.6, in opposition to tripping out where it remains almost constant. However, since the angular displacement is severely dissipated due to friction on Model II, the fluctuations disappear on Figure 5.8. This can be easily explained by looking again at Figures 5.5 and 5.6. Since the angular displacement is reduced close to zero for Model II, the tripping in case approaches the tripping out case, thus leading to what is seen on Figure 5.8: the normal force for tripping in approaches the normal force for tripping out. It is still inconclusive if this small difference in normal forces can lead to a difference in friction forces; therefore, the friction forces must be compared as well.

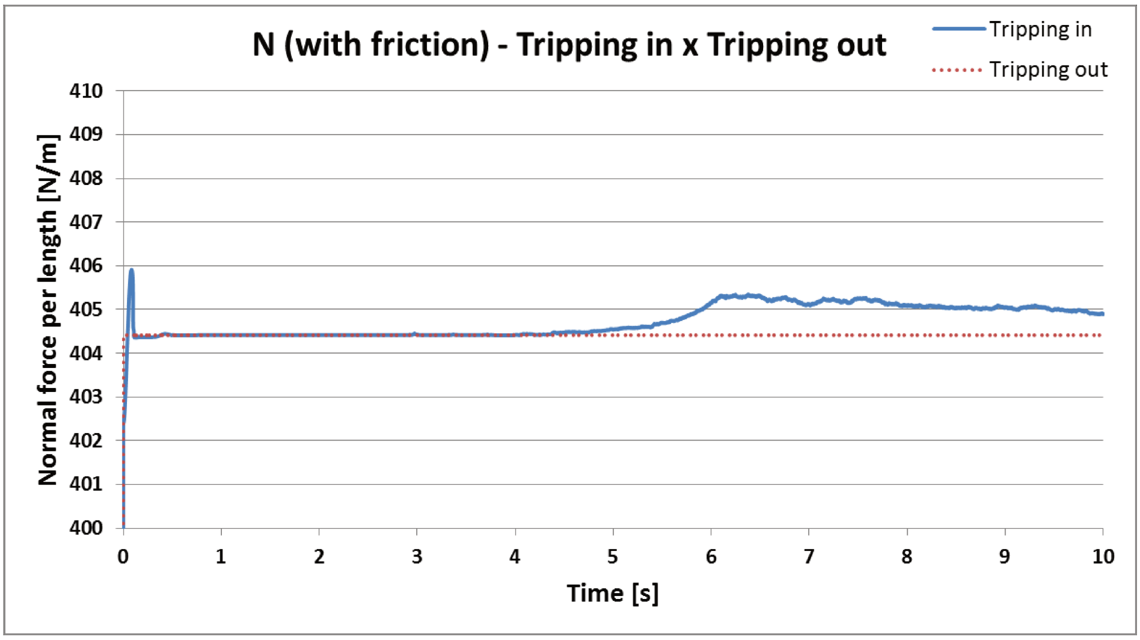

Figure 5.8: Comparison of the normal contact force per unit of length for tripping in and tripping out, in Newton per meter, as a function of time, in seconds, for Model II. The forces used are for the point at $x = 500$ m.

Figure 5.9 provides a comparison between the friction forces for tripping and tripping out on Model II. The friction force shown is the total force acting through the whole column. The graph is cut at $t = 2$ s – the time instant in which the transient part begins to vanish for tripping out – because there is a numerical instability after the dynamic solution converges to the static solution. This happens because the discretization used has low order; consequently, the errors pile up with the static solution.

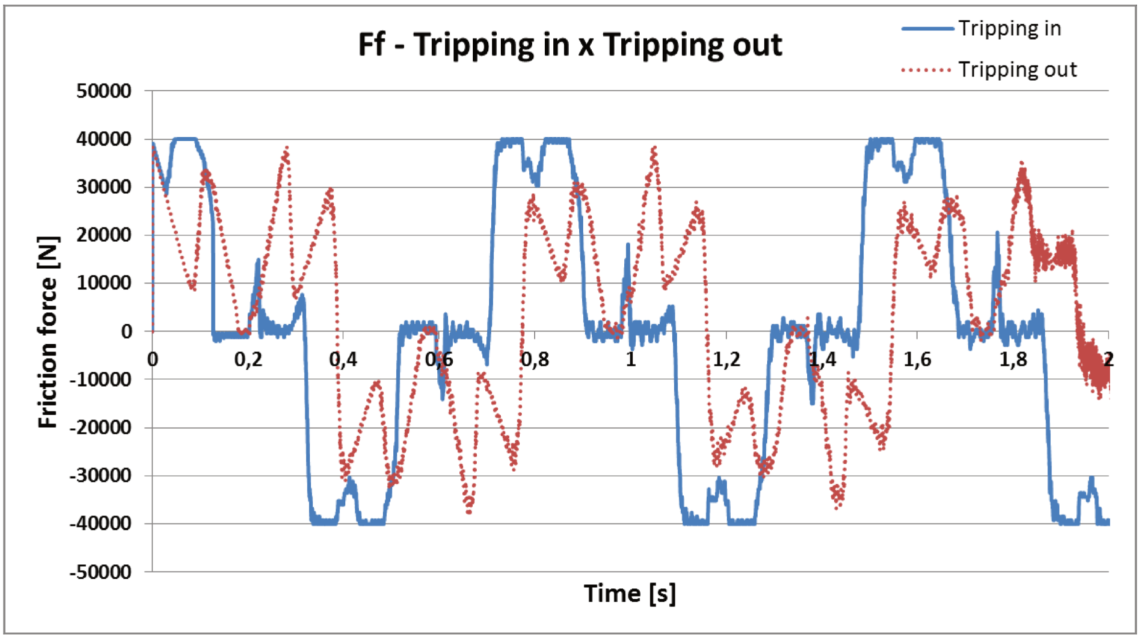

Figure 5.9: Comparison of the friction force for tripping in and tripping out, in Newton, as a function of time, in seconds, for Model II. The values shown are the total force acting through the whole column.

As can be seen on Figure 5.9, the friction forces are indeed different for tripping in and tripping out, thus being in agreement with the main hypothesis of this work. Taking a look again at section 3.2, the friction force is dependent of the horizontal displacement, the angular displacement and the normal contact force; therefore, even though the angular displacement and the normal force for tripping in approach the tripping out case, the difference is enough to cause a significant difference on the horizontal displacement, which then leads to a difference on the friction forces. Comparing Eqs. (29) and (32) through their $\hat{\imath}$ component, it can be seen that the difference between tripping in and out is given by the term $C_f = \left|\frac{\partial u_x}{\partial t}\right| / \sqrt{\left(\frac{\partial u_x}{\partial t}\right)^2 + r^2\left(\frac{\partial \theta}{\partial t}\right)^2}$. As long as $C_f \neq 1$, the friction forces will be different; to have $C_f \neq 1$ means that the angular displacement must be $\theta \neq 0$. This conclusion aligns with the hypothesis used previously – that the ratio of the friction coefficients on the axial and lateral directions is proportional to the ratio of the velocities on said directions. Therefore, since the normal contact force in both cases is not really different – as seen on Figure 5.8 – the real cause for the different friction forces is the angular displacement – and, indirectly, the axial displacement. Another comparison of the friction forces can be seen on Figure 5.10, now by taking the force per unit of length as a function of the position. The data is again taken from t = 1 s.

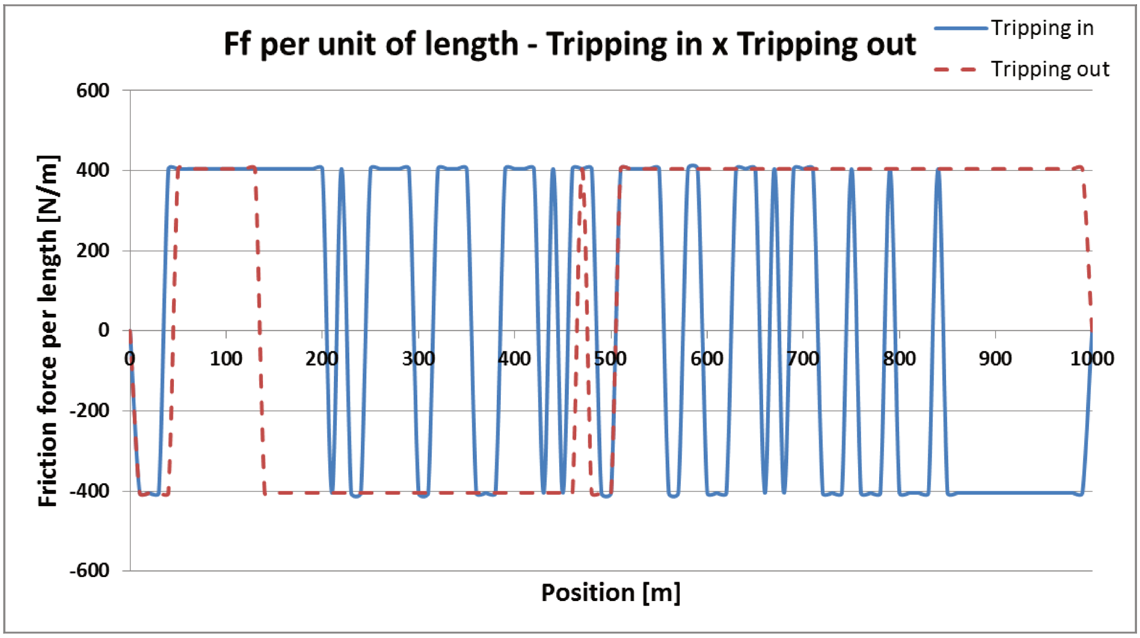

Figure 5.10: Comparison of the friction force for tripping in and tripping out, in Newton per meter, as a function of position, in meters, for Model II. The forces used are for the time instant $t = 1$ s.

As can be seen on Figure 5.10, while on tripping out the friction force per unit of length remains almost constant, it fluctuates heavily for the tripping in case, thus causing a difference on the total friction force when the contributions at each point are added up. This is another aspect that contributes towards the result shown on Figure 5.9.

For Models III and IV, the horizontal well trajectory shown on Figure 4.2 will be used. Starting with Model III, Figures 5.11 and 5.12 show the horizontal displacement for several inclinations for the tripping in case and the tripping out case, respectively. The inclinations were taken from specific points along the well trajectory: $\alpha = 0°$ at $x = 500$ m on the vertical segment, $\alpha = 37°$ at $x = 1500$ m on the first build-up segment, $\alpha = 55°$ at $x = 2000$ m on the slant segment, $\alpha = 73°$ at $x = 2500$ m on the second build-up segment and $\alpha = 90°$ at $x = 3000$ m on the horizontal segment.

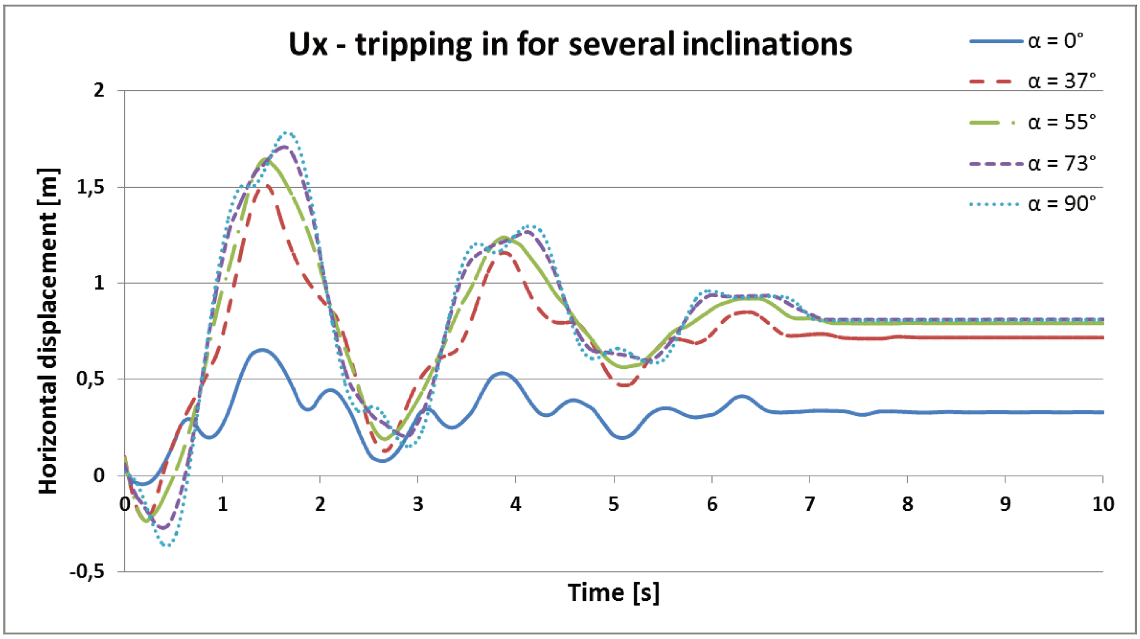

Figure 5.11: Comparison of the horizontal displacement during tripping in for several inclinations, in meters, as a function of time, in seconds, for Model III. The data is taken from points located at x = *500* m, x = *1500* m, x = *2000* m, x = *2500* m and x = *3000* m.

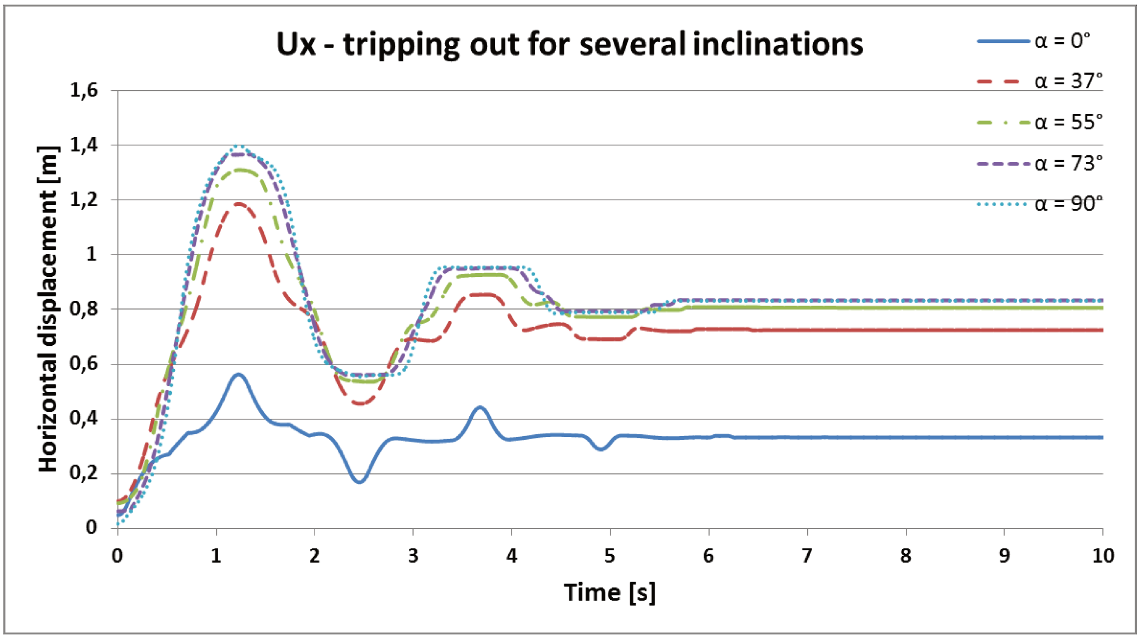

Figure 5.12: Comparison of the horizontal displacement during tripping out for several inclinations, in meters, as a function of time, in seconds, for Model III. The data is taken from points located at x = *500* m, x = *1500* m, x = *2000* m, x = *2500* m and x = *3000* m.

As can be observed from both Figures 5.11 and 5.12, the displacements are greater the higher the angle, remembering that *0°* is the vertical position and *90°* is the horizontal position. This provides an interesting result when coupled with Figure 5.13 below. Figure 5.13 shows the normal contact force per unit of length during tripping in for several inclinations. It can be seen that the greater the angle, the higher the normal force; this makes sense physically considering that the contact weakens as the column moves to the vertical position, thus reducing the normal force. If the normal force reduces, so does the friction force, which is directly proportional; finally, if the friction forces reduces as the column approaches the vertical position, the horizontal displacement should be higher for small angles, but this is not the case as observed on Figures 5.11 and 5.12. Instead, the opposite occurs: the points with greater angles, which are located deep down on the well, are the ones with greater displacements. To check the aforementioned result, the same column length was simulated for five scenarios with constant inclination using the five angles from Figures 5.11 and 5.12 and then the time histories of the same five points at the same five depths were taken – one point from each of the five scenarios. This is shown on Figure 5.14 below. Except for $\alpha = 0°$, in this case the expected outcome was observed: the higher displacements are at lower angles, in which the friction force is smaller and thus it dissipate less. It was also observed that for small inclinations, greater displacements are seen when a segment with constant inclination is used rather than when the full trajectory is applied; meanwhile, for large inclinations, greater displacements are seen when the full trajectory is used instead. This comparison between the two analyses shows that the well curvature combined with the buckling effect are affecting the axial behavior of the column by diminishing displacements for small angles while causing greater displacements for larger angles. This can be explained by the friction being distributed throughout the whole well: the friction at small angles is actually higher than initially thought, causing smaller displacements; meanwhile, the friction at large angles is actually lesser than initially thought, causing larger displacements. Therefore, this is an interesting result that can only be seen when a full trajectory is applied to the model and would not be seen otherwise if a segment with constant inclination was simulated instead. Also, as in Model II, the displacements dissipate due to friction and remain on a stationary value, which is the static displacement of the column.

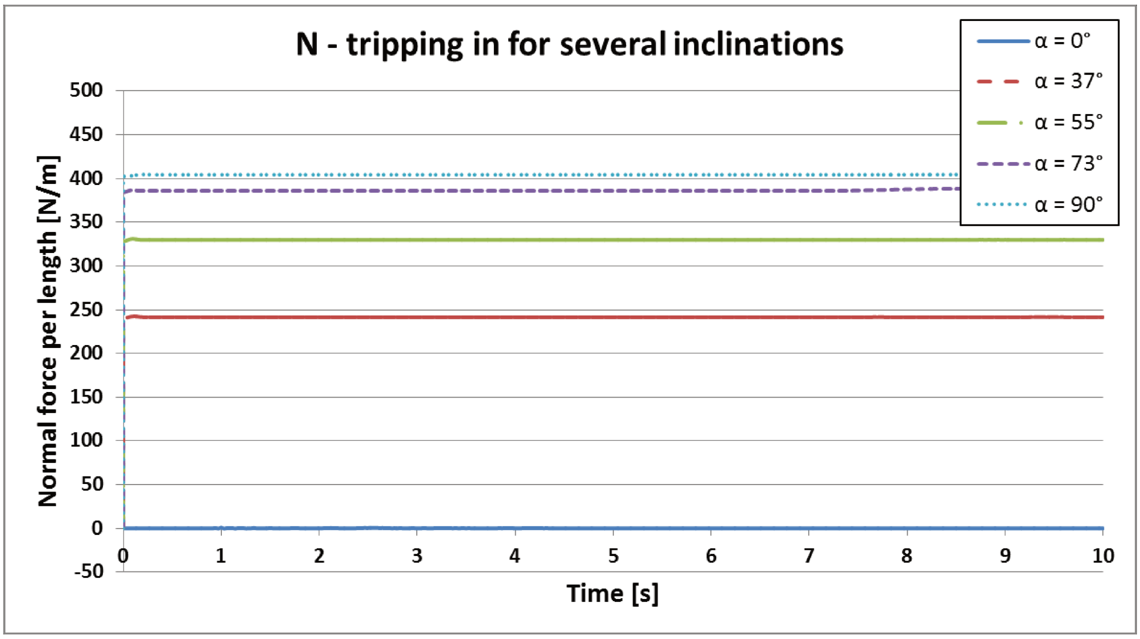

Figure 5.13: Comparison of the normal contact force per unit of length during tripping in for several inclinations, in Newton per meter, as a function of time, in seconds, for Model III. The data is taken from points located at x = *500* m, x = *1500* m, x = *2000* m, x = *2500* m and x = *3000* m.

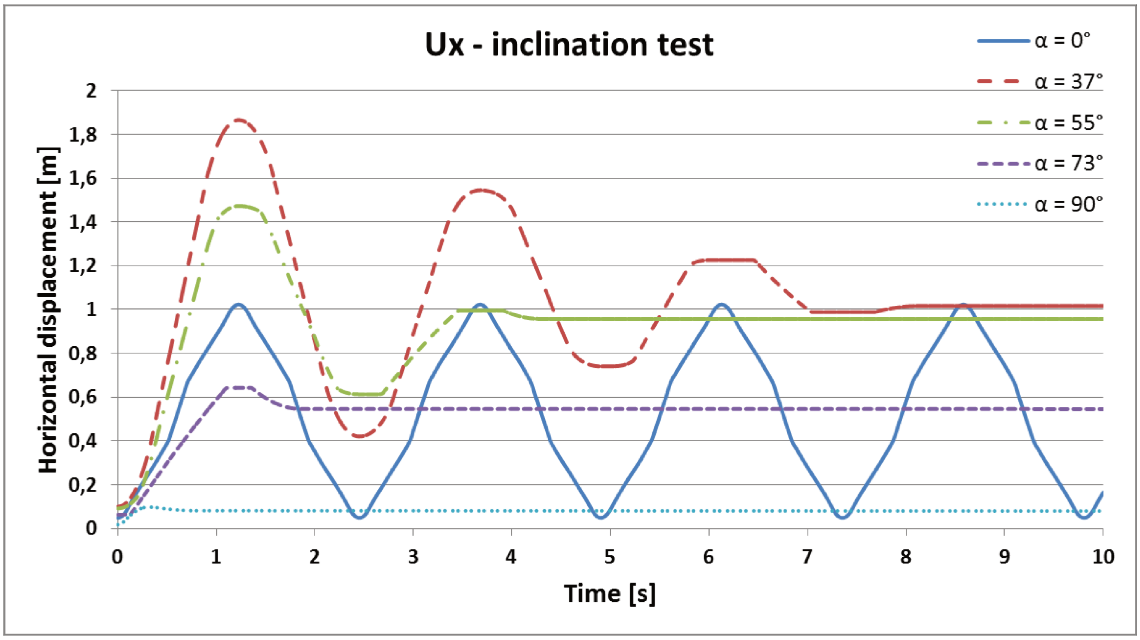

Figure 5.14: Axial displacement for different inclinations for comparison with Figures 5.11 and 5.12, in meters, as a function of time, in seconds, for Model III. The data is taken from points located at x = *500* m, x = *1500* m, x = *2000* m, x = *2500* m and x = *3000* m.

Figure 5.15 shows the angular displacement during tripping in for several inclinations. Except for $\alpha = 0°$, the results are in good agreement with Figures 5.5 and 5.6 for Models I and II. For $\alpha = 0°$, the angular displacement possesses an unusual behavior, which is to be expected considering the hypotheses of this model. As mentioned before, the column is considered to always remain in contact with the wellbore, but this may not be entirely true for the whole vertical segment where $\alpha = 0°$, despite being a good hypothesis for almost the whole range between $0°$ and $90°$. Since the angular displacement caused by this effect is not completely out-of-scale when compared with the angular displacements at other points, the results remain valid.

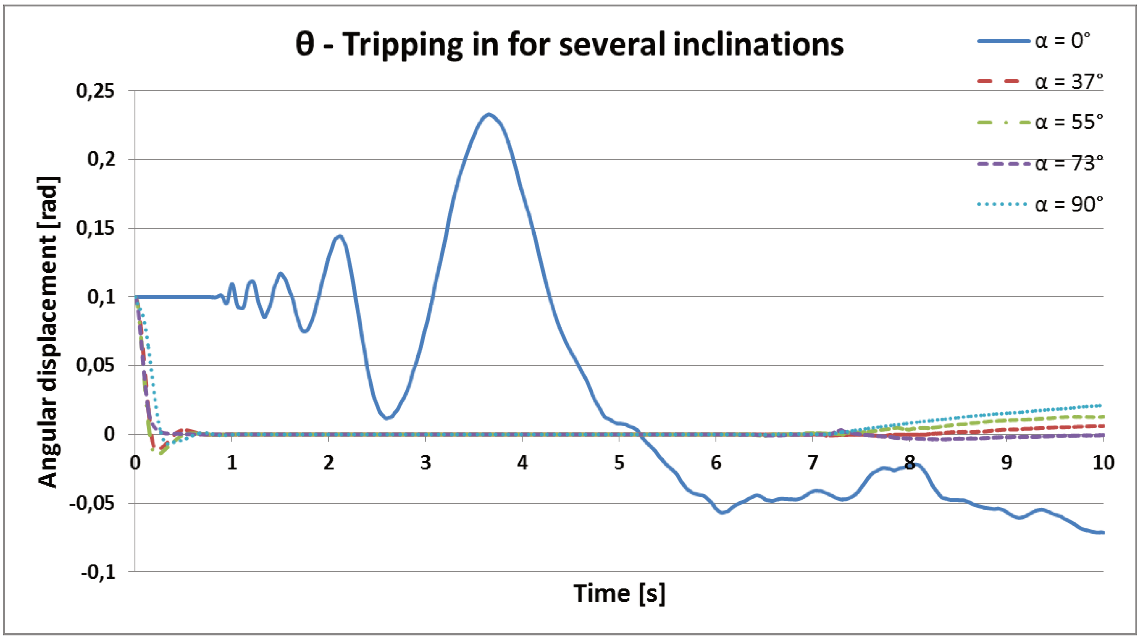

Figure 5.15: Comparison of the angular displacement during tripping in for several inclinations, in radians, as a function of time, in seconds, for Model III. The data is taken from points located at $x = 500$ m, $x = 1500$ m, $x = 2000$ m, $x = 2500$ m and $x = 3000$ m.

For a deeper analysis regarding the angle, a more refined graph can be made. Figure 5.16 shows the angular displacement for small angle values: $\alpha = 0°$, $\alpha = 2°$, $\alpha = 5°$ and $\alpha = 10°$. The effect observed on Figure 5.15 is more pronounced for angles up to $2°$; at $5°$, the angular displacement dissipates more quickly, while at $10°$ the expect behavior from Figure 5.15 already occurs. Therefore, the solution seems to be in accordance for $\alpha > 2°$, while for $\alpha < 2°$ the solution can still be used but loses precision due to the hypothesis used.

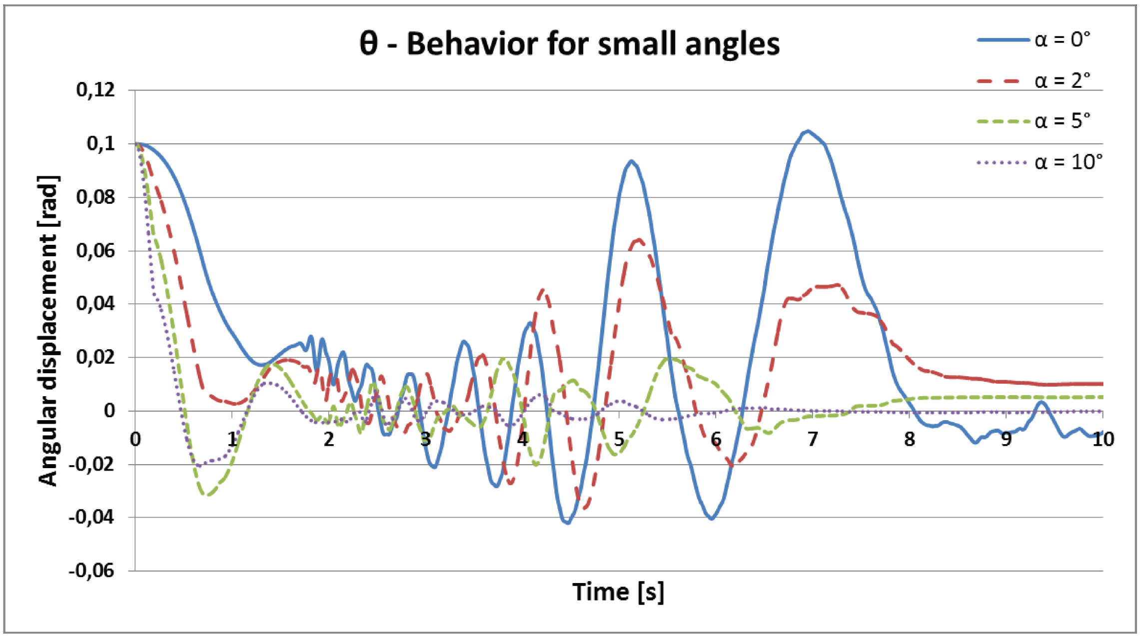

Figure 5.16: Angular displacement θ for small angles, in radians, as a function of time, in seconds, for Model III. The data is taken from points located at $x = 950$ m, $x = 980$ m, $x = 1030$ m and $x = 1100$ m.

Finally, Figure 5.17 shows the total friction force comparison during tripping in and tripping out for Model III by adding up the contributions through the whole well trajectory. Once more, the total friction force remains different for both tripping in and tripping out cases, thus further agreeing with the initial hypothesis of this work. Again, the graph was cut – now at $t = 5$ s – for the same reason as Figure 5.9.

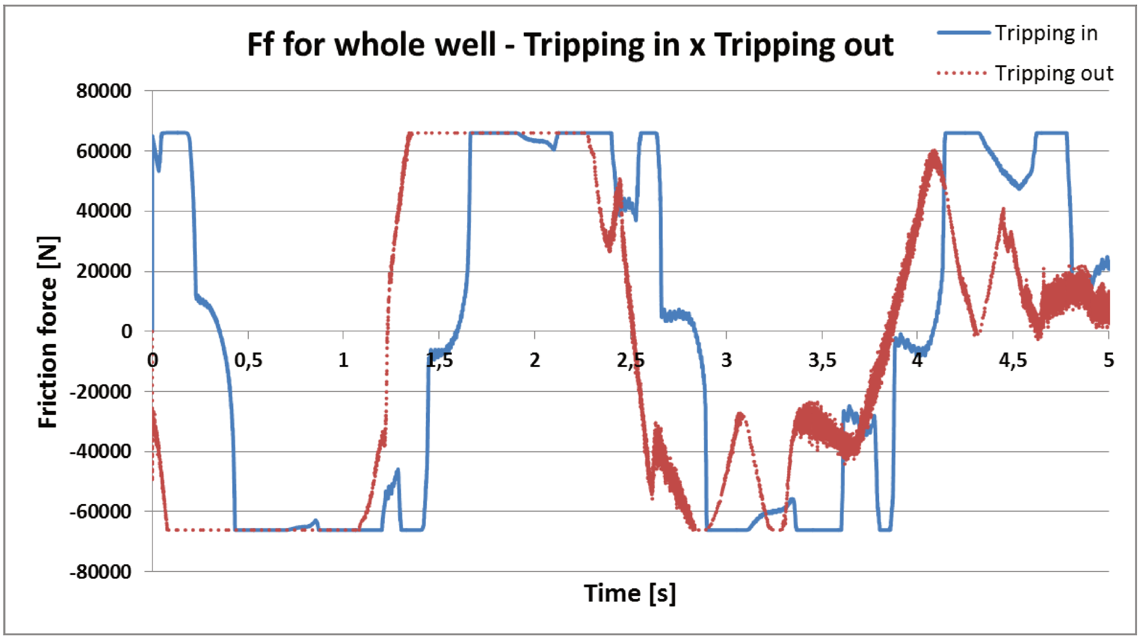

Figure 5.17: Comparison of the total friction force for the whole well trajectory during tripping in and tripping out, in Newton, as a function of time, in seconds, for Model III.

Now moving to Model IV, similar results are achieved as can be seen on Figures 5.18 and 5.19 for the horizontal displacements during tripping in and tripping out for several inclinations. The only difference regarding Models III and IV is that in Model IV the variables no longer reach a stationary value, due to the presence of a periodic excitation – the heave motion. The solution can now be divided into two parts: the transient solution, which contains the system characteristics, and the permanent solution, which contains the external periodic excitation characteristics. As can be seen on Figures 5.18 and 5.19, a periodic motion starts around *6* seconds, which is a consequence of the heave motion. For a heave amplitude of *0.5* m, it can be seen that the heave motion becomes significant on the overall response of the system.

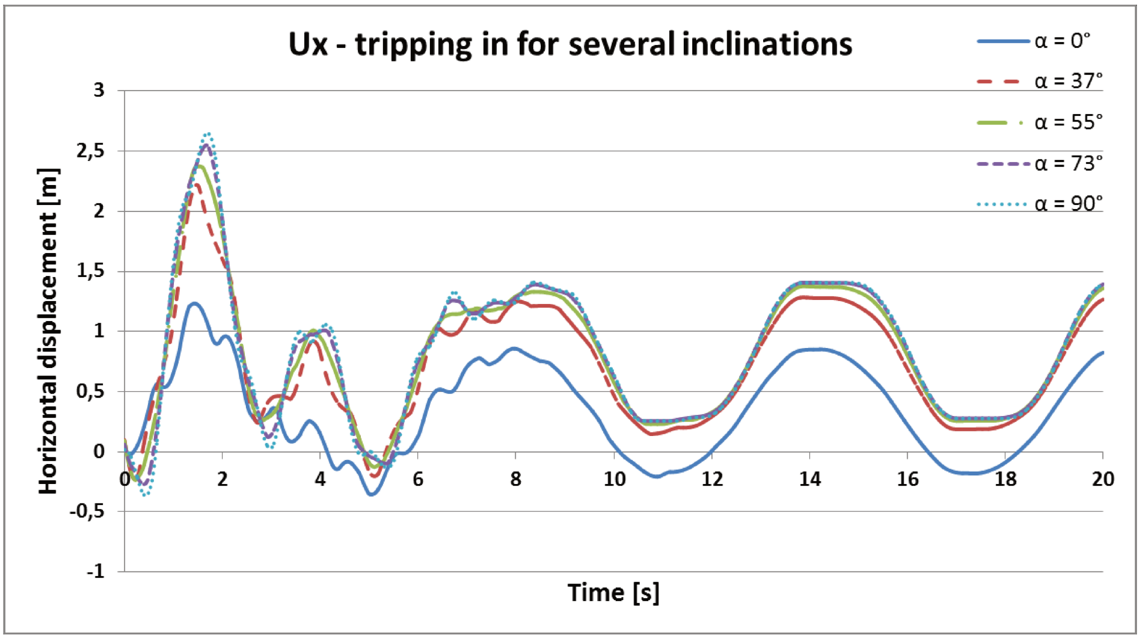

Figure 5.18: Comparison of the horizontal displacement during tripping in for several inclinations, in meters, as a function of time, in seconds, for Model IV. The data is taken from points located at x = *500* m, x = *1500* m, x = *2000* m, x = *2500* m and x = *3000* m.

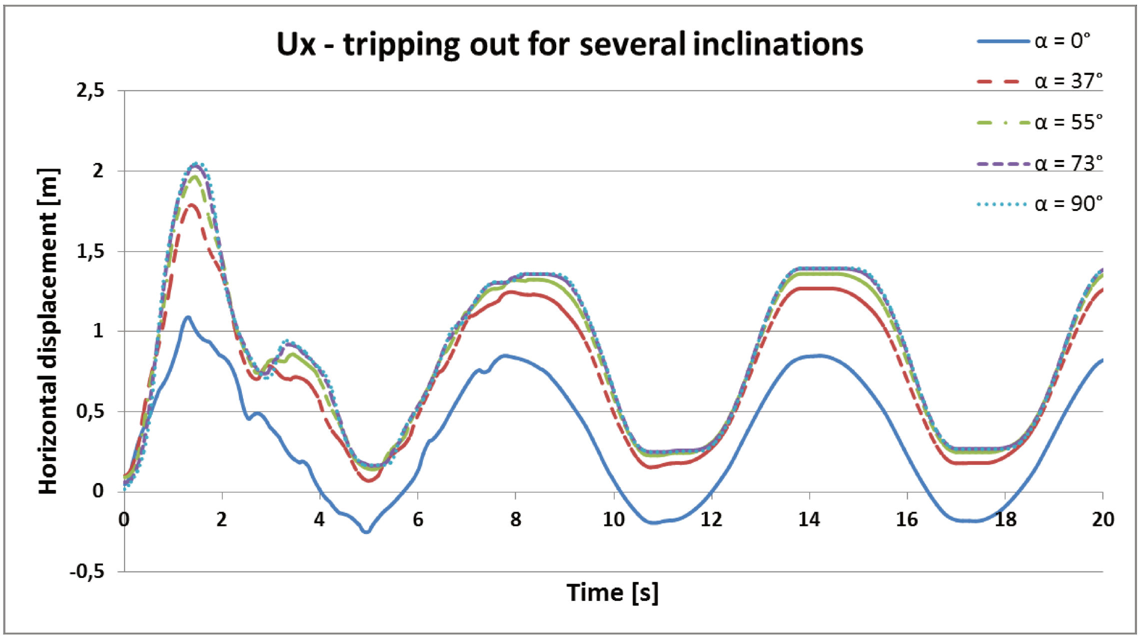

Figure 5.19: Comparison of the horizontal displacement during tripping out for several inclinations, in meters, as a function of time, in seconds, for Model IV. The data is taken from points located at x = *500* m, x = *1500* m, x = *2000* m, x = *2500* m and x = *3000* m.

Once more, the total friction force comparison during tripping in and tripping out is shown on Figure 5.20, now for Model IV. The total friction force is still different for both tripping in and tripping out cases, thus still agreeing with the initial hypothesis of this work.

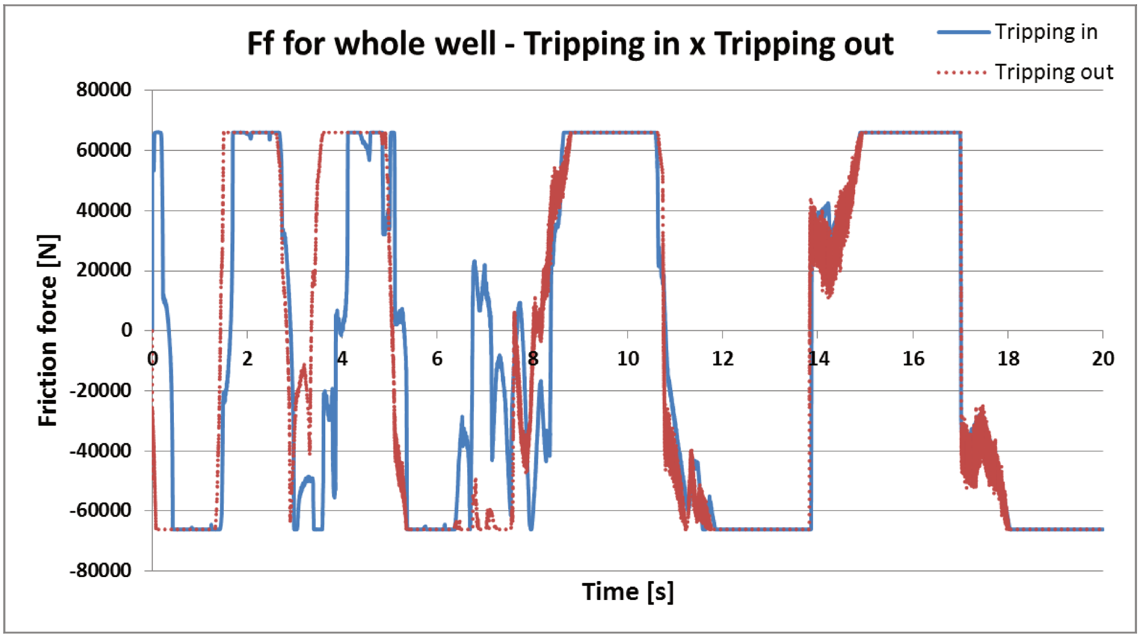

Figure 5.20: Comparison of the total friction force for the whole well trajectory during tripping in and tripping out, in Newton, as a function of time, in seconds, for Model IV.

Lastly, a quick comparison between the horizontal displacement of Models III and IV is made on Figure 5.21, by using the displacements for α = *37°*. As already explained, the only difference between the two models is the presence of a periodic motion on Model IV response once the transient part of the solution vanishes – around 6 seconds.

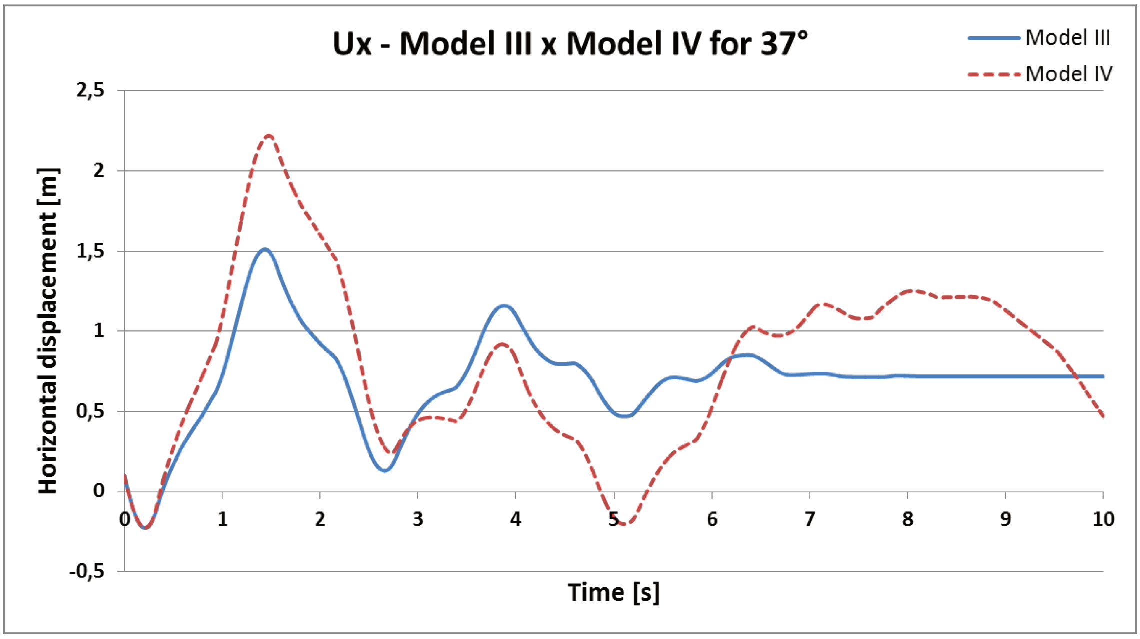

Figure 5.21: Comparison of the horizontal displacement, in meters, as a function of time, in seconds, between Models III and IV. The data is taken from a point located at $x = 1500$ m.

6. CONCLUSIONS

On the present work, a dynamic model was developed to understand the behavior of columns constrained inside directional wells during completion operations, such as running a tubing inside a cased hole, running a coiled tubing inside a tubing or running a sand screen inside an open hole. The development was done through four different models, with each one increasing the problem complexity: Model I considered a frictionless column inside a horizontal portion of well; Model II added the effect of friction to the problem; Model III considered the well inclination, thus being able to analyze the behavior of a column inside any well trajectory; and, finally, Model IV considered the effect of heave motion transmitted through the column, thus moving from an onshore to an offshore environment.

The results for Models I and II, given by Figures 5.1 through 5.10, show that, in fact, the friction force is different during tripping in and tripping out a column inside a well. Therefore, the results are in good agreement with this work initial hypothesis that the difference on the friction forces during tripping in and out is a consequence of the dynamic buckling of the column. Also, the effect of the friction force on the variables was shown: the friction dissipates the motion, thus turning a solution that was initially permanent into a transient one, with the response decaying to its static response as time passes.

The effect of the well inclination – Model III – was also seen on Figures 5.11 through 5.17. An interesting effect was observed on Figures 5.11 through 5.14: despite the normal contact force decreasing as the well inclination becomes closer to vertical – which reduces the friction force and thus would increase the horizontal displacement – a decrease on the horizontal displacement was seen instead. This is a result that can only be seen if the full well trajectory is applied to the model, in opposition to simulating separately several well segments of constant inclination. Also, the hypothesis of the column being in contact with the wellbore through its whole length is not entirely valid for angles too close to $0°$, as seen on Figures 5.15 and 5.16.

Lastly, the effect of the heave motion – Model IV – is seen on Figures 5.18 through 5.21. As discussed, the only effect that the heave causes is introducing a permanent component on the solution of this system. Instead of dissipating its motion entirely, the column remains vibrating indefinitely thanks to the heave motion, with the same angular frequency of the heave and with amplitude which varies along the column length.

Suggestions for future works

For future works, this author suggests improving the hypotheses presented through the models and/or improving the numerical discretization, leading to more accurate solutions.

- Firstly, a validation with real data is needed. Currently, data collected specifically in order to solve this problem is still taken with a static mindset – which means that no variable involved is measured as a function of time, only as a function of position. With these models, this author intend to raise awareness on the issue of dynamic buckling while also hoping to acquire real data for validating this work in the future;
- Include the effect of external and internal fluid, since they will induce both viscous damping – which attenuates the column vibration and consequently the buckling effect – and a buoyancy force;
- Consider that the column no longer needs to remain in contact with the wellbore, which is necessary not only for accurately describing vertical segments of well, but also for inclined segments, since the column may lose contact along the trajectory;
- Improve the finite difference discretization or even propose a finite elements discretization. On this work, the discretization used was of the simplest form available with the lowest order; more complex and higher-order discretizations such as Runge-Kutta can be employed to obtain more accurate results;
- Consider that the column is actually moving forward or backward – and not only vibrating around an equilibrium position – while being assembled or disassembled, respectively.
- Apply the model for similar problems – in which a column is constrained inside another column – such as on the sucker-rod pumping method, which is used for artificially lifting from a well.

REFERENCES

ANP. **Poços – Dados Estatísticos (Wells – Statistical Data) – 2012**. In: Banco de Dados de Exploração e Produção (Production and Exploration Database). Available at: http://www.bdep.gov.br/SITE/acao/download/?id=6236. Accessed on May 24, 2016.

ARFKEN, G. **Mathematical Methods For Physicists**. 3rd edition, 985 pp. San Diego: Academic Press, Inc., 1985.

ARSLAN, M.; OZBAYOGLU, E. M.; MISKA, S. Z.; YU, M.; TAKACH, N.; MITCHELL, R. F. **Buckling of Buoyancy-Assisted Tubulars**. SPE Drilling & Completion, Vol 29(4), pp 372-385, SPE 159747-PA, 2014. http://dx.doi.org/10.2118/159747-PA

BAILEY, J. J.; FINNIE, I. **An Analytical Study of Drill-String Vibration**. ASME J. Eng. Ind., Vol 82(2), pp 122-127, 1960. http://dx.doi.org/10.1115/1.3663017

BOURGOYNE, A. T.; MILLHEIM, K. K.; CHENEVERT, M. E.; YOUNG, F. S. **Applied Drilling Engineering**. SPE Textbook Series Vol. 2. 502 pp. Richardson: Society of Petroleum Engineers, 1986.

CHAKRABARTI, S. K.. **Hydrodynamics of Offshore Structures**. 464 pp. Ashurst: Wit Press / Computational Mechanics, 2003.

CHEN, Y.; LIN, Y.; CHEATHAM, J. B. **Tubing and Casing Buckling in Horizontal Wells**. Journal of Petroleum Technology, Vol 42(2), pp 140-191, SPE 19176-PA, 1990. http://dx.doi.org/10.2118/19176-PA

CHIN, W. C. **Wave Propagation in Drilling, Well Logging and Reservoir Applications**. Advances in Petroleum Engineering. 456 pp. Beverly: Scrivener Publishing, 2014.

CHUNG, J. S.; WHITNEY, A. K. **Dynamic Vertical Stretching Oscillation of an 18000 ft Ocean Mining Pipe**. Offshore Technology Conference, 4-7 May, Houston, Texas. OTC 4092-MS, 1981. http://dx.doi.org/10.4043/4092-MS

COURANT, R.; FRIEDRICHS, K.; LEWY, H. **On the Partial Difference Equations of Mathematical Physics**. Mathematische Annalen Vol 100, pp 32-74, 1928.

DAWSON, R.; PASLAY, P. R. **Drillpipe Buckling in Inclined Holes**. Journal of Petroleum Technology, Vol 36(10), pp 1734-1738, SPE 11167-PA, 1984. http://dx.doi.org/10.2118/11167-PA

FINNIE, I; BAILEY, J. J.. **An Experimental Study of Drill-String Vibration**. ASME J. Eng. Ind., Vol 82(2), pp 129-135, 1960. http://dx.doi.org/10.1115/1.3663020

FORNBERG, B. **Generation of Finite Difference Formulas on Arbitrarily Spaced Grids**. Mathematics of Computation Vol 51 Nr 184, pp 699-706, 1988. . http://dx.doi.org/10.1090/S0025-5718-1988-0935077-0

GAO, G.; MISKA, S. **Dynamic Buckling and Snaking Motion of Rotating Drilling Pipe in a Horizontal Well**. SPE Journal, Vol 15(3) pp 867-877, SPE 113883-PA, 2010a. http://dx.doi.org/10.2118/113883-PA

GAO, G.; MISKA, S. **Effects of Boundary Conditions and Friction on Static Buckling of Pipe in a Horizontal Well**. SPE Journal, Vol 14(4) pp 782-796, SPE 111511-PA, 2009. http://dx.doi.org/10.2118/111511-PA

GAO, G.; MISKA, S. **Effects of Friction on Post-Buckling Behavior and Axial Load Transfer in a Horizontal Well**. SPE Production and Operations Symposium, 4-8 April, Oklahoma City, Oklahoma, SPE 120084-MS, 2010b. http://dx.doi.org/10.2118/120084-MS

HAN, S. M.; BENAROYA, H. **Nonlinear and Stochastic Dynamics of Compliant Offshore Structures**. Solid Mechanics and Its Applications. 274 pp. Dordrecht: Springer Science+Business Media Dordrecht, 2002.

HE, X.; KYLLINGSTAD, A. **Helical Buckling and Lock-up Conditions for Coiled Tubing in Curved Wells**. SPE Drilling & Completion, Vol 10(1), pp 10-15, SPE 25370-PA, 1995. http://dx.doi.org/10.2118/25370-PA

HUANG, W.; GAO, D.; WEI, S.; CHEN, P. **Boundary Conditions A Key Factor In Tubular-String Buckling**. SPE Journal, Vol 20(6), pp 1409-1420, SPE 174087-PA, 2015. http://dx.doi.org/10.2118/174087-PA

HUANG, W.; GAO, D.; LIU, F. **Buckling Analysis of Tubular Strings in Horizontal Wells**. SPE Journal, Vol 20(2), pp 405-416, SPE 171551-PA, 2015. http://dx.doi.org/10.2118/171551-PA

LEVEQUE, R. J. **Finite Difference Methods for Differential Equations**. University of Washington, AMath 585-586 Notes, 2005.

LUBINSKI, A.; ALTHOUSE, W. S.; LOGAN, J. J. **Helical Buckling of Tubing Sealed in Packers**. Petroleum Transactions, Vol 14(6), pp 655-670, SPE 178-PA, 1962. http://dx.doi.org/10.2118/178-PA

MISKA, S.; CUNHA, J. C. **An Analysis of Helical Buckling of Tubulars Subjected to Axial and Torsional Loading in Inclined Wellbores**. SPE Production Operations Symposium, 2-4 April, Oklahoma City, Oklahoma, SPE 29460-MS, 1995. http://dx.doi.org/10.2118/29460-MS

MITCHELL, R. F. **A Buckling Criterion for Constant-Curvature Wellbores**. SPE Journal, Vol 4(4), pp 349-352, SPE 57896-PA, 1999. http://dx.doi.org/10.2118/57896-PA

MITCHELL, R. F. **Buckling Analysis in Deviated Wells - A Practical Method**. SPE Annual Technical Conference and Exhibition, 6-9 October, Denver, Colorado, SPE 36761-MS, 1996a. http://dx.doi.org/10.2118/36761-MS

MITCHELL, R. F. **Comprehensive Analysis of Buckling with Friction**. SPE Drilling & Completion, Vol 11(3), pp 178-184, SPE 29457-PA, 1996b. http://dx.doi.org/10.2118/29457-PA

MITCHELL, R. F. **Effects of Well Deviation on Helical Buckling**. SPE Drilling & Completion, Vol 12(1), pp 63-70, SPE 29462-PA, 1997. http://dx.doi.org/10.2118/29462-PA

MITCHELL, R. F. **Exact Analytic Solutions for Pipe Buckling in Vertical and Horizontal Wells**. SPE Journal, Vol 7(4), pp 373-390, SPE 72079-PA, 2002. http://dx.doi.org/10.2118/72079-PA

MITCHELL, R. F. **New Concepts for Helical Buckling**. SPE Drilling Engineering, Vol 3(3), pp 303-310, SPE 15470-PA, 1988. http://dx.doi.org/10.2118/15470-PA

MITCHELL, R. F. **Simple Frictional Analysis of Helical Buckling of Tubing**. SPE Drilling Engineering, Vol 1(6), pp 457-465, SPE 13064-PA, 1986. http://dx.doi.org/10.2118/13064-PA

MITCHELL, R. F. **The Effect of Friction on Initial Buckling of Tubing and Flowlines**. SPE Drilling & Completions, Vol 22(2), pp 112-118, SPE 99099-PA, 2007. http://dx.doi.org/10.2118/99099-PA

MITCHELL, R. F. **Tubing Buckling - The State of the Art**. SPE Drilling & Completions, Vol 23(4), SPE 104267-PA, 2008. http://dx.doi.org/10.2118/104267-PA

NIEDZWECKI, J. M.; THAMPI, S. K. **Heave Response of Long Riserless Drill Strings**. Ocean Engineering, Vol 15(5), pp 457-469, 1988. http://dx.doi.org/10.1016/0029-8018(88)90010-8

PARK, H. I.; HONG, Y. P.; NAKAMURA, M. KOTERAYAMA, W. **An Experimental Study on Transverse Vibrations of A Highly Flexible Free-Hanging Pipe in Water**. Proceedings of the The Twelfth International Offshore and Polar Engineering Conference, 26-31 May, Kitakyushu, Japan, 2002.

PASLAY, P. R.; BOGY, D. B. **The Stability of a Circular Rod Laterally Constrained to be in Contact with an Inclined Circular Cylinder**. ASME J. Appl. Mech, Vol 31(4), pp 605-610, 1964. http://dx.doi.org/10.1115/1.3629721

QIU, W.; MISKA, S.; VOLK, L. **Drill Pipe & Coiled Tubing Buckling Analysis in a Hole of Constant Curvature**. SPE Permian Basin Oil and Gas Recovery Conference, 23-26 March, Midland, Texas, SPE 39795-MS, 1998. http://dx.doi.org/10.2118/39795-MS

QIU, W.; MISKA, S. Z.; VOLK, L. J. **Effect of Coiled-Tubing Initial Configuration on Buckling Behavior in a Constant-Curvature Hole**. SPE Journal, Vol 4(1), pp 64-71, SPE 55682-PA, 1999. http://dx.doi.org/10.2118/55682-PA

RAO, S. S. **Vibration of Continuous Systems**. 744 pp. Hoboken: John Wiley & Sons, Inc., 2007.

ROCHA, L. A. S.; AZUAGA, D.; ANDRADE, R.; VIEIRA, J. L. B.; SANTOS, O. L. A. **Perfuração Direcional (Directional Drilling)**. 342 pp. Rio de Janeiro: Editora Interciência, 2006.

SALIÉS, J. B. **Experimental Study and Mathematical Modeling of Helical Buckling of Tubulars in Inclined Wellbores**. 1994. PhD Thesis, The University of Tulsa, Tulsa.

SPARKS, C. P.; CABILLIC, J. P.; SCHAWANN, J. **Longitudinal Resonant Behavior of Very Deep Water Risers**. Offshore Technology Conference, 3-6 May, Houston, Texas. OTC 4317-MS, 1982. http://dx.doi.org/10.4043/4317-MS

SPARKS, C. P. **Transverse Modal Vibrations of Vertical Tensioned Risers – A Simplified Analytical Approach**. Oil & Gas Science and Technology, Vol 57(1), pp 71-86, 2002. http://dx.doi.org/10.2516/ogst:2002005

STRANG, G. **Computational Science and Engineering**. 725 pp. Wellesley: Wellesley-Cambridge Press, 2007.

SUN, Y.; YU, Y.; LIU, B. **Closed form solutions for predicting static and dynamic buckling behaviors of a drillstring in a horizontal well**. European Journal of Mechanics A/Solids, Vol 49, pp 362-372, 2014. http://dx.doi.org/10.1016/j.euromechsol.2014.08.008

TIMOSHENKO, S. **Vibration Problems in Engineering**. 476 pp. Princeton: D. Van Nostrand Company, Inc., 1937.

WICKS, N.; WARDLE, B. L.; PAFITIS, D. **Horizontal cylinder-in-cylinder buckling under compression and torsion: Review and application to composite drill pipe**. International Journal of Mechanical Sciences, Vol 50(3), pp 538-549, 2007. http://dx.doi.org/10.1016/j.ijmecsci.2007.08.005

APPENDIX A – MATHEMATICAL DEDUCTION FOR MODELS I, II AND III

On this appendix, the mathematical deductions for Models I through III are shown in full detail, according to the definitions presented on chapter 3. Since Model IV only modifies a boundary condition, it is already fully explained on chapter 3.

A.1. Model I – Column without friction

The hypotheses behind this model were explained on section 3.1. Here, only the deduction of the motion equations and their solution through the finite differences method will be shown.

A.1.1. Model for tripping in

As explained before, during tripping in, the column will be subjected to compressive loads which will cause buckling. Therefore, the point C_0 from Figure 3.2(a) which is initially on the lower portion of the well with coordinates *(x, 0, -r)* will displace to the position of point *C* from Figure 3.2(b) with coordinates *(x + ux, r*sinθ, -r*cosθ)* on a certain time t. To keep the sign convention consistent, the displacement u_x is added up on Eq. (A.1), despite being negative since it is a contraction. This displacement includes the effects of axial contraction u_a and bending contraction u_b. The coordinate x is the initial position along the horizontal segment of well, the coordinate θ is the angle defined between the z axis and the normal vector $\hat{p}$ and the distance r is the difference between the well radius and the column radius – also known as clearance.

Starting from the origin defined at *(0, 0, 0)*, the position vector $\vec{r}$ between point *C* and this origin is given by Eq. (A.1):

$$\vec{r}(x,t) = (x + u_x)\hat{\imath} + r\,sin\,\theta\,\hat{\jmath} - r\,cos\,\theta\,\hat{k} \tag{A.1}$$

The unitary vector $\vec{\tau}$, tangential to the column axial axis, is defined by Eq. (A.2):

$$\vec{\tau}(x,t) = \frac{1}{c}\frac{\partial \vec{r}}{\partial x} \tag{A.2}$$

Where c is the vector norm of $\partial\vec{r}/\partial x$. Developing Eq. (A.2):

$$\vec{\tau}(x,t) = \frac{1}{c}\frac{\partial}{\partial x}\left[(x+u_x)\hat{\imath} + r\,sin\,\theta\,\hat{\jmath} - r\,cos\,\theta\,\hat{k}\right] \tag{A.3}$$

$$\vec{\tau}(x,t) = \frac{1}{c}\left[\left(1+\frac{\partial u_x}{\partial x}\right)\hat{\imath} + r\,cos\,\theta\frac{\partial\theta}{\partial x}\hat{\jmath} + r\,sin\,\theta\frac{\partial\theta}{\partial x}\hat{k}\right] \tag{A.4}$$

It is noted that the norm c is given by $\sqrt{1+r^2\frac{\partial^2\theta}{\partial x^2}}$. Considering that r is very small ($r << 1$), then $c \approx 1$. Also, $\frac{\partial u_x}{\partial x} \ll 1$, therefore this term can be neglected on the component $\hat{\imath}$. Introducing the unitary vector $\hat{q}$, corresponding to the tangential direction on the contact as seen on Figure 3.1, defined by:

$$\hat{q} = cos\,\theta\,\hat{\jmath} + sin\,\theta\,\hat{k} \tag{A.5}$$

Eq. (A.4) can be simplified by using Eq. (A.5):

$$\vec{\tau}(x,t) = \hat{\imath} + r\frac{\partial\theta}{\partial x}\hat{q} \tag{A.6}$$

As said before, Eq. (A.5) provides the unitary vector $\vec{\tau}$, which is tangential to the column axial axis for each coordinate x. In order to find the normal unitary vector to $\vec{\tau}$, namely $\vec{n}$, the derivative of $\vec{\tau}$ is taken, according to Eq. (A.7):

$$\vec{n} = \frac{1}{k}\frac{\partial\vec{\tau}}{\partial x} \tag{A.7}$$

Where k is vector norm of $\partial\vec{\tau}/\partial x$. Taking the derivative of Eq. (A.4):

$$\frac{\partial\vec{\tau}}{\partial x} = \frac{\partial}{\partial x}\left[\hat{\imath} + r\,cos\,\theta\frac{\partial\theta}{\partial x}\hat{\jmath} + r\,sin\,\theta\frac{\partial\theta}{\partial x}\hat{k}\right] \tag{A.8}$$

$$\frac{\partial \vec{\tau}}{\partial x} = -r \sin\theta \left(\frac{\partial \theta}{\partial x}\right)^2 \hat{\jmath} + r \cos\theta \frac{\partial^2 \theta}{\partial x^2} \hat{\jmath} + r \cos\theta \left(\frac{\partial \theta}{\partial x}\right)^2 \hat{k} + r \sin\theta \frac{\partial^2 \theta}{\partial x^2} \hat{k} \tag{A.9}$$

Introducing the unitary vector $\hat{p}$, corresponding to the normal direction on the contact as seen on Figure 3.1 and defined by:

$$\hat{p} = \sin\theta\, \hat{\jmath} - \cos\theta\, \hat{k} \tag{A.10}$$

Substituting Eqs. (A.5) and (A.10) into Eq. (A.9):

$$\frac{\partial \vec{\tau}}{\partial x} = -r \left(\frac{\partial \theta}{\partial x}\right)^2 \hat{p} + r \frac{\partial^2 \theta}{\partial x^2} \hat{q} \tag{A.11}$$

$$\frac{\partial \vec{\tau}}{\partial x} = k_r \hat{p} + k_\theta \hat{q} \tag{A.12}$$

Where k_r and k_θ on Eq. (A.12) are given by:

$$k_r = -r \left(\frac{\partial \theta}{\partial x}\right)^2 \tag{A.13}$$

$$k_\theta = r \frac{\partial^2 \theta}{\partial x^2} \tag{A.14}$$

Thus, the modulus k from Eq. (A.7) is given by:

$$k = \sqrt{k_r^2 + k_\theta^2} \tag{A.15}$$

Therefore, Eq. (A.7) becomes:

$$k\vec{n} = k_r \hat{p} + k_\theta \hat{q} \tag{A.16}$$

Lastly, the binormal unitary vector $\vec{b}$ – which is perpendicular to both $\vec{\tau}$ and $\vec{n}$ – is defined by Eq. (A.17):

$$\vec{b} = \vec{\tau}\ x\ \vec{n} \tag{A.17}$$

Or alternatively:

$$k\vec{b} = \vec{\tau}\ x\ k\vec{n} \tag{A.18}$$

Substituting Eqs. (A.4) and (A.9) into Eq. (A.18):

$$\begin{aligned} k\vec{b} = &\left(\hat{\imath} + r\cos\theta\frac{\partial\theta}{\partial x}\hat{\jmath} + r\sin\theta\frac{\partial\theta}{\partial x}\hat{k}\right)\ x\ \left(-r\sin\theta\left(\frac{\partial\theta}{\partial x}\right)^2\hat{\jmath}\right. \\ &\left. + r\cos\theta\frac{\partial^2\theta}{\partial x^2}\hat{\jmath} + r\cos\theta\left(\frac{\partial\theta}{\partial x}\right)^2\hat{k} + r\sin\theta\frac{\partial^2\theta}{\partial x^2}\hat{k}\right) \end{aligned} \tag{A.19}$$

$$\begin{aligned} k\vec{b} = &\, r\cos\theta\frac{\partial\theta}{\partial x}r\cos\theta\left(\frac{\partial\theta}{\partial x}\right)^2\hat{\imath} + r\cos\theta\frac{\partial\theta}{\partial x}r\sin\theta\frac{\partial^2\theta}{\partial x^2}\hat{\imath} \\ &+ r\sin\theta\frac{\partial\theta}{\partial x}r\sin\theta\left(\frac{\partial\theta}{\partial x}\right)^2\hat{\imath} - r\sin\theta\frac{\partial\theta}{\partial x}r\cos\theta\frac{\partial^2\theta}{\partial x^2}\hat{\imath} \\ &- r\cos\theta\left(\frac{\partial\theta}{\partial x}\right)^2\hat{\jmath} - r\sin\theta\frac{\partial^2\theta}{\partial x^2}\hat{\jmath} - r\sin\theta\left(\frac{\partial\theta}{\partial x}\right)^2\hat{k} \\ &+ r\cos\theta\frac{\partial^2\theta}{\partial x^2}\hat{k} \end{aligned} \tag{A.20}$$

$$\begin{aligned} k\vec{b} = &\, r^2\cos^2\theta\left(\frac{\partial\theta}{\partial x}\right)^3\hat{\imath} + r^2\sin^2\theta\left(\frac{\partial\theta}{\partial x}\right)^3\hat{\imath} - r\cos\theta\left(\frac{\partial\theta}{\partial x}\right)^2\hat{\jmath} \\ &- r\sin\theta\frac{\partial^2\theta}{\partial x^2}\hat{\jmath} - r\sin\theta\left(\frac{\partial\theta}{\partial x}\right)^2\hat{k} + r\cos\theta\frac{\partial^2\theta}{\partial x^2}\hat{k} \end{aligned} \tag{A.21}$$

$$k\vec{b} = \left[r^2\left(\frac{\partial\theta}{\partial x}\right)^3 + r^2\left(\frac{\partial\theta}{\partial x}\right)^3\right]\hat{\imath} - r\frac{\partial^2\theta}{\partial x^2}\hat{p} - r\left(\frac{\partial\theta}{\partial x}\right)^2\hat{q} \tag{A.22}$$

The term of component $\hat{\imath}$ can be neglected since it is too small when compared with the terms from components $\hat{p}$ and $\hat{q}$, since the value of *r* is very small. Using Eqs. (A.13) and (A.14) into Eq. (A.22):

$$k\vec{b} = -k_\theta\hat{p} + k_r\hat{q} \tag{A.23}$$

Up to this point, the derivatives of the position vector $\vec{r}$ were taken in respect to space. Since this is a dynamic problem, derivatives in respect to time must be taken as well. The velocity vector $\vec{v}$ will be given by Eq. (A.24):

$$\vec{v}(x,t) = \frac{\partial \vec{r}}{\partial t} \tag{A.24}$$

Substituting Eq. (A.1) into Eq. (A.24):

$$\vec{v}(x,t) = \frac{\partial}{\partial t}\left[(x+u_x)\hat{\imath} + r\,sin\,\theta\,\hat{\jmath} - r\,cos\,\theta\,\hat{k}\right] \tag{A.25}$$

$$\vec{v}(x,t) = \frac{\partial u_x}{\partial t}\hat{\imath} + r\,cos\,\theta\frac{\partial \theta}{\partial t}\hat{\jmath} + r\,sin\,\theta\frac{\partial \theta}{\partial t}\hat{k} \tag{A.26}$$

$$\vec{v}(x,t) = \frac{\partial u_x}{\partial t}\hat{\imath} + r\frac{\partial \theta}{\partial t}\hat{q} \tag{A.27}$$

Both Eq. (A.5) and the knowledge that $\partial x/\partial t = 0$, since *x* is an independent coordinate, were used. The acceleration vector $\vec{a}$ will be given by Eq. (A.28):

$$\vec{a}(x,t) = \frac{\partial \vec{v}}{\partial t} \tag{A.28}$$

Substituting Eq. (A.26) into Eq. (A.28):

$$\vec{a}(x,t) = \frac{\partial}{\partial t}\left[\frac{\partial u_x}{\partial t}\hat{\imath} + r\,cos\,\theta\frac{\partial \theta}{\partial t}\hat{\jmath} + r\,sin\,\theta\frac{\partial \theta}{\partial t}\hat{k}\right] \tag{A.29}$$

$$\begin{aligned}\vec{a}(x,t) = \frac{\partial^2 u_x}{\partial t^2}\hat{\imath} + \left[-r\,sin\,\theta\left(\frac{\partial \theta}{\partial t}\right)^2 + r\,cos\,\theta\frac{\partial^2 \theta}{\partial t^2}\right]\hat{\jmath} \\ + \left[r\,cos\,\theta\left(\frac{\partial \theta}{\partial t}\right)^2 + r\,sin\,\theta\frac{\partial^2 \theta}{\partial t^2}\right]\hat{k}\end{aligned} \tag{A.30}$$

$$\vec{a}(x,t) = \frac{\partial^2 u_x}{\partial t^2}\hat{\imath} - r\left(\frac{\partial \theta}{\partial t}\right)^2\hat{p} + r\frac{\partial^2 \theta}{\partial t^2}\hat{q} \tag{A.31}$$

Eqs. (A.5) and (A.10) were used. Since the problem is also related to the angular rotation of the column, it is necessary to define an angular velocity vector $\vec{\Omega}$, which has contributions from both the column own rotary speed ω as well as the change in direction given by the derivative of $\vec{\tau}$:

$$\vec{\Omega}(x,t) = \omega\vec{\tau} + \frac{\partial\vec{\tau}}{\partial t} \tag{A.32}$$

Substituting Eq. (A.4) into Eq. (A.32):

$$\begin{aligned}\vec{\Omega}(x,t) = \omega\left[\hat{\imath} + r\cos\theta\frac{\partial\theta}{\partial x}\hat{\jmath} + r\sin\theta\frac{\partial\theta}{\partial x}\hat{k}\right] \\ + \frac{\partial}{\partial t}\left[\hat{\imath} + r\cos\theta\frac{\partial\theta}{\partial x}\hat{\jmath} + r\sin\theta\frac{\partial\theta}{\partial x}\hat{k}\right]\end{aligned} \tag{A.33}$$

$$\begin{aligned}\vec{\Omega}(x,t) = \omega\hat{\imath} + \omega r\cos\theta\frac{\partial\theta}{\partial x}\hat{\jmath} + \omega r\sin\theta\frac{\partial\theta}{\partial x}\hat{k} - r\sin\theta\frac{\partial\theta}{\partial t}\frac{\partial\theta}{\partial x}\hat{\jmath} \\ + r\cos\theta\frac{\partial^2\theta}{\partial x\partial t}\hat{\jmath} + r\cos\theta\frac{\partial\theta}{\partial t}\frac{\partial\theta}{\partial x}\hat{k} + r\sin\theta\frac{\partial^2\theta}{\partial x\partial t}\hat{k}\end{aligned} \tag{A.34}$$

$$\vec{\Omega}(x,t) = \omega\hat{\imath} + \omega r\frac{\partial\theta}{\partial x}\hat{q} - r\frac{\partial\theta}{\partial t}\frac{\partial\theta}{\partial x}\hat{p} + r\frac{\partial^2\theta}{\partial x\partial t}\hat{q} \tag{A.35}$$

$$\vec{\Omega}(x,t) = \omega\hat{\imath} + \omega_r\hat{p} + \left(\omega r\frac{\partial\theta}{\partial x} + \omega_\theta\right)\hat{q} \tag{A.36}$$

Where ω_r and ω_θ on Eq. (A.36) are given by:

$$\omega_r = -r\frac{\partial\theta}{\partial t}\frac{\partial\theta}{\partial x} \tag{A.37}$$

$$\omega_\theta = r\frac{\partial^2\theta}{\partial x\partial t} \tag{A.38}$$

On Eq. (A.36), the terms of coordinates $\hat{p}$ and $\hat{q}$ will generate angular moments much smaller than the angular moment from coordinate $\hat{\imath}$ and thus can be neglected. Finally, in order to relate position, linear velocity, angular velocity and acceleration with forces and moments, it is necessary to calculate the linear and angular momentums of an infinitesimal column element with length *dx*. Firstly, the linear momentum:

$$\vec{P}(x,t) = m_p \vec{v} dx \tag{A.39}$$

Where m_p is the column mass per unit of length. Substituting Eq. (A.27) into Eq. (A.39):

$$\vec{P}(x,t) = m_p \frac{\partial u_x}{\partial t} dx\hat{\imath} + m_p r \frac{\partial \theta}{\partial t} dx\hat{q} \tag{A.40}$$

Then, the angular moment:

$$\vec{H}_0(x,t) = \left(m_p \vec{r}\ x\ \vec{v} + I_p \omega \vec{\tau}\right) dx \tag{A.41}$$

Where I_p is the mass moment of inertia per unit of length and is related with the area moment of inertia I through the expression $I_p = 2\rho I$, where ρ is the specific mass of the material. The cross product $\vec{r}\ x\ \vec{v}$ is too small when compared to the angular moment generated by ω and can be neglected (Gao & Miska, 2010a). Thus, neglecting this term and substituting Eq. (A.4) into Eq. (A.41):

$$\vec{H}_0(x,t) = \left[I_p \omega \left(\hat{\imath} + r\cos\theta \frac{\partial \theta}{\partial x}\hat{\jmath} + r\sin\theta \frac{\partial \theta}{\partial x}\hat{k}\right)\right] dx \tag{A.42}$$

$$\vec{H}_0(x,t) = \left[I_p \omega \hat{\imath} + I_p \omega r \frac{\partial \theta}{\partial x}\hat{q}\right] dx \tag{A.43}$$

The loads acting on the column can be seen on Figure A.1. The column will be subjected to internal forces and internal moments due to axial tension/compression and bending, respectively, and also its own weight and the normal contact force with respect to the wellbore.

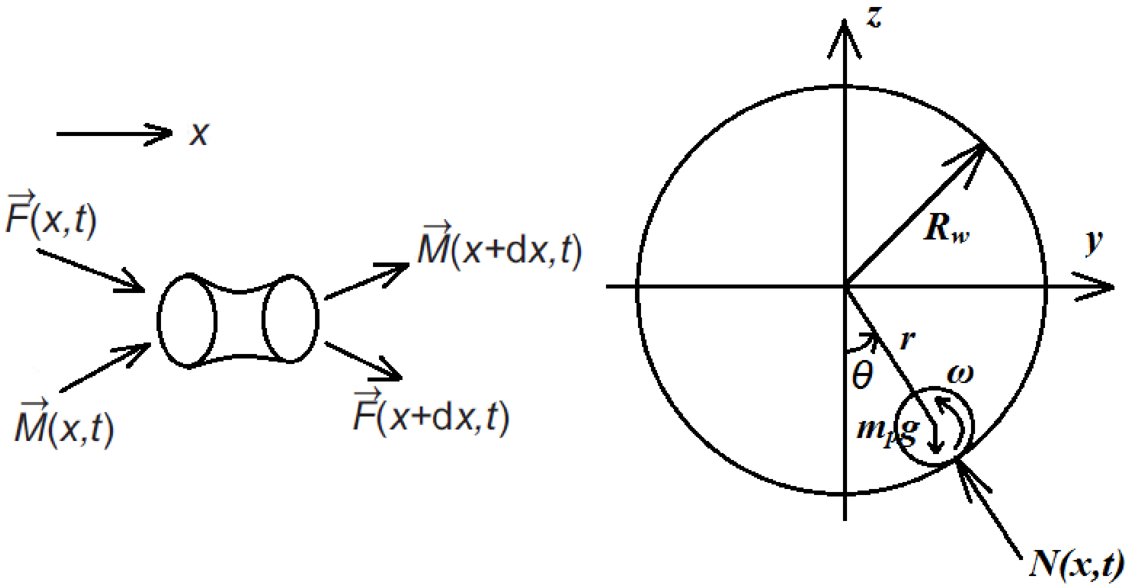

Figure A.1: Loads acting on the column. On the left side, the internal forces and moments acting on an infinitesimal element. On the right one, the weight and the normal contact force (Gao & Miska, 2010a).

The internal force $\vec{F}$ can be written as a function of either the coordinates $\hat{\imath}$, $\hat{\jmath}$ and $\hat{k}$ or $\hat{\imath}$, $\hat{p}$ and $\hat{q}$. For convenience, since the vector decomposition will be made later on the $\hat{\imath}$, $\hat{p}$ and $\hat{q}$ coordinates, $\vec{F}$ is defined as being:

$$\vec{F} = F_x\hat{\imath} + F_r\hat{p} + F_\theta\hat{q} \tag{A.44}$$

Where F_x, F_r and F_θ are the components of $\vec{F}$. To calculate the space derivative of $\vec{F}$, it can be more interesting to return to coordinates $\hat{\imath}$, $\hat{\jmath}$ and $\hat{k}$. Substituting Eqs. (A.5) and (A.10) into Eq. (A.44):

$$\vec{F} = F_x\hat{\imath} + F_r\left(\sin\theta\,\hat{\jmath} - \cos\theta\,\hat{k}\right) + F_\theta\left(\cos\theta\,\hat{\jmath} + \sin\theta\,\hat{k}\right) \tag{A.45}$$

$$\vec{F} = F_x\hat{\imath} + (F_r\sin\theta + F_\theta\cos\theta)\hat{\jmath} + (-F_r\cos\theta + F_\theta\sin\theta)\hat{k} \tag{A.46}$$

Taking the spatial derivative of Eq. (A.46):

$$\frac{\partial\vec{F}}{\partial x} = \frac{\partial}{\partial x}\left[F_x\hat{\imath} + (F_r\sin\theta + F_\theta\cos\theta)\hat{\jmath} + (-F_r\cos\theta + F_\theta\sin\theta)\hat{k}\right] \tag{A.47}$$

$$\frac{\partial \vec{F}}{\partial x} = \frac{\partial F_x}{\partial x}\hat{\imath} + \frac{\partial F_r}{\partial x} sin\,\theta\,\hat{\jmath} + F_r\,cos\,\theta\,\frac{\partial \theta}{\partial x}\hat{\jmath} + \frac{\partial F_\theta}{\partial x} cos\,\theta\,\hat{\jmath} - F_\theta\,sin\,\theta\,\frac{\partial \theta}{\partial x}\hat{\jmath} - \frac{\partial F_r}{\partial x} cos\,\theta\,\hat{k} + F_r\,sin\,\theta\,\frac{\partial \theta}{\partial x}\hat{k} + \frac{\partial F_\theta}{\partial x} sin\,\theta\,\hat{k} + F_\theta\,cos\,\theta\,\frac{\partial \theta}{\partial x}\hat{k} \tag{A.48}$$

Substituting Eqs. (A.5) and (A.10) once again:

$$\frac{\partial \vec{F}}{\partial x} = \frac{\partial F_x}{\partial x}\hat{\imath} + \left(\frac{\partial F_r}{\partial x} - F_\theta \frac{\partial \theta}{\partial x}\right)\hat{p} + \left(\frac{\partial F_\theta}{\partial x} + F_r \frac{\partial \theta}{\partial x}\right)\hat{q} \tag{A.49}$$

Similarly to the internal force $\vec{F}$, the internal moment $\vec{M}$ can be written on both sets of coordinates. There is no contribution on $\hat{\imath}$ since there is no applied torque on the column. Therefore:

$$\vec{M} = M_r\hat{p} + M_\theta\hat{q} \tag{A.50}$$

Where M_r and M_θ are the components of $\vec{M}$. Again, using the $\hat{\imath}$, $\hat{\jmath}$ and $\hat{k}$ coordinates to calculate the spatial derivative:

$$\vec{M} = M_r\left(sin\,\theta\,\hat{\jmath} - cos\,\theta\,\hat{k}\right) + M_\theta\left(cos\,\theta\,\hat{\jmath} + sin\,\theta\,\hat{k}\right) \tag{A.51}$$

$$\vec{M} = (M_r\,sin\,\theta + M_\theta\,cos\,\theta)\hat{\jmath} + (-M_r\,cos\,\theta + M_\theta\,sin\,\theta)\hat{k} \tag{A.52}$$

Taking the spatial derivative of Eq. (A.52):

$$\frac{\partial \vec{M}}{\partial x} = \frac{\partial}{\partial x}\left[(M_r\,sin\,\theta + M_\theta\,cos\,\theta)\hat{\jmath} + (-M_r\,cos\,\theta + M_\theta\,sin\,\theta)\hat{k}\right] \tag{A.53}$$

$$\frac{\partial \vec{M}}{\partial x} = \frac{\partial M_r}{\partial x} sin\,\theta\,\hat{\jmath} + M_r\,cos\,\theta\,\frac{\partial \theta}{\partial x}\hat{\jmath} + \frac{\partial M_\theta}{\partial x} cos\,\theta\,\hat{\jmath} - M_\theta\,sin\,\theta\,\frac{\partial \theta}{\partial x}\hat{\jmath} - \frac{\partial M_r}{\partial x} cos\,\theta\,\hat{k} + M_r\,sin\,\theta\,\frac{\partial \theta}{\partial x}\hat{k} + \frac{\partial M_\theta}{\partial x} sin\,\theta\,\hat{k} + M_\theta\,cos\,\theta\,\frac{\partial \theta}{\partial x}\hat{k} \tag{A.54}$$

Substituting again Eqs. (A.5) and (A.10):

$$\frac{\partial \vec{M}}{\partial x} = \left(\frac{\partial M_r}{\partial x} - M_\theta \frac{\partial \theta}{\partial x}\right)\hat{p} + \left(\frac{\partial M_\theta}{\partial x} + M_r \frac{\partial \theta}{\partial x}\right)\hat{q} \tag{A.55}$$

The column own weight per unit of length $\vec{q}_p$ acts on the central axis and on the negative direction of the z axis. Therefore:

$$\vec{q}_p = -m_p g dx \hat{k} \tag{A.56}$$

Where, once more, m_p is the column mass per unit of length, g is the gravitational acceleration and dx is the length of an infinitesimal element. Changing to $\hat{p}$ and $\hat{q}$ coordinates once more:

$$\vec{q}_p = m_p g dx \cos\theta\, \hat{p} - m_p g dx \sin\theta\, \hat{q} \tag{A.57}$$

It can be noted that $\hat{k} = \cos\theta\, \hat{p} - \sin\theta\, \hat{q}$ by using Eqs. (A.5) and (A.10). The normal contact force is already aligned to $\hat{p}$ but on the opposite direction defined on Figure 3.1. Therefore:

$$\vec{N} = -N dx \hat{p} \tag{A.58}$$

Where N is the normal contact force per unit of length – thus having units of N/m. The total external force per unit of length is obtained by adding them up:

$$\vec{f} = \frac{\vec{q}_p}{dx} + \frac{\vec{N}}{dx} \tag{A.59}$$

Substituting Eqs. (A.57) and (A.58) into Eq. (A.59):

$$\vec{f} = \left(m_p g \cos\theta - N\right)\hat{p} - m_p g \sin\theta\, \hat{q} \tag{A.60}$$

From the Strength of Materials, it is known that internal forces and internal moments are directly tied to displacements and strains. Defining the total axial displacement u_x as being:

$$u_x = u_a + u_b \tag{A.61}$$

Where u_a is the axial displacement caused by axial tension and compression and u_b is the axial displacement caused due to bending. The displacement u_a comes from Hooke's Law:

$$F_x(x,t) = -EA\frac{\partial u_a}{\partial x} \tag{A.62}$$

Where E is the material Young's modulus and A is the cross sectional area. The displacement u_b can be obtained by (Gao & Miska, 2010a):

$$u_b = -\frac{1}{2}r^2\int_0^x \left(\frac{\partial\theta}{\partial x}\right)^2 dx \tag{A.63}$$

Taking the spatial derivative of Eq. (A.61) and substituting Eqs. (A.62) and (A.63), with r constant:

$$\frac{\partial u_x}{\partial x} = \frac{\partial u_a}{\partial x} + \frac{\partial u_b}{\partial x} \tag{A.64}$$

$$\frac{\partial u_x}{\partial x} = -\frac{F_x(x,t)}{EA} - \frac{1}{2}r^2\left(\frac{\partial\theta}{\partial x}\right)^2 \tag{A.65}$$

$$F_x(x,t) = -EA\frac{\partial u_x}{\partial x} - \frac{1}{2}EAr^2\left(\frac{\partial\theta}{\partial x}\right)^2 \tag{A.66}$$

Meanwhile, the bending moment can be obtained through its relation with the curvature radius, in this case given by the binormal vector (Gao & Miska, 2010a):

$$\vec{M}(x,t) = -EIk\vec{b} \tag{A.67}$$

Where I is the area moment of inertia. Substituting Eq. (A.22) into Eq. (A.67):

$$\vec{M}(x,t) = -EI\left[-r\frac{\partial^2\theta}{\partial x^2}\hat{p} - r\left(\frac{\partial\theta}{\partial x}\right)^2\hat{q}\right] \tag{A.68}$$

$$\vec{M}(x,t) = EIr\frac{\partial^2\theta}{\partial x^2}\hat{p} + EIr\left(\frac{\partial\theta}{\partial x}\right)^2\hat{q} \tag{A.69}$$

Comparing Eq. (A.69) with Eq. (A.50), it can be concluded that:

$$M_r = EIr\frac{\partial^2\theta}{\partial x^2} \tag{A.70}$$

$$M_\theta = EIr\left(\frac{\partial\theta}{\partial x}\right)^2 \tag{A.71}$$

Now that the loads and linear and angular momentums were defined, it is time to apply Newton's Second Law to find the motion equations for the column. Starting with the linear momentum:

$$\sum \vec{F}_i = \frac{\partial\vec{P}}{\partial t} \tag{A.72}$$

Substituting Eq. (A.39) into Eq. (A.72) and introducing the loads defined previously according to the convention of Figure A.1:

$$\vec{F} - \left(\vec{F} + \frac{\partial\vec{F}}{\partial x}dx\right) + \vec{f}dx = m_p\frac{\partial\vec{v}}{\partial t}dx \tag{A.73}$$

Simplifying Eq. (A.73):

$$\frac{\partial\vec{F}}{\partial x} - \vec{f} + m_p\frac{\partial\vec{v}}{\partial t} = 0 \tag{A.74}$$

Substituting Eqs. (A.31), (A.49) and (A.60) into Eq. (A.74):

$$\frac{\partial F_x}{\partial x}\hat{\imath}+\left(\frac{\partial F_r}{\partial x}-F_\theta\frac{\partial\theta}{\partial x}\right)\hat{p}+\left(\frac{\partial F_\theta}{\partial x}+F_r\frac{\partial\theta}{\partial x}\right)\hat{q}-\left(m_p g\cos\theta-N\right)\hat{p}+m_p g\sin\theta\,\hat{q}+m_p\left[\frac{\partial^2 u_x}{\partial t^2}\hat{\imath}-r\left(\frac{\partial\theta}{\partial t}\right)^2\hat{p}+r\frac{\partial^2\theta}{\partial t^2}\hat{q}\right]=0 \tag{A.75}$$

$$\left(\frac{\partial F_x}{\partial x}+m_p\frac{\partial^2 u_x}{\partial t^2}\right)\hat{\imath}+\left(\frac{\partial F_r}{\partial x}-F_\theta\frac{\partial\theta}{\partial x}+N-m_p g\cos\theta-m_p r\left(\frac{\partial\theta}{\partial t}\right)^2\right)\hat{p}+\left(\frac{\partial F_\theta}{\partial x}+F_r\frac{\partial\theta}{\partial x}+m_p g\sin\theta+m_p r\frac{\partial^2\theta}{\partial t^2}\right)\hat{q}=0 \tag{A.76}$$

Separating Eq. (A.76) into components $\hat{\imath}$, $\hat{p}$ and $\hat{q}$:

$$\frac{\partial F_x}{\partial x}+m_p\frac{\partial^2 u_x}{\partial t^2}=0 \tag{A.77}$$

$$\frac{\partial F_r}{\partial x}-F_\theta\frac{\partial\theta}{\partial x}+N-m_p g\cos\theta-m_p r\left(\frac{\partial\theta}{\partial t}\right)^2=0 \tag{A.78}$$

$$\frac{\partial F_\theta}{\partial x}+F_r\frac{\partial\theta}{\partial x}+m_p g\sin\theta+m_p r\frac{\partial^2\theta}{\partial t^2}=0 \tag{A.79}$$

Substituting Eq. (A.66) into Eq. (A.77):

$$\frac{\partial}{\partial x}\left[-EA\frac{\partial u_x}{\partial x}-\frac{1}{2}EAr^2\left(\frac{\partial\theta}{\partial x}\right)^2\right]+m_p\frac{\partial^2 u_x}{\partial t^2}=0 \tag{A.80}$$

Manipulating Eq. (A.80), a motion equation relating the axial displacement u_x and the angular displacement θ is found:

$$EA\frac{\partial^2 u_x}{\partial x^2}-m_p\frac{\partial^2 u_x}{\partial t^2}+EAr^2\frac{\partial\theta}{\partial x}\frac{\partial^2\theta}{\partial x^2}=0 \tag{A.81}$$

Eq. (A.81) still has two unknowns; another equation is needed to calculate the two displacements. It can be obtained also from Newton's Second Law, but now applied to moments:

$$\sum_i \vec{M} = \frac{\partial \vec{H}_0}{\partial t} \tag{A.82}$$

Substituting the simplified Eq. (A.41) on Eq. (A.82) and introducing the loads defined previously according to the convention of Figure A.1:

$$\vec{M} - \left(\vec{M} + \frac{\partial \vec{M}}{\partial x} dx\right) - \vec{r}\ x\ \vec{F} = \frac{\partial}{\partial t}\left(I_p \omega \vec{\tau} dx\right) \tag{A.83}$$

Simplifying Eq. (A.83) and taking the spatial derivative of $\vec{r}$:

$$\frac{\partial \vec{M}}{\partial x} + \vec{\tau}\ x\ \vec{F} + I_p \omega \frac{\partial \vec{\tau}}{\partial t} = 0 \tag{A.84}$$

Substituting Eqs. (A.6), (A.44) and (A.55) and a part of Eq. (A.36) into Eq. (A.84):

$$\begin{aligned}\left(\frac{\partial M_r}{\partial x} - M_\theta \frac{\partial \theta}{\partial x}\right)\hat{p} + \left(\frac{\partial M_\theta}{\partial x} + M_r \frac{\partial \theta}{\partial x}\right)\hat{q} \\ + \left(\hat{\imath} + r\frac{\partial \theta}{\partial x}\hat{q}\right) x\ (F_x \hat{\imath} + F_r \hat{p} + F_\theta \hat{q}) \\ + I_p \omega(\omega_r \hat{p} + \omega_\theta \hat{q}) = 0\end{aligned} \tag{A.85}$$

$$\begin{aligned}\left(-F_r r \frac{\partial \theta}{\partial x}\right)\hat{\imath} + \left(\frac{\partial M_r}{\partial x} - M_\theta \frac{\partial \theta}{\partial x} + F_x r \frac{\partial \theta}{\partial x} - F_\theta + I_p \omega \omega_r\right)\hat{p} \\ + \left(\frac{\partial M_\theta}{\partial x} + M_r \frac{\partial \theta}{\partial x} + F_r + I_p \omega \omega_\theta\right)\hat{q} = 0\end{aligned} \tag{A.86}$$

Separating Eq. (A.86) into components $\hat{\imath}$, $\hat{p}$ and $\hat{q}$:

$$-F_r r \frac{\partial \theta}{\partial x} = 0 \tag{A.87}$$

$$\frac{\partial M_r}{\partial x} - M_\theta \frac{\partial \theta}{\partial x} + F_x r \frac{\partial \theta}{\partial x} - F_\theta + I_p \omega \omega_r = 0 \tag{A.88}$$

$$\frac{\partial M_\theta}{\partial x} + M_r \frac{\partial \theta}{\partial x} + F_r + I_p \omega \omega_\theta = 0 \tag{A.89}$$

Eq. (A.87) does not give much information; meanwhile, Eqs. (A.88) and (A.89) can be further developed. Substituting Eqs. (A.70) and (A.71) into Eq. (A.88):

$$\frac{\partial}{\partial x}\left[EIr\frac{\partial^2\theta}{\partial x^2}\right]-\left[EIr\left(\frac{\partial\theta}{\partial x}\right)^2\right]\frac{\partial\theta}{\partial x}+F_x r\frac{\partial\theta}{\partial x}-F_\theta+I_p\omega\omega_r=0 \tag{A.90}$$

Isolating the F_θ component:

$$EIr\left[\frac{\partial^3\theta}{\partial x^3}-\left(\frac{\partial\theta}{\partial x}\right)^3\right]+F_x r\frac{\partial\theta}{\partial x}-F_\theta+I_p\omega\omega_r=0 \tag{A.91}$$

$$F_\theta=EIr\left[\frac{\partial^3\theta}{\partial x^3}-\left(\frac{\partial\theta}{\partial x}\right)^3\right]+F_x r\frac{\partial\theta}{\partial x}+I_p\omega\omega_r \tag{A.92}$$

Once more, substituting Eqs. (A.70) and (A.71) but now on Eq. (A.89):

$$\frac{\partial}{\partial x}\left[EIr\left(\frac{\partial\theta}{\partial x}\right)^2\right]+\left[EIr\frac{\partial^2\theta}{\partial x^2}\right]\frac{\partial\theta}{\partial x}+F_r+I_p\omega\omega_\theta=0 \tag{A.93}$$

Isolating the F_r component:

$$3EIr\frac{\partial\theta}{\partial x}\frac{\partial^2\theta}{\partial x^2}+F_r+I_p\omega\omega_\theta=0 \tag{A.94}$$

$$F_r=-3EIr\frac{\partial\theta}{\partial x}\frac{\partial^2\theta}{\partial x^2}-I_p\omega\omega_\theta \tag{A.95}$$

Now, by knowing components F_r and F_θ, substituting Eqs. (A.92) and (A.95) into Eq. (A.78):

$$\begin{aligned}\frac{\partial}{\partial x}&\left[-3EIr\frac{\partial\theta}{\partial x}\frac{\partial^2\theta}{\partial x^2}-I_p\omega\omega_\theta\right]\\&-\left[EIr\left[\frac{\partial^3\theta}{\partial x^3}-\left(\frac{\partial\theta}{\partial x}\right)^3\right]+F_x r\frac{\partial\theta}{\partial x}+I_p\omega\omega_r\right]\frac{\partial\theta}{\partial x}+N\\&-m_p g\cos\theta-m_p r\left(\frac{\partial\theta}{\partial t}\right)^2=0\end{aligned} \tag{A.96}$$

Isolating for the normal contact force per unit of length N:

$$EIr\left[\left(\frac{\partial\theta}{\partial x}\right)^4 - 3\left(\frac{\partial^2\theta}{\partial x^2}\right)^2 - 4\frac{\partial^3\theta}{\partial x^3}\frac{\partial\theta}{\partial x}\right] - F_x r\left(\frac{\partial\theta}{\partial x}\right)^2 - I_p\omega\left[\frac{\partial\omega_\theta}{\partial x} + \omega_r\frac{\partial\theta}{\partial x}\right] + N - m_p g\cos\theta - m_p r\left(\frac{\partial\theta}{\partial t}\right)^2 = 0 \quad \text{(A.97)}$$

$$N(x,t) = -EIr\left[\left(\frac{\partial\theta}{\partial x}\right)^4 - 3\left(\frac{\partial^2\theta}{\partial x^2}\right)^2 - 4\frac{\partial^3\theta}{\partial x^3}\frac{\partial\theta}{\partial x}\right] + F_x r\left(\frac{\partial\theta}{\partial x}\right)^2 + I_p\omega\left[\frac{\partial\omega_\theta}{\partial x} + \omega_r\frac{\partial\theta}{\partial x}\right] + m_p g\cos\theta + m_p r\left(\frac{\partial\theta}{\partial t}\right)^2 \quad \text{(A.98)}$$

Lastly, repeating the procedure for Eq. (A.79):

$$\frac{\partial}{\partial x}\left[EIr\left[\frac{\partial^3\theta}{\partial x^3} - \left(\frac{\partial\theta}{\partial x}\right)^3\right] + F_x r\frac{\partial\theta}{\partial x} + I_p\omega\omega_r\right] + \left[-3EIr\frac{\partial\theta}{\partial x}\frac{\partial^2\theta}{\partial x^2} - I_p\omega\omega_\theta\right]\frac{\partial\theta}{\partial x} + m_p g\sin\theta + m_p r\frac{\partial^2\theta}{\partial t^2} = 0 \quad \text{(A.99)}$$

Simplifying Eq. (A.99), an equation for the angular displacement is obtained:

$$EIr\left[\frac{\partial^4\theta}{\partial x^4} - 6\left(\frac{\partial\theta}{\partial x}\right)^2\frac{\partial^2\theta}{\partial x^2}\right] + r\left[F_x\frac{\partial^2\theta}{\partial x^2} + \frac{\partial F_x}{\partial x}\frac{\partial\theta}{\partial x}\right] + I_p\omega\left[\frac{\partial\omega_r}{\partial x} - \omega_\theta\frac{\partial\theta}{\partial x}\right] + m_p g\sin\theta + m_p r\frac{\partial^2\theta}{\partial t^2} = 0 \quad \text{(A.100)}$$

It is possible to simplify even further Eqs. (A.98) and (A.100) by usage of Eqs. (A.37), (A.38) and (A.66):

$$\begin{aligned}N(x,t) = &-EIr\left[\left(\frac{\partial\theta}{\partial x}\right)^4 - 3\left(\frac{\partial^2\theta}{\partial x^2}\right)^2 - 4\frac{\partial^3\theta}{\partial x^3}\frac{\partial\theta}{\partial x}\right] \\ &- EAr\left[\frac{\partial u_x}{\partial x}\left(\frac{\partial\theta}{\partial x}\right)^2 + \frac{1}{2}r^2\left(\frac{\partial\theta}{\partial x}\right)^4\right] \\ &+ I_p r\omega\left[\frac{\partial^3\theta}{\partial x^2\partial t} - \frac{\partial\theta}{\partial t}\left(\frac{\partial\theta}{\partial x}\right)^2\right] + m_p g\cos\theta \\ &+ m_p r\left(\frac{\partial\theta}{\partial t}\right)^2\end{aligned} \tag{A.101}$$

$$\begin{aligned}&EIr\left[\frac{\partial^4\theta}{\partial x^4} - 6\left(\frac{\partial\theta}{\partial x}\right)^2\frac{\partial^2\theta}{\partial x^2}\right] \\ &\quad - EAr\left[\frac{\partial u_x}{\partial x}\frac{\partial^2\theta}{\partial x^2} + \frac{\partial^2 u_x}{\partial x^2}\frac{\partial\theta}{\partial x} + \frac{3}{2}r^2\frac{\partial^2\theta}{\partial x^2}\left(\frac{\partial\theta}{\partial x}\right)^2\right] \\ &\quad - I_p r\omega\left[2\frac{\partial^2\theta}{\partial x\partial t}\frac{\partial\theta}{\partial x} + \frac{\partial\theta}{\partial t}\frac{\partial^2\theta}{\partial x^2}\right] + m_p g\sin\theta \\ &\quad + m_p r\frac{\partial^2\theta}{\partial t^2} = 0\end{aligned} \tag{A.102}$$

Summing up, the final problem consists of four equations to determine four unknowns: Eqs. (A.66), (A.81), (A.101) and (A.102) which relate F_x, u_x, N and θ.

A.1.2. Model for tripping out

As explained before, for the problem of tripping out the equations previously presented are severely simplified. This happens because the column does not suffer buckling and thus remains in contact with the lowest portion of the well for its whole length and for the whole time. During tripping out, the point C_0 from Figure 3.2(a) displaces itself from $(x, 0, -r)$ to $(x + u_x, 0, -r)$. On this case, the position vector $\vec{r}$ is given by:

$$\vec{r}(x,t) = (x + u_x)\hat{\imath} - r\hat{k} \tag{A.103}$$

The procedure now is similar than before, but some steps are no longer needed. Firstly, the unitary vector $\vec{\tau}$ from the tangential direction:

$$\vec{\tau}(x,t) = \frac{1}{c}\frac{\partial\vec{r}}{\partial x} \tag{A.104}$$

Where *c* is the vector norm of $\partial\vec{r}/\partial x$. Substituting Eq. (A.103) into Eq. (A.104):

$$\vec{\tau}(x,t) = \frac{1}{c}\frac{\partial}{\partial x}\left[(x+u_x)\hat{\imath} - r\hat{k}\right] \tag{A.105}$$

$$\vec{\tau}(x,t) = \hat{\imath} \tag{A.106}$$

The vector norm *c* is *1* in this case and just like before, the term $\partial u_x/dx$ can be neglected. The velocity vector will be given by:

$$\vec{v}(x,t) = \frac{\partial\vec{r}}{\partial t} \tag{A.107}$$

Substituting Eq. (A.103) into Eq. (A.107):

$$\vec{v}(x,t) = \frac{\partial}{\partial t}\left[(x+u_x)\hat{\imath} - r\hat{k}\right] \tag{A.108}$$

$$\vec{v}(x,t) = \frac{\partial u_x}{\partial t}\hat{\imath} \tag{A.109}$$

Once again remembering that $\partial x/\partial t = 0$ since *x* is an independent coordinate. The acceleration vector $\vec{a}$ will be given by:

$$\vec{a}(x,t) = \frac{\partial\vec{v}}{\partial t} \tag{A.110}$$

Substituting Eq. (A.103) into Eq. (A.110):

$$\vec{a}(x,t) = \frac{\partial}{\partial t}\left[\frac{\partial u_x}{\partial t}\hat{\imath}\right] \tag{A.111}$$

$$\vec{a}(x,t) = \frac{\partial^2 u_x}{\partial t^2}\hat{\imath} \tag{A.112}$$

The linear momentum $\vec{P}$ of an infinitesimal element dx will be given by:

$$\vec{P}(x,t) = m_p \vec{v} dx \tag{A.113}$$

Substituting Eq. (A.109) into Eq. (A.113):

$$\vec{P}(x,t) = m_p \frac{\partial u_x}{\partial t} dx\hat{\imath} \tag{A.114}$$

The angular velocity vector $\vec{\Omega}$ will be given by:

$$\vec{\Omega}(x,t) = \omega\vec{\tau} + \frac{\partial \vec{\tau}}{\partial t} \tag{A.115}$$

Substituting Eq. (A.106) into Eq. (A.115):

$$\vec{\Omega}(x,t) = \omega[\hat{\imath}] + \frac{\partial}{\partial t}[\hat{\imath}] \tag{A.116}$$

$$\vec{\Omega}(x,t) = \omega\hat{\imath} \tag{A.117}$$

Lastly, the angular momentum $\vec{H}_0$ from an infinitesimal element *dx*:

$$\vec{H}_0(x,t) = \left(m_p \vec{r}\ x\ \vec{v} + I_p \omega \vec{\tau}\right) dx \tag{A.118}$$

Substituting Eqs. (A.103), (A.106) and (A.109) into Eq. (A.118):

$$\vec{H}_0(x,t) = \left[m_p \left((x+u_x)\hat{\imath} - r\hat{k}\right) x \left(\frac{\partial u_x}{\partial t}\hat{\imath}\right) + I_p \omega \hat{\imath}\right] dx \tag{A.119}$$

$$\vec{H}_0(x,t) = \left[I_p \omega \hat{\imath} - m_p r \frac{\partial u_x}{\partial t}\hat{\jmath}\right] dx \tag{A.120}$$

During tripping out, there will not be any moments, since the column is not subjected to bending. This simplified the following equations. Since the column remains on the lowest portion of the well, there is no need for the unitary vectors $\hat{p}$ and $\hat{q}$. Therefore, the internal force $\vec{F}$ can be written on the $\hat{\imath}$, $\hat{\jmath}$ and $\hat{k}$ coordinates:

$$\vec{F} = F_x\hat{\imath} + F_y\hat{\jmath} + F_z\hat{k} \tag{A.121}$$

Taking the spatial derivative of Eq. (A.121):

$$\frac{\partial \vec{F}}{\partial x} = \frac{\partial F_x}{\partial x}\hat{\imath} + \frac{\partial F_y}{\partial x}\hat{\jmath} + \frac{\partial F_z}{\partial x}\hat{k} \tag{A.122}$$

As said above, there are no bending moments, thus:

$$\vec{M} = 0 \tag{A.123}$$

Consequently, the spatial derivative of Eq. (A.123) will be:

$$\frac{\partial \vec{M}}{\partial x} = 0 \tag{A.124}$$

As in the previous case, the column own weight per unit of length $\vec{q}_p$ acts on the central axis and on the negative direction of the *z* axis. Therefore:

$$\vec{q}_p = -m_p g dx\hat{k} \tag{A.125}$$

The normal contact force has the same modulus than before, but it is now aligned to the *z* axis on its positive direction.

$$\vec{N} = Ndx\hat{k} \tag{A.126}$$

Adding up these two forces, the total external force per unit of length will be the same as before:

$$\vec{f} = \frac{\vec{q}_p}{dx} + \frac{\vec{N}}{dx} \tag{A.127}$$

Substituting Eqs. (A.125) and (A.126) into Eq. (A.127):

$$\vec{f} = \left(-m_p g + N\right)\hat{k} \tag{A.128}$$

Once again, from the Strength of Materials, it is known that the internal forces are directly tied with displacements and strains. On this case, the total axial displacement u_x is the same as the axial displacement u_a, since there is not a displacement due to bending:

$$u_x = u_a \tag{A.129}$$

The displacement u_a from Eq. (A.129) is obtained once again from Hooke's Law:

$$F_x(x,t) = -EA\frac{\partial u_a}{\partial x} \tag{A.130}$$

Combining Eq. (A.129) with Eq. (A.130):

$$F_x(x,t) = -EA\frac{\partial u_x}{\partial x} \tag{A.131}$$

As before, applying Newton's Second Law to find the motion equation for the column, starting for the linear momentum:

$$\sum \vec{F}_i = \frac{\partial \vec{P}}{\partial t} \tag{A.132}$$

Substituting Eq. (A.113) into Eq. (A.132) and introducing the loadings defined through the convention from Figure A.1:

$$\vec{F} - \left(\vec{F} + \frac{\partial \vec{F}}{\partial x}dx\right) + \vec{f}dx = m_p\frac{\partial \vec{v}}{\partial t}dx \tag{A.133}$$

Simplifying Eq. (A.133):

$$\frac{\partial \vec{F}}{\partial x} - \vec{f} + m_p\frac{\partial \vec{v}}{\partial t} = 0 \tag{A.134}$$

Substituting Eqs. (A.112), (A.122) and (A.128) into Eq. (A.134):

$$\frac{\partial F_x}{\partial x}\hat{\imath} + \frac{\partial F_y}{\partial x}\hat{\jmath} + \frac{\partial F_z}{\partial x}\hat{k} - \left(-m_p g + N\right)\hat{k} + m_p\left[\frac{\partial^2 u_x}{\partial t^2}\hat{\imath}\right] = 0 \tag{A.135}$$

$$\left(\frac{\partial F_x}{\partial x} + m_p\frac{\partial^2 u_x}{\partial t^2}\right)\hat{\imath} + \left(\frac{\partial F_y}{\partial x}\right)\hat{\jmath} + \left(\frac{\partial F_z}{\partial x} + m_p g - N\right)\hat{k} = 0 \tag{A.136}$$

Separating Eq. (A.136) into its components, three motion equations are obtained:

$$\frac{\partial F_x}{\partial x} + m_p\frac{\partial^2 u_x}{\partial t^2} = 0 \tag{A.137}$$

$$\frac{\partial F_y}{\partial x} = 0 \tag{A.138}$$

$$\frac{\partial F_z}{\partial x} + m_p g - N = 0 \tag{A.139}$$

Substituting Eq. (A.131) into Eq. (A.137):

$$\frac{\partial}{\partial x}\left[-EA\frac{\partial u_x}{\partial x}\right] + m_p\frac{\partial^2 u_x}{\partial t^2} = 0 \tag{A.140}$$

Manipulating Eq. (A.140), an equation for the axial displacement is found:

$$EA\frac{\partial^2 u_x}{\partial x^2} - m_p\frac{\partial^2 u_x}{\partial t^2} = 0 \tag{A.141}$$

Applying Newton’s Second Law now to the angular momentum:

$$\sum \vec{M}_i = \frac{\partial \vec{H}_0}{\partial t} \tag{A.142}$$

Substituting Eq. (A.118) into Eq. (A.142) and introducing the loadings defined previously on Figure A.1:

$$\vec{M} - \left(\vec{M} + \frac{\partial \vec{M}}{\partial x} dx\right) - \vec{r} \; x \; \vec{F} = \frac{\partial}{\partial t}\left[\left(m_p \vec{r} \; x \; \vec{v} + I_p \omega \vec{\tau}\right) dx\right] \tag{A.143}$$

Simplifying Eq. (A.143) and taking the spatial derivative of $\vec{r}$:

$$\frac{\partial \vec{M}}{\partial x} + \vec{\tau} \; x \; \vec{F} + \frac{\partial}{\partial t}\left[m_p \vec{r} \; x \; \vec{v} + I_p \omega \vec{\tau}\right] = 0 \tag{A.144}$$

Substituting Eqs. (A.106), (A.120), (A.121) and (A.124) into Eq. (A.144):

$$(\hat{\imath}) x \left(F_x \hat{\imath} + F_y \hat{\jmath} + F_z \hat{k}\right) - m_p r \frac{\partial^2 u_x}{\partial t^2} \hat{\jmath} = 0 \tag{A.145}$$

The term $I_p \omega \vec{\tau}$ disappears from the equation since $\vec{\tau} = \hat{\imath}$ and $\partial I_p \omega \hat{\imath} / \partial t = 0$. Manipulating Eq. (A.145):

$$\left(-F_z - m_p r \frac{\partial^2 u_x}{\partial t^2}\right) \hat{\jmath} + F_y k = 0 \tag{A.146}$$

Separating Eq. (A.146) into its components, two motion equations are obtained:

$$F_z = -m_p r \frac{\partial^2 u_x}{\partial t^2} \tag{A.147}$$

$$F_y = 0 \tag{A.148}$$

Substituting Eq. (A.147) into Eq. (A.139):

$$\frac{\partial}{\partial x}\left[-m_p r \frac{\partial^2 u_x}{\partial t^2}\right] + m_p g - N = 0 \tag{A.149}$$

Isolating the normal contact force per unit of length *N*:

$$N(x,t) = -m_p r \frac{\partial^3 u_x}{\partial x \partial t^2} + m_p g \tag{A.150}$$

Summing up, the final problem is now only three equations for three unknowns: Eqs. (A.131), (A.141) and (A.150) which relate F_x, u_x and N.

A.1.3. Solution for tripping in

Due to the complexity of the problem of tripping in, an analytical solution is not possible. Therefore, a numerical solution using the finite differences method will be used. For convenience, the four final equations of the model are repeated here:

$$EA\frac{\partial^2 u_x}{\partial x^2} - m_p\frac{\partial^2 u_x}{\partial t^2} + EAr^2\frac{\partial\theta}{\partial x}\frac{\partial^2\theta}{\partial x^2} = 0 \tag{A.151}$$

$$\begin{aligned} EIr&\left[\frac{\partial^4\theta}{\partial x^4} - 6\left(\frac{\partial\theta}{\partial x}\right)^2\frac{\partial^2\theta}{\partial x^2}\right] \\ &- EAr\left[\frac{\partial u_x}{\partial x}\frac{\partial^2\theta}{\partial x^2} + \frac{\partial^2 u_x}{\partial x^2}\frac{\partial\theta}{\partial x} + \frac{3}{2}r^2\frac{\partial^2\theta}{\partial x^2}\left(\frac{\partial\theta}{\partial x}\right)^2\right] \\ &- I_p r\omega\left[2\frac{\partial^2\theta}{\partial x\partial t}\frac{\partial\theta}{\partial x} + \frac{\partial\theta}{\partial t}\frac{\partial^2\theta}{\partial x^2}\right] + m_p g\sin\theta \\ &+ m_p r\frac{\partial^2\theta}{\partial t^2} = 0 \end{aligned} \tag{A.152}$$

$$F_x(x,t) = -EA\frac{\partial u_x}{\partial x} - \frac{1}{2}EAr^2\left(\frac{\partial\theta}{\partial x}\right)^2 \tag{A.153}$$

$$\begin{aligned} N(x,t) = -EIr&\left[\left(\frac{\partial\theta}{\partial x}\right)^4 - 3\left(\frac{\partial^2\theta}{\partial x^2}\right)^2 - 4\frac{\partial^3\theta}{\partial x^3}\frac{\partial\theta}{\partial x}\right] \\ &- EAr\left[\frac{\partial u_x}{\partial x}\left(\frac{\partial\theta}{\partial x}\right)^2 + \frac{1}{2}r^2\left(\frac{\partial\theta}{\partial x}\right)^4\right] \\ &+ I_p r\omega\left[\frac{\partial^3\theta}{\partial x^2\partial t} - \frac{\partial\theta}{\partial t}\left(\frac{\partial\theta}{\partial x}\right)^2\right] + m_p g\cos\theta \\ &+ m_p r\left(\frac{\partial\theta}{\partial t}\right)^2 \end{aligned} \tag{A.154}$$

Eqs. (A.151) and (A.152) related directly the axial displacement u_x with the angular displacement θ, while Eqs. (A.153) and (A.154) allow calculating the axial and normal forces if the displacements are known. Therefore, this set of equations is not a system; it is possible to find first the displacements and only then calculate the forces. Also, discretizing the time derivatives using the centered formula, the problem becomes implicit and decouples Eqs. (A.151) and (A.152), since the coupling between u_x and θ only happens on the spatial derivatives. Discretizing Eqs. (A.151), (A.152), (A.153) and (A.154):

$$EA\left(\frac{U_{i+1,j}-2U_{i,j}+U_{i-1,j}}{\Delta x^2}\right)-m_p\left(\frac{U_{i,j+1}-2U_{i,j}+U_{i,j-1}}{\Delta t^2}\right) + EAr^2\left(\frac{\theta_{i+1,j}-\theta_{i-1,j}}{2\Delta x}\right)\left(\frac{\theta_{i+1,j}-2\theta_{i,j}+\theta_{i-1,j}}{\Delta x^2}\right)=0 \quad \text{(A.155)}$$

$$\begin{aligned} &EIr\left[\left(\frac{\theta_{i+2,j}-4\theta_{i+1,j}+6\theta_{i,j}-4\theta_{i-1,j}+\theta_{i-2,j}}{\Delta x^4}\right)\right.\\ &\left.-6\left(\frac{\theta_{i+1,j}-\theta_{i-1,j}}{2\Delta x}\right)^2\left(\frac{\theta_{i+1,j}-2\theta_{i,j}+\theta_{i-1,j}}{\Delta x^2}\right)\right]\\ &-EAr\left[\left(\frac{U_{i+1,j}-U_{i-1,j}}{2\Delta x}\right)\left(\frac{\theta_{i+1,j}-2\theta_{i,j}+\theta_{i-1,j}}{\Delta x^2}\right)\right.\\ &+\left(\frac{U_{i+1,j}-2U_{i,j}+U_{i-1,j}}{\Delta x^2}\right)\left(\frac{\theta_{i+1,j}-\theta_{i-1,j}}{2\Delta x}\right)\\ &\left.+\frac{3}{2}r^2\left(\frac{\theta_{i+1,j}-2\theta_{i,j}+\theta_{i-1,j}}{\Delta x^2}\right)\left(\frac{\theta_{i+1,j}-\theta_{i-1,j}}{2\Delta x}\right)^2\right]\\ &-I_pr\omega\left[2\left(\frac{\theta_{i+1,j+1}-\theta_{i-1,j+1}-\theta_{i+1,j-1}+\theta_{i-1,j-1}}{4\Delta x\Delta t}\right)\left(\frac{\theta_{i+1,j}-\theta_{i-1,j}}{2\Delta x}\right)\right.\\ &\left.+\left(\frac{\theta_{i,j+1}-\theta_{i,j-1}}{2\Delta t}\right)\left(\frac{\theta_{i+1,j}-2\theta_{i,j}+\theta_{i-1,j}}{\Delta x^2}\right)\right]+m_pg\sin\theta_{i,j}\\ &+m_pr\left(\frac{\theta_{i,j+1}-2\theta_{i,j}+\theta_{i,j-1}}{\Delta t^2}\right)=0 \end{aligned} \quad \text{(A.156)}$$

$$F_{i,j}=-\frac{EA}{2\Delta x}\left(U_{i+1,j}-U_{i-1,j}\right)-\frac{1}{2}EAr^2\left(\frac{\theta_{i+1,j}-\theta_{i-1,j}}{2\Delta x}\right)^2 \quad \text{(A.157)}$$

$$
\begin{aligned}
& N_{i,j} \\
& = -EIr\left[\left(\frac{\theta_{i+1,j}-\theta_{i-1,j}}{2\Delta x}\right)^4 - 3\left(\frac{\theta_{i+1,j}-2\theta_{i,j}+\theta_{i-1,j}}{\Delta x^2}\right)^2\right. \\
& \left. - 4\left(\frac{\theta_{i+2,j}-2\theta_{i+1,j}+2\theta_{i-1,j}-\theta_{i-2,j}}{2\Delta x^3}\right)\left(\frac{\theta_{i+1,j}-\theta_{i-1,j}}{2\Delta x}\right)\right] \\
& - EAr\left[\left(\frac{U_{i+1,j}-U_{i-1,j}}{2\Delta x}\right)\left(\frac{\theta_{i+1,j}-\theta_{i-1,j}}{2\Delta x}\right)^2\right. \\
& \left. + \frac{1}{2}r^2\left(\frac{\theta_{i+1,j}-\theta_{i-1,j}}{2\Delta x}\right)^4\right] \\
& + I_p r\omega\left[\left(\frac{\theta_{i+1,j}-2\theta_{i,j}+\theta_{i-1,j}-\theta_{i+1,j-2}+2\theta_{i,j-2}-\theta_{i-1,j-2}}{2\Delta x^2\Delta t}\right)\right. \\
& \left. - \left(\frac{\theta_{i,j}-\theta_{i,j-2}}{2\Delta t}\right)\left(\frac{\theta_{i+1,j}-\theta_{i-1,j}}{2\Delta x}\right)^2\right] + m_p g\cos\theta_{i,j} \\
& + m_p r\left(\frac{\theta_{i,j}-\theta_{i,j-2}}{2\Delta t}\right)^2
\end{aligned} \tag{A.158}
$$

Where subscript i denotes the space and subscript j represents time. Manipulating Eqs. (A.155), (A.156), (A.157) and (A.158):

$$
\begin{aligned}
U_{i,j+1} = 2U_{i,j} - U_{i,j-1} &+ \frac{EA\Delta t^2}{m_p\Delta x^2}\left(U_{i+1,j}-2U_{i,j}+U_{i-1,j}\right) \\
&+ \frac{EAr^2\Delta t^2}{2m_p\Delta x^3}\left(\theta_{i+1,j}-\theta_{i-1,j}\right)\left(\theta_{i+1,j}-2\theta_{i,j}+\theta_{i-1,j}\right)
\end{aligned} \tag{A.159}
$$

$$
\begin{aligned}
&\frac{I_p r\omega\left(\theta_{i+1,j}-\theta_{i-1,j}\right)}{4\Delta x^2\Delta t}\theta_{i+1,j+1} \\
&\quad+\left[\frac{I_p r\omega\left(\theta_{i+1,j}-2\theta_{i,j}+\theta_{i-1,j}\right)}{2\Delta x^2\Delta t}-\frac{m_p r}{\Delta t^2}\right]\theta_{i,j+1} \\
&\quad-\frac{I_p r\omega\left(\theta_{i+1,j}-\theta_{i-1,j}\right)}{4\Delta x^2\Delta t}\theta_{i-1,j+1} \\
&\quad=\frac{I_p r\omega\left(\theta_{i+1,j}-2\theta_{i,j}+\theta_{i-1,j}\right)}{2\Delta x^2\Delta t}\theta_{i,j-1} \\
&\quad-\frac{I_p r\omega\left(\theta_{i+1,j}-\theta_{i-1,j}\right)}{4\Delta x^2\Delta t}\left(-\theta_{i+1,j-1}+\theta_{i-1,j-1}\right) \\
&\quad+\frac{m_p r}{\Delta t^2}\left(-2\theta_{i,j}+\theta_{i,j-1}\right) \\
&\quad+\frac{EIr}{\Delta x^4}\left[\left(\theta_{i+2,j}-4\theta_{i+1,j}+6\theta_{i,j}-4\theta_{i-1,j}+\theta_{i-2,j}\right)\right. \\
&\quad\left.-\frac{3}{2}\left(\theta_{i+1,j}-\theta_{i-1,j}\right)^2\left(\theta_{i+1,j}-2\theta_{i,j}+\theta_{i-1,j}\right)\right] \\
&\quad-\frac{EAr}{2\Delta x^3}\left[\left(U_{i+1,j}-U_{i-1,j}\right)\left(\theta_{i+1,j}-2\theta_{i,j}+\theta_{i-1,j}\right)\right. \\
&\quad+\left(U_{i+1,j}-2U_{i,j}+U_{i-1,j}\right)\left(\theta_{i+1,j}-\theta_{i-1,j}\right) \\
&\quad\left.+\frac{3r^2}{4\Delta x}\left(\theta_{i+1,j}-2\theta_{i,j}+\theta_{i-1,j}\right)\left(\theta_{i+1,j}-\theta_{i-1,j}\right)^2\right] \\
&\quad+m_p g\sin\theta_{i,j}
\end{aligned}
\tag{A.160}
$$

$$
F_{i,j}=-\frac{EA}{2\Delta x}\left[\left(U_{i+1,j}-U_{i-1,j}\right)+\frac{r^2}{4\Delta x}\left(\theta_{i+1,j}-\theta_{i-1,j}\right)^2\right]
\tag{A.161}
$$

$$
\begin{aligned}
N_{i,j}=-\frac{EIr}{\Delta x^4}&\left[\frac{1}{16}\left(\theta_{i+1,j}-\theta_{i-1,j}\right)^4-3\left(\theta_{i+1,j}-2\theta_{i,j}+\theta_{i-1,j}\right)^2\right. \\
&-\left(\theta_{i+2,j}-2\theta_{i+1,j}+2\theta_{i-1,j}-\theta_{i-2,j}\right)\left(\theta_{i+1,j}\right. \\
&\left.\left.-\theta_{i-1,j}\right)\right] \\
&-\frac{EAr}{8\Delta x^3}\left[\left(U_{i+1,j}-U_{i-1,j}\right)\left(\theta_{i+1,j}-\theta_{i-1,j}\right)^2\right. \\
&\left.+\frac{r^2}{4\Delta x}\left(\theta_{i+1,j}-\theta_{i-1,j}\right)^4\right] \\
&+\frac{I_p r\omega}{2\Delta x^2\Delta t}\left[\left(\theta_{i+1,j}-2\theta_{i,j}+\theta_{i-1,j}-\theta_{i+1,j-2}\right.\right. \\
&\left.+2\theta_{i,j-2}-\theta_{i-1,j-2}\right) \\
&\left.-\frac{1}{4}\left(\theta_{i,j}-\theta_{i,j-2}\right)\left(\theta_{i+1,j}-\theta_{i-1,j}\right)^2\right]+m_p g\cos\theta_{i,j} \\
&+\frac{m_p r}{4\Delta t^2}\left(\theta_{i,j}-\theta_{i,j-2}\right)^2
\end{aligned}
\tag{A.162}
$$

Remains to be defined the initial conditions and the boundary conditions of the problem, so then the equations for points $i = 0$ and $i = N$ and for points $j = 1$ and $j =$

2 can be found. Considering that the column is fixed at $x = 0$ but free to move in $x = L$, as seen on Figure A.2, the boundary conditions will be given by:

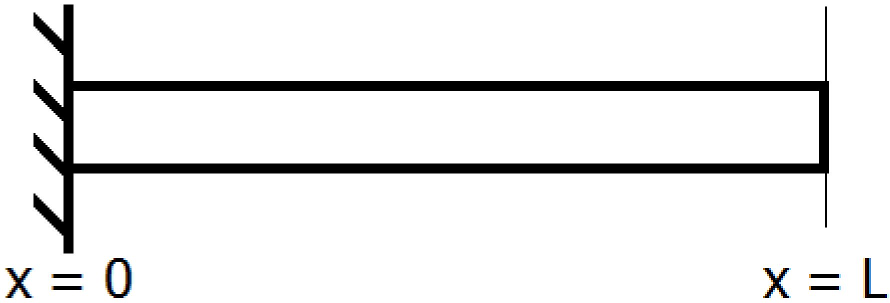

Figure A.2: Example of a cantilever beam, which has a fixed end on x = 0 and a free end on x = L.

$$u(0) = 0 \tag{A.163}$$

$$\left.\frac{\partial u}{\partial x}\right|_{x=L} + \frac{r^2}{2}\left(\left.\frac{\partial \theta}{\partial x}\right|_{x=L}\right)^2 = 0 \tag{A.164}$$

$$\theta(0) = 0 \tag{A.165}$$

$$\left.\frac{\partial^2 \theta}{\partial x^2}\right|_{x=0} = 0 \tag{A.166}$$

$$\left.\frac{\partial^2 \theta}{\partial x^2}\right|_{x=L} = 0 \tag{A.167}$$

$$\left.\frac{\partial^3 \theta}{\partial x^3}\right|_{x=L} = 0 \tag{A.168}$$

Discretizing Eqs. (A.163), (A.164), (A.165), (A.166), (A.167) and (A.168):

$$U_{0,j} = 0 \tag{A.169}$$

$$U_{N+1,j} - U_{N-1,j} + \frac{r^2}{4\Delta x}\left(\theta_{N+1,j} - \theta_{N-1,j}\right)^2 = 0 \rightarrow U_{N+1,j} = U_{N-1,j} - \frac{r^2}{\Delta x}{\theta_{N-1,j}}^2 \tag{A.170}$$

$$\theta_{0,j} = 0 \tag{A.171}$$

$$\theta_{1,j} - 2\theta_{0,j} + \theta_{-1,j} = 0 \rightarrow \theta_{-1,j} = -\theta_{1,j} \tag{A.172}$$

$$\theta_{N+1,j} - 2\theta_{N,j} + \theta_{N-1,j} = 0 \rightarrow \theta_{N+1,j} = -\theta_{N-1,j} \tag{A.173}$$

$$\begin{aligned}\theta_{N+2,j} - 2\theta_{N+1,j} + 2\theta_{N-1,j} - \theta_{N-2,j} = 0 \rightarrow \theta_{N+2,j} \\ = \theta_{N-2,j} - 4\theta_{N-1,j}\end{aligned} \tag{A.174}$$

From Eqs. (A.169), (A.170), (A.171), (A.172), (A.173) and (A.174), the equations for points $i = 1$, $i = N - 1$ and $i = N$ are found substituting into Eqs. (A.159) e (A.160) – the point $i = 0$ is not needed since the displacements are already known as being zero. For point $i = 1$:

$$\begin{aligned}U_{1,j+1} = 2U_{1,j} - U_{1,j-1} + \frac{EA\Delta t^2}{m_p\Delta x^2}\left(U_{2,j} - 2U_{1,j}\right) \\ + \frac{EAr^2\Delta t^2}{2m_p\Delta x^3}\theta_{2,j}\left(\theta_{2,j} - 2\theta_{1,j}\right)\end{aligned} \tag{A.175}$$

$$\begin{aligned}\frac{I_p r\omega\theta_{2,j}}{4\Delta x^2\Delta t}\theta_{2,j+1} + \left[\frac{I_p r\omega\left(\theta_{2,j} - 2\theta_{1,j}\right)}{2\Delta x^2\Delta t} - \frac{m_p r}{\Delta t^2}\right]\theta_{1,j+1} \\ = \frac{I_p r\omega\left(\theta_{2,j} - 2\theta_{1,j}\right)}{2\Delta x^2\Delta t}\theta_{1,j-1} - \frac{I_p r\omega\theta_{2,j}}{4\Delta x^2\Delta t}\left(-\theta_{2,j-1}\right) \\ + \frac{m_p r}{\Delta t^2}\left(-2\theta_{1,j} + \theta_{1,j-1}\right) \\ + \frac{EIr}{\Delta x^4}\Big[\left(\theta_{3,j} - 4\theta_{2,j} + 5\theta_{1,j}\right) \\ - \frac{3}{2}\left(\theta_{2,j}\right)^2\left(\theta_{2,j} - 2\theta_{1,j}\right)\Big] \\ - \frac{EAr}{2\Delta x^3}\Big[U_{2,j}\left(\theta_{2,j} - 2\theta_{1,j}\right) + \theta_{2,j}\left(U_{2,j} - 2U_{1,j}\right) \\ + \frac{3r^2}{4\Delta x}\theta_{2,j}{}^2\left(\theta_{2,j} - 2\theta_{1,j}\right)\Big] + m_p g \sin\theta_{1,j}\end{aligned} \tag{A.176}$$

While for point $i = N - 1$:

$$U_{N-1,j+1} = 2U_{N-1,j} - U_{N-1,j-1} + \frac{EA\Delta t^2}{m_p \Delta x^2}\left(U_{N,j} - 2U_{N-1,j} + U_{N-2,j}\right) + \frac{EAr^2\Delta t^2}{2m_p\Delta x^3}\left(\theta_{N,j} - \theta_{N-2,j}\right)\left(\theta_{N,j} - 2\theta_{N-1,j} + \theta_{N-2,j}\right) \tag{A.177}$$

$$\begin{aligned}\frac{I_p r\omega\left(\theta_{N,j} - \theta_{N-2,j}\right)}{4\Delta x^2 \Delta t}\theta_{N,j+1} &+ \left[\frac{I_p r\omega\left(\theta_{N,j} - 2\theta_{N-1,j} + \theta_{N-2,j}\right)}{2\Delta x^2\Delta t} - \frac{m_p r}{\Delta t^2}\right]\theta_{N-1,j+1} \\ &- \frac{I_p r\omega\left(\theta_{N,j} - \theta_{N-2,j}\right)}{4\Delta x^2\Delta t}\theta_{N-2,j+1} \\ &= \frac{I_p r\omega\left(\theta_{N,j} - 2\theta_{N-1,j} + \theta_{N-2,j}\right)}{2\Delta x^2\Delta t}\theta_{N-1,j-1} \\ &- \frac{I_p r\omega\left(\theta_{N,j} - \theta_{N-2,j}\right)}{4\Delta x^2\Delta t}\left(-\theta_{N,j-1} + \theta_{N-2,j-1}\right) \\ &+ \frac{m_p r}{\Delta t^2}\left(-2\theta_{N-1,j} + \theta_{N-1,j-1}\right) \\ &+ \frac{EIr}{\Delta x^4}\Big[\left(-4\theta_{N,j} + 5\theta_{N-1,j} - 4\theta_{N-2,j} + \theta_{N-3,j}\right) \\ &- \frac{3}{2}\left(\theta_{N,j} - \theta_{N-2,j}\right)^2\left(\theta_{N,j} - 2\theta_{N-1,j} + \theta_{N-2,j}\right)\Big] \\ &- \frac{EAr}{2\Delta x^3}\Big[\left(\theta_{N,j} - \theta_{N-2,j}\right)\left(\theta_{N,j} - 2\theta_{N-1,j} + \theta_{N-2,j}\right) \\ &+ \left(U_{N,j} - 2U_{N-1,j} + U_{N-2,j}\right)\left(\theta_{N,j} - \theta_{N-2,j}\right) \\ &+ \frac{3r^2}{4\Delta x}\left(\theta_{N,j} - 2\theta_{N-1,j} + \theta_{N-2,j}\right)\left(\theta_{N,j} - \theta_{N-2,j}\right)^2\Big] \\ &+ m_p g \sin\theta_{N-1,j}\end{aligned} \tag{A.178}$$

Lastly, for point $i = N$:

$$U_{N,j+1} = 2U_{N,j} - U_{N,j-1} + \frac{EA\Delta t^2}{m_p\Delta x^2}\left(-2U_{N,j} + 2U_{N-1,j} - \frac{r^2}{\Delta x}{\theta_{N-1,j}}^2\right) + \frac{EAr^2\Delta t^2}{2m_p\Delta x^3}\left(-2\theta_{N-1,j}\right)\left(-2\theta_{N,j}\right) \tag{A.179}$$

$$\left[\frac{I_p r\omega\left(-2\theta_{N,j}\right)}{2\Delta x^2\Delta t}-\frac{m_p r}{\Delta t^2}\right]\theta_{N,j+1}-2\,\frac{I_p r\omega\left(-2\theta_{N-1,j}\right)}{4\Delta x^2\Delta t}\theta_{N-1,j+1}$$
$$\begin{aligned}
&=\frac{I_p r\omega\left(-2\theta_{N,j}\right)}{2\Delta x^2\Delta t}\theta_{N,j-1}\\
&-\frac{I_p r\omega\left(-2\theta_{N-1,j}\right)}{4\Delta x^2\Delta t}\left(2\theta_{N-1,j-1}\right)\\
&+\frac{m_p r}{\Delta t^2}\left(-2\theta_{N,j}+\theta_{N,j-1}\right)\\
&+\frac{EIr}{\Delta x^4}\left[\left(6\theta_{N,j}-4\theta_{N-1,j}+2\theta_{N-2,j}\right)\right.\\
&\left.-\frac{3}{2}\left(-2\theta_{N-1,j}\right)^2\left(-2\theta_{N,j}\right)\right]\\
&-\frac{EAr}{2\Delta x^3}\left[\left(-\frac{r^2}{\Delta x}\theta_{N-1,j}{}^2\right)\left(-2\theta_{N,j}\right)\right.\\
&+\left(-2U_{N,j}+2U_{N-1,j}\right)\left(-2\theta_{N-1,j}\right)\\
&\left.+\frac{3r^2}{4\Delta x}\left(-2\theta_{N,j}\right)\left(-2\theta_{N-1,j}\right)^2\right]+m_p g\sin\theta_{N,j}
\end{aligned} \tag{A.180}$$

Now for the initial conditions, an initial displacement is imposed for u_x and θ and the initial velocities are considered zero. A small value is given to θ for convergence purposes.

$$u(x,0)=U_0\sin\left(\frac{\pi x}{L}\right) \tag{A.181}$$

$$\frac{\partial u(x,0)}{\partial t}=0 \tag{A.182}$$

$$\theta(x,0)=0.1 \tag{A.183}$$

$$\frac{\partial \theta(x,0)}{\partial t}=0 \tag{A.184}$$

Discretizing Eqs. (A.181), (A.182), (A.183) and (A.184):

$$U_{i,1}=U_0\sin\left(\frac{\pi i\Delta x}{L}\right) \tag{A.185}$$

$$\frac{U_{i,2}-U_{i,0}}{2\Delta t}=0\rightarrow U_{i,0}=U_{i,2}\rightarrow U_{i,2}$$
$$=U_{i,1}+\frac{EA\Delta t^2}{2m_p\Delta x^2}\left(U_{i+1,1}-2U_{i,1}+U_{i-1,1}\right)$$
$$+\frac{EAr^2\Delta t^2}{4m_p\Delta x^3}\left(\theta_{i+1,1}-\theta_{i-1,1}\right)\left(\theta_{i+1,1}-2\theta_{i,1}+\theta_{i-1,1}\right) \quad \text{(A.186)}$$

$$\theta_{i,1}=0.1 \quad \text{(A.187)}$$

$$\frac{\theta_{i,2}-\theta_{i,0}}{2\Delta t}=0\rightarrow \theta_{i,0}=\theta_{i,2}$$
$$\rightarrow \frac{I_p r\omega\left(\theta_{i+1,j}-\theta_{i-1,j}\right)}{2\Delta x^2\Delta t}\theta_{i+1,2}$$
$$+\left[\frac{I_p r\omega\left(\theta_{i+1,1}-2\theta_{i,1}+\theta_{i-1,1}\right)}{2\Delta x^2\Delta t}-\frac{m_p r}{\Delta t^2}\right]\theta_{i,2}$$
$$-\frac{I_p r\omega\left(\theta_{i+1,1}-\theta_{i-1,1}\right)}{2\Delta x^2\Delta t}\theta_{i-1,2}$$
$$=\frac{m_p r}{\Delta t^2}\left(-2\theta_{i,1}\right)$$
$$+\frac{EIr}{\Delta x^4}\left[\left(\theta_{i+2,1}-4\theta_{i+1,1}+6\theta_{i,1}-4\theta_{i-1,1}+\theta_{i-2,1}\right)\right.$$
$$\left.-\frac{3}{2}\left(\theta_{i+1,1}-\theta_{i-1,1}\right)^2\left(\theta_{i+1,1}-2\theta_{i,1}+\theta_{i-1,1}\right)\right]$$
$$-\frac{EAr}{2\Delta x^3}\left[\left(U_{i+1,1}-U_{i-1,1}\right)\left(\theta_{i+1,1}-2\theta_{i,1}+\theta_{i-1,1}\right)\right.$$
$$+\left(U_{i+1,1}-2U_{i,1}+U_{i-1,1}\right)\left(\theta_{i+1,1}-\theta_{i-1,1}\right)$$
$$\left.+\frac{3r^2}{4\Delta x}\left(\theta_{i+1,1}-2\theta_{i,1}+\theta_{i-1,1}\right)\left(\theta_{i+1,1}-\theta_{i-1,1}\right)^2\right]$$
$$+m_p g\sin\theta_{i,1} \quad \text{(A.188)}$$

A.1.4. Solution for tripping out

Differently from the tripping in case, the equations for tripping out the column are simpler and possess an analytical solution. Therefore, on this case, there are two possible ways of solving the equations: analytic and numeric – through the finite differences method. The three equations are repeated here for convenience:

$$EA\frac{\partial^2 u_x}{\partial x^2}-m_p\frac{\partial^2 u_x}{\partial t^2}=0 \quad \text{(A.189)}$$

$$F_x(x,t)=-EA\frac{\partial u_x}{\partial x} \quad \text{(A.190)}$$

$$N(x,t) = -m_p r \frac{\partial^3 u_x}{\partial x \partial t^2} + m_p g \tag{A.191}$$

The analytical solution of Eq. (A.189) is simple and is already known in the literature since it is the wave equation. The axial displacement can be obtained through a separation of variables $u_x(x,t) = X(x)T(t)$. The solution for this equation is given by:

$$u_x(x,t) = \left[A_1 \cos\left(\sqrt{\frac{m_p}{EA}}\omega x\right) + A_2 \sin\left(\sqrt{\frac{m_p}{EA}}\omega x\right)\right][B_1 \cos(\omega t) + B_2 \sin(\omega t)] \tag{A.192}$$

Consequently, the axial and normal forces will be given by:

$$F_x(x,t) = \omega\sqrt{m_p EA}\left[A_1 \sin\left(\sqrt{\frac{m_p}{EA}}\omega x\right) - A_2 \cos\left(\sqrt{\frac{m_p}{EA}}\omega x\right)\right][B_1 \cos(\omega t) + B_2 \sin(\omega t)] \tag{A.193}$$

$$N(x,t) = \omega^3 m_p r\sqrt{\frac{m_p}{EA}}\left[-A_1 \sin\left(\sqrt{\frac{m_p}{EA}}\omega x\right) + A_2 \cos\left(\sqrt{\frac{m_p}{EA}}\omega x\right)\right][B_1 \cos(\omega t) + B_2 \sin(\omega t)] + m_p g \tag{A.194}$$

Where constants A_1, A_2, $B_1$and B_2 must be obtained from the boundary and initial conditions. Just like the previous case, the column is fixed on $x = 0$ and free on $x = L$.

$$X(0) = 0 \tag{A.195}$$

$$X'(L) = 0 \tag{A.196}$$

Where the function *X(x)* is given by:

$$X(x) = A_1 \cos\left(\sqrt{\frac{m_p}{EA}}\omega x\right) + A_2 \sin\left(\sqrt{\frac{m_p}{EA}}\omega x\right) \tag{A.197}$$

Substituting Eqs. (A.195) and (A.196) into Eq. (A.197), constants A_1 and A_2 are found:

$$A_1 = 0 \tag{A.198}$$

$$A_2\sqrt{\frac{m_p}{EA}}\omega \cos\left(\sqrt{\frac{m_p}{EA}}\omega L\right) = 0 \tag{A.199}$$

Since the value of A_2 cannot be zero on Eq. (A.199) – which would lead to the trivial solution $X(x) = 0$ – then it must be:

$$\cos\left(\sqrt{\frac{m_p}{EA}}\omega L\right) = 0 \tag{A.200}$$

$$\sqrt{\frac{m_p}{EA}}\omega_n L = \pi\left(n - \frac{1}{2}\right) \tag{A.201}$$

$$\omega_n = \left(n - \frac{1}{2}\right)\frac{\pi}{L}\sqrt{\frac{EA}{m_p}} \tag{A.202}$$

Where ω_n are the eigenvalues, physically known as the natural frequencies of the system. The analytical solution allows finding the natural frequencies but does not allow solving for all constants on the final solution. This happens because there are only two boundary conditions for three unknowns: two constants A_1 and A_2 from the solution and the eigenvalues ω_n. The numerical solution, however, uses the two boundary conditions to obtain the final solution without calculating the eigenvalues. Since the objective is to compare the column response during its tripping in and tripping out, the numerical solution is preferable, even though an analytical solution is possible. Discretizing Eqs. (A.189), (A.190) and (A.191):

$$\frac{EA}{\Delta x^2}\left(U_{i+1,j} - 2U_{i,j} + U_{i-1,j}\right) - \frac{m_p}{\Delta t^2}\left(U_{i,j+1} - 2U_{i,j} + U_{i,j-1}\right) = 0 \tag{A.203}$$

$$F_{i,j} = -\frac{EA}{2\Delta x}\left(U_{i+1,j} - U_{i-1,j}\right) \tag{A.204}$$

$$\begin{aligned} N_{i,j} = -\frac{m_p r}{2\Delta x \Delta t^2}\big(U_{i+1,j} - U_{i-1,j} - 2U_{i+1,j-1} + 2U_{i-1,j-1} \\ + U_{i+1,j-2} - U_{i-1,j-2}\big) + m_p g \end{aligned} \tag{A.205}$$

Manipulating Eq. (A.203):

$$U_{i,j+1} = 2U_{i,j} - U_{i,j-1} + \frac{EA\Delta t^2}{m_p \Delta x^2}\left(U_{i+1,j} - 2U_{i,j} + U_{i-1,j}\right) \tag{A.206}$$

As in the tripping in case, first Eq. (A.206) is solved to find and the axial displacements and only then Eqs. (A.204) and (A.205) are solved to find the axial and normal forces. Remains to be defined the boundary and initial conditions. As said before, the column is fixed in $x = 0$ and free on $x = L$. The boundary conditions will then be given by:

$$u(0) = 0 \tag{A.207}$$

$$\left.\frac{\partial u}{\partial x}\right|_{x=L} = 0 \tag{A.208}$$

Discretizing Eqs. (A.207) and (A.208):

$$U_{0,j} = 0 \tag{A.209}$$

$$U_{N+1,j} - U_{N-1,j} = 0 \rightarrow U_{N+1,j} = U_{N-1,j} \tag{A.210}$$

From Eqs. (A.209) and (A.210), the equations for the points $i = 1$, $i = N - 1$ and $i = N$ are found by substituting on Eq. (A.206). For point $i = 1$:

$$U_{1,j+1} = 2U_{1,j} - U_{1,j-1} + \frac{EA\Delta t^2}{m_p \Delta x^2}\left(U_{2,j} - 2U_{1,j}\right) \tag{A.211}$$

For point $i = N - 1$:

$$U_{N-1,j+1} = 2U_{N-1,j} - U_{N-1,j-1} + \frac{EA\Delta t^2}{m_p \Delta x^2}\left(U_{N,j} - 2U_{N-1,j} + U_{N-2,j}\right) \quad (A.212)$$

While for point $i = N$:

$$U_{N,j+1} = 2U_{N,j} - U_{N,j-1} + \frac{EA\Delta t^2}{m_p \Delta x^2}\left(-2U_{N,j} + 2U_{N-1,j}\right) \quad (A.213)$$

Lastly, the initial conditions will be the same from the tripping in case:

$$u(x,0) = U_0 \, sin\left(\frac{\pi x}{L}\right) \quad (A.214)$$

$$\frac{\partial u(x,0)}{\partial t} = 0 \quad (A.215)$$

Discretizing Eqs. (A.214) and (A.215):

$$U_{i,1} = U_0 \, sin\left(\frac{\pi i \Delta x}{L}\right) \quad (A.216)$$

$$\frac{U_{i,2} - U_{i,0}}{2\Delta t} = 0 \rightarrow U_{i,0} = U_{i,2} \rightarrow U_{i,2} = U_{i,1} + \frac{EA\Delta t^2}{2m_p \Delta x^2}\left(U_{i+1,1} - 2U_{i,1} + U_{i-1,1}\right) \quad (A.217)$$

A.2. Model II – Column with friction

The hypotheses behind this model were explained on section 3.2. Here, only the deduction of the motion equations and their solution through the finite differences method will be shown.

A.2.1. Model for tripping in

The friction force has two components and thus can be written as:

$$\vec{F}_f(x,t) = \vec{F}_{f1}(x,t)\hat{\imath} + \vec{F}_{f2}(x,t)\hat{q} \quad (A.218)$$

$\vec{F}_{f1}$ is the axial component while $\vec{F}_{f2}$ is the lateral one. The modulus of component $\vec{F}_{f1}$ will be given by:

$$\left|\vec{F}_{f1}\right| = f_1 N dx \tag{A.219}$$

Where f_1 is the dynamic friction coefficient on the axial direction, N is the normal contact force per unit of length and dx is an infinitesimal element of length. Since $\vec{F}_{f1}$ is dependent of the sign of $\partial u_x/\partial t$:

$$\vec{F}_{f1}(x,t) = -\,sgn\left(\frac{\partial u_x}{\partial t}\right) f_1 N dx \hat{\imath} \tag{A.220}$$

Where *sgn* is the sign function. If the velocity is positive, the sign function has value of *1* and the friction force is on the negative direction; if the velocity is negative, the sign function has value of *–1* and the friction force is on the positive direction; and if the velocity is zero, the sign function has value *0* and then there is no dynamic friction force. The same procedure is valid for the component $\vec{F}_{f2}$, but on this case it is dependent of the sign of $\partial\theta/\partial t$:

$$\left|\vec{F}_{f2}\right| = f_2 N dx \tag{A.221}$$

$$\vec{F}_{f2}(x,t) = -\,sgn\left(\frac{\partial \theta}{\partial t}\right) f_2 N dx \hat{q} \tag{A.222}$$

Where f_2 is the dynamic friction coefficient on the lateral direction. It is possible to manipulate the two friction coefficients $f_1$and f_2 by introducing a single total dynamic friction coefficient f. Through Eq. (A.218), the following relation is valid:

$$\left|\vec{F}_{f}^{2}\right| = \left|\vec{F}_{f1}^{2}\right| + \left|\vec{F}_{f2}^{2}\right| \tag{A.223}$$

Substituting the modulus of the vectors:

$$f^2 N^2 dx^2 = f_1^2 N^2 dx^2 + f_2^2 N^2 dx^2 \tag{A.224}$$

$$f^2 = f_1^2 + f_2^2 \tag{A.225}$$

Another possible relation is to consider that f_1 and f_2 are proportional to the respective axial velocity v_1 and lateral velocity v_2. For small velocities, this linear relation is acceptable (Gao & Miska, 2009). Therefore:

$$\frac{f_1}{f_2} = \frac{v_1(x,t)}{v_2(x,t)} \tag{A.226}$$

Where v_1 and v_2 are the components of the velocity on the $\hat{\imath}$ and $\hat{q}$ directions, as given by Eq. (A.27). Starting from Eq. (A.226), each friction coefficient can be isolated:

$$f_1 = f_2 \frac{v_1(x,t)}{v_2(x,t)} \tag{A.227}$$

$$f_2 = f_1 \frac{v_2(x,t)}{v_1(x,t)} \tag{A.228}$$

Combining Eq. (A.228) with Eq. (A.225):

$$f^2 = f_1^2 + f_1^2 \frac{v_2^2}{v_1^2} \tag{A.229}$$

$$v_1^2 f^2 = v_1^2 f_1^2 + v_2^2 f_1^2 \tag{A.230}$$

$$f_1^2 = \frac{v_1^2 f^2}{v_1^2 + v_2^2} \tag{A.231}$$

$$f_1 = \frac{|v_1| f}{\sqrt{v_1^2 + v_2^2}} \tag{A.232}$$

Now combining Eq. (A.227) with Eq. (A.225):

$$f^2 = f_2^2 \frac{v_1^2}{v_2^2} + f_2^2 \tag{A.233}$$

$$\mathrm{v}_2^2\mathrm{f}^2 = \mathrm{v}_1^2\mathrm{f}_2^2 + \mathrm{v}_2^2\mathrm{f}_2^2 \tag{A.234}$$

$$f_2^2 = \frac{v_2^2 f^2}{v_1^2 + v_2^2} \tag{A.235}$$

$$f_2 = \frac{|v_2| f}{\sqrt{v_1^2 + v_2^2}} \tag{A.236}$$

Substituting Eqs. (A.220), (A.222), (A.232) and (A.236) into Eq. (A.218):

$$\begin{aligned} \vec{F}_f(x,t) = &- sgn\left(\frac{\partial u_x}{\partial t}\right)\frac{|v_1| f}{\sqrt{v_1^2 + v_2^2}} N dx \hat{\imath} \\ &- sgn\left(\frac{\partial \theta}{\partial t}\right)\frac{|v_2| f}{\sqrt{v_1^2 + v_2^2}} N dx \hat{q} \end{aligned} \tag{A.237}$$

$$\vec{F}_f(x,t) = -\frac{fNdx}{\sqrt{v_1^2 + v_2^2}}\left[sgn\left(\frac{\partial u_x}{\partial t}\right)|v_1|\hat{\imath} + sgn\left(\frac{\partial \theta}{\partial t}\right)|v_2|\hat{q}\right] \tag{A.238}$$

Knowing that $v_1 = \partial u_x/\partial t$ and $v_2 = r\partial\theta/\partial t$, according to Eq. (A.27), and substituting into Eq. (A.238):

$$\begin{aligned} \vec{F}_f(x,t) = -\frac{fNdx}{\sqrt{\left(\frac{\partial u_x}{\partial t}\right)^2 + r^2\left(\frac{\partial \theta}{\partial t}\right)^2}} &\left[sgn\left(\frac{\partial u_x}{\partial t}\right)\left|\frac{\partial u_x}{\partial t}\right|\hat{\imath}\right. \\ &\left. + sgn\left(\frac{\partial \theta}{\partial t}\right) r \left|\frac{\partial \theta}{\partial t}\right|\hat{q}\right] \end{aligned} \tag{A.239}$$

Therefore, the total external force per unit of length is now given by:

$$\vec{f} = \frac{\vec{q}_p}{dx} + \frac{\vec{N}}{dx} + \frac{\vec{F}_f}{dx} \tag{A.240}$$

Substituting Eqs. (A.57), (A.58) and (A.239) into Eq. (A.240):

$$\vec{f} = m_p g \cos\theta\,\hat{p} - m_p g \sin\theta\,\hat{q} - N\hat{p} - \frac{fN}{\sqrt{\left(\frac{\partial u_x}{\partial t}\right)^2 + r^2\left(\frac{\partial \theta}{\partial t}\right)^2}}\left[sgn\left(\frac{\partial u_x}{\partial t}\right)\left|\frac{\partial u_x}{\partial t}\right|\hat{\imath} + sgn\left(\frac{\partial \theta}{\partial t}\right) r \left|\frac{\partial \theta}{\partial t}\right|\hat{q}\right] \tag{A.241}$$

Manipulating Eq. (A.241):

$$\vec{f} = -\frac{sgn\left(\frac{\partial u_x}{\partial t}\right) fN \left|\frac{\partial u_x}{\partial t}\right|}{\sqrt{\left(\frac{\partial u_x}{\partial t}\right)^2 + r^2\left(\frac{\partial \theta}{\partial t}\right)^2}}\hat{\imath} + \left(m_p g \cos\theta - N\right)\hat{p} - \left(m_p g \sin\theta + \frac{sgn\left(\frac{\partial \theta}{\partial t}\right) fNr \left|\frac{\partial \theta}{\partial t}\right|}{\sqrt{\left(\frac{\partial u_x}{\partial t}\right)^2 + r^2\left(\frac{\partial \theta}{\partial t}\right)^2}}\right)\hat{q} \tag{A.242}$$

The summation of forces is still given by Eq. (A.74):

$$\frac{\partial \vec{F}}{\partial x} - \vec{f} + m_p \frac{\partial \vec{v}}{\partial t} = 0 \tag{A.243}$$

Substituting Eqs. (A.31), (A.49) and (A.242) into Eq. (A.243):

$$\frac{\partial F_x}{\partial x}\hat{\imath} + \left(\frac{\partial F_r}{\partial x} - F_\theta \frac{\partial \theta}{\partial x}\right)\hat{p} + \left(\frac{\partial F_\theta}{\partial x} + F_r \frac{\partial \theta}{\partial x}\right)\hat{q} + \frac{sgn\left(\frac{\partial u_x}{\partial t}\right) fN \left|\frac{\partial u_x}{\partial t}\right|}{\sqrt{\left(\frac{\partial u_x}{\partial t}\right)^2 + r^2\left(\frac{\partial \theta}{\partial t}\right)^2}}\hat{\imath} - \left(m_p g \cos\theta - N\right)\hat{p} + \left(m_p g \sin\theta + \frac{sgn\left(\frac{\partial \theta}{\partial t}\right) fNr \left|\frac{\partial \theta}{\partial t}\right|}{\sqrt{\left(\frac{\partial u_x}{\partial t}\right)^2 + r^2\left(\frac{\partial \theta}{\partial t}\right)^2}}\right)\hat{q} + m_p\left[\frac{\partial^2 u_x}{\partial t^2}\hat{\imath} - r\left(\frac{\partial \theta}{\partial t}\right)^2\hat{p} + r\frac{\partial^2 \theta}{\partial t^2}\hat{q}\right] = 0 \tag{A.244}$$

Manipulating Eq. (A.244):

$$\left[\frac{\partial F_x}{\partial x} + \frac{sgn\left(\frac{\partial u_x}{\partial t}\right) fN \left|\frac{\partial u_x}{\partial t}\right|}{\sqrt{\left(\frac{\partial u_x}{\partial t}\right)^2 + r^2 \left(\frac{\partial \theta}{\partial t}\right)^2}} + m_p \frac{\partial^2 u_x}{\partial t^2}\right]\hat{\imath} + \left[\frac{\partial F_r}{\partial x} - F_\theta \frac{\partial \theta}{\partial x} + N - m_p g \cos\theta - m_p r \left(\frac{\partial \theta}{\partial t}\right)^2\right]\hat{p} + \left[\frac{\partial F_\theta}{\partial x} + F_r \frac{\partial \theta}{\partial x} + m_p g \sin\theta + \frac{sgn\left(\frac{\partial \theta}{\partial t}\right) fNr \left|\frac{\partial \theta}{\partial t}\right|}{\sqrt{\left(\frac{\partial u_x}{\partial t}\right)^2 + r^2 \left(\frac{\partial \theta}{\partial t}\right)^2}} + m_p r \frac{\partial^2 \theta}{\partial t^2}\right]\hat{q} = 0 \tag{A.245}$$

Separating Eq. (A.245) into components:

$$\frac{\partial F_x}{\partial x} + \frac{sgn\left(\frac{\partial u_x}{\partial t}\right) fN \left|\frac{\partial u_x}{\partial t}\right|}{\sqrt{\left(\frac{\partial u_x}{\partial t}\right)^2 + r^2 \left(\frac{\partial \theta}{\partial t}\right)^2}} + m_p \frac{\partial^2 u_x}{\partial t^2} = 0 \tag{A.246}$$

$$\frac{\partial F_r}{\partial x} - F_\theta \frac{\partial \theta}{\partial x} + N - m_p g \cos\theta - m_p r \left(\frac{\partial \theta}{\partial t}\right)^2 = 0 \tag{A.247}$$

$$\frac{\partial F_\theta}{\partial x} + F_r \frac{\partial \theta}{\partial x} + m_p g \sin\theta + \frac{sgn\left(\frac{\partial \theta}{\partial t}\right) fNr \left|\frac{\partial \theta}{\partial t}\right|}{\sqrt{\left(\frac{\partial u_x}{\partial t}\right)^2 + r^2 \left(\frac{\partial \theta}{\partial t}\right)^2}} + m_p r \frac{\partial^2 \theta}{\partial t^2} = 0 \tag{A.248}$$

Looking at the analysis made on the previous section, it is easy to conclude that the calculations to find the components F_x, F_r and F_θ from $\vec{F}$ will not change with the introduction of the friction force. Therefore, substituting Eqs. (A.66), (A.92) and (A.95) into Eqs. (A.246), (A.247), (A.248), with Eqs. (A.37) and (A.38):

$$\frac{\partial}{\partial x}\left[-EA\frac{\partial u_x}{\partial x} - \frac{1}{2}EAr^2\left(\frac{\partial \theta}{\partial x}\right)^2\right] + \frac{sgn\left(\frac{\partial u_x}{\partial t}\right) fN \left|\frac{\partial u_x}{\partial t}\right|}{\sqrt{\left(\frac{\partial u_x}{\partial t}\right)^2 + r^2 \left(\frac{\partial \theta}{\partial t}\right)^2}} + m_p \frac{\partial^2 u_x}{\partial t^2} = 0 \tag{A.249}$$

$$\frac{\partial}{\partial x}\left[-3EIr\frac{\partial\theta}{\partial x}\frac{\partial^2\theta}{\partial x^2}-I_p\omega r\frac{\partial^2\theta}{\partial x\partial t}\right] - \left[EIr\left[\frac{\partial^3\theta}{\partial x^3}-\left(\frac{\partial\theta}{\partial x}\right)^3\right] + \left[-EA\frac{\partial u_x}{\partial x}-\frac{1}{2}EAr^2\left(\frac{\partial\theta}{\partial x}\right)^2\right]r\frac{\partial\theta}{\partial x} + I_p\omega\left(-r\frac{\partial\theta}{\partial t}\frac{\partial\theta}{\partial x}\right)\right]\frac{\partial\theta}{\partial x} + N - m_p g\cos\theta - m_p r\left(\frac{\partial\theta}{\partial t}\right)^2 = 0 \tag{A.250}$$

$$\frac{\partial}{\partial x}\left[EIr\left[\frac{\partial^3\theta}{\partial x^3}-\left(\frac{\partial\theta}{\partial x}\right)^3\right] + \left[-EA\frac{\partial u_x}{\partial x}-\frac{1}{2}EAr^2\left(\frac{\partial\theta}{\partial x}\right)^2\right]r\frac{\partial\theta}{\partial x} + I_p\omega\left(-r\frac{\partial\theta}{\partial t}\frac{\partial\theta}{\partial x}\right)\right] + \left[-3EIr\frac{\partial\theta}{\partial x}\frac{\partial^2\theta}{\partial x^2}-I_p\omega r\frac{\partial^2\theta}{\partial x\partial t}\right]\frac{\partial\theta}{\partial x} + m_p g\sin\theta + \frac{sgn\left(\frac{\partial\theta}{\partial t}\right)fNr\left|\frac{\partial\theta}{\partial t}\right|}{\sqrt{\left(\frac{\partial u_x}{\partial t}\right)^2+r^2\left(\frac{\partial\theta}{\partial t}\right)^2}} + m_p r\frac{\partial^2\theta}{\partial t^2} = 0 \tag{A.251}$$

Manipulating Eqs. (A.249), (A.250) and (A.251):

$$EA\frac{\partial^2 u_x}{\partial x^2} - m_p\frac{\partial^2 u_x}{\partial t^2} + EAr^2\frac{\partial\theta}{\partial x}\frac{\partial^2\theta}{\partial x^2} - \frac{sgn\left(\frac{\partial u_x}{\partial t}\right)fN\left|\frac{\partial u_x}{\partial t}\right|}{\sqrt{\left(\frac{\partial u_x}{\partial t}\right)^2+r^2\left(\frac{\partial\theta}{\partial t}\right)^2}} = 0 \tag{A.252}$$

$$N = -EIr\left[\left(\frac{\partial\theta}{\partial x}\right)^4 - 3\left(\frac{\partial^2\theta}{\partial x^2}\right)^2 - 4\frac{\partial^3\theta}{\partial x^3}\frac{\partial\theta}{\partial x}\right] - EAr\left[\frac{\partial u_x}{\partial x}\left(\frac{\partial\theta}{\partial x}\right)^2 + \frac{1}{2}r^2\left(\frac{\partial\theta}{\partial x}\right)^4\right] + I_p r\omega\left[\frac{\partial^3\theta}{\partial x^2\partial t} - \frac{\partial\theta}{\partial t}\left(\frac{\partial\theta}{\partial x}\right)^2\right] + m_p g\cos\theta + m_p r\left(\frac{\partial\theta}{\partial t}\right)^2 \tag{A.253}$$

$$
\begin{aligned}
&EIr\left[\frac{\partial^4\theta}{\partial x^4} - 6\left(\frac{\partial\theta}{\partial x}\right)^2\frac{\partial^2\theta}{\partial x^2}\right] \\
&\qquad - EAr\left[\frac{\partial u_x}{\partial x}\frac{\partial^2\theta}{\partial x^2} + \frac{\partial^2 u_x}{\partial x^2}\frac{\partial\theta}{\partial x} + \frac{3}{2}r^2\frac{\partial^2\theta}{\partial x^2}\left(\frac{\partial\theta}{\partial x}\right)^2\right] \\
&\qquad - I_p r\omega\left[2\frac{\partial^2\theta}{\partial x\partial t}\frac{\partial\theta}{\partial x} + \frac{\partial\theta}{\partial t}\frac{\partial^2\theta}{\partial x^2}\right] + m_p g\, sin\,\theta \\
&\qquad + m_p r\frac{\partial^2\theta}{\partial t^2} + \frac{sgn\left(\frac{\partial\theta}{\partial t}\right) fNr\left|\frac{\partial\theta}{\partial t}\right|}{\sqrt{\left(\frac{\partial u_x}{\partial t}\right)^2 + r^2\left(\frac{\partial\theta}{\partial t}\right)^2}} = 0
\end{aligned}
\tag{A.254}
$$

Eq. (A.253) for the normal contact force is exactly the same as Eq. (A.101) obtained previously without friction. Substituting Eq. (A.253) into Eqs. (A.252) and (A.254):

$$
\begin{aligned}
&EA\frac{\partial^2 u_x}{\partial x^2} - m_p\frac{\partial^2 u_x}{\partial t^2} + EAr^2\frac{\partial\theta}{\partial x}\frac{\partial^2\theta}{\partial x^2} \\
&\qquad - \frac{sgn\left(\frac{\partial u_x}{\partial t}\right) f\left|\frac{\partial u_x}{\partial t}\right|}{\sqrt{\left(\frac{\partial u_x}{\partial t}\right)^2 + r^2\left(\frac{\partial\theta}{\partial t}\right)^2}}\left\{-EIr\left[\left(\frac{\partial\theta}{\partial x}\right)^4 - 3\left(\frac{\partial^2\theta}{\partial x^2}\right)^2\right.\right. \\
&\qquad \left. - 4\frac{\partial^3\theta}{\partial x^3}\frac{\partial\theta}{\partial x}\right] - EAr\left[\frac{\partial u_x}{\partial x}\left(\frac{\partial\theta}{\partial x}\right)^2 + \frac{1}{2}r^2\left(\frac{\partial\theta}{\partial x}\right)^4\right] \\
&\qquad + I_p r\omega\left[\frac{\partial^3\theta}{\partial x^2\partial t} - \frac{\partial\theta}{\partial t}\left(\frac{\partial\theta}{\partial x}\right)^2\right] + m_p g\, cos\,\theta \\
&\qquad \left. + m_p r\left(\frac{\partial\theta}{\partial t}\right)^2\right\} = 0
\end{aligned}
\tag{A.255}
$$

$$
\begin{aligned}
& EIr\left[\frac{\partial^4\theta}{\partial x^4}-6\left(\frac{\partial\theta}{\partial x}\right)^2\frac{\partial^2\theta}{\partial x^2}\right] \\
&\quad - EAr\left[\frac{\partial u_x}{\partial x}\frac{\partial^2\theta}{\partial x^2}+\frac{\partial^2 u_x}{\partial x^2}\frac{\partial\theta}{\partial x}+\frac{3}{2}r^2\frac{\partial^2\theta}{\partial x^2}\left(\frac{\partial\theta}{\partial x}\right)^2\right] \\
&\quad - I_p r\omega\left[2\frac{\partial^2\theta}{\partial x\partial t}\frac{\partial\theta}{\partial x}+\frac{\partial\theta}{\partial t}\frac{\partial^2\theta}{\partial x^2}\right]+m_p g\sin\theta \\
&\quad + m_p r\frac{\partial^2\theta}{\partial t^2} \\
&\quad + \frac{sgn\left(\frac{\partial\theta}{\partial t}\right)fr\left|\frac{\partial\theta}{\partial t}\right|}{\sqrt{\left(\frac{\partial u_x}{\partial t}\right)^2+r^2\left(\frac{\partial\theta}{\partial t}\right)^2}}\left\{-EIr\left[\left(\frac{\partial\theta}{\partial x}\right)^4-3\left(\frac{\partial^2\theta}{\partial x^2}\right)^2\right.\right. \\
&\quad \left. - 4\frac{\partial^3\theta}{\partial x^3}\frac{\partial\theta}{\partial x}\right]-EAr\left[\frac{\partial u_x}{\partial x}\left(\frac{\partial\theta}{\partial x}\right)^2+\frac{1}{2}r^2\left(\frac{\partial\theta}{\partial x}\right)^4\right] \\
&\quad + I_p r\omega\left[\frac{\partial^3\theta}{\partial x^2\partial t}-\frac{\partial\theta}{\partial t}\left(\frac{\partial\theta}{\partial x}\right)^2\right]+m_p g\cos\theta \\
&\quad \left. + m_p r\left(\frac{\partial\theta}{\partial t}\right)^2\right\}=0
\end{aligned}
\tag{A.256}
$$

Eqs. (A.255) and (A.256) allow calculating the axial displacement u_x and angular displacement θ. Knowing the displacements, the forces F_x and N can then be calculated as well.

A.2.2. Model for tripping out

As in the model without friction, the motion equations become simplified for the tripping out problem. The friction force, in this case, has only one component and is given by:

$$\vec{F}_f(x,t)=\vec{F}_{f1}(x,t)\hat{\imath} \tag{A.257}$$

Similarly, this component will be given by:

$$\left|\vec{F}_{f1}\right|=f_1 N dx \tag{A.258}$$

$$\vec{F}_{f1}(x,t)=-sgn\left(\frac{\partial u_x}{\partial t}\right)f_1 N dx\hat{\imath} \tag{A.259}$$

However, in this case, since there is not another friction component, $f = f_1$. Substituting Eq. (A.259) into Eq. (A.257):

$$\vec{F}_f(x,t) = -sgn\left(\frac{\partial u_x}{\partial t}\right) fNdx\hat{\imath} \quad \text{(A.260)}$$

It is interesting to point that the $\hat{\imath}$ component for the friction force during tripping out, given by Eq. (A.260) is different from the $\hat{\imath}$ component for the friction force during tripping in. This suggests that the friction force in the axial direction is, indeed, different during tripping in and tripping out the column. The total external force per unit of length will be given by:

$$\vec{f} = \frac{\vec{q}_p}{dx} + \frac{\vec{N}}{dx} + \frac{\vec{F}_f}{dx} \quad \text{(A.261)}$$

Substituting Eqs. (A.125), (A.126) and (A.260) into Eq. (A.261):

$$\vec{f} = -m_p g\hat{k} + N\hat{k} - sgn\left(\frac{\partial u_x}{\partial t}\right) fN\hat{\imath} \quad \text{(A.262)}$$

$$\vec{f} = -sgn\left(\frac{\partial u_x}{\partial t}\right) fN\hat{\imath} + \left(-m_p g + N\right)\hat{k} \quad \text{(A.263)}$$

The summation of forces will be given by Eq. (A.134). Substituting Eqs. (A.112), (A.122) and (A.263) into Eq. (A.134):

$$\begin{gathered}\frac{\partial F_x}{\partial x}\hat{\imath} + \frac{\partial F_y}{\partial x}\hat{\jmath} + \frac{\partial F_z}{\partial x}\hat{k} + sgn\left(\frac{\partial u_x}{\partial t}\right) fN\hat{\imath} - \left(-m_p g + N\right)\hat{k} \\ + m_p\left[\frac{\partial^2 u_x}{\partial t^2}\hat{\imath}\right] = 0\end{gathered} \quad \text{(A.264)}$$

Manipulating Eq. (A.264):

$$\begin{gathered}\left(\frac{\partial F_x}{\partial x} + m_p\frac{\partial^2 u_x}{\partial t^2} + sgn\left(\frac{\partial u_x}{\partial t}\right) fN\right)\hat{\imath} + \left(\frac{\partial F_y}{\partial x}\right)\hat{\jmath} \\ + \left(\frac{\partial F_z}{\partial x} + m_p g - N\right)\hat{k} = 0\end{gathered} \quad \text{(A.265)}$$

Separating Eq. (A.265) into components:

$$\frac{\partial F_x}{\partial x} + m_p \frac{\partial^2 u_x}{\partial t^2} + sgn\left(\frac{\partial u_x}{\partial t}\right) fN = 0 \tag{A.266}$$

$$\frac{\partial F_y}{\partial x} = 0 \tag{A.267}$$

$$\frac{\partial F_z}{\partial x} + m_p g - N = 0 \tag{A.268}$$

Once again looking at the previous analysis, it is easy to see that the calculations for F_x, F_y and F_z of $\vec{F}$ will not change with the friction force. Therefore, substituting Eqs. (A.131), (A.147) and (A.148) into Eqs. (A.266), (A.267) and (A.268), it is easy to note that Eq. (A.267) becomes irrelevant and only two equations remain:

$$\frac{\partial}{\partial x}\left[-EA\frac{\partial u_x}{\partial x}\right] + m_p \frac{\partial^2 u_x}{\partial t^2} + sgn\left(\frac{\partial u_x}{\partial t}\right) fN = 0 \tag{A.269}$$

$$\frac{\partial}{\partial x}\left[-m_p r\frac{\partial^2 u_x}{\partial t^2}\right] + m_p g - N = 0 \tag{A.270}$$

Manipulating Eqs. (A.269) and (A.270):

$$EA\frac{\partial^2 u_x}{\partial x^2} - m_p \frac{\partial^2 u_x}{\partial t^2} - sgn\left(\frac{\partial u_x}{\partial t}\right) fN = 0 \tag{A.271}$$

$$N = -m_p r\frac{\partial^3 u_x}{\partial x \partial t^2} + m_p g \tag{A.272}$$

Substituting Eq. (A.272) into Eq. (A.271):

$$EA\frac{\partial^2 u_x}{\partial x^2} - m_p \frac{\partial^2 u_x}{\partial t^2} - sgn\left(\frac{\partial u_x}{\partial t}\right) f\left[-m_p r\frac{\partial^3 u_x}{\partial x \partial t^2} + m_p g\right] = 0 \tag{A.273}$$

Eq. (A.273) allows calculating the axial displacement u_x. After that, the forces F_x and N can be calculated.

A.2.3. Solution for tripping in

As in the previous case, the solution here must be numeric. Repeating the four final equations:

$$
\begin{aligned}
&EA\frac{\partial^2 u_x}{\partial x^2} - m_p\frac{\partial^2 u_x}{\partial t^2} + EAr^2\frac{\partial\theta}{\partial x}\frac{\partial^2\theta}{\partial x^2} \\
&\quad - \frac{sgn\left(\frac{\partial u_x}{\partial t}\right) f\left|\frac{\partial u_x}{\partial t}\right|}{\sqrt{\left(\frac{\partial u_x}{\partial t}\right)^2 + r^2\left(\frac{\partial\theta}{\partial t}\right)^2}}\Bigg\{-EIr\left[\left(\frac{\partial\theta}{\partial x}\right)^4 - 3\left(\frac{\partial^2\theta}{\partial x^2}\right)^2\right. \\
&\quad\left. - 4\frac{\partial^3\theta}{\partial x^3}\frac{\partial\theta}{\partial x}\right] - EAr\left[\frac{\partial u_x}{\partial x}\left(\frac{\partial\theta}{\partial x}\right)^2 + \frac{1}{2}r^2\left(\frac{\partial\theta}{\partial x}\right)^4\right] \\
&\quad + I_p r\omega\left[\frac{\partial^3\theta}{\partial x^2\partial t} - \frac{\partial\theta}{\partial t}\left(\frac{\partial\theta}{\partial x}\right)^2\right] + m_p g\cos\theta \\
&\quad + m_p r\left(\frac{\partial\theta}{\partial t}\right)^2\Bigg\} = 0
\end{aligned}
\tag{A.274}
$$

$$
\begin{aligned}
&EIr\left[\frac{\partial^4\theta}{\partial x^4} - 6\left(\frac{\partial\theta}{\partial x}\right)^2\frac{\partial^2\theta}{\partial x^2}\right] \\
&\quad - EAr\left[\frac{\partial u_x}{\partial x}\frac{\partial^2\theta}{\partial x^2} + \frac{\partial^2 u_x}{\partial x^2}\frac{\partial\theta}{\partial x} + \frac{3}{2}r^2\frac{\partial^2\theta}{\partial x^2}\left(\frac{\partial\theta}{\partial x}\right)^2\right] \\
&\quad - I_p r\omega\left[2\frac{\partial^2\theta}{\partial x\partial t}\frac{\partial\theta}{\partial x} + \frac{\partial\theta}{\partial t}\frac{\partial^2\theta}{\partial x^2}\right] + m_p g\sin\theta \\
&\quad + m_p r\frac{\partial^2\theta}{\partial t^2} \\
&\quad + \frac{sgn\left(\frac{\partial\theta}{\partial t}\right) fr\left|\frac{\partial\theta}{\partial t}\right|}{\sqrt{\left(\frac{\partial u_x}{\partial t}\right)^2 + r^2\left(\frac{\partial\theta}{\partial t}\right)^2}}\Bigg\{-EIr\left[\left(\frac{\partial\theta}{\partial x}\right)^4 - 3\left(\frac{\partial^2\theta}{\partial x^2}\right)^2\right. \\
&\quad\left. - 4\frac{\partial^3\theta}{\partial x^3}\frac{\partial\theta}{\partial x}\right] - EAr\left[\frac{\partial u_x}{\partial x}\left(\frac{\partial\theta}{\partial x}\right)^2 + \frac{1}{2}r^2\left(\frac{\partial\theta}{\partial x}\right)^4\right] \\
&\quad + I_p r\omega\left[\frac{\partial^3\theta}{\partial x^2\partial t} - \frac{\partial\theta}{\partial t}\left(\frac{\partial\theta}{\partial x}\right)^2\right] + m_p g\cos\theta \\
&\quad + m_p r\left(\frac{\partial\theta}{\partial t}\right)^2\Bigg\} = 0
\end{aligned}
\tag{A.275}
$$

$$
F_x = -EA\frac{\partial u_x}{\partial x} - \frac{1}{2}EAr^2\left(\frac{\partial\theta}{\partial x}\right)^2 \tag{A.276}
$$

$$
\begin{aligned}
N = -EIr\left[\left(\frac{\partial\theta}{\partial x}\right)^4 - 3\left(\frac{\partial^2\theta}{\partial x^2}\right)^2 - 4\frac{\partial^3\theta}{\partial x^3}\frac{\partial\theta}{\partial x}\right] \\
- EAr\left[\frac{\partial u_x}{\partial x}\left(\frac{\partial\theta}{\partial x}\right)^2 + \frac{1}{2}r^2\left(\frac{\partial\theta}{\partial x}\right)^4\right] \\
+ I_p r\omega\left[\frac{\partial^3\theta}{\partial x^2\partial t} - \frac{\partial\theta}{\partial t}\left(\frac{\partial\theta}{\partial x}\right)^2\right] + m_p g\cos\theta \\
+ m_p r\left(\frac{\partial\theta}{\partial t}\right)^2
\end{aligned}
\tag{A.277}
$$

Discretizing Eqs. (A.274), (A.275), (A.276) and (A.277):

$$
\begin{aligned}
& EA\left(\frac{U_{i+1,j} - 2U_{i,j} + U_{i-1,j}}{\Delta x^2}\right) - m_p\left(\frac{U_{i,j+1} - 2U_{i,j} + U_{i,j-1}}{\Delta t^2}\right) \\
& + EAr^2\left(\frac{\theta_{i+1,j} - \theta_{i-1,j}}{2\Delta x}\right)\left(\frac{\theta_{i+1,j} - 2\theta_{i,j} + \theta_{i-1,j}}{\Delta x^2}\right) \\
& - \frac{sgn\left(U_{i,j} - U_{i,j-1}\right) f \left|\frac{U_{i,j}-U_{i,j-2}}{2\Delta t}\right|}{\sqrt{\left(\frac{U_{i,j}-U_{i,j-2}}{2\Delta t}\right)^2 + r^2\left(\frac{\theta_{i,j}-\theta_{i,j-2}}{2\Delta t}\right)^2}}\left\{-EIr\left[\left(\frac{\theta_{i+1,j} - \theta_{i-1,j}}{2\Delta x}\right)^4\right.\right. \\
& - 3\left(\frac{\theta_{i+1,j} - 2\theta_{i,j} + \theta_{i-1,j}}{\Delta x^2}\right)^2 \\
& \left. - 4\left(\frac{\theta_{i+2,j} - 2\theta_{i+1,j} + 2\theta_{i-1,j} - \theta_{i-2,j}}{2\Delta x^3}\right)\left(\frac{\theta_{i+1,j} - \theta_{i-1,j}}{2\Delta x}\right)\right] \\
& - EAr\left[\left(\frac{U_{i+1,j} - U_{i-1,j}}{2\Delta x}\right)\left(\frac{\theta_{i+1,j} - \theta_{i-1,j}}{2\Delta x}\right)^2\right. \\
& \left. + \frac{1}{2}r^2\left(\frac{\theta_{i+1,j} - \theta_{i-1,j}}{2\Delta x}\right)^4\right] \\
& + I_p r\omega\left[\left(\frac{\theta_{i+1,j} - 2\theta_{i,j} + \theta_{i-1,j} - \theta_{i+1,j-2} + 2\theta_{i,j-2} - \theta_{i-1,j-2}}{2\Delta x^2\Delta t}\right)\right. \\
& \left. - \left(\frac{\theta_{i,j} - \theta_{i,j-2}}{2\Delta t}\right)\left(\frac{\theta_{i+1,j} - \theta_{i-1,j}}{2\Delta x}\right)^2\right] + m_p g\cos\theta_{i,j} \\
& \left. + m_p r\left(\frac{\theta_{i,j} - \theta_{i,j-2}}{2\Delta t}\right)^2\right\} = 0
\end{aligned}
\tag{A.278}
$$

$$
\begin{aligned}
&EIr\left[\left(\frac{\theta_{i+2,j}-4\theta_{i+1,j}+6\theta_{i,j}-4\theta_{i-1,j}+\theta_{i-2,j}}{\Delta x^4}\right)\right.\\
&\left.-6\left(\frac{\theta_{i+1,j}-\theta_{i-1,j}}{2\Delta x}\right)^2\left(\frac{\theta_{i+1,j}-2\theta_{i,j}+\theta_{i-1,j}}{\Delta x^2}\right)\right]\\
&-EAr\left[\left(\frac{U_{i+1,j}-U_{i-1,j}}{2\Delta x}\right)\left(\frac{\theta_{i+1,j}-2\theta_{i,j}+\theta_{i-1,j}}{\Delta x^2}\right)\right.\\
&+\left(\frac{U_{i+1,j}-2U_{i,j}+U_{i-1,j}}{\Delta x^2}\right)\left(\frac{\theta_{i+1,j}-\theta_{i-1,j}}{2\Delta x}\right)\\
&\left.+\frac{3}{2}r^2\left(\frac{\theta_{i+1,j}-2\theta_{i,j}+\theta_{i-1,j}}{\Delta x^2}\right)\left(\frac{\theta_{i+1,j}-\theta_{i-1,j}}{2\Delta x}\right)^2\right]\\
&-I_pr\omega\left[2\left(\frac{\theta_{i+1,j+1}-\theta_{i-1,j+1}-\theta_{i+1,j-1}+\theta_{i-1,j-1}}{4\Delta x\Delta t}\right)\left(\frac{\theta_{i+1,j}-\theta_{i-1,j}}{2\Delta x}\right)\right.\\
&\left.+\left(\frac{\theta_{i,j+1}-\theta_{i,j-1}}{2\Delta t}\right)\left(\frac{\theta_{i+1,j}-2\theta_{i,j}+\theta_{i-1,j}}{\Delta x^2}\right)\right]+m_pg\sin\theta_{i,j}\\
&+m_pr\left(\frac{\theta_{i,j+1}-2\theta_{i,j}+\theta_{i,j-1}}{\Delta t^2}\right)\\
&+\frac{sgn\left(\theta_{i,j}-\theta_{i,j-1}\right)fr\left|\frac{\theta_{i,j}-\theta_{i,j-2}}{2\Delta t}\right|}{\sqrt{\left(\frac{U_{i,j}-U_{i,j-2}}{2\Delta t}\right)^2+r^2\left(\frac{\theta_{i,j}-\theta_{i,j-2}}{2\Delta t}\right)^2}}\left\{-EIr\left[\left(\frac{\theta_{i+1,j}-\theta_{i-1,j}}{2\Delta x}\right)^4\right.\right.\\
&-3\left(\frac{\theta_{i+1,j}-2\theta_{i,j}+\theta_{i-1,j}}{\Delta x^2}\right)^2\\
&\left.-4\left(\frac{\theta_{i+2,j}-2\theta_{i+1,j}+2\theta_{i-1,j}-\theta_{i-2,j}}{2\Delta x^3}\right)\left(\frac{\theta_{i+1,j}-\theta_{i-1,j}}{2\Delta x}\right)\right]\\
&-EAr\left[\left(\frac{U_{i+1,j}-U_{i-1,j}}{2\Delta x}\right)\left(\frac{\theta_{i+1,j}-\theta_{i-1,j}}{2\Delta x}\right)^2+\frac{1}{2}r^2\left(\frac{\theta_{i+1,j}-\theta_{i-1,j}}{2\Delta x}\right)^4\right]\\
&+I_pr\omega\left[\left(\frac{\theta_{i+1,j}-2\theta_{i,j}+\theta_{i-1,j}-\theta_{i+1,j-2}+2\theta_{i,j-2}-\theta_{i-1,j-2}}{2\Delta x^2\Delta t}\right)\right.\\
&\left.-\left(\frac{\theta_{i,j}-\theta_{i,j-2}}{2\Delta t}\right)\left(\frac{\theta_{i+1,j}-\theta_{i-1,j}}{2\Delta x}\right)^2\right]+m_pg\cos\theta_{i,j}\\
&\left.+m_pr\left(\frac{\theta_{i,j}-\theta_{i,j-2}}{2\Delta t}\right)^2\right\}=0
\end{aligned}
\tag{A.279}
$$

$$
F_{i,j}=-\frac{EA}{2\Delta x}\left(U_{i+1,j}-U_{i-1,j}\right)-\frac{1}{2}EAr^2\left(\frac{\theta_{i+1,j}-\theta_{i-1,j}}{2\Delta x}\right)^2 \tag{A.280}
$$

$$N_{i,j} = -EIr\left[\left(\frac{\theta_{i+1,j}-\theta_{i-1,j}}{2\Delta x}\right)^4 - 3\left(\frac{\theta_{i+1,j}-2\theta_{i,j}+\theta_{i-1,j}}{\Delta x^2}\right)^2 - 4\left(\frac{\theta_{i+2,j}-2\theta_{i+1,j}+2\theta_{i-1,j}-\theta_{i-2,j}}{2\Delta x^3}\right)\left(\frac{\theta_{i+1,j}-\theta_{i-1,j}}{2\Delta x}\right)\right] - EAr\left[\left(\frac{U_{i+1,j}-U_{i-1,j}}{2\Delta x}\right)\left(\frac{\theta_{i+1,j}-\theta_{i-1,j}}{2\Delta x}\right)^2 + \frac{1}{2}r^2\left(\frac{\theta_{i+1,j}-\theta_{i-1,j}}{2\Delta x}\right)^4\right] + I_p r\omega\left[\left(\frac{\theta_{i+1,j}-2\theta_{i,j}+\theta_{i-1,j}-\theta_{i+1,j-2}+2\theta_{i,j-2}-\theta_{i-1,j-2}}{2\Delta x^2\Delta t}\right) - \left(\frac{\theta_{i,j}-\theta_{i,j-2}}{2\Delta t}\right)\left(\frac{\theta_{i+1,j}-\theta_{i-1,j}}{2\Delta x}\right)^2\right] + m_p g\cos\theta_{i,j} + m_p r\left(\frac{\theta_{i,j}-\theta_{i,j-2}}{2\Delta t}\right)^2 \tag{A.281}$$

Manipulating Eqs. (A.278), (A.279), (A.280) and (A.281):

$$U_{i,j+1} = 2U_{i,j} - U_{i,j-1} + \frac{EA\Delta t^2}{m_p\Delta x^2}\left(U_{i+1,j}-2U_{i,j}+U_{i-1,j}\right) + \frac{EAr^2\Delta t^2}{2m_p\Delta x^3}\left(\theta_{i+1,j}-\theta_{i-1,j}\right)\left(\theta_{i+1,j}-2\theta_{i,j}+\theta_{i-1,j}\right) - \frac{sgn\left(U_{i,j}-U_{i,j-1}\right) f\Delta t\left|U_{i,j}-U_{i,j-2}\right|}{2m_p\sqrt{\left(\frac{U_{i,j}-U_{i,j-2}}{2\Delta t}\right)^2 + r^2\left(\frac{\theta_{i,j}-\theta_{i,j-2}}{2\Delta t}\right)^2}}\left\{-\frac{EIr}{\Delta x^4}\left[\frac{1}{16}\left(\theta_{i+1,j}-\theta_{i-1,j}\right)^4 - 3\left(\theta_{i+1,j}-2\theta_{i,j}+\theta_{i-1,j}\right)^2 - \left(\theta_{i+2,j}-2\theta_{i+1,j}+2\theta_{i-1,j}-\theta_{i-2,j}\right)\left(\theta_{i+1,j}-\theta_{i-1,j}\right)\right] - \frac{EAr}{8\Delta x^3}\left[\left(U_{i+1,j}-U_{i-1,j}\right)\left(\theta_{i+1,j}-\theta_{i-1,j}\right)^2 + \frac{r^2}{4\Delta x}\left(\theta_{i+1,j}-\theta_{i-1,j}\right)^4\right] + \frac{I_p r\omega}{2\Delta x^2\Delta t}\left[\left(\theta_{i+1,j}-2\theta_{i,j}+\theta_{i-1,j}-\theta_{i+1,j-2}+2\theta_{i,j-2}-\theta_{i-1,j-2}\right) - \frac{1}{4}\left(\theta_{i,j}-\theta_{i,j-2}\right)\left(\theta_{i+1,j}-\theta_{i-1,j}\right)^2\right] + m_p g\cos\theta_{i,j} + \frac{m_p r}{4\Delta t^2}\left(\theta_{i,j}-\theta_{i,j-2}\right)^2\right\} \tag{A.282}$$

$$
\begin{aligned}
&\frac{I_p r\omega\left(\theta_{i+1,j}-\theta_{i-1,j}\right)}{4\Delta x^2\Delta t}\theta_{i+1,j+1} \\
&+\left[\frac{I_p r\omega\left(\theta_{i+1,j}-2\theta_{i,j}+\theta_{i-1,j}\right)}{2\Delta x^2\Delta t}-\frac{m_p r}{\Delta t^2}\right]\theta_{i,j+1} \\
&-\frac{I_p r\omega\left(\theta_{i+1,j}-\theta_{i-1,j}\right)}{4\Delta x^2\Delta t}\theta_{i-1,j+1} \\
&=\frac{I_p r\omega\left(\theta_{i+1,j}-2\theta_{i,j}+\theta_{i-1,j}\right)}{2\Delta x^2\Delta t}\theta_{i,j-1} \\
&-\frac{I_p r\omega\left(\theta_{i+1,j}-\theta_{i-1,j}\right)}{4\Delta x^2\Delta t}\left(-\theta_{i+1,j-1}+\theta_{i-1,j-1}\right) \\
&+\frac{m_p r}{\Delta t^2}\left(-2\theta_{i,j}+\theta_{i,j-1}\right) \\
&+\frac{EIr}{\Delta x^4}\left[\left(\theta_{i+2,j}-4\theta_{i+1,j}+6\theta_{i,j}-4\theta_{i-1,j}+\theta_{i-2,j}\right)\right. \\
&\left.-\frac{3}{2}\left(\theta_{i+1,j}-\theta_{i-1,j}\right)^2\left(\theta_{i+1,j}-2\theta_{i,j}+\theta_{i-1,j}\right)\right] \\
&-\frac{EAr}{2\Delta x^3}\left[\left(U_{i+1,j}-U_{i-1,j}\right)\left(\theta_{i+1,j}-2\theta_{i,j}+\theta_{i-1,j}\right)\right. \\
&+\left(U_{i+1,j}-2U_{i,j}+U_{i-1,j}\right)\left(\theta_{i+1,j}-\theta_{i-1,j}\right) \\
&\left.+\frac{3r^2}{4\Delta x}\left(\theta_{i+1,j}-2\theta_{i,j}+\theta_{i-1,j}\right)\left(\theta_{i+1,j}-\theta_{i-1,j}\right)^2\right]+m_p g\sin\theta_{i,j} \\
&+\frac{sgn\left(\theta_{i,j}-\theta_{i,j-1}\right)fr\left|\theta_{i,j}-\theta_{i,j-2}\right|}{2\Delta t\sqrt{\left(\frac{U_{i,j}-U_{i,j-2}}{2\Delta t}\right)^2+r^2\left(\frac{\theta_{i,j}-\theta_{i,j-2}}{2\Delta t}\right)^2}}\left\{-\frac{EIr}{\Delta x^4}\left[\frac{1}{16}\left(\theta_{i+1,j}-\theta_{i-1,j}\right)^4\right.\right. \\
&-3\left(\theta_{i+1,j}-2\theta_{i,j}+\theta_{i-1,j}\right)^2 \\
&\left.-\left(\theta_{i+2,j}-2\theta_{i+1,j}+2\theta_{i-1,j}-\theta_{i-2,j}\right)\left(\theta_{i+1,j}-\theta_{i-1,j}\right)\right] \\
&-\frac{EAr}{8\Delta x^3}\left[\left(U_{i+1,j}-U_{i-1,j}\right)\left(\theta_{i+1,j}-\theta_{i-1,j}\right)^2\right. \\
&\left.+\frac{r^2}{4\Delta x}\left(\theta_{i+1,j}-\theta_{i-1,j}\right)^4\right] \\
&+\frac{I_p r\omega}{2\Delta x^2\Delta t}\left[\left(\theta_{i+1,j}-2\theta_{i,j}+\theta_{i-1,j}-\theta_{i+1,j-2}+2\theta_{i,j-2}-\theta_{i-1,j-2}\right)\right. \\
&\left.-\frac{1}{4}\left(\theta_{i,j}-\theta_{i,j-2}\right)\left(\theta_{i+1,j}-\theta_{i-1,j}\right)^2\right]+m_p g\cos\theta_{i,j} \\
&\left.+\frac{m_p r}{4\Delta t^2}\left(\theta_{i,j}-\theta_{i,j-2}\right)^2\right\}
\end{aligned}
\tag{A.283}
$$

$$
F_{i,j}=-\frac{EA}{2\Delta x}\left[\left(U_{i+1,j}-U_{i-1,j}\right)+\frac{r^2}{4\Delta x}\left(\theta_{i+1,j}-\theta_{i-1,j}\right)^2\right] \tag{A.284}
$$

$$N_{i,j} = -\frac{EIr}{\Delta x^4}\left[\frac{1}{16}\left(\theta_{i+1,j} - \theta_{i-1,j}\right)^4 - 3\left(\theta_{i+1,j} - 2\theta_{i,j} + \theta_{i-1,j}\right)^2 - \left(\theta_{i+2,j} - 2\theta_{i+1,j} + 2\theta_{i-1,j} - \theta_{i-2,j}\right)\left(\theta_{i+1,j} - \theta_{i-1,j}\right)\right] - \frac{EAr}{8\Delta x^3}\left[\left(U_{i+1,j} - U_{i-1,j}\right)\left(\theta_{i+1,j} - \theta_{i-1,j}\right)^2 + \frac{r^2}{4\Delta x}\left(\theta_{i+1,j} - \theta_{i-1,j}\right)^4\right] + \frac{I_p r\omega}{2\Delta x^2 \Delta t}\left[\left(\theta_{i+1,j} - 2\theta_{i,j} + \theta_{i-1,j} - \theta_{i+1,j-2} + 2\theta_{i,j-2} - \theta_{i-1,j-2}\right) - \frac{1}{4}\left(\theta_{i,j} - \theta_{i,j-2}\right)\left(\theta_{i+1,j} - \theta_{i-1,j}\right)^2\right] + m_p g \cos\theta_{i,j} + \frac{m_p r}{4\Delta t^2}\left(\theta_{i,j} - \theta_{i,j-2}\right)^2 \tag{A.285}$$

The boundary conditions are the same given by Eqs. (A.163), (A.164), (A.165), (A.166), (A.167) and (A.168), with their discretizations given by Eqs. (A.169), (A.170), (A.171), (A.172), (A.173) and (A.174). Substituting $i = 1$ in Eqs. (A.282) and (A.283) and using the boundary conditions:

$$U_{1,j+1} = 2U_{1,j} - U_{1,j-1} + \frac{EA\Delta t^2}{m_p \Delta x^2}\left(U_{2,j} - 2U_{1,j}\right) + \frac{EAr^2\Delta t^2}{2m_p\Delta x^3}\theta_{2,j}\left(\theta_{2,j} - 2\theta_{1,j}\right) - \frac{sgn\left(U_{1,j} - U_{1,j-1}\right) f\Delta t\left|U_{1,j} - U_{1,j-2}\right|}{2m_p\sqrt{\left(\frac{U_{1,j}-U_{1,j-2}}{2\Delta t}\right)^2 + r^2\left(\frac{\theta_{1,j}-\theta_{1,j-2}}{2\Delta t}\right)^2}}\left\{-\frac{EIr}{\Delta x^4}\left[\frac{1}{16}{\theta_{2,j}}^4 - 3\left(\theta_{2,j} - 2\theta_{1,j}\right)^2 - \left(\theta_{3,j} - 2\theta_{2,j} + \theta_{1,j}\right)\theta_{2,j}\right] - \frac{EAr}{8\Delta x^3}\left[U_{2,j}{\theta_{2,j}}^2 + \frac{r^2}{4\Delta x}{\theta_{2,j}}^4\right] + \frac{I_p r\omega}{2\Delta x^2\Delta t}\left[\left(\theta_{2,j} - 2\theta_{1,j} - \theta_{2,j-2} + 2\theta_{1,j-2}\right) - \frac{1}{4}\left(\theta_{1,j} - \theta_{1,j-2}\right){\theta_{2,j}}^2\right] + m_p g\cos\theta_{1,j} + \frac{m_p r}{4\Delta t^2}\left(\theta_{1,j} - \theta_{1,j-2}\right)^2\right\} \tag{A.286}$$

$$\frac{I_p r\omega\theta_{2,j}}{4\Delta x^2\Delta t}\theta_{2,j+1} + \left[\frac{I_p r\omega\left(\theta_{2,j} - 2\theta_{1,j}\right)}{2\Delta x^2\Delta t} - \frac{m_p r}{\Delta t^2}\right]\theta_{1,j+1}$$
$$= \frac{I_p r\omega\left(\theta_{2,j} - 2\theta_{1,j}\right)}{2\Delta x^2\Delta t}\theta_{1,j-1} - \frac{I_p r\omega\theta_{2,j}}{4\Delta x^2\Delta t}\left(-\theta_{2,j-1}\right)$$
$$+ \frac{m_p r}{\Delta t^2}\left(-2\theta_{1,j} + \theta_{1,j-1}\right)$$
$$+ \frac{EIr}{\Delta x^4}\left[\left(\theta_{3,j} - 4\theta_{2,j} + 5\theta_{1,j}\right) - \frac{3}{2}\left(\theta_{2,j}\right)^2\left(\theta_{2,j} - 2\theta_{1,j}\right)\right]$$
$$- \frac{EAr}{2\Delta x^3}\left[U_{2,j}\left(\theta_{2,j} - 2\theta_{1,j}\right) + \theta_{2,j}\left(U_{2,j} - 2U_{1,j}\right)\right.$$
$$\left. + \frac{3r^2}{4\Delta x}{\theta_{2,j}}^2\left(\theta_{2,j} - 2\theta_{1,j}\right)\right] + m_p g\sin\theta_{1,j} \tag{A.287}$$
$$+ \frac{sgn\left(\theta_{1,j} - \theta_{1,j-1}\right) fr\left|\theta_{1,j} - \theta_{1,j-2}\right|}{2\Delta t\sqrt{\left(\frac{U_{1,j} - U_{1,j-2}}{2\Delta t}\right)^2 + r^2\left(\frac{\theta_{1,j} - \theta_{1,j-2}}{2\Delta t}\right)^2}}\left\{-\frac{EIr}{\Delta x^4}\left[\frac{1}{16}{\theta_{2,j}}^4\right.\right.$$
$$\left. - 3\left(\theta_{2,j} - 2\theta_{1,j}\right)^2 - \left(\theta_{3,j} - 2\theta_{2,j} + \theta_{1,j}\right)\theta_{2,j}\right]$$
$$- \frac{EAr}{8\Delta x^3}\left[U_{2,j}{\theta_{2,j}}^2 + \frac{r^2}{4\Delta x}{\theta_{2,j}}^4\right]$$
$$+ \frac{I_p r\omega}{2\Delta x^2\Delta t}\left[\left(\theta_{2,j} - 2\theta_{1,j} - \theta_{2,j-2} + 2\theta_{1,j-2}\right)\right.$$
$$\left.\left. - \frac{1}{4}\left(\theta_{1,j} - \theta_{1,j-2}\right){\theta_{2,j}}^2\right] + m_p g\cos\theta_{1,j} + \frac{m_p r}{4\Delta t^2}\left(\theta_{1,j} - \theta_{1,j-2}\right)^2\right\}$$

Substituting $i = N - 1$ in Eqs. (A.282) and (A.283) and using the boundary conditions:

$$
\begin{aligned}
&U_{N-1,j+1} \\
&= 2U_{N-1,j} - U_{N-1,j-1} + \frac{EA\Delta t^2}{m_p \Delta x^2}\left(U_{N,j} - 2U_{N-1,j} + U_{N-2,j}\right) \\
&+ \frac{EAr^2\Delta t^2}{2m_p \Delta x^3}\left(\theta_{N,j} - \theta_{N-2,j}\right)\left(\theta_{N,j} - 2\theta_{N-1,j} + \theta_{N-2,j}\right) \\
&- \frac{sgn\left(U_{N-1,j} - U_{N-1,j-1}\right) f\Delta t\left|U_{N-1,j} - U_{N-1,j-2}\right|}{2m_p\sqrt{\left(\frac{U_{N-1,j}-U_{N-1,j-2}}{2\Delta t}\right)^2 + r^2\left(\frac{\theta_{N-1,j}-\theta_{N-1,j-2}}{2\Delta t}\right)^2}}\left\{-\frac{EIr}{\Delta x^4}\left[\frac{1}{16}\left(\theta_{N,j}\right.\right.\right. \\
&\left.- \theta_{N-2,j}\right)^4 - 3\left(\theta_{N,j} - 2\theta_{N-1,j} + \theta_{N-2,j}\right)^2 \\
&\left.- \left(-2\theta_{N,j} - \theta_{N-1,j} + 2\theta_{N-2,j} - \theta_{N-3,j}\right)\left(\theta_{N,j} - \theta_{N-2,j}\right)\right] \\
&- \frac{EAr}{8\Delta x^3}\left[\left(U_{N,j} - U_{N-2,j}\right)\left(\theta_{N,j} - \theta_{N-2,j}\right)^2 + \frac{r^2}{4\Delta x}\left(\theta_{N,j} - \theta_{N-2,j}\right)^4\right] \\
&+ \frac{I_p r\omega}{2\Delta x^2\Delta t}\left[\left(\theta_{N,j} - 2\theta_{N-1,j} + \theta_{N-2,j} - \theta_{N,j-2} + 2\theta_{N-1,j-2}\right.\right. \\
&\left.\left.- \theta_{N-2,j-2}\right) - \frac{1}{4}\left(\theta_{N-1,j} - \theta_{N-1,j-2}\right)\left(\theta_{N,j} - \theta_{N-2,j}\right)^2\right] \\
&\left.+ m_p g\cos\theta_{N-1,j} + \frac{m_p r}{4\Delta t^2}\left(\theta_{N-1,j} - \theta_{N-1,j-2}\right)^2\right\}
\end{aligned}
\tag{A.288}
$$

$$
\begin{aligned}
&\frac{I_p r\omega\left(\theta_{N,j}-\theta_{N-2,j}\right)}{4\Delta x^2\Delta t}\theta_{N,j+1} \\
&+\left[\frac{I_p r\omega\left(\theta_{N,j}-2\theta_{N-1,j}+\theta_{N-2,j}\right)}{2\Delta x^2\Delta t}-\frac{m_p r}{\Delta t^2}\right]\theta_{N-1,j+1} \\
&-\frac{I_p r\omega\left(\theta_{N,j}-\theta_{N-2,j}\right)}{4\Delta x^2\Delta t}\theta_{N-2,j+1} \\
&=\frac{I_p r\omega\left(\theta_{N,j}-2\theta_{N-1,j}+\theta_{N-2,j}\right)}{2\Delta x^2\Delta t}\theta_{N-1,j-1} \\
&-\frac{I_p r\omega\left(\theta_{N,j}-\theta_{N-2,j}\right)}{4\Delta x^2\Delta t}\left(-\theta_{N,j-1}+\theta_{N-2,j-1}\right) \\
&+\frac{m_p r}{\Delta t^2}\left(-2\theta_{N-1,j}+\theta_{N-1,j-1}\right) \\
&+\frac{EIr}{\Delta x^4}\Big[\left(-4\theta_{N,j}+5\theta_{N-1,j}-4\theta_{N-2,j}+\theta_{N-3,j}\right) \\
&-\frac{3}{2}\left(\theta_{N,j}-\theta_{N-2,j}\right)^2\left(\theta_{N,j}-2\theta_{N-1,j}+\theta_{N-2,j}\right)\Big] \\
&-\frac{EAr}{2\Delta x^3}\Big[\left(\theta_{N,j}-\theta_{N-2,j}\right)\left(\theta_{N,j}-2\theta_{N-1,j}+\theta_{N-2,j}\right) \\
&+\left(U_{N,j}-2U_{N-1,j}+U_{N-2,j}\right)\left(\theta_{N,j}-\theta_{N-2,j}\right) \\
&+\frac{3r^2}{4\Delta x}\left(\theta_{N,j}-2\theta_{N-1,j}+\theta_{N-2,j}\right)\left(\theta_{N,j}-\theta_{N-2,j}\right)^2\Big]+m_p g\sin\theta_{N-1,j} \\
&+\frac{sgn\left(\theta_{N-1,j}-\theta_{N-1,j-1}\right)fr\left|\theta_{N-1,j}-\theta_{N-1,j-2}\right|}{2\Delta t\sqrt{\left(\frac{U_{N-1,j}-U_{N-1,j-2}}{2\Delta t}\right)^2+r^2\left(\frac{\theta_{N-1,j}-\theta_{N-1,j-2}}{2\Delta t}\right)^2}}\Big\{-\frac{EIr}{\Delta x^4}\Big[\frac{1}{16}\big(\theta_{N,j} \\
&-\theta_{N-2,j}\big)^4-3\left(\theta_{N,j}-2\theta_{N-1,j}+\theta_{N-2,j}\right)^2 \\
&-\left(-2\theta_{N,j}-\theta_{N-1,j}+2\theta_{N-2,j}-\theta_{N-3,j}\right)\left(\theta_{N,j}-\theta_{N-2,j}\right)\Big] \\
&-\frac{EAr}{8\Delta x^3}\left[\left(U_{N,j}-U_{N-2,j}\right)\left(\theta_{N,j}-\theta_{N-2,j}\right)^2+\frac{r^2}{4\Delta x}\left(\theta_{N,j}-\theta_{N-2,j}\right)^4\right] \\
&+\frac{I_p r\omega}{2\Delta x^2\Delta t}\Big[\big(\theta_{N,j}-2\theta_{N-1,j}+\theta_{N-2,j}-\theta_{N,j-2}+2\theta_{N-1,j-2} \\
&-\theta_{N-2,j-2}\big)-\frac{1}{4}\left(\theta_{N-1,j}-\theta_{N-1,j-2}\right)\left(\theta_{N,j}-\theta_{N-2,j}\right)^2\Big] \\
&+m_p g\cos\theta_{N-1,j}+\frac{m_p r}{4\Delta t^2}\left(\theta_{N-1,j}-\theta_{N-1,j-2}\right)^2\Big\}
\end{aligned}
\tag{A.289}
$$

Substituting $i = N$ in Eqs. (A.282) and (A.283) and using the boundary conditions:

$$
\begin{aligned}
&U_{N,j+1} \\
&= 2U_{N,j} - U_{N,j-1} + \frac{EA\Delta t^2}{m_p\Delta x^2}\left(-2U_{N,j} + 2U_{N-1,j} - \frac{r^2}{\Delta x}\theta_{N-1,j}{}^2\right) \\
&+ \frac{EAr^2\Delta t^2}{2m_p\Delta x^3}\left(-2\theta_{N-1,j}\right)\left(-2\theta_{N,j}\right) \\
&- \frac{sgn\left(U_{N,j} - U_{N,j-1}\right) f\Delta t\left|U_{N,j} - U_{N,j-2}\right|}{2m_p\sqrt{\left(\frac{U_{N,j}-U_{N,j-2}}{2\Delta t}\right)^2 + r^2\left(\frac{\theta_{N,j}-\theta_{N,j-2}}{2\Delta t}\right)^2}}\left\{-\frac{EIr}{\Delta x^4}\left[\frac{1}{16}\left(-2\theta_{N-1,j}\right)^4\right.\right. \\
&\left.- 3\left(-2\theta_{N,j}\right)^2\right] \\
&- \frac{EAr}{8\Delta x^3}\left[\left(-\frac{r^2}{\Delta x}\theta_{N-1,j}{}^2\right)\left(-2\theta_{N-1,j}\right)^2 + \frac{r^2}{4\Delta x}\left(-2\theta_{N-1,j}\right)^4\right] \\
&+ \frac{I_p r\omega}{2\Delta x^2\Delta t}\left[\left(-2\theta_{N,j} + 2\theta_{N,j-2}\right) - \frac{1}{4}\left(\theta_{N,j} - \theta_{N,j-2}\right)\left(-2\theta_{N-1,j}\right)^2\right] \\
&\left.+ m_p g\cos\theta_{N,j} + \frac{m_p r}{4\Delta t^2}\left(\theta_{N,j} - \theta_{N,j-2}\right)^2\right\}
\end{aligned}
\tag{A.290}
$$

$$
\begin{aligned}
&\left[\frac{I_p r\omega\left(-2\theta_{N,j}\right)}{2\Delta x^2\Delta t} - \frac{m_p r}{\Delta t^2}\right]\theta_{N,j+1} - 2\frac{I_p r\omega\left(-2\theta_{N-1,j}\right)}{4\Delta x^2\Delta t}\theta_{N-1,j+1} \\
&= \frac{I_p r\omega\left(-2\theta_{N,j}\right)}{2\Delta x^2\Delta t}\theta_{N,j-1} - \frac{I_p r\omega\left(-2\theta_{N-1,j}\right)}{4\Delta x^2\Delta t}\left(2\theta_{N-1,j-1}\right) \\
&+ \frac{m_p r}{\Delta t^2}\left(-2\theta_{N,j} + \theta_{N,j-1}\right) \\
&+ \frac{EIr}{\Delta x^4}\left[\left(6\theta_{N,j} - 4\theta_{N-1,j} + 2\theta_{N-2,j}\right) - \frac{3}{2}\left(-2\theta_{N-1,j}\right)^2\left(-2\theta_{N,j}\right)\right] \\
&- \frac{EAr}{2\Delta x^3}\left[\left(-\frac{r^2}{\Delta x}\theta_{N-1,j}{}^2\right)\left(-2\theta_{N,j}\right)\right. \\
&\left.+ \left(-2U_{N,j} + 2U_{N-1,j}\right)\left(-2\theta_{N-1,j}\right) + \frac{3r^2}{4\Delta x}\left(-2\theta_{N,j}\right)\left(-2\theta_{N-1,j}\right)^2\right] \\
&+ m_p g\sin\theta_{N,j} \\
&+ \frac{sgn\left(\theta_{N,j} - \theta_{N,j-1}\right) fr\left|\theta_{N,j} - \theta_{N,j-2}\right|}{2\Delta t\sqrt{\left(\frac{U_{N,j}-U_{N,j-2}}{2\Delta t}\right)^2 + r^2\left(\frac{\theta_{N,j}-\theta_{N,j-2}}{2\Delta t}\right)^2}}\left\{-\frac{EIr}{\Delta x^4}\left[\frac{1}{16}\left(-2\theta_{N-1,j}\right)^4\right.\right. \\
&\left.- 3\left(-2\theta_{N,j}\right)^2\right] \\
&- \frac{EAr}{8\Delta x^3}\left[\left(-\frac{r^2}{\Delta x}\theta_{N-1,j}{}^2\right)\left(-2\theta_{N-1,j}\right)^2 + \frac{r^2}{4\Delta x}\left(-2\theta_{N-1,j}\right)^4\right] \\
&+ \frac{I_p r\omega}{2\Delta x^2\Delta t}\left[\left(-2\theta_{N,j} + 2\theta_{N,j-2}\right) - \frac{1}{4}\left(\theta_{N,j} - \theta_{N,j-2}\right)\left(-2\theta_{N-1,j}\right)^2\right] \\
&\left.+ m_p g\cos\theta_{N,j} + \frac{m_p r}{4\Delta t^2}\left(\theta_{N,j} - \theta_{N,j-2}\right)^2\right\}
\end{aligned}
\tag{A.291}
$$

Lastly, the initial conditions are the same given by Eqs. (A.182), (A.183), (A.184) and (A.185). Their discretizations will be:

$$U_{i,1} = U_0 \, sin\left(\frac{\pi i \Delta x}{L}\right) \tag{A.292}$$

$$\begin{aligned}
\frac{U_{i,2} - U_{i,0}}{2\Delta t} = 0 \to U_{i,0} = U_{i,2} \to U_{i,2} \\
&= U_{i,1} + \frac{EA\Delta t^2}{2m_p \Delta x^2}\left(U_{i+1,1} - 2U_{i,1} + U_{i-1,1}\right) \\
&+ \frac{EAr^2\Delta t^2}{4m_p\Delta x^3}\left(\theta_{i+1,1} - \theta_{i-1,1}\right)\left(\theta_{i+1,1} - 2\theta_{i,1} + \theta_{i-1,1}\right) \\
&- \frac{sgn\left(U_{i,1}\right) f\Delta t\left|U_{i,1}\right|}{4m_p\sqrt{\left(\frac{U_{i,1}}{2\Delta t}\right)^2 + r^2\left(\frac{\theta_{i,1}}{2\Delta t}\right)^2}}\left\{-\frac{EIr}{\Delta x^4}\left[\frac{1}{16}\left(\theta_{i+1,1}\right.\right.\right. \\
&\left. - \theta_{i-1,1}\right)^4 - 3\left(\theta_{i+1,1} - 2\theta_{i,1} + \theta_{i-1,1}\right)^2 \\
&- \left(\theta_{i+2,1} - 2\theta_{i+1,1} + 2\theta_{i-1,1} - \theta_{i-2,1}\right)\left(\theta_{i+1,1}\right. \\
&\left.\left. - \theta_{i-1,1}\right)\right] \\
&- \frac{EAr}{8\Delta x^3}\left[\left(U_{i+1,1} - U_{i-1,1}\right)\left(\theta_{i+1,1} - \theta_{i-1,1}\right)^2\right. \\
&\left. + \frac{r^2}{4\Delta x}\left(\theta_{i+1,1} - \theta_{i-1,1}\right)^4\right] \\
&+ \frac{I_p r\omega}{2\Delta x^2\Delta t}\left[\left(\theta_{i+1,1} - 2\theta_{i,1} + \theta_{i-1,1}\right)\right. \\
&\left. - \frac{1}{4}\theta_{i,1}\left(\theta_{i+1,1} - \theta_{i-1,1}\right)^2\right] + m_p g \cos\theta_{i,1} \\
&\left. + \frac{m_p r}{4\Delta t^2}{\theta_{i,1}}^2\right\}
\end{aligned} \tag{A.293}$$

$$\theta_{i,1} = 0.1 \tag{A.294}$$

$$
\begin{aligned}
\frac{\theta_{i,2}-\theta_{i,0}}{2\Delta t} = 0 \rightarrow \theta_{i,0} = \theta_{i,2} \\
&\rightarrow \frac{I_p r\omega\left(\theta_{i+1,j}-\theta_{i-1,j}\right)}{2\Delta x^2 \Delta t}\theta_{i+1,2} \\
&+ \left[\frac{I_p r\omega\left(\theta_{i+1,1}-2\theta_{i,1}+\theta_{i-1,1}\right)}{2\Delta x^2 \Delta t} - \frac{m_p r}{\Delta t^2}\right]\theta_{i,2} \\
&- \frac{I_p r\omega\left(\theta_{i+1,1}-\theta_{i-1,1}\right)}{2\Delta x^2 \Delta t}\theta_{i-1,2} \\
&= \frac{m_p r}{\Delta t^2}\left(-2\theta_{i,1}\right) \\
&+ \frac{EIr}{\Delta x^4}\Big[\left(\theta_{i+2,1}-4\theta_{i+1,1}+6\theta_{i,1}-4\theta_{i-1,1}+\theta_{i-2,1}\right) \\
&- \frac{3}{2}\left(\theta_{i+1,1}-\theta_{i-1,1}\right)^2\left(\theta_{i+1,1}-2\theta_{i,1}+\theta_{i-1,1}\right)\Big] \\
&- \frac{EAr}{2\Delta x^3}\Big[\left(U_{i+1,1}-U_{i-1,1}\right)\left(\theta_{i+1,1}-2\theta_{i,1}+\theta_{i-1,1}\right) \\
&+ \left(U_{i+1,1}-2U_{i,1}+U_{i-1,1}\right)\left(\theta_{i+1,1}-\theta_{i-1,1}\right) \\
&+ \frac{3r^2}{4\Delta x}\left(\theta_{i+1,1}-2\theta_{i,1}+\theta_{i-1,1}\right)\left(\theta_{i+1,1}-\theta_{i-1,1}\right)^2\Big] \\
&+ m_p g \sin\theta_{i,1} \\
&+ \frac{sgn\left(\theta_{i,1}\right) fr\left|\theta_{i,1}\right|}{2\Delta t\sqrt{\left(\frac{U_{i,1}}{2\Delta t}\right)^2 + r^2\left(\frac{\theta_{i,1}}{2\Delta t}\right)^2}}\Bigg\{-\frac{EIr}{\Delta x^4}\Big[\frac{1}{16}\left(\theta_{i+1,1}\right. \\
&\left.-\theta_{i-1,1}\right)^4 - 3\left(\theta_{i+1,1}-2\theta_{i,1}+\theta_{i-1,1}\right)^2 \\
&- \left(\theta_{i+2,1}-2\theta_{i+1,1}+2\theta_{i-1,1}-\theta_{i-2,1}\right)\left(\theta_{i+1,1}\right. \\
&\left.-\theta_{i-1,1}\right)\Big] \\
&- \frac{EAr}{8\Delta x^3}\Big[\left(U_{i+1,1}-U_{i-1,1}\right)\left(\theta_{i+1,1}-\theta_{i-1,1}\right)^2 \\
&+ \frac{r^2}{4\Delta x}\left(\theta_{i+1,1}-\theta_{i-1,1}\right)^4\Big] \\
&+ \frac{I_p r\omega}{2\Delta x^2 \Delta t}\Big[\left(\theta_{i+1,1}-2\theta_{i,1}+\theta_{i-1,1}\right) \\
&- \frac{1}{4}\theta_{i,1}\left(\theta_{i+1,1}-\theta_{i-1,1}\right)^2\Big] + m_p g \cos\theta_{i,1} \\
&+ \frac{m_p r}{4\Delta t^2}{\theta_{i,1}}^2\Bigg\}
\end{aligned}
\tag{A.295}
$$

A.2.4. Solution for tripping out

Differently from the model without friction, this time there is no analytical solution if friction is included. Repeating the three equations from the model:

$$EA\frac{\partial^2 u_x}{\partial x^2} - m_p\frac{\partial^2 u_x}{\partial t^2} - sgn\left(\frac{\partial u_x}{\partial t}\right) f\left[-m_p r\frac{\partial^3 u_x}{\partial x\partial t^2} + m_p g\right] = 0 \tag{A.296}$$

$$F_x(x,t) = -EA\frac{\partial u_x}{\partial x} \tag{A.297}$$

$$N(x,t) = -m_p r\frac{\partial^3 u_x}{\partial x\partial t^2} + m_p g \tag{A.298}$$

Discretizing Eqs. (A.296), (A.297) and (A.298):

$$\begin{aligned} EA\left(\frac{U_{i+1,j} - 2U_{i,j} + U_{i-1,j}}{\Delta x^2}\right) - m_p\left(\frac{U_{i,j+1} - 2U_{i,j} + U_{i,j-1}}{\Delta t^2}\right) \\ - sgn(U_{i,j} - U_{i,j-1}) f\Big[-\frac{m_p r}{2\Delta x\Delta t^2}\big(U_{i+1,j} - U_{i-1,j} \\ - 2U_{i+1,j-1} + 2U_{i-1,j-1} + U_{i+1,j-2} - U_{i-1,j-2}\big) \\ + m_p g\Big] = 0 \end{aligned} \tag{A.299}$$

$$F_{i,j} = -\frac{EA}{2\Delta x}\left(U_{i+1,j} - U_{i-1,j}\right) \tag{A.300}$$

$$\begin{aligned} N_{i,j} = -\frac{m_p r}{2\Delta x\Delta t^2}\big(U_{i+1,j} - U_{i-1,j} - 2U_{i+1,j-1} + 2U_{i-1,j-1} \\ + U_{i+1,j-2} - U_{i-1,j-2}\big) + m_p g \end{aligned} \tag{A.301}$$

Manipulating Eq. (A.299):

$$\begin{aligned} U_{i,j+1} = 2U_{i,j} - U_{i,j-1} + \frac{EA\Delta t^2}{m_p\Delta x^2}\left(U_{i+1,j} - 2U_{i,j} + U_{i-1,j}\right) \\ - sgn(U_{i,j} - U_{i,j-1}) f\Big[-\frac{r}{2\Delta x}\big(U_{i+1,j} - U_{i-1,j} \\ - 2U_{i+1,j-1} + 2U_{i-1,j-1} + U_{i+1,j-2} - U_{i-1,j-2}\big) \\ + g\Delta t^2\Big] \end{aligned} \tag{A.302}$$

Once more, the boundary conditions are Eqs. (A.207) and (A.208), with Eqs. (A.209) and (A.210) being the discretizations. Substituting *i = 1* in Eq. (A.302):

$$U_{1,j+1} = 2U_{1,j} - U_{1,j-1} + \frac{EA\Delta t^2}{m_p \Delta x^2}\left(U_{2,j} - 2U_{1,j}\right) - sgn\left(U_{1,j} - U_{1,j-1}\right) f \left[-\frac{r}{2\Delta x}\left(U_{2,j} - 2U_{2,j-1} + U_{2,j-2}\right) + g\Delta t^2\right] \tag{A.303}$$

Substituting $i = N - 1$ in Eq. (A.302):

$$U_{N-1,j+1} = 2U_{N-1,j} - U_{N-1,j-1} + \frac{EA\Delta t^2}{m_p \Delta x^2}\left(U_{N,j} - 2U_{N-1,j} + U_{N-2,j}\right) - sgn\left(U_{N-1,j} - U_{N-1,j-1}\right) f \left[-\frac{r}{2\Delta x}\left(U_{N,j} - U_{N-2,j} - 2U_{N,j-1} + 2U_{N-2,j-1} + U_{N,j-2} - U_{N-2,j-2}\right) + g\Delta t^2\right] \tag{A.304}$$

Substituting $i = N$ in Eq. (A.302):

$$U_{N,j+1} = 2U_{N,j} - U_{N,j-1} + \frac{EA\Delta t^2}{m_p \Delta x^2}\left(-2U_{N,j} + 2U_{N-1,j}\right) - sgn\left(U_{N,j} - U_{N,j-1}\right) fg\Delta t^2 \tag{A.305}$$

The initial conditions are given by Eqs. (A.214) and (A.215) with the discretizations being:

$$U_{i,1} = U_0 \sin\left(\frac{\pi i \Delta x}{L}\right) \tag{A.306}$$

$$\frac{U_{i,2} - U_{i,0}}{2\Delta t} = 0 \rightarrow U_{i,0} = U_{i,2} \rightarrow -\frac{sgn\left(U_{i,1}\right) fr}{2\Delta x} U_{i-1,2} + U_{i,2} + \frac{sgn\left(U_{i,1}\right) fr}{2\Delta x} U_{i+1,2} = U_{i,1} + \frac{EA\Delta t^2}{2m_p \Delta x^2}\left(U_{i+1,1} - 2U_{i,1} + U_{i-1,1}\right) - \frac{sgn\left(U_{i,1}\right) f}{2}\left[-\frac{r}{2\Delta x}\left(U_{i+1,1} - U_{i-1,1}\right) + g\Delta t^2\right] \tag{A.307}$$

A.3. Model III – Slant wells

The hypotheses behind this model were explained on section 3.3. Here, only the deduction of the motion equations and their solution through the finite differences method will be shown.

A.3.1. Model for tripping in

The decomposition of the weight for the configuration given by Figure 3.6(b) will be:

$$\vec{q}_p = m_p g dx \cos\alpha\,\hat{\imath} + m_p g dx \sin\alpha \cos\theta\,\hat{p} - m_p g dx \sin\alpha \sin\theta\,\hat{q} \qquad \text{(A.308)}$$

For $\alpha = 90°$ it can be noted that Eq. (A.308) reduces itself to Eq. (A.57) defined previously. Substituting Eqs. (A.58), (A.239) and (A.308) into Eq. (A.240):

$$\begin{aligned}\vec{f} = {} & m_p g \cos\alpha\,\hat{\imath} + m_p g \sin\alpha\cos\theta\,\hat{p} - m_p g \sin\alpha \sin\theta\,\hat{q} - N\hat{p} \\ & - \frac{fN}{\sqrt{\left(\frac{\partial u_x}{\partial t}\right)^2 + r^2\left(\frac{\partial \theta}{\partial t}\right)^2}}\left[sgn\left(\frac{\partial u_x}{\partial t}\right)\left|\frac{\partial u_x}{\partial t}\right|\hat{\imath}\right. \\ & \left. + sgn\left(\frac{\partial \theta}{\partial t}\right) r \left|\frac{\partial \theta}{\partial t}\right|\hat{q}\right]\end{aligned} \qquad \text{(A.309)}$$

$$\begin{aligned}\vec{f} = {} & \left(m_p g \cos\alpha - \frac{sgn\left(\frac{\partial u_x}{\partial t}\right) fN \left|\frac{\partial u_x}{\partial t}\right|}{\sqrt{\left(\frac{\partial u_x}{\partial t}\right)^2 + r^2\left(\frac{\partial \theta}{\partial t}\right)^2}}\right)\hat{\imath} \\ & + \left(m_p g \sin\alpha \cos\theta - N\right)\hat{p} \\ & - \left(m_p g \sin\alpha \sin\theta + \frac{sgn\left(\frac{\partial \theta}{\partial t}\right) fNr \left|\frac{\partial \theta}{\partial t}\right|}{\sqrt{\left(\frac{\partial u_x}{\partial t}\right)^2 + r^2\left(\frac{\partial \theta}{\partial t}\right)^2}}\right)\hat{q}\end{aligned} \qquad \text{(A.310)}$$

Substituting Eqs. (A.31), (A.49) and (A.310) into Eq. (A.74):

$$\frac{\partial F_x}{\partial x}\hat{\imath} + \left(\frac{\partial F_r}{\partial x} - F_\theta \frac{\partial \theta}{\partial x}\right)\hat{p} + \left(\frac{\partial F_\theta}{\partial x} + F_r \frac{\partial \theta}{\partial x}\right)\hat{q} - \left(m_p g \cos\alpha - \frac{sgn\left(\frac{\partial u_x}{\partial t}\right) fN \left|\frac{\partial u_x}{\partial t}\right|}{\sqrt{\left(\frac{\partial u_x}{\partial t}\right)^2 + r^2\left(\frac{\partial \theta}{\partial t}\right)^2}}\right)\hat{\imath} - \left(m_p g \sin\alpha\cos\theta - N\right)\hat{p} + \left(m_p g \sin\alpha\sin\theta + \frac{sgn\left(\frac{\partial \theta}{\partial t}\right) fNr \left|\frac{\partial \theta}{\partial t}\right|}{\sqrt{\left(\frac{\partial u_x}{\partial t}\right)^2 + r^2\left(\frac{\partial \theta}{\partial t}\right)^2}}\right)\hat{q} + m_p\left[\frac{\partial^2 u_x}{\partial t^2}\hat{\imath} - r\left(\frac{\partial \theta}{\partial t}\right)^2\hat{p} + r\frac{\partial^2 \theta}{\partial t^2}\hat{q}\right] = 0 \tag{A.311}$$

$$\left[\frac{\partial F_x}{\partial x} - m_p g\cos\alpha + \frac{sgn\left(\frac{\partial u_x}{\partial t}\right) fN \left|\frac{\partial u_x}{\partial t}\right|}{\sqrt{\left(\frac{\partial u_x}{\partial t}\right)^2 + r^2\left(\frac{\partial \theta}{\partial t}\right)^2}} + m_p\frac{\partial^2 u_x}{\partial t^2}\right]\hat{\imath} + \left[\frac{\partial F_r}{\partial x} - F_\theta\frac{\partial \theta}{\partial x} + N - m_p g\sin\alpha\cos\theta - m_p r\left(\frac{\partial \theta}{\partial t}\right)^2\right]\hat{p} + \left[\frac{\partial F_\theta}{\partial x} + F_r\frac{\partial \theta}{\partial x} + m_p g\sin\alpha\sin\theta + \frac{sgn\left(\frac{\partial \theta}{\partial t}\right) fNr \left|\frac{\partial \theta}{\partial t}\right|}{\sqrt{\left(\frac{\partial u_x}{\partial t}\right)^2 + r^2\left(\frac{\partial \theta}{\partial t}\right)^2}} + m_p r\frac{\partial^2 \theta}{\partial t^2}\right]\hat{q} = 0 \tag{A.312}$$

Decomposing Eq. (A.312) into components:

$$\frac{\partial F_x}{\partial x} - m_p g\cos\alpha + \frac{sgn\left(\frac{\partial u_x}{\partial t}\right) fN \left|\frac{\partial u_x}{\partial t}\right|}{\sqrt{\left(\frac{\partial u_x}{\partial t}\right)^2 + r^2\left(\frac{\partial \theta}{\partial t}\right)^2}} + m_p\frac{\partial^2 u_x}{\partial t^2} \tag{A.313}$$

$$\frac{\partial F_r}{\partial x} - F_\theta\frac{\partial \theta}{\partial x} + N - m_p g\sin\alpha\cos\theta - m_p r\left(\frac{\partial \theta}{\partial t}\right)^2 \tag{A.314}$$

$$\frac{\partial F_\theta}{\partial x} + F_r\frac{\partial \theta}{\partial x} + m_p g\sin\alpha\sin\theta + \frac{sgn\left(\frac{\partial \theta}{\partial t}\right) fNr \left|\frac{\partial \theta}{\partial t}\right|}{\sqrt{\left(\frac{\partial u_x}{\partial t}\right)^2 + r^2\left(\frac{\partial \theta}{\partial t}\right)^2}} + m_p r\frac{\partial^2 \theta}{\partial t^2} \tag{A.315}$$

The expressions for F_x, F_r and F_θ from $\vec{F}$ do not modify from the previous cases. Therefore, substituting Eqs. (A.66), (A.92) and (A.95) into Eqs. (A.313), (A.314) and (A.315), while using Eqs. (A.37) and (A.38):

$$\frac{\partial}{\partial x}\left[-EA\frac{\partial u_x}{\partial x}-\frac{1}{2}EAr^2\left(\frac{\partial\theta}{\partial x}\right)^2\right]-m_p g\cos\alpha+\frac{sgn\left(\frac{\partial u_x}{\partial t}\right)fN\left|\frac{\partial u_x}{\partial t}\right|}{\sqrt{\left(\frac{\partial u_x}{\partial t}\right)^2+r^2\left(\frac{\partial\theta}{\partial t}\right)^2}} + m_p\frac{\partial^2 u_x}{\partial t^2}=0 \tag{A.316}$$

$$\frac{\partial}{\partial x}\left[-3EIr\frac{\partial\theta}{\partial x}\frac{\partial^2\theta}{\partial x^2}-I_p\omega r\frac{\partial^2\theta}{\partial x\partial t}\right] - \left[EIr\left[\frac{\partial^3\theta}{\partial x^3}-\left(\frac{\partial\theta}{\partial x}\right)^3\right] + \left[-EA\frac{\partial u_x}{\partial x}-\frac{1}{2}EAr^2\left(\frac{\partial\theta}{\partial x}\right)^2\right]r\frac{\partial\theta}{\partial x} + I_p\omega\left(-r\frac{\partial\theta}{\partial t}\frac{\partial\theta}{\partial x}\right)\right]\frac{\partial\theta}{\partial x}+N-m_p g\sin\alpha\cos\theta - m_p r\left(\frac{\partial\theta}{\partial t}\right)^2=0 \tag{A.317}$$

$$\frac{\partial}{\partial x}\left[EIr\left[\frac{\partial^3\theta}{\partial x^3}-\left(\frac{\partial\theta}{\partial x}\right)^3\right]+\left[-EA\frac{\partial u_x}{\partial x}-\frac{1}{2}EAr^2\left(\frac{\partial\theta}{\partial x}\right)^2\right]r\frac{\partial\theta}{\partial x} + I_p\omega\left(-r\frac{\partial\theta}{\partial t}\frac{\partial\theta}{\partial x}\right)\right] + \left[-3EIr\frac{\partial\theta}{\partial x}\frac{\partial^2\theta}{\partial x^2}-I_p\omega r\frac{\partial^2\theta}{\partial x\partial t}\right]\frac{\partial\theta}{\partial x} + m_p g\sin\alpha\sin\theta+\frac{sgn\left(\frac{\partial\theta}{\partial t}\right)fNr\left|\frac{\partial\theta}{\partial t}\right|}{\sqrt{\left(\frac{\partial u_x}{\partial t}\right)^2+r^2\left(\frac{\partial\theta}{\partial t}\right)^2}}+m_p r\frac{\partial^2\theta}{\partial t^2} = 0 \tag{A.318}$$

Manipulating Eqs. (A.316), (A.317) and (A.318):

$$EA\frac{\partial^2 u_x}{\partial x^2}-m_p\frac{\partial^2 u_x}{\partial t^2}+EAr^2\frac{\partial\theta}{\partial x}\frac{\partial^2\theta}{\partial x^2}-\frac{sgn\left(\frac{\partial u_x}{\partial t}\right)fN\left|\frac{\partial u_x}{\partial t}\right|}{\sqrt{\left(\frac{\partial u_x}{\partial t}\right)^2+r^2\left(\frac{\partial\theta}{\partial t}\right)^2}} + m_p g\cos\alpha=0 \tag{A.319}$$

$$N = -EIr\left[\left(\frac{\partial\theta}{\partial x}\right)^4 - 3\left(\frac{\partial^2\theta}{\partial x^2}\right)^2 - 4\frac{\partial^3\theta}{\partial x^3}\frac{\partial\theta}{\partial x}\right] - EAr\left[\frac{\partial u_x}{\partial x}\left(\frac{\partial\theta}{\partial x}\right)^2 + \frac{1}{2}r^2\left(\frac{\partial\theta}{\partial x}\right)^4\right] + I_p r\omega\left[\frac{\partial^3\theta}{\partial x^2\partial t} - \frac{\partial\theta}{\partial t}\left(\frac{\partial\theta}{\partial x}\right)^2\right] + m_p g\, sin\, \alpha\, cos\, \theta + m_p r\left(\frac{\partial\theta}{\partial t}\right)^2 \tag{A.320}$$

$$EIr\left[\frac{\partial^4\theta}{\partial x^4} - 6\left(\frac{\partial\theta}{\partial x}\right)^2\frac{\partial^2\theta}{\partial x^2}\right] - EAr\left[\frac{\partial u_x}{\partial x}\frac{\partial^2\theta}{\partial x^2} + \frac{\partial^2 u_x}{\partial x^2}\frac{\partial\theta}{\partial x} + \frac{3}{2}r^2\frac{\partial^2\theta}{\partial x^2}\left(\frac{\partial\theta}{\partial x}\right)^2\right] - I_p r\omega\left[2\frac{\partial^2\theta}{\partial x\partial t}\frac{\partial\theta}{\partial x} + \frac{\partial\theta}{\partial t}\frac{\partial^2\theta}{\partial x^2}\right] + m_p g\, sin\, \alpha\, sin\, \theta + m_p r\frac{\partial^2\theta}{\partial t^2} + \frac{sgn\left(\frac{\partial\theta}{\partial t}\right) fNr\left|\frac{\partial\theta}{\partial t}\right|}{\sqrt{\left(\frac{\partial u_x}{\partial t}\right)^2 + r^2\left(\frac{\partial\theta}{\partial t}\right)^2}} = 0 \tag{A.321}$$

Lastly, substituting the normal contact force given by Eq. (A.320) into Eqs. (A.319) and (A.321):

$$EA\frac{\partial^2 u_x}{\partial x^2} - m_p\frac{\partial^2 u_x}{\partial t^2} + EAr^2\frac{\partial\theta}{\partial x}\frac{\partial^2\theta}{\partial x^2} - \frac{sgn\left(\frac{\partial u_x}{\partial t}\right) f\left|\frac{\partial u_x}{\partial t}\right|}{\sqrt{\left(\frac{\partial u_x}{\partial t}\right)^2 + r^2\left(\frac{\partial\theta}{\partial t}\right)^2}}\left\{-EIr\left[\left(\frac{\partial\theta}{\partial x}\right)^4 - 3\left(\frac{\partial^2\theta}{\partial x^2}\right)^2 - 4\frac{\partial^3\theta}{\partial x^3}\frac{\partial\theta}{\partial x}\right] - EAr\left[\frac{\partial u_x}{\partial x}\left(\frac{\partial\theta}{\partial x}\right)^2 + \frac{1}{2}r^2\left(\frac{\partial\theta}{\partial x}\right)^4\right] + I_p r\omega\left[\frac{\partial^3\theta}{\partial x^2\partial t} - \frac{\partial\theta}{\partial t}\left(\frac{\partial\theta}{\partial x}\right)^2\right] + m_p g\, sin\, \alpha\, cos\, \theta + m_p r\left(\frac{\partial\theta}{\partial t}\right)^2\right\} + m_p g\, cos\, \alpha = 0 \tag{A.322}$$

$$
\begin{aligned}
&EIr\left[\frac{\partial^4\theta}{\partial x^4}-6\left(\frac{\partial\theta}{\partial x}\right)^2\frac{\partial^2\theta}{\partial x^2}\right]\\
&\qquad -EAr\left[\frac{\partial u_x}{\partial x}\frac{\partial^2\theta}{\partial x^2}+\frac{\partial^2 u_x}{\partial x^2}\frac{\partial\theta}{\partial x}+\frac{3}{2}r^2\frac{\partial^2\theta}{\partial x^2}\left(\frac{\partial\theta}{\partial x}\right)^2\right]\\
&\qquad -I_p r\omega\left[2\frac{\partial^2\theta}{\partial x\partial t}\frac{\partial\theta}{\partial x}+\frac{\partial\theta}{\partial t}\frac{\partial^2\theta}{\partial x^2}\right]+m_p g\sin\alpha\sin\theta\\
&\qquad +m_p r\frac{\partial^2\theta}{\partial t^2}\\
&\qquad +\frac{sgn\left(\frac{\partial\theta}{\partial t}\right)fr\left|\frac{\partial\theta}{\partial t}\right|}{\sqrt{\left(\frac{\partial u_x}{\partial t}\right)^2+r^2\left(\frac{\partial\theta}{\partial t}\right)^2}}\left\{-EIr\left[\left(\frac{\partial\theta}{\partial x}\right)^4-3\left(\frac{\partial^2\theta}{\partial x^2}\right)^2\right.\right.\\
&\qquad \left.-4\frac{\partial^3\theta}{\partial x^3}\frac{\partial\theta}{\partial x}\right]-EAr\left[\frac{\partial u_x}{\partial x}\left(\frac{\partial\theta}{\partial x}\right)^2+\frac{1}{2}r^2\left(\frac{\partial\theta}{\partial x}\right)^4\right]\\
&\qquad +I_p r\omega\left[\frac{\partial^3\theta}{\partial x^2\partial t}-\frac{\partial\theta}{\partial t}\left(\frac{\partial\theta}{\partial x}\right)^2\right]+m_p g\sin\alpha\cos\theta\\
&\qquad \left.+m_p r\left(\frac{\partial\theta}{\partial t}\right)^2\right\}=0
\end{aligned}
\tag{A.323}
$$

The problem consists in solving Eqs. (A.320), (A.322) and (A.323) in order to find the axial and angular displacements and the normal contact force, besides Eq. (A.66) for the axial force.

A.3.2. Model for tripping out

For the case of tripping out, the weight decomposition according to Figure 3.6(b) will be given by:

$$\vec{q}_p = m_p g dx\cos\alpha\,\hat{\imath} - m_p g dx\sin\alpha\,\hat{k} \tag{A.324}$$

For $\alpha = 90°$, Eq. (A.324) reduces itself to Eq. (A.125) previously defined. Substituting Eqs. (A.126), (A.260) and (A.324) into Eq. (A.261):

$$\vec{f} = m_p g\cos\alpha\,\hat{\imath} - m_p g\sin\alpha\,\hat{k} + N\hat{k} - sgn\left(\frac{\partial u_x}{\partial t}\right)fN\hat{\imath} \tag{A.325}$$

$$\vec{f} = \left(m_p g\cos\alpha - sgn\left(\frac{\partial u_x}{\partial t}\right)fN\right)\hat{\imath} + \left(-m_p g\sin\alpha + N\right)\hat{k} \tag{A.326}$$

Substituting Eqs. (A.112), (A.122) and (A.326) into Eq. (A.134):

$$\begin{aligned}\frac{\partial F_x}{\partial x}\hat{\imath}+\frac{\partial F_y}{\partial x}\hat{\jmath}+\frac{\partial F_z}{\partial x}\hat{k}+sgn\left(\frac{\partial u_x}{\partial t}\right)fN\hat{\imath}\\-\left[\left(m_p g\cos\alpha-sgn\left(\frac{\partial u_x}{\partial t}\right)fN\right)\hat{\imath}\right.\\\left.+\left(-m_p g\sin\alpha+N\right)\hat{k}\right]+m_p\left[\frac{\partial^2 u_x}{\partial t^2}\hat{\imath}\right]=0\end{aligned} \tag{A.327}$$

$$\begin{aligned}\left(\frac{\partial F_x}{\partial x}+m_p\frac{\partial^2 u_x}{\partial t^2}-m_p g\cos\alpha+sgn\left(\frac{\partial u_x}{\partial t}\right)fN\right)\hat{\imath}+\left(\frac{\partial F_y}{\partial x}\right)\hat{\jmath}\\+\left(\frac{\partial F_z}{\partial x}+m_p g\sin\alpha-N\right)\hat{k}=0\end{aligned} \tag{A.328}$$

Separating Eq. (A.328) into its components:

$$\frac{\partial F_x}{\partial x}+m_p\frac{\partial^2 u_x}{\partial t^2}-m_p g\cos\alpha+sgn\left(\frac{\partial u_x}{\partial t}\right)fN=0 \tag{A.329}$$

$$\frac{\partial F_y}{\partial x}=0 \tag{A.330}$$

$$\frac{\partial F_z}{\partial x}+m_p g\sin\alpha-N=0 \tag{A.331}$$

Once again, the expressions for F_x, F_y and F_z from $\vec{F}$ do not modify from the previous cases. Therefore, substituting Eqs. (A.131), (A.147) and (A.148) into Eqs. (A.329), (A.330) and (A.331), two equations of motion are obtained since Eq. (A.330) is irrelevant:

$$\frac{\partial}{\partial x}\left[-EA\frac{\partial u_x}{\partial x}\right]+m_p\frac{\partial^2 u_x}{\partial t^2}-m_p g\cos\alpha+sgn\left(\frac{\partial u_x}{\partial t}\right)fN=0 \tag{A.332}$$

$$\frac{\partial}{\partial x}\left[-m_p r\frac{\partial^2 u_x}{\partial t^2}\right]+m_p g\sin\alpha-N=0 \tag{A.333}$$

Manipulating Eqs. (A.332) and (A.333):

$$EA\frac{\partial^2 u_x}{\partial x^2}-m_p\frac{\partial^2 u_x}{\partial t^2}+m_p g\cos\alpha-sgn\left(\frac{\partial u_x}{\partial t}\right)fN=0 \tag{A.334}$$

$$N = -m_p r \frac{\partial^3 u_x}{\partial x \partial t^2} + m_p g \sin\alpha \tag{A.335}$$

Finally, substituting Eq. (A.335) into Eq. (A.334):

$$\begin{aligned} &EA\frac{\partial^2 u_x}{\partial x^2} - m_p\frac{\partial^2 u_x}{\partial t^2} + m_p g \cos\alpha \\ &\qquad - sgn\left(\frac{\partial u_x}{\partial t}\right) f \left[-m_p r \frac{\partial^3 u_x}{\partial x \partial t^2} + m_p g \sin\alpha\right] = 0 \end{aligned} \tag{A.336}$$

The problem consists of solving Eqs. (A.335) and (A.336) to find the axial displacement and normal contact force, besides Eq. (A.131) for the axial force.

A.3.3. Solution for tripping in

Discretizing Eqs. (A.66), (A.320), (A.322) and (A.323):

$$\begin{aligned} &EA\left(\frac{U_{i+1,j} - 2U_{i,j} + U_{i-1,j}}{\Delta x^2}\right) - m_p\left(\frac{U_{i,j+1} - 2U_{i,j} + U_{i,j-1}}{\Delta t^2}\right) \\ &+ EAr^2\left(\frac{\theta_{i+1,j} - \theta_{i-1,j}}{2\Delta x}\right)\left(\frac{\theta_{i+1,j} - 2\theta_{i,j} + \theta_{i-1,j}}{\Delta x^2}\right) \\ &- \frac{sgn\left(U_{i,j} - U_{i,j-1}\right) f \left|\frac{U_{i,j} - U_{i,j-2}}{2\Delta t}\right|}{\sqrt{\left(\frac{U_{i,j} - U_{i,j-2}}{2\Delta t}\right)^2 + r^2\left(\frac{\theta_{i,j} - \theta_{i,j-2}}{2\Delta t}\right)^2}}\left\{-EIr\left[\left(\frac{\theta_{i+1,j} - \theta_{i-1,j}}{2\Delta x}\right)^4\right.\right. \\ &- 3\left(\frac{\theta_{i+1,j} - 2\theta_{i,j} + \theta_{i-1,j}}{\Delta x^2}\right)^2 \\ &\left.- 4\left(\frac{\theta_{i+2,j} - 2\theta_{i+1,j} + 2\theta_{i-1,j} - \theta_{i-2,j}}{2\Delta x^3}\right)\left(\frac{\theta_{i+1,j} - \theta_{i-1,j}}{2\Delta x}\right)\right] \\ &- EAr\left[\left(\frac{U_{i+1,j} - U_{i-1,j}}{2\Delta x}\right)\left(\frac{\theta_{i+1,j} - \theta_{i-1,j}}{2\Delta x}\right)^2\right. \\ &\left.+ \frac{1}{2}r^2\left(\frac{\theta_{i+1,j} - \theta_{i-1,j}}{2\Delta x}\right)^4\right] \\ &+ I_p r\omega\left[\left(\frac{\theta_{i+1,j} - 2\theta_{i,j} + \theta_{i-1,j} - \theta_{i+1,j-2} + 2\theta_{i,j-2} - \theta_{i-1,j-2}}{2\Delta x^2 \Delta t}\right)\right. \\ &\left.- \left(\frac{\theta_{i,j} - \theta_{i,j-2}}{2\Delta t}\right)\left(\frac{\theta_{i+1,j} - \theta_{i-1,j}}{2\Delta x}\right)^2\right] + m_p g \sin\alpha \cos\theta_{i,j} \\ &\left.+ m_p r\left(\frac{\theta_{i,j} - \theta_{i,j-2}}{2\Delta t}\right)^2\right\} + m_p g \cos\alpha = 0 \end{aligned} \tag{A.337}$$

$$
\begin{aligned}
&EIr\left[\left(\frac{\theta_{i+2,j}-4\theta_{i+1,j}+6\theta_{i,j}-4\theta_{i-1,j}+\theta_{i-2,j}}{\Delta x^4}\right)\right.\\
&\left.-6\left(\frac{\theta_{i+1,j}-\theta_{i-1,j}}{2\Delta x}\right)^2\left(\frac{\theta_{i+1,j}-2\theta_{i,j}+\theta_{i-1,j}}{\Delta x^2}\right)\right]\\
&-EAr\left[\left(\frac{U_{i+1,j}-U_{i-1,j}}{2\Delta x}\right)\left(\frac{\theta_{i+1,j}-2\theta_{i,j}+\theta_{i-1,j}}{\Delta x^2}\right)\right.\\
&+\left(\frac{U_{i+1,j}-2U_{i,j}+U_{i-1,j}}{\Delta x^2}\right)\left(\frac{\theta_{i+1,j}-\theta_{i-1,j}}{2\Delta x}\right)\\
&\left.+\frac{3}{2}r^2\left(\frac{\theta_{i+1,j}-2\theta_{i,j}+\theta_{i-1,j}}{\Delta x^2}\right)\left(\frac{\theta_{i+1,j}-\theta_{i-1,j}}{2\Delta x}\right)^2\right]\\
&-I_p r\omega\left[2\left(\frac{\theta_{i+1,j+1}-\theta_{i-1,j+1}-\theta_{i+1,j-1}+\theta_{i-1,j-1}}{4\Delta x\Delta t}\right)\left(\frac{\theta_{i+1,j}-\theta_{i-1,j}}{2\Delta x}\right)\right.\\
&\left.+\left(\frac{\theta_{i,j+1}-\theta_{i,j-1}}{2\Delta t}\right)\left(\frac{\theta_{i+1,j}-2\theta_{i,j}+\theta_{i-1,j}}{\Delta x^2}\right)\right]+m_p g\sin\alpha\sin\theta_{i,j}\\
&+m_p r\left(\frac{\theta_{i,j+1}-2\theta_{i,j}+\theta_{i,j-1}}{\Delta t^2}\right)\\
&+\frac{sgn\left(\theta_{i,j}-\theta_{i,j-1}\right)fr\left|\frac{\theta_{i,j}-\theta_{i,j-2}}{2\Delta t}\right|}{\sqrt{\left(\frac{U_{i,j}-U_{i,j-2}}{2\Delta t}\right)^2+r^2\left(\frac{\theta_{i,j}-\theta_{i,j-2}}{2\Delta t}\right)^2}}\left\{-EIr\left[\left(\frac{\theta_{i+1,j}-\theta_{i-1,j}}{2\Delta x}\right)^4\right.\right.\\
&-3\left(\frac{\theta_{i+1,j}-2\theta_{i,j}+\theta_{i-1,j}}{\Delta x^2}\right)^2\\
&\left.-4\left(\frac{\theta_{i+2,j}-2\theta_{i+1,j}+2\theta_{i-1,j}-\theta_{i-2,j}}{2\Delta x^3}\right)\left(\frac{\theta_{i+1,j}-\theta_{i-1,j}}{2\Delta x}\right)\right]\\
&-EAr\left[\left(\frac{U_{i+1,j}-U_{i-1,j}}{2\Delta x}\right)\left(\frac{\theta_{i+1,j}-\theta_{i-1,j}}{2\Delta x}\right)^2+\frac{1}{2}r^2\left(\frac{\theta_{i+1,j}-\theta_{i-1,j}}{2\Delta x}\right)^4\right]\\
&+I_p r\omega\left[\left(\frac{\theta_{i+1,j}-2\theta_{i,j}+\theta_{i-1,j}-\theta_{i+1,j-2}+2\theta_{i,j-2}-\theta_{i-1,j-2}}{2\Delta x^2\Delta t}\right)\right.\\
&\left.-\left(\frac{\theta_{i,j}-\theta_{i,j-2}}{2\Delta t}\right)\left(\frac{\theta_{i+1,j}-\theta_{i-1,j}}{2\Delta x}\right)^2\right]+m_p g\sin\alpha\cos\theta_{i,j}\\
&\left.+m_p r\left(\frac{\theta_{i,j}-\theta_{i,j-2}}{2\Delta t}\right)^2\right\}=0
\end{aligned}
\tag{A.338}
$$

$$
F_{i,j}=-\frac{EA}{2\Delta x}\left(U_{i+1,j}-U_{i-1,j}\right)-\frac{1}{2}EAr^2\left(\frac{\theta_{i+1,j}-\theta_{i-1,j}}{2\Delta x}\right)^2 \tag{A.339}
$$

$$
\begin{aligned}
&N_{i,j} \\
&= -EIr\left[\left(\frac{\theta_{i+1,j}-\theta_{i-1,j}}{2\Delta x}\right)^4 - 3\left(\frac{\theta_{i+1,j}-2\theta_{i,j}+\theta_{i-1,j}}{\Delta x^2}\right)^2\right. \\
&\left.- 4\left(\frac{\theta_{i+2,j}-2\theta_{i+1,j}+2\theta_{i-1,j}-\theta_{i-2,j}}{2\Delta x^3}\right)\left(\frac{\theta_{i+1,j}-\theta_{i-1,j}}{2\Delta x}\right)\right] \\
&- EAr\left[\left(\frac{U_{i+1,j}-U_{i-1,j}}{2\Delta x}\right)\left(\frac{\theta_{i+1,j}-\theta_{i-1,j}}{2\Delta x}\right)^2\right. \\
&\left.+ \frac{1}{2}r^2\left(\frac{\theta_{i+1,j}-\theta_{i-1,j}}{2\Delta x}\right)^4\right] \\
&+ I_p r\omega\left[\left(\frac{\theta_{i+1,j}-2\theta_{i,j}+\theta_{i-1,j}-\theta_{i+1,j-2}+2\theta_{i,j-2}-\theta_{i-1,j-2}}{2\Delta x^2\Delta t}\right)\right. \\
&\left.- \left(\frac{\theta_{i,j}-\theta_{i,j-2}}{2\Delta t}\right)\left(\frac{\theta_{i+1,j}-\theta_{i-1,j}}{2\Delta x}\right)^2\right] + m_p g\, sin\,\alpha\, cos\,\theta_{i,j} \\
&+ m_p r\left(\frac{\theta_{i,j}-\theta_{i,j-2}}{2\Delta t}\right)^2
\end{aligned}
\tag{A.340}
$$

Manipulating Eqs. (A.337), (A.338), (A.339) and (A.340):

$$
\begin{aligned}
&U_{i,j+1} \\
&= 2U_{i,j} - U_{i,j-1} + \frac{EA\Delta t^2}{m_p\Delta x^2}\left(U_{i+1,j}-2U_{i,j}+U_{i-1,j}\right) \\
&+ \frac{EAr^2\Delta t^2}{2m_p\Delta x^3}\left(\theta_{i+1,j}-\theta_{i-1,j}\right)\left(\theta_{i+1,j}-2\theta_{i,j}+\theta_{i-1,j}\right) \\
&- \frac{sgn\left(U_{i,j}-U_{i,j-1}\right) f\Delta t\left|U_{i,j}-U_{i,j-2}\right|}{2m_p\sqrt{\left(\frac{U_{i,j}-U_{i,j-2}}{2\Delta t}\right)^2 + r^2\left(\frac{\theta_{i,j}-\theta_{i,j-2}}{2\Delta t}\right)^2}}\left\{-\frac{EIr}{\Delta x^4}\left[\frac{1}{16}\left(\theta_{i+1,j}\right.\right.\right. \\
&\left.- \theta_{i-1,j}\right)^4 - 3\left(\theta_{i+1,j}-2\theta_{i,j}+\theta_{i-1,j}\right)^2 \\
&\left.- \left(\theta_{i+2,j}-2\theta_{i+1,j}+2\theta_{i-1,j}-\theta_{i-2,j}\right)\left(\theta_{i+1,j}-\theta_{i-1,j}\right)\right] \\
&- \frac{EAr}{8\Delta x^3}\left[\left(U_{i+1,j}-U_{i-1,j}\right)\left(\theta_{i+1,j}-\theta_{i-1,j}\right)^2\right. \\
&\left.+ \frac{r^2}{4\Delta x}\left(\theta_{i+1,j}-\theta_{i-1,j}\right)^4\right] \\
&+ \frac{I_p r\omega}{2\Delta x^2\Delta t}\left[\left(\theta_{i+1,j}-2\theta_{i,j}+\theta_{i-1,j}-\theta_{i+1,j-2}+2\theta_{i,j-2}-\theta_{i-1,j-2}\right)\right. \\
&\left.- \frac{1}{4}\left(\theta_{i,j}-\theta_{i,j-2}\right)\left(\theta_{i+1,j}-\theta_{i-1,j}\right)^2\right] + m_p g\, sin\,\alpha\, cos\,\theta_{i,j} \\
&\left.+ \frac{m_p r}{4\Delta t^2}\left(\theta_{i,j}-\theta_{i,j-2}\right)^2\right\} + \Delta t^2 g\, cos\,\alpha
\end{aligned}
\tag{A.341}
$$

$$
\begin{aligned}
&\frac{I_p r\omega\left(\theta_{i+1,j}-\theta_{i-1,j}\right)}{4\Delta x^2\Delta t}\theta_{i+1,j+1} \\
&+\left[\frac{I_p r\omega\left(\theta_{i+1,j}-2\theta_{i,j}+\theta_{i-1,j}\right)}{2\Delta x^2\Delta t}-\frac{m_p r}{\Delta t^2}\right]\theta_{i,j+1} \\
&-\frac{I_p r\omega\left(\theta_{i+1,j}-\theta_{i-1,j}\right)}{4\Delta x^2\Delta t}\theta_{i-1,j+1} \\
&=\frac{I_p r\omega\left(\theta_{i+1,j}-2\theta_{i,j}+\theta_{i-1,j}\right)}{2\Delta x^2\Delta t}\theta_{i,j-1} \\
&-\frac{I_p r\omega\left(\theta_{i+1,j}-\theta_{i-1,j}\right)}{4\Delta x^2\Delta t}\left(-\theta_{i+1,j-1}+\theta_{i-1,j-1}\right) \\
&+\frac{m_p r}{\Delta t^2}\left(-2\theta_{i,j}+\theta_{i,j-1}\right) \\
&+\frac{EIr}{\Delta x^4}\Big[\left(\theta_{i+2,j}-4\theta_{i+1,j}+6\theta_{i,j}-4\theta_{i-1,j}+\theta_{i-2,j}\right) \\
&-\frac{3}{2}\left(\theta_{i+1,j}-\theta_{i-1,j}\right)^2\left(\theta_{i+1,j}-2\theta_{i,j}+\theta_{i-1,j}\right)\Big] \\
&-\frac{EAr}{2\Delta x^3}\Big[\left(U_{i+1,j}-U_{i-1,j}\right)\left(\theta_{i+1,j}-2\theta_{i,j}+\theta_{i-1,j}\right) \\
&+\left(U_{i+1,j}-2U_{i,j}+U_{i-1,j}\right)\left(\theta_{i+1,j}-\theta_{i-1,j}\right) \\
&+\frac{3r^2}{4\Delta x}\left(\theta_{i+1,j}-2\theta_{i,j}+\theta_{i-1,j}\right)\left(\theta_{i+1,j}-\theta_{i-1,j}\right)^2\Big] \\
&+m_p g\sin\alpha\sin\theta_{i,j} \\
&+\frac{sgn\left(\theta_{i,j}-\theta_{i,j-1}\right)fr\left|\theta_{i,j}-\theta_{i,j-2}\right|}{2\Delta t\sqrt{\left(\frac{U_{i,j}-U_{i,j-2}}{2\Delta t}\right)^2+r^2\left(\frac{\theta_{i,j}-\theta_{i,j-2}}{2\Delta t}\right)^2}}\Big\{-\frac{EIr}{\Delta x^4}\Big[\frac{1}{16}\left(\theta_{i+1,j}-\theta_{i-1,j}\right)^4 \\
&-3\left(\theta_{i+1,j}-2\theta_{i,j}+\theta_{i-1,j}\right)^2 \\
&-\left(\theta_{i+2,j}-2\theta_{i+1,j}+2\theta_{i-1,j}-\theta_{i-2,j}\right)\left(\theta_{i+1,j}-\theta_{i-1,j}\right)\Big] \\
&-\frac{EAr}{8\Delta x^3}\Big[\left(U_{i+1,j}-U_{i-1,j}\right)\left(\theta_{i+1,j}-\theta_{i-1,j}\right)^2 \\
&+\frac{r^2}{4\Delta x}\left(\theta_{i+1,j}-\theta_{i-1,j}\right)^4\Big] \\
&+\frac{I_p r\omega}{2\Delta x^2\Delta t}\Big[\left(\theta_{i+1,j}-2\theta_{i,j}+\theta_{i-1,j}-\theta_{i+1,j-2}+2\theta_{i,j-2}-\theta_{i-1,j-2}\right) \\
&-\frac{1}{4}\left(\theta_{i,j}-\theta_{i,j-2}\right)\left(\theta_{i+1,j}-\theta_{i-1,j}\right)^2\Big]+m_p g\sin\alpha\cos\theta_{i,j} \\
&+\frac{m_p r}{4\Delta t^2}\left(\theta_{i,j}-\theta_{i,j-2}\right)^2\Big\}
\end{aligned}
\tag{A.342}
$$

$$
F_{i,j}=-\frac{EA}{2\Delta x}\left[\left(U_{i+1,j}-U_{i-1,j}\right)+\frac{r^2}{4\Delta x}\left(\theta_{i+1,j}-\theta_{i-1,j}\right)^2\right] \tag{A.343}
$$

$$
\begin{aligned}
N_{i,j} = -\frac{EIr}{\Delta x^4}\Bigg[&\frac{1}{16}\left(\theta_{i+1,j} - \theta_{i-1,j}\right)^4 - 3\left(\theta_{i+1,j} - 2\theta_{i,j} + \theta_{i-1,j}\right)^2 \\
&- \left(\theta_{i+2,j} - 2\theta_{i+1,j} + 2\theta_{i-1,j} - \theta_{i-2,j}\right)\left(\theta_{i+1,j}\right. \\
&\left.- \theta_{i-1,j}\right)\Bigg] \\
&- \frac{EAr}{8\Delta x^3}\left[\left(U_{i+1,j} - U_{i-1,j}\right)\left(\theta_{i+1,j} - \theta_{i-1,j}\right)^2\right. \\
&\left.+ \frac{r^2}{4\Delta x}\left(\theta_{i+1,j} - \theta_{i-1,j}\right)^4\right] \\
&+ \frac{I_p r\omega}{2\Delta x^2 \Delta t}\left[\left(\theta_{i+1,j} - 2\theta_{i,j} + \theta_{i-1,j} - \theta_{i+1,j-2}\right.\right. \\
&\left.+ 2\theta_{i,j-2} - \theta_{i-1,j-2}\right) \\
&\left.- \frac{1}{4}\left(\theta_{i,j} - \theta_{i,j-2}\right)\left(\theta_{i+1,j} - \theta_{i-1,j}\right)^2\right] \\
&+ m_p g \sin\alpha \cos\theta_{i,j} + \frac{m_p r}{4\Delta t^2}\left(\theta_{i,j} - \theta_{i,j-2}\right)^2
\end{aligned} \tag{A.344}
$$

The boundary conditions are the same ones given by Eqs. (A.163), (A.164), (A.165), (A.166), (A.167) and (A.168), with discretizations given by Eqs. (A.169), (A.170), (A.171), (A.172), (A.173) and (A.174). For $i = 1$:

$$
\begin{aligned}
&U_{1,j+1} \\
&= 2U_{1,j} - U_{1,j-1} + \frac{EA\Delta t^2}{m_p \Delta x^2}\left(U_{2,j} - 2U_{1,j}\right) \\
&+ \frac{EAr^2\Delta t^2}{2m_p\Delta x^3}\theta_{2,j}\left(\theta_{2,j} - 2\theta_{1,j}\right) \\
&- \frac{sgn\left(U_{1,j} - U_{1,j-1}\right) f\Delta t\left|U_{1,j} - U_{1,j-2}\right|}{2m_p\sqrt{\left(\frac{U_{1,j}-U_{1,j-2}}{2\Delta t}\right)^2 + r^2\left(\frac{\theta_{1,j}-\theta_{1,j-2}}{2\Delta t}\right)^2}}\left\{-\frac{EIr}{\Delta x^4}\left[\frac{1}{16}{\theta_{2,j}}^4\right.\right. \\
&\left.- 3\left(\theta_{2,j} - 2\theta_{1,j}\right)^2 - \left(\theta_{3,j} - 2\theta_{2,j} + \theta_{1,j}\right)\theta_{2,j}\right] \\
&- \frac{EAr}{8\Delta x^3}\left[U_{2,j}{\theta_{2,j}}^2 + \frac{r^2}{4\Delta x}{\theta_{2,j}}^4\right] \\
&+ \frac{I_p r\omega}{2\Delta x^2\Delta t}\left[\left(\theta_{2,j} - 2\theta_{1,j} - \theta_{2,j-2} + 2\theta_{1,j-2}\right)\right. \\
&\left.- \frac{1}{4}\left(\theta_{1,j} - \theta_{1,j-2}\right){\theta_{2,j}}^2\right] + m_p g \sin\alpha\cos\theta_{1,j} \\
&\left.+ \frac{m_p r}{4\Delta t^2}\left(\theta_{1,j} - \theta_{1,j-2}\right)^2\right\} + \Delta t^2 g\cos\alpha
\end{aligned} \tag{A.345}
$$

$$
\begin{aligned}
&\frac{I_p r\omega\theta_{2,j}}{4\Delta x^2\Delta t}\theta_{2,j+1} + \left[\frac{I_p r\omega\left(\theta_{2,j} - 2\theta_{1,j}\right)}{2\Delta x^2\Delta t} - \frac{m_p r}{\Delta t^2}\right]\theta_{1,j+1} \\
&= \frac{I_p r\omega\left(\theta_{2,j} - 2\theta_{1,j}\right)}{2\Delta x^2\Delta t}\theta_{1,j-1} - \frac{I_p r\omega\theta_{2,j}}{4\Delta x^2\Delta t}\left(-\theta_{2,j-1}\right) \\
&+ \frac{m_p r}{\Delta t^2}\left(-2\theta_{1,j} + \theta_{1,j-1}\right) \\
&+ \frac{EIr}{\Delta x^4}\left[\left(\theta_{3,j} - 4\theta_{2,j} + 5\theta_{1,j}\right) - \frac{3}{2}\left(\theta_{2,j}\right)^2\left(\theta_{2,j} - 2\theta_{1,j}\right)\right] \\
&- \frac{EAr}{2\Delta x^3}\left[U_{2,j}\left(\theta_{2,j} - 2\theta_{1,j}\right) + \theta_{2,j}\left(U_{2,j} - 2U_{1,j}\right)\right. \\
&\left. + \frac{3r^2}{4\Delta x}{\theta_{2,j}}^2\left(\theta_{2,j} - 2\theta_{1,j}\right)\right] + m_p g \sin\alpha \sin\theta_{1,j} \\
&+ \frac{sgn\left(\theta_{1,j} - \theta_{1,j-1}\right) fr\left|\theta_{1,j} - \theta_{1,j-2}\right|}{2\Delta t\sqrt{\left(\frac{U_{1,j}-U_{1,j-2}}{2\Delta t}\right)^2 + r^2\left(\frac{\theta_{1,j}-\theta_{1,j-2}}{2\Delta t}\right)^2}}\left\{-\frac{EIr}{\Delta x^4}\left[\frac{1}{16}{\theta_{2,j}}^4\right.\right. \\
&\left. - 3\left(\theta_{2,j} - 2\theta_{1,j}\right)^2 - \left(\theta_{3,j} - 2\theta_{2,j} + \theta_{1,j}\right)\theta_{2,j}\right] \\
&- \frac{EAr}{8\Delta x^3}\left[U_{2,j}{\theta_{2,j}}^2 + \frac{r^2}{4\Delta x}{\theta_{2,j}}^4\right] \\
&+ \frac{I_p r\omega}{2\Delta x^2\Delta t}\left[\left(\theta_{2,j} - 2\theta_{1,j} - \theta_{2,j-2} + 2\theta_{1,j-2}\right)\right. \\
&\left. - \frac{1}{4}\left(\theta_{1,j} - \theta_{1,j-2}\right){\theta_{2,j}}^2\right] + m_p g \sin\alpha \cos\theta_{1,j} \\
&\left. + \frac{m_p r}{4\Delta t^2}\left(\theta_{1,j} - \theta_{1,j-2}\right)^2\right\}
\end{aligned}
\tag{A.346}
$$

While for $i = N - 1$:

$$
\begin{aligned}
&U_{N-1,j+1} \\
&= 2U_{N-1,j} - U_{N-1,j-1} + \frac{EA\Delta t^2}{m_p \Delta x^2}\left(U_{N,j} - 2U_{N-1,j} + U_{N-2,j}\right) \\
&+ \frac{EAr^2\Delta t^2}{2m_p\Delta x^3}\left(\theta_{N,j} - \theta_{N-2,j}\right)\left(\theta_{N,j} - 2\theta_{N-1,j} + \theta_{N-2,j}\right) \\
&- \frac{sgn\left(U_{N-1,j} - U_{N-1,j-1}\right) f \Delta t \left|U_{N-1,j} - U_{N-1,j-2}\right|}{2m_p\sqrt{\left(\frac{U_{N-1,j}-U_{N-1,j-2}}{2\Delta t}\right)^2 + r^2\left(\frac{\theta_{N-1,j}-\theta_{N-1,j-2}}{2\Delta t}\right)^2}}\left\{-\frac{EIr}{\Delta x^4}\left[\frac{1}{16}\left(\theta_{N,j}\right.\right.\right. \\
&\left. - \theta_{N-2,j}\right)^4 - 3\left(\theta_{N,j} - 2\theta_{N-1,j} + \theta_{N-2,j}\right)^2 \\
&\left. - \left(-2\theta_{N,j} - \theta_{N-1,j} + 2\theta_{N-2,j} - \theta_{N-3,j}\right)\left(\theta_{N,j} - \theta_{N-2,j}\right)\right] \\
&- \frac{EAr}{8\Delta x^3}\left[\left(U_{N,j} - U_{N-2,j}\right)\left(\theta_{N,j} - \theta_{N-2,j}\right)^2 + \frac{r^2}{4\Delta x}\left(\theta_{N,j} - \theta_{N-2,j}\right)^4\right] \\
&+ \frac{I_p r\omega}{2\Delta x^2\Delta t}\left[\left(\theta_{N,j} - 2\theta_{N-1,j} + \theta_{N-2,j} - \theta_{N,j-2} + 2\theta_{N-1,j-2}\right.\right. \\
&\left.\left. - \theta_{N-2,j-2}\right) - \frac{1}{4}\left(\theta_{N-1,j} - \theta_{N-1,j-2}\right)\left(\theta_{N,j} - \theta_{N-2,j}\right)^2\right] \\
&\left. + m_p g \sin\alpha \cos\theta_{N-1,j} + \frac{m_p r}{4\Delta t^2}\left(\theta_{N-1,j} - \theta_{N-1,j-2}\right)^2\right\} + \Delta t^2 g \cos\alpha
\end{aligned}
\tag{A.347}
$$

$$
\begin{aligned}
&\frac{I_p r\omega\left(\theta_{N,j}-\theta_{N-2,j}\right)}{4\Delta x^2\Delta t}\theta_{N,j+1} \\
&+\left[\frac{I_p r\omega\left(\theta_{N,j}-2\theta_{N-1,j}+\theta_{N-2,j}\right)}{2\Delta x^2\Delta t}-\frac{m_p r}{\Delta t^2}\right]\theta_{N-1,j+1} \\
&-\frac{I_p r\omega\left(\theta_{N,j}-\theta_{N-2,j}\right)}{4\Delta x^2\Delta t}\theta_{N-2,j+1} \\
&=\frac{I_p r\omega\left(\theta_{N,j}-2\theta_{N-1,j}+\theta_{N-2,j}\right)}{2\Delta x^2\Delta t}\theta_{N-1,j-1} \\
&-\frac{I_p r\omega\left(\theta_{N,j}-\theta_{N-2,j}\right)}{4\Delta x^2\Delta t}\left(-\theta_{N,j-1}+\theta_{N-2,j-1}\right) \\
&+\frac{m_p r}{\Delta t^2}\left(-2\theta_{N-1,j}+\theta_{N-1,j-1}\right) \\
&+\frac{EIr}{\Delta x^4}\Big[\left(-4\theta_{N,j}+5\theta_{N-1,j}-4\theta_{N-2,j}+\theta_{N-3,j}\right) \\
&-\frac{3}{2}\left(\theta_{N,j}-\theta_{N-2,j}\right)^2\left(\theta_{N,j}-2\theta_{N-1,j}+\theta_{N-2,j}\right)\Big] \\
&-\frac{EAr}{2\Delta x^3}\Big[\left(\theta_{N,j}-\theta_{N-2,j}\right)\left(\theta_{N,j}-2\theta_{N-1,j}+\theta_{N-2,j}\right) \\
&+\left(U_{N,j}-2U_{N-1,j}+U_{N-2,j}\right)\left(\theta_{N,j}-\theta_{N-2,j}\right) \\
&+\frac{3r^2}{4\Delta x}\left(\theta_{N,j}-2\theta_{N-1,j}+\theta_{N-2,j}\right)\left(\theta_{N,j}-\theta_{N-2,j}\right)^2\Big] \\
&+m_p g\sin\alpha\sin\theta_{N-1,j} \\
&+\frac{sgn\left(\theta_{N-1,j}-\theta_{N-1,j-1}\right)fr\left|\theta_{N-1,j}-\theta_{N-1,j-2}\right|}{2\Delta t\sqrt{\left(\frac{U_{N-1,j}-U_{N-1,j-2}}{2\Delta t}\right)^2+r^2\left(\frac{\theta_{N-1,j}-\theta_{N-1,j-2}}{2\Delta t}\right)^2}}\Big\{-\frac{EIr}{\Delta x^4}\Big[\frac{1}{16}\big(\theta_{N,j} \\
&-\theta_{N-2,j}\big)^4-3\left(\theta_{N,j}-2\theta_{N-1,j}+\theta_{N-2,j}\right)^2 \\
&-\left(-2\theta_{N,j}-\theta_{N-1,j}+2\theta_{N-2,j}-\theta_{N-3,j}\right)\left(\theta_{N,j}-\theta_{N-2,j}\right)\Big] \\
&-\frac{EAr}{8\Delta x^3}\left[\left(U_{N,j}-U_{N-2,j}\right)\left(\theta_{N,j}-\theta_{N-2,j}\right)^2+\frac{r^2}{4\Delta x}\left(\theta_{N,j}-\theta_{N-2,j}\right)^4\right] \\
&+\frac{I_p r\omega}{2\Delta x^2\Delta t}\Big[\big(\theta_{N,j}-2\theta_{N-1,j}+\theta_{N-2,j}-\theta_{N,j-2}+2\theta_{N-1,j-2} \\
&-\theta_{N-2,j-2}\big)-\frac{1}{4}\left(\theta_{N-1,j}-\theta_{N-1,j-2}\right)\left(\theta_{N,j}-\theta_{N-2,j}\right)^2\Big] \\
&+m_p g\sin\alpha\cos\theta_{N-1,j}+\frac{m_p r}{4\Delta t^2}\left(\theta_{N-1,j}-\theta_{N-1,j-2}\right)^2\Big\}
\end{aligned}
\tag{A.348}
$$

Lastly for $i = N$:

$$
\begin{aligned}
&U_{N,j+1} \\
&= 2U_{N,j} - U_{N,j-1} + \frac{EA\Delta t^2}{m_p \Delta x^2}\left(-2U_{N,j} + 2U_{N-1,j} - \frac{r^2}{\Delta x}\theta_{N-1,j}{}^2\right) \\
&+ \frac{EAr^2\Delta t^2}{2m_p\Delta x^3}\left(-2\theta_{N-1,j}\right)\left(-2\theta_{N,j}\right) \\
&- \frac{sgn\left(U_{N,j} - U_{N,j-1}\right) f\Delta t\left|U_{N,j} - U_{N,j-2}\right|}{2m_p\sqrt{\left(\frac{U_{N,j}-U_{N,j-2}}{2\Delta t}\right)^2 + r^2\left(\frac{\theta_{N,j}-\theta_{N,j-2}}{2\Delta t}\right)^2}}\left\{-\frac{EIr}{\Delta x^4}\left[\frac{1}{16}\left(-2\theta_{N-1,j}\right)^4\right.\right. \\
&\left.- 3\left(-2\theta_{N,j}\right)^2\right] \\
&- \frac{EAr}{8\Delta x^3}\left[\left(-\frac{r^2}{\Delta x}\theta_{N-1,j}{}^2\right)\left(-2\theta_{N-1,j}\right)^2 + \frac{r^2}{4\Delta x}\left(-2\theta_{N-1,j}\right)^4\right] \\
&+ \frac{I_p r\omega}{2\Delta x^2\Delta t}\left[\left(-2\theta_{N,j} + 2\theta_{N,j-2}\right) - \frac{1}{4}\left(\theta_{N,j} - \theta_{N,j-2}\right)\left(-2\theta_{N-1,j}\right)^2\right] \\
&\left.+ m_p g \sin\alpha \cos\theta_{N,j} + \frac{m_p r}{4\Delta t^2}\left(\theta_{N,j} - \theta_{N,j-2}\right)^2\right\} + \Delta t^2 g \cos\alpha
\end{aligned}
\tag{A.349}
$$

$$
\begin{aligned}
&\left[\frac{I_p r\omega\left(-2\theta_{N,j}\right)}{2\Delta x^2\Delta t} - \frac{m_p r}{\Delta t^2}\right]\theta_{N,j+1} - 2\frac{I_p r\omega\left(-2\theta_{N-1,j}\right)}{4\Delta x^2\Delta t}\theta_{N-1,j+1} \\
&= \frac{I_p r\omega\left(-2\theta_{N,j}\right)}{2\Delta x^2\Delta t}\theta_{N,j-1} - \frac{I_p r\omega\left(-2\theta_{N-1,j}\right)}{4\Delta x^2\Delta t}\left(2\theta_{N-1,j-1}\right) \\
&+ \frac{m_p r}{\Delta t^2}\left(-2\theta_{N,j} + \theta_{N,j-1}\right) \\
&+ \frac{EIr}{\Delta x^4}\left[\left(6\theta_{N,j} - 4\theta_{N-1,j} + 2\theta_{N-2,j}\right) - \frac{3}{2}\left(-2\theta_{N-1,j}\right)^2\left(-2\theta_{N,j}\right)\right] \\
&- \frac{EAr}{2\Delta x^3}\left[\left(-\frac{r^2}{\Delta x}\theta_{N-1,j}{}^2\right)\left(-2\theta_{N,j}\right)\right. \\
&\left.+ \left(-2U_{N,j} + 2U_{N-1,j}\right)\left(-2\theta_{N-1,j}\right) + \frac{3r^2}{4\Delta x}\left(-2\theta_{N,j}\right)\left(-2\theta_{N-1,j}\right)^2\right] \\
&+ m_p g \sin\alpha \sin\theta_{N,j} \\
&+ \frac{sgn\left(\theta_{N,j} - \theta_{N,j-1}\right) fr\left|\theta_{N,j} - \theta_{N,j-2}\right|}{2\Delta t\sqrt{\left(\frac{U_{N,j}-U_{N,j-2}}{2\Delta t}\right)^2 + r^2\left(\frac{\theta_{N,j}-\theta_{N,j-2}}{2\Delta t}\right)^2}}\left\{-\frac{EIr}{\Delta x^4}\left[\frac{1}{16}\left(-2\theta_{N-1,j}\right)^4\right.\right. \\
&\left.- 3\left(-2\theta_{N,j}\right)^2\right] \\
&- \frac{EAr}{8\Delta x^3}\left[\left(-\frac{r^2}{\Delta x}\theta_{N-1,j}{}^2\right)\left(-2\theta_{N-1,j}\right)^2 + \frac{r^2}{4\Delta x}\left(-2\theta_{N-1,j}\right)^4\right] \\
&+ \frac{I_p r\omega}{2\Delta x^2\Delta t}\left[\left(-2\theta_{N,j} + 2\theta_{N,j-2}\right) - \frac{1}{4}\left(\theta_{N,j} - \theta_{N,j-2}\right)\left(-2\theta_{N-1,j}\right)^2\right] \\
&\left.+ m_p g \sin\alpha \cos\theta_{N,j} + \frac{m_p r}{4\Delta t^2}\left(\theta_{N,j} - \theta_{N,j-2}\right)^2\right\}
\end{aligned}
\tag{A.350}
$$

The initial conditions are the same ones from Eqs. (A.182), (A.183), (A.184) and (A.185), with discretizations given by:

$$U_{i,1} = U_0 \, sin\left(\frac{\pi i \Delta x}{L}\right) \tag{A.351}$$

$$\begin{aligned}
\frac{U_{i,2} - U_{i,0}}{2\Delta t} = 0 \rightarrow U_{i,0} = U_{i,2} \rightarrow U_{i,2} \\
&= U_{i,1} + \frac{EA\Delta t^2}{2m_p \Delta x^2}\left(U_{i+1,1} - 2U_{i,1} + U_{i-1,1}\right) \\
&+ \frac{EAr^2\Delta t^2}{4m_p \Delta x^3}\left(\theta_{i+1,1} - \theta_{i-1,1}\right)\left(\theta_{i+1,1} - 2\theta_{i,1} + \theta_{i-1,1}\right) \\
&- \frac{sgn\left(U_{i,1}\right) f \Delta t \left|U_{i,1}\right|}{4m_p\sqrt{\left(\frac{U_{i,1}}{2\Delta t}\right)^2 + r^2\left(\frac{\theta_{i,1}}{2\Delta t}\right)^2}}\left\{-\frac{EIr}{\Delta x^4}\left[\frac{1}{16}\left(\theta_{i+1,1}\right.\right.\right. \\
&\left. - \theta_{i-1,1}\right)^4 - 3\left(\theta_{i+1,1} - 2\theta_{i,1} + \theta_{i-1,1}\right)^2 \\
&- \left(\theta_{i+2,1} - 2\theta_{i+1,1} + 2\theta_{i-1,1} - \theta_{i-2,1}\right)\left(\theta_{i+1,1}\right. \\
&\left.\left. - \theta_{i-1,1}\right)\right] \\
&- \frac{EAr}{8\Delta x^3}\left[\left(U_{i+1,1} - U_{i-1,1}\right)\left(\theta_{i+1,1} - \theta_{i-1,1}\right)^2\right. \\
&\left. + \frac{r^2}{4\Delta x}\left(\theta_{i+1,1} - \theta_{i-1,1}\right)^4\right] \\
&+ \frac{I_p r\omega}{2\Delta x^2 \Delta t}\left[\left(\theta_{i+1,1} - 2\theta_{i,1} + \theta_{i-1,1}\right)\right. \\
&\left. - \frac{1}{4}\theta_{i,1}\left(\theta_{i+1,1} - \theta_{i-1,1}\right)^2\right] + m_p g \, sin\,\alpha \, cos\,\theta_{i,1} \\
&\left. + \frac{m_p r}{4\Delta t^2}\theta_{i,1}{}^2\right\} + \frac{\Delta t^2 g \, cos\,\alpha}{2}
\end{aligned} \tag{A.352}$$

$$\theta_{i,1} = 0.1 \tag{A.353}$$

$$
\begin{aligned}
\frac{\theta_{i,2}-\theta_{i,0}}{2\Delta t} = 0 \rightarrow \theta_{i,0} = \theta_{i,2}& \\
&\rightarrow \frac{I_p r\omega\left(\theta_{i+1,j}-\theta_{i-1,j}\right)}{2\Delta x^2 \Delta t}\theta_{i+1,2} \\
&+\left[\frac{I_p r\omega\left(\theta_{i+1,1}-2\theta_{i,1}+\theta_{i-1,1}\right)}{2\Delta x^2 \Delta t}-\frac{m_p r}{\Delta t^2}\right]\theta_{i,2} \\
&-\frac{I_p r\omega\left(\theta_{i+1,1}-\theta_{i-1,1}\right)}{2\Delta x^2 \Delta t}\theta_{i-1,2} \\
&=\frac{m_p r}{\Delta t^2}\left(-2\theta_{i,1}\right) \\
&+\frac{EIr}{\Delta x^4}\Big[\left(\theta_{i+2,1}-4\theta_{i+1,1}+6\theta_{i,1}-4\theta_{i-1,1}+\theta_{i-2,1}\right) \\
&-\frac{3}{2}\left(\theta_{i+1,1}-\theta_{i-1,1}\right)^2\left(\theta_{i+1,1}-2\theta_{i,1}+\theta_{i-1,1}\right)\Big] \\
&-\frac{EAr}{2\Delta x^3}\Big[\left(U_{i+1,1}-U_{i-1,1}\right)\left(\theta_{i+1,1}-2\theta_{i,1}+\theta_{i-1,1}\right) \\
&+\left(U_{i+1,1}-2U_{i,1}+U_{i-1,1}\right)\left(\theta_{i+1,1}-\theta_{i-1,1}\right) \\
&+\frac{3r^2}{4\Delta x}\left(\theta_{i+1,1}-2\theta_{i,1}+\theta_{i-1,1}\right)\left(\theta_{i+1,1}-\theta_{i-1,1}\right)^2\Big] \\
&+m_p g \sin\alpha \sin\theta_{i,1} \\
&+\frac{sgn\left(\theta_{i,1}\right) fr\left|\theta_{i,1}\right|}{2\Delta t\sqrt{\left(\frac{U_{i,1}}{2\Delta t}\right)^2+r^2\left(\frac{\theta_{i,1}}{2\Delta t}\right)^2}}\Big\{-\frac{EIr}{\Delta x^4}\Big[\frac{1}{16}\big(\theta_{i+1,1} \\
&-\theta_{i-1,1}\big)^4-3\left(\theta_{i+1,1}-2\theta_{i,1}+\theta_{i-1,1}\right)^2 \\
&-\left(\theta_{i+2,1}-2\theta_{i+1,1}+2\theta_{i-1,1}-\theta_{i-2,1}\right)\big(\theta_{i+1,1} \\
&-\theta_{i-1,1}\big)\Big] \\
&-\frac{EAr}{8\Delta x^3}\Big[\left(U_{i+1,1}-U_{i-1,1}\right)\left(\theta_{i+1,1}-\theta_{i-1,1}\right)^2 \\
&+\frac{r^2}{4\Delta x}\left(\theta_{i+1,1}-\theta_{i-1,1}\right)^4\Big] \\
&+\frac{I_p r\omega}{2\Delta x^2 \Delta t}\Big[\left(\theta_{i+1,1}-2\theta_{i,1}+\theta_{i-1,1}\right) \\
&-\frac{1}{4}\theta_{i,1}\left(\theta_{i+1,1}-\theta_{i-1,1}\right)^2\Big]+m_p g \sin\alpha \cos\theta_{i,1} \\
&+\frac{m_p r}{4\Delta t^2}{\theta_{i,1}}^2\Big\}
\end{aligned}
\tag{A.354}
$$

A.3.4. Solution for tripping out

Discretizing Eqs. (A.131), (A.335) and (A.336):

$$EA\left(\frac{U_{i+1,j} - 2U_{i,j} + U_{i-1,j}}{\Delta x^2}\right) - m_p\left(\frac{U_{i,j+1} - 2U_{i,j} + U_{i,j-1}}{\Delta t^2}\right) + m_p g \cos\alpha - sgn\left(U_{i,j} - U_{i,j-1}\right) f\left[\frac{-m_p r}{2\Delta x \Delta t^2}\left(U_{i+1,j} - U_{i-1,j} - 2U_{i+1,j-1} + 2U_{i-1,j-1} + U_{i+1,j-2} - U_{i-1,j-2}\right) + m_p g \sin\alpha\right] = 0 \tag{A.355}$$

$$F_{i,j} = -\frac{EA}{2\Delta x}\left(U_{i+1,j} - U_{i-1,j}\right) \tag{A.356}$$

$$N_{i,j} = -\frac{m_p r}{2\Delta x \Delta t^2}\left(U_{i+1,j} - U_{i-1,j} - 2U_{i+1,j-1} + 2U_{i-1,j-1} + U_{i+1,j-2} - U_{i-1,j-2}\right) + m_p g \sin\alpha \tag{A.357}$$

Manipulating Eq. (A.355):

$$U_{i,j+1} = 2U_{i,j} - U_{i,j-1} + \frac{EA\Delta t^2}{m_p \Delta x^2}\left(U_{i+1,j} - 2U_{i,j} + U_{i-1,j}\right) + g\Delta t^2 \cos\alpha - sgn\left(U_{i,j} - U_{i,j-1}\right) f\left[-\frac{r}{2\Delta x}\left(U_{i+1,j} - U_{i-1,j} - 2U_{i+1,j-1} + 2U_{i-1,j-1} + U_{i+1,j-2} - U_{i-1,j-2}\right) + g\Delta t^2 \sin\alpha\right] \tag{A.358}$$

The boundary conditions are the same given by Eqs. (A.207) and (A.208), with the discretizations given by Eqs. (A.209) and (A.210). For $i = 1$:

$$U_{1,j+1} = 2U_{1,j} - U_{1,j-1} + \frac{EA\Delta t^2}{m_p \Delta x^2}\left(U_{2,j} - 2U_{1,j}\right) + g\Delta t^2 \cos\alpha - sgn\left(U_{1,j} - U_{1,j-1}\right) f\left[-\frac{r}{2\Delta x}\left(U_{2,j} - 2U_{2,j-1} + U_{2,j-2}\right) + g\Delta t^2 \sin\alpha\right] \tag{A.359}$$

While for $i = N - 1$:

$$\begin{aligned} U_{N-1,j+1} = 2U_{N-1,j} - U_{N-1,j-1} \\ + \frac{EA\Delta t^2}{m_p \Delta x^2}\left(U_{N,j} - 2U_{N-1,j} + U_{N-2,j}\right) + g\Delta t^2 \cos\alpha \\ - sgn\left(U_{N-1,j} - U_{N-1,j-1}\right) f \Big[-\frac{r}{2\Delta x}\left(U_{N,j} - U_{N-2,j}\right. \\ \left. - 2U_{N,j-1} + 2U_{N-2,j-1} + U_{N,j-2} - U_{N-2,j-2}\right) \\ + g\Delta t^2 \sin\alpha\Big] \end{aligned} \tag{A.360}$$

Lastly for $i = N$:

$$\begin{aligned} U_{N,j+1} = 2U_{N,j} - U_{N,j-1} + \frac{EA\Delta t^2}{m_p \Delta x^2}\left(-2U_{N,j} + 2U_{N-1,j}\right) \\ + g\Delta t^2 \cos\alpha - sgn\left(U_{N,j} - U_{N,j-1}\right) f g\Delta t^2 \sin\alpha \end{aligned} \tag{A.361}$$

The initial conditions are the same ones given by Eqs. (A.214) and (A.215), with their discretizations given by:

$$U_{i,1} = U_0 \sin\left(\frac{\pi i \Delta x}{L}\right) \tag{A.362}$$

$$\begin{aligned} \frac{U_{i,2} - U_{i,0}}{2\Delta t} = 0 \rightarrow U_{i,0} = U_{i,2} \\ \rightarrow -\frac{sgn\left(U_{i,1}\right) fr}{2\Delta x} U_{i-1,2} + U_{i,2} + \frac{sgn\left(U_{i,1}\right) fr}{2\Delta x} U_{i+1,2} \\ = U_{i,1} + \frac{EA\Delta t^2}{2m_p \Delta x^2}\left(U_{i+1,1} - 2U_{i,1} + U_{i-1,1}\right) \\ + \frac{g\Delta t^2 \cos\alpha}{2} \\ - \frac{sgn\left(U_{i,1}\right) f}{2}\Big[-\frac{r}{2\Delta x}\left(U_{i+1,1} - U_{i-1,1}\right) \\ + g\Delta t^2 \sin\alpha\Big] \end{aligned} \tag{A.363}$$

APPENDIX B – FINITE DIFFERENCES METHODS

On this appendix, the finite differences method is discussed in more detail by presenting the discretization formulas needed for applying the method. A discussion regarding the method stability is made, since this restricts the choice of the discretization intervals Δx and Δt. Finally, badly-scaled matrices are also discussed, since they are a common issue that arises whenever the finite differences method is used.

B.1. Introduction

Due to the complexity of the equations associated to a physical phenomenon, it is not always possible to find an analytical solution. Consequently, the only resort is to employ numerical methods to find approximated solution for these equations. The most commonly used methods are the finite differences and the finite elements; on the present work, only the finite differences method will be used. Despite having a higher computational cost than the finite elements, it is much easier to do the discretization for finite differences.

The finite differences method consists in doing a discretization for all the derivatives on the equations, using the information from adjacent points – also commonly called nodes. It is worth explaining, however, the concept of adjacent: since the derivatives can be either in respect to space or to time, the word adjacent has different implications. Consider an arbitrary structure divided in N points, with an arbitrary internal point named i, and a time interval T divided in subintervals, with an arbitrary point in time named j. To do the discretization for the displacement derivative in space – also known as the strain – of an arbitrary point i, information from at least the adjacent points $i - 1$ and $i + 1$ will be needed. Meanwhile, for the displacement derivative in time – also known as the velocity – of an arbitrary point i on the time point j, at least $j - 1$ and $j + 1$ will be needed. It also a common practice to instead use points $j - 1$ and $j - 2$ for time derivatives; that will define if the scheme is either explicit or implicit. The problem is explicit when the discretization of the time derivatives uses information from time intervals already known, such as $j - 1$ and $j - 2$; meanwhile, in the implicit problem, information from a future time interval is needed, such as $j + 1$.

The practical consequences of these methods in solving partial differential equations are that the explicit problem will result in a system of equations for all the points in space being solved at each time step, while in the implicit problem the equation for each point in space is decoupled from the adjacent points, speeding up the calculations. Depending on the type of partial differential equation, there can be differences on the algorithm stability as well.

The discretization most commonly used for the finite differences methods are the Euler's approximations, which are based on the Taylor's series expansion. The advantage from this discretization when compared to others is its simplicity, since it requires less adjacent points for the discretization of each derivative. However, since the information from only a few adjacent points are used, the error associated to the discretization is bigger than in other methods – in other words, it is also said that the methods is of lower order. Strang (2007) does an extensive discussion regarding the advantages and disadvantages of each type of approximation used for the finite differences method.

Another possibility is the approach known as the methods of lines, in which only the spatial derivative is discretized, keeping the time derivatives intact, thus reaching a system of ordinary differential equations. This method is also discussed in Strang (2007).

B.2. First Order Derivative

To deduct the derivatives discretization formulas, it is necessary to use the Taylor's series expansion. The Taylor's series is a series expansion of a function around a specific point. The expansion of a function *f(x)* around point $x = a$ is given by Eq. (B.1):

$$\begin{gathered} f(x) = f(a) + f'(a)(x-a) + \frac{f''(a)}{2!}(x-a)^2 + \cdots \\ + \frac{f^{(n)}(a)}{n!}(x-a)^n + \cdots \end{gathered} \tag{B.1}$$

Applying the Taylor's series expansion around points $x + h$ and $x - h$, Eqs. (B.2) and (B.3) are obtained:

$$f(x+h) = f(x) + hf'(x) + \frac{1}{2}h^2 f''(x) + \frac{1}{6}h^3 f'''(x) + O(h^4) \qquad \text{(B.2)}$$

$$f(x-h) = f(x) - hf'(x) + \frac{1}{2}h^2 f''(x) - \frac{1}{6}h^3 f'''(x) + O(h^4) \qquad \text{(B.3)}$$

Isolating *f'(x)* on Eqs. (B.2) and (B.3), Eqs. (B.4) and (B.5) are reached:

$$\begin{aligned} f'(x) &= \frac{f(x+h) - f(x)}{h} - \frac{1}{2}hf''(x) - \frac{1}{6}h^2 f'''(x) - O(h^3) \\ &= \frac{f(x+h) - f(x)}{h} - O(h) \end{aligned} \qquad \text{(B.4)}$$

$$\begin{aligned} f'(x) &= \frac{f(x) - f(x-h)}{h} + \frac{1}{2}hf''(x) + \frac{1}{6}h^2 f'''(x) + O(h^3) \\ &= \frac{f(x) - f(x-h)}{h} + O(h) \end{aligned} \qquad \text{(B.5)}$$

Eq. (B.4) is known as the forward difference, while Eq. (B.5) is known as the backward difference. The errors associated with the approximations given by Eqs. (B.4) and (B.5) have order of *h*; for this reason, they are known as first order approximations.

Another approximation possibility is obtained by taking the difference between Eqs. (B.2) and (B.3), resulting in Eq. (B.6). The terms dependent of *h* to an even exponent are canceled, thus remaining only terms dependent of *h* to an odd exponent.

$$f(x+h) - f(x-h) = 2hf'(x) + \frac{1}{3}h^3 f'''(x) + O(h^5) \qquad \text{(B.6)}$$

Rearranging Eq. (B.6) to isolate *f'(x)*, Eq. (B.7) is obtained:

$$\begin{aligned} f'(x) &= \frac{f(x+h) - f(x-h)}{2h} - \frac{1}{6}h^2 f'''(x) - O(h^4) \\ &= \frac{f(x+h) - f(x-h)}{2h} - O(h^2) \end{aligned} \qquad \text{(B.7)}$$

Eq. (B.7) is known as the centered difference. Differently from Eqs. (B.4) and (B.5), the error of this approximation has order of h^2, thus being more precise than the forward and backward differences. Graphically, the three approximations can be seen on Figure B.1, where $D_{+}u(\bar{x})$ represents the forward difference, $D_{-}u(\bar{x})$ represents the backward difference, $D_{0}u(\bar{x})$ represents the centered difference and $u'(\bar{x})$ represents the real derivative of function $u(x)$ on point $\bar{x}$. As can be seen, the centered difference is closer to the real derivative $u'(\bar{x})$, reiterating the lesser error associated with this approximation.

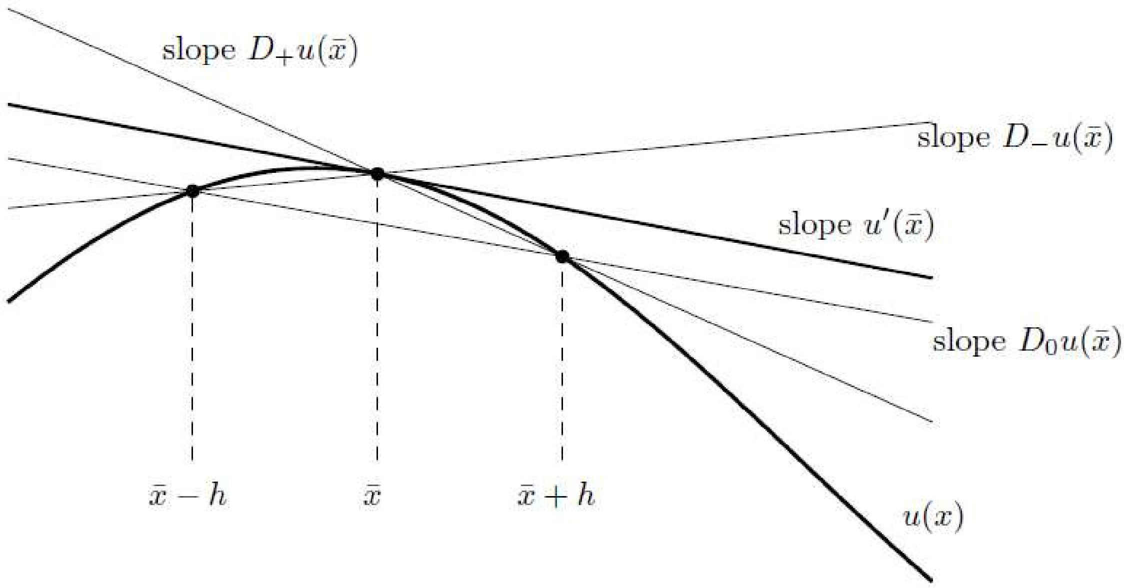

Figure B.1: Graphical representation of the comparison between forward, backward and centered differences for the real derivative $u'(\bar{x})$ of function $u(x)$ on point $\bar{x}$ (Leveque, 2005).

B.3. Higher Order Derivatives

The simplest way to obtain the discretization for higher order derivatives is through Eqs. (B.4), (B.5) and (B.7), obtained for the first order derivative. Writing the second derivative as two consecutive first derivatives, Eq. (B.8) is obtained:

$$f''(x) = \left(f'(x)\right)' = \frac{1}{h}\left(f'(x+h) - f'(x)\right) \tag{B.8}$$

On this step, the forward difference was used. Applying again the discretization on Eq. (B.8), Eq. (B.9) is obtained:

$$f''(x) = \frac{1}{h}\left(\frac{f(x+h) - f(x)}{h} - \frac{f(x) - f(x-h)}{h}\right) = \frac{1}{h^2}[f(x+h) - 2f(x) + f(x-h)] \tag{B.9}$$

Meanwhile, on this step, the backward difference was applied. This combination guarantees that the discretization error will be of order h^2. The same result could be obtained if the centered difference was applied twice with step *h/2* instead.

As previously discussed, for time derivatives it is possible to use either centered or backward differences. The centered difference is given by Eq. (B.9) and has error of order h^2, while the backward one is given by Eq. (B.10) and has error of order h.

$$f''(x) = \frac{1}{h^2}[f(x) - 2f(x-h) + f(x-2h)] \tag{B.10}$$

Derivatives of higher order are needed for the physical problem of a column buckling inside a well – especially the discretization for the fourth derivative. Firstly, for the third derivative, the same procedure is used, resulting on Eq. (B.11):

$$f'''(x) = \frac{1}{2h^3}[f(x+2h) - 2f(x+h) + 2f(x-h) - f(x-2h)] \tag{B.11}$$

Eq. (B.11) has error of order h^2. Lastly, for the fourth derivative, Eq. (B.12) is obtained:

$$f''''(x) = \frac{1}{h^4}[f(x+2h) - 4f(x+h) + 6f(x) - 4f(x-h) + f(x-2h)] \tag{B.12}$$

Eq. (B.12) also has error of order h^2. The discretizations given by Eqs. (B.4), (B.5), (B.7), (B.9), (B.10), (B.11) e (B.12) have precision order varying from h to h^2. It is possible to obtain discretizations with higher order of precision, as seen in Fornberg (1988). However, despite improving precision, the usage of these approximations will not solve problems regarding the algorithm stability.

B.4. Mixed Derivatives

Up to this point, the deducted discretizations only apply to derivatives of one variable. Despite the displacement being a function of both space and time, on the derivatives of one variable only the desired variable is taken into account during discretization; for example, the discretization of a spatial derivative only uses information from adjacent points in space, but all information is situated on the same time step. However, on the desired problem, there is the necessity to discretize some mixed derivatives – derivatives dependent of both space and time simultaneously. In special, three mixed derivatives appear on the developed motion equations: second derivative, being one in space and one in time; third derivative, being two in space and one in time; and third derivative, being one in space and two in time. The discretizations for these cases are given by Eqs. (B.13), (B.14) and (B.15).

$$\frac{\partial^2 f(x,t)}{\partial x \partial t} = \frac{1}{4hj}[f(x+h,t+j) - f(x-h,t+j) - f(x+h,t-j) + f(x-h,t-j)] \tag{B.13}$$

$$\frac{\partial^3 f(x,t)}{\partial x^2 \partial t} = \frac{1}{2h^2 j}[f(x+h,t+j) - 2f(x,t+j) + f(x-h,t+j) - f(x+h,t-j) + 2f(x,t-j) - f(x-h,t-j)] \tag{B.14}$$

$$\frac{\partial^3 f(x,t)}{\partial x \partial t^2} = \frac{1}{2hj^2}[f(x+h,t+j) - f(x-h,t+j) - 2f(x+h,t) + 2f(x-h,t) + f(x+h,t-j) - f(x-h,t-j)] \tag{B.15}$$

B.5. Stability

On this work, both derivatives will be discretized, using centered differences for both space and time. On this kind of problem – hyperbolic partial differential equations such as the wave equation – the increments of space *Δx* and time *Δt* cannot be chosen freely when doing an explicit scheme. There is a restriction on this choice, first noted by Courant et al. (1928), originating the Courant number – also known as the Courant-Friedrichs-Lewy stability condition. The physical principle behind this condition is that if a wave moves through a mesh of discrete points in space and its amplitude must be known as a function of time, the time step from the discretization must be less than the time spent for the wave to move through two adjacent points of this mesh. Therefore, the Courant number is directly tied to the propagation speed of waves on the media.

To find out what must be the intervals of discretization, it is necessary to find the growth factor of the differential equation and determine the values in which this factor decays instead of growing indefinitely. Such analysis is beyond the scope of this work and can be seen in Leveque (2005) and Strang (2007). For practical purposes, only the Courant number is of any use, which is given by Eq. (B.16):

$$C = c\frac{\Delta t}{\Delta x} \leq 1 \tag{B.16}$$

Where C is the Courant number, dimensionless, c is the propagation speed of waves on the medium, in m/s, Δt is the time step, in s, and Δx is the space step, in m. For an unidimensional solid media, such is the case for the vibration of continuous media, the propagation speed of waves is given by Eq. (B.17):

$$c = \sqrt{\frac{E}{\rho}} \tag{B.17}$$

Where E is the material Young's modulus, in Pa, and ρ is the material specific mass, in kg/m³. Therefore, the procedure to choose the appropriate increments would be defining the space step Δx, calculate the propagation speed of waves on the media c and choose a time step Δt that obeys the inequality given by Eq. (B.18):

$$\Delta t \leq \frac{\Delta x}{c} \tag{B.18}$$

According to Strang (2007), the Courant-Friedrichs-Lewy stability condition is a necessary condition for convergence in this kind of problem, but it is not a sufficient condition; obeying this relation does not guarantee that the problem solution will be stable, since other numerical problems might occur, such as the instability caused by badly-scaled matrices. Also, this analysis is only valid for the wave equation, which is a linear equation; other linear partial differential equations, as well as nonlinear differential equations, have different stability conditions. Since the motion equation of the problem, despite not being linear, is close to the wave equation – and deducting the proper stability condition would be an incredible hard task – it is possible to use the criterion from Eq. (B.18) as a first guess. This criterion might not be enough, however, and the need to be even more conservative when choosing Δt may arise; in this case, trial-and-error becomes the best possibility. On the present work – in which the material used is steel – the propagation speed is $c = 5172$ m/s. To ensure that the nonlinearities would not cause any trouble, a discretization speed $\Delta x/\Delta t = 50000$ m/s was adopted instead. Finally, while the CFL condition applies only to explicit finite difference schemes – and this work uses an implicit scheme – it was observed that the solution was not behaving properly if the CFL condition was not respected – which may be associated to the nonlinearities present on the equation. Therefore, the discretization will be chosen such as it respects this CFL restriction, despite it being implicit.

B.6. Badly-scaled Matrices

Another problem that arises during discretization of partial differential equations is badly-scaled matrices. A matrix is said to be badly-scaled if its determinant is close to zero – thus making it numerically singular – because the value of the determinant is too close to the numerical method precision, inducing large errors while solving the associated linear system.

After the discretization is made through the finite differences method, the partial differential equation is transformed into a set of algebraic linear equations, with the form of Eq. (B.19). However, two factors might forbid the solution of this system: either the matrix *A* of the problem is sparse – which means that there is large number of zero elements – or the matrix *A* has non-zero values with discrepant orders of magnitude. These two factors can render matrix *A* badly-scaled and hamper its solution.

$$[A]\{x\} = [B] \tag{B.19}$$

In the case of problems solved using finite differences, the system matrix *A* is always sparse. This occurs because the value of an arbitrary point of the structure is only a function of the adjacent points and not all the points in the structure. Therefore, matrix *A* becomes tridiagonal, which means that all information of the system is contained on the main diagonal and the two adjacent ones, as shown on Eq. (B.20).

$$A = \begin{bmatrix} A_{1,1} & A_{1,2} & 0 & \cdots & \cdots & \cdots & \cdots & \cdots & 0 \\ A_{2,1} & A_{2,2} & A_{2,3} & 0 & \cdots & \cdots & \cdots & \cdots & 0 \\ \vdots & \vdots & \vdots & \vdots & \vdots & \vdots & \vdots & \vdots & \vdots \\ 0 & \cdots & 0 & A_{i,j-1} & A_{i,j} & A_{i,j+1} & 0 & \cdots & 0 \\ \vdots & \vdots & \vdots & \vdots & \vdots & \vdots & \vdots & \vdots & \vdots \\ 0 & \cdots & \cdots & \cdots & \cdots & 0 & A_{N-1,N-2} & A_{N-1,N-1} & A_{N-1,N} \\ 0 & \cdots & \cdots & \cdots & \cdots & \cdots & 0 & A_{N,N-1} & A_{N,N} \end{bmatrix} \quad \text{(B.20)}$$

Where index *i* represents the lines, index *j* represents the columns and *N* is the matrix order. The elements $A_{i,j-1}$ and $A_{i,j+1}$ from the adjacent diagonals normally have the same module, but opposite signs; meanwhile, the element $A_{i,j}$ from the main diagonal can have a discrepant module when compared to the adjacent ones. Whenever the value of $A_{i,j}$ is way higher than the values of $A_{i,j-1}$ and $A_{i,j+1}$, the matrix is usually well conditioned; this happens because the main diagonal dominates the matrix determinant and the adjacent diagonals become negligible. Since in this case only the values from the main diagonal are relevant, the matrix determinant becomes the product of the elements from the main diagonal, thus being non-zero. However, when the value of $A_{i,j}$ is a lot less than the values of $A_{i,j-1}$ and $A_{i,j+1}$, the adjacent diagonals dominate the main diagonal and the determinant gets closer to zero, implying a numerically singular matrix.

One of the ways to measure the conditioning of a matrix is through its conditioning number (Arfken, 1985). By definition, the conditioning number is the ratio between the matrix highest and lowest singular values, obtained through the singular value decomposition (SVD). This number can range from *1* to infinite, with well-conditioned matrices having values close to *1*, whereas numerically singular matrices having values close to infinite – a singular matrix has an infinite conditioning number. The procedure for doing the singular value decomposition is out of the scope of this work, thus mathematical software will be used to calculate the conditioning number directly in case the problem of badly-scaled matrices arises.